ISSN 0257 – 3660

ACTA MINERALOGICA PAKISTANICA

Volume 6 1992

NATIONAL CENTRE OF EXCELLENCE IN MINERALOGY
(UNIVERSITY OF BALOCHISTAN), QUETTA, PAKISTAN

ACTA MINERALOGICA PAKISTANICA

VOLUME 6, 1992

CHIEF EDITOR: ZULFIQAR AHMED

REFEREES FOR THIS VOLUME :

ABUL FARAH, ISLAMABAD, PAKISTAN.
AFTAB AHMAD BUTT, PUNJAB UNIVERSITY, LAHORE, PAKISTAN.
ALI NASIR FATMI, QUETTA, PAKISTAN.
ANTHONY HALL, R.H.B. NEW COLLEGE, LONDON UNIVERSITY, UK.
DUANE M. MOORE, ILLINOIS STATE GEOLOGICAL SURVEY, USA.
FAIZ AHMED SHAMS, PUNJAB UNIVERSITY, LAHORE, PAKISTAN.
FAROOQ AHMED KHAN, P.O.L., RAWALPINDI, PAKISTAN.
FAYYAZ UR REHMAN, PCSIR, LAHORE, PAKISTAN.
FAZAL UR REHMAN, P.A.E. MINERALS CENTRE, LAHORE, PAKISTAN.
GEORGE R. McCORMICK, IOWA UNIVERSITY, USA.
KHALIL A. MALLICK, KARACHI UNIVERSITY, PAKISTAN.
M. AZAM MALIK, O.G.D.C., ISLAMABAD, PAKISTAN.
M. JAVED KHAN, PESHAWAR UNIVERSITY, PAKISTAN.
MOHAMMAD MAJID, PESHAWAR UNIVERSITY, PAKISTAN.
P.G. COORAY, SRI LANKA.
R.A. HOWIE, LONDON, U.K.
R.A. KHAN TAHIRKHELI, PESHAWAR, PAKISTAN.
RIAZ AHMAD SHEIKH, PUNJAB UNIVERSITY, LAHORE, PAKISTAN.
RHYS G. DAVIES, SURREY, U.K.
SHAFEEQ AHMAD, PUNJAB UNIVERSITY, LAHORE, PAKISTAN.
SHAH JEHAN, P.M.D.C., ISLAMABAD, PAKISTAN.
ZULFIQAR AHMED, NCE MINERALOGY, QUETTA, PAKISTAN.

ISSN 0257 — 3660

PRICE:

PREPAID ORDERS FROM PAKISTAN: RS. 100
OTHER COUNTRIES: U.S. $ 12.00 OR U.K. £ 8.00
This price includes postage and handling charges.

Published in December each year.
Printed at **KASHMIR OFFSET PRESS, QUETTA, PAKISTAN.**

ACTA MINERALOGICA PAKISTANICA VOLUME 6, 1992

CONTENTS

C. SHORT COMMUNICATIONS

D. REPORTS

PICTURES ON THE OUTSIDE COVER

Features from the leucocratic rocks of Bela ophiolite.

Top, left : Anatectic acidic rock outcrop at Purwait Bhut mound at latitude 27° 12' 32" N and longitude 66° 20' 20" E.

Top, right : Plane-polarized light photomicrograph of plagiogranite sample from Kurki Jhal (stream) area at latitude 27° 01' 40" N and longitude 66° 22' E. A euhedral albite grain is surrounded by quartz-albite intergrowths. A thin ilmenite plate is also visible.
View-size is 2.25 mm x 1.5 mm.

Bottom, left : Photomicrograph under plan-polarized light of an anatectic biotite-granite located 2 km W of Karku Jhal at latitude 27° 45' 30" N and longitude 66° 8' 14" E. Phases include brown biotite flakes, clear quartz, slightly dirtier feldspar, and a tiny zircon. View-size is 2.25 mm x 1.5 mm.

Bottom, right : Crossed-nicols photomicrograph of the same view as in the picture to the left, showing up twinning in feldspar.

(Responsibility : Zulfiqar Ahmed).

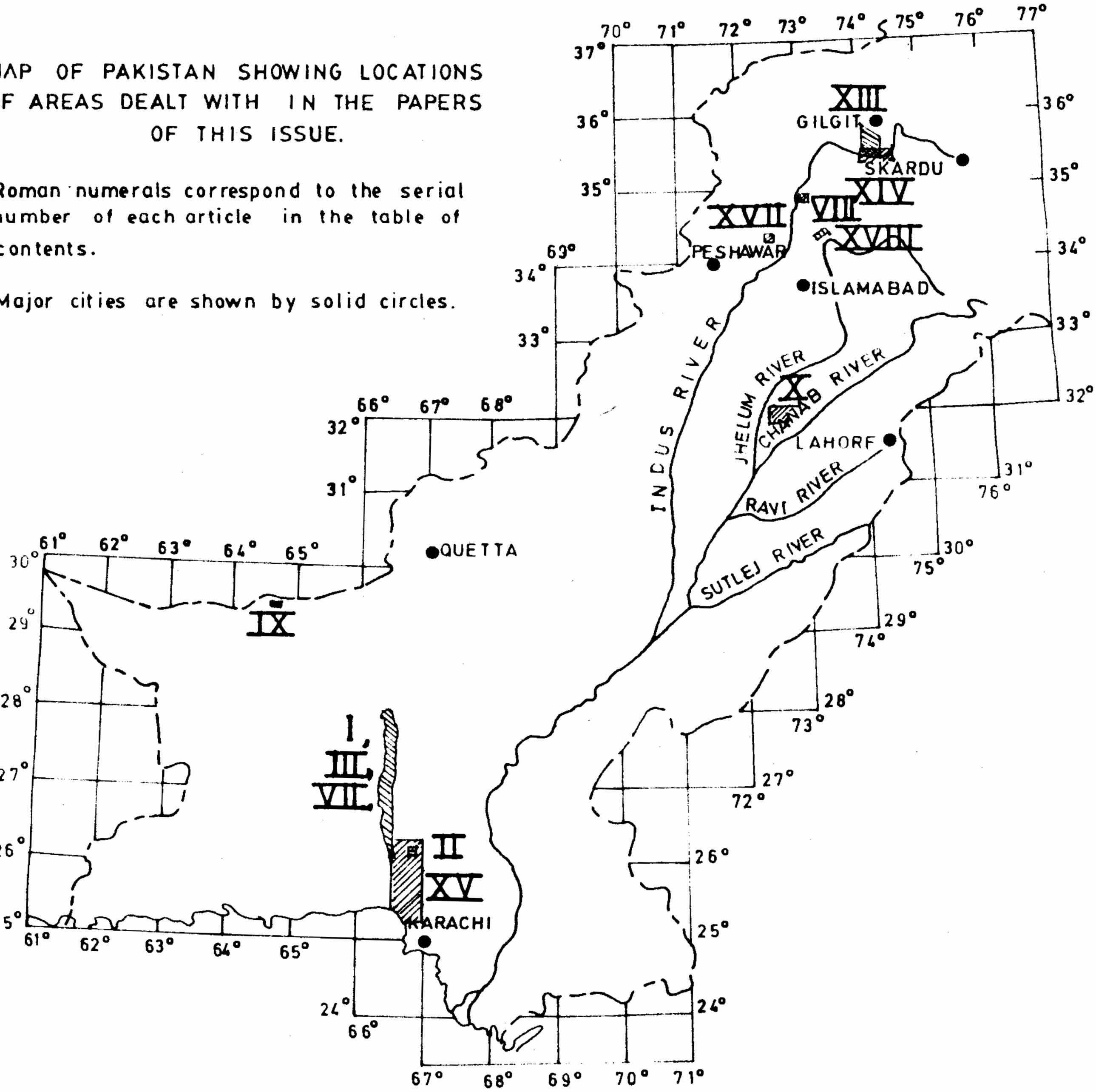

MAP OF PAKISTAN SHOWING LOCATIONS OF AREAS DEALT WITH IN THE PAPERS OF THIS ISSUE.

Roman numerals correspond to the serial number of each article in the table of contents.

Major cities are shown by solid circles.

ACTA MINERALOGICA PAKISTANICA
VOLUME 6 (1992) PP. 4–20

COMPOSITION OF CHROMITE FROM THE NORTHERN PART OF BELA OPHIOLITE, KHUZDAR DISTRICT, PAKISTAN.

ZULFIQAR AHMED

National Centre of Excellence in Mineralogy, University of Balochistan, G.P.O. Box 43, Quetta, Pakistan.

ABSTRACT: Bela ophiolite contains abundant mineable chromite segregations in addition to the accessory chromite in dunite, lherzolite, harzburgite, wehrlite and pyroxenite. This paper presents first account of the composition of ore as well as accessory chromite determined by the microprobe. An ore body with nodular chromitite texture has Al-rich composition distinct from the Cr-rich compositions for the more common ore from other parts showing non-nodular textures. The Mg/(Mg+Fe^{2+}) ratios are higher for segregated chromites compared to the accessory chromites, except for the rare basalt-hosted chromite. The Cr/(Cr+ Al) ratios exceed those known from the mid-ocean ridge type as well as the island arc type ophiolites and resemble those from the transitional type ophiolites.

INTRODUCTION

Chemical composition of chromite is important not only for its industrial applications but also as an indicator of magmatic and tectonic environment and host-rock petrogenesis (e.g., Thayer, 1970; Irvine, 1965,1967; Dick & Bullen, 1984; Zhou & Kerrich, 1992; Gartos et al., 1990).

Chromite is known to occur widely in the Bela ophiolite (Ahmed, 1986) and segregations are being actively mined. However, its chemical characterization is still lacking.

The Bela ophiolite represents oceanic crust - mantle obducted onto the western margin of the Indian continental plate. However, the initial ophiolitic tectonic environment is not precisely known. Previous literature is small and controversial. (e.g., Sarwar, 1992). Supporting chemical data is very poor. This study is a small contribution towards this goal.

This communication presents the chemistry of segregated ore as well as rock-forming accessory chromite from the Bela ophiolite, determined by an electron microprobe.

GEOLOGY OF THE BELA OPHIOLITE

The Bela ophiolite makes a more or less continuous outcrop elongated in an approximately due north direction that occurs along the western margin of the Indian plate for over 400 km. The east-west width of such outcrops averages to about 10 km. An ophiolitic mélange dominates on all outcrops and the ophiolite has suffered severe tectonics but at many places parts of the sequence are still intact. All the lithologies of a typical ophiolite sequence are present. The crustal sequence is more developed than the mantle sequence. One large segment of the ophiolite, the Lak Baran massif, displays a complete ophiolite sequence. This massif includes the chromite mines of Pahar Khan Bidrang (Table 1) as well. Chromite is abundant as ore- grade segregations, and is ubiquitous as an accessory phase in ultramafic rocks in addition to its presence in certain basalts.

CHROMITE OCCURRENCE

Mineable chromite occurrences at a few localities were reported by Hunting Survey Corporation Ltd. (1960). More recently, chromite occurrences have been found at many other localities, as small sized podiform bodies of irregular, lenticular and layer-like shapes. Major localities are given below:

I. *Upstream Karku Jhal.* These bodies are hosted by dunite exposed in the extreme northern part of the Bela ophiolite, in the upper reaches of the stream called Karku Jhal. Some bodies occur in more southerly exposures of dunite west of Karku Jhal near the Karku peak.

II. *Karku.* Two ore bodies are being mined surrounded by a harzburgite outcrop that shows little phase variation.

III. *Nal.* A big harzburgite outcrop lacks chromite ore, but a small dunite body towards west contains ore.

IV. *Laya Garr.* A 5 m thick layer-like body of massive chrome ore is present in the dunite body that outcrops SSW of Wadh town. This dunite is in thrust contact with the granite-intruded sheeted dyke complex overlain by basalt-chert exposed towards west.

V. *Pahar Khan Bidrang.* In this area, chromite segregations are relatively more abundant and occur as lenticular to layer-like bodies. The host cumulus dunite overlies harzburgite and lherzolite. Harzburgite and dunite oucrops have an intermediary zone of interlayered dunite and harzburgite. This layering frequently parallels the attitudes of chromite bodies. The area is a part of the Lak Baran massif where the intact ophiolitic sequence is most complete. The chromitites of this locality mainly occur only a small distance below the contact of layered gabbro and ultramafic rocks. The harzburgite of Lak Baran continues towards ESE for a few kms where it is tectonically in contact with Jurassic sediments. The harzburgite contains a mineable ore segregation of subconcordant type as defined by Cassard et al. (1981).

VI. *Lak Baran.* The harzburgite and lherzolite form base of the cumulate series and contain small bodies of chromitite inside the dunitic envelopes. At one locality, chromitite with massive, disseminated, regularly banded, graded layered, chromite -net and occluded-silicate textures is present. Generally the pseudolayering is developed which appears parallel to the attitudes of chromitites.

VII. *East Sonaro.* East of Sonaro village, clinopyroxene- harzburgite and dunite occur alongwith small lensoid to irregular chromitite bodies near Tibbi Jhal.

VIII. *Upstream Bora Jhal.* In the western upper reaches of stream of Bora Jhal, chromitite makes three mineable bodies in harzburgite and dunite which immediately underlie gabbro. The remainder of the mafic rock sequence of the ophiolite is exposed further eastwards. The chromite deposits are tectonically separated from the rest of the deposits of the ophiolite.

IX. *Ophiolitic Mélange.* The widespread ophiolitic melange contains blocks of ultramafic rock with chromite segregations including some mineable ore bodies. Some bodies are hosted by very small blocks with maximum dimensions of a few tens of metres. Examples are the dunite blocks at Samand Jhal area, and harzburgitic blocks at Jani Jhal area east of Jani peak. At latter occurrence , a massive magnetite body of lenticular shape occurs in the harzburgite block.

The number and size of the chromite bodies is not related to the size of the enclosing ultramafic body. Large harzburgitic outcrops either lack chromite bodies or contain only a few (e.g., near Nal). However, the dunite bodies contain more ore.

Host rocks of accessory chromite include lherzolite, clinopyroxene-harzburgite, harzburgite, dunite, wehrlite, clinopyroxenite and pillowed basalt (Table 1). Some of the peridotites are strongly serpentinized.

MINERAL CHEMISTRY

Method

Polished thin sections were made from various rock units of Bela ophiolite that contained chromian spinel. The analyses were performed at the California Institute of Technology (Caltech), U.S.A., employing Jeol Superprobe 733 instrument.

The analytical accuracy is estimated to be within ± 1.5 % for the major elements present in amounts > 5 %. Total iron determined by the microprobe analyses was partitioned between Fe^{3+} and Fe^{2+} on the basis of $RO / R_2O_3 = 1 : 1$, and using

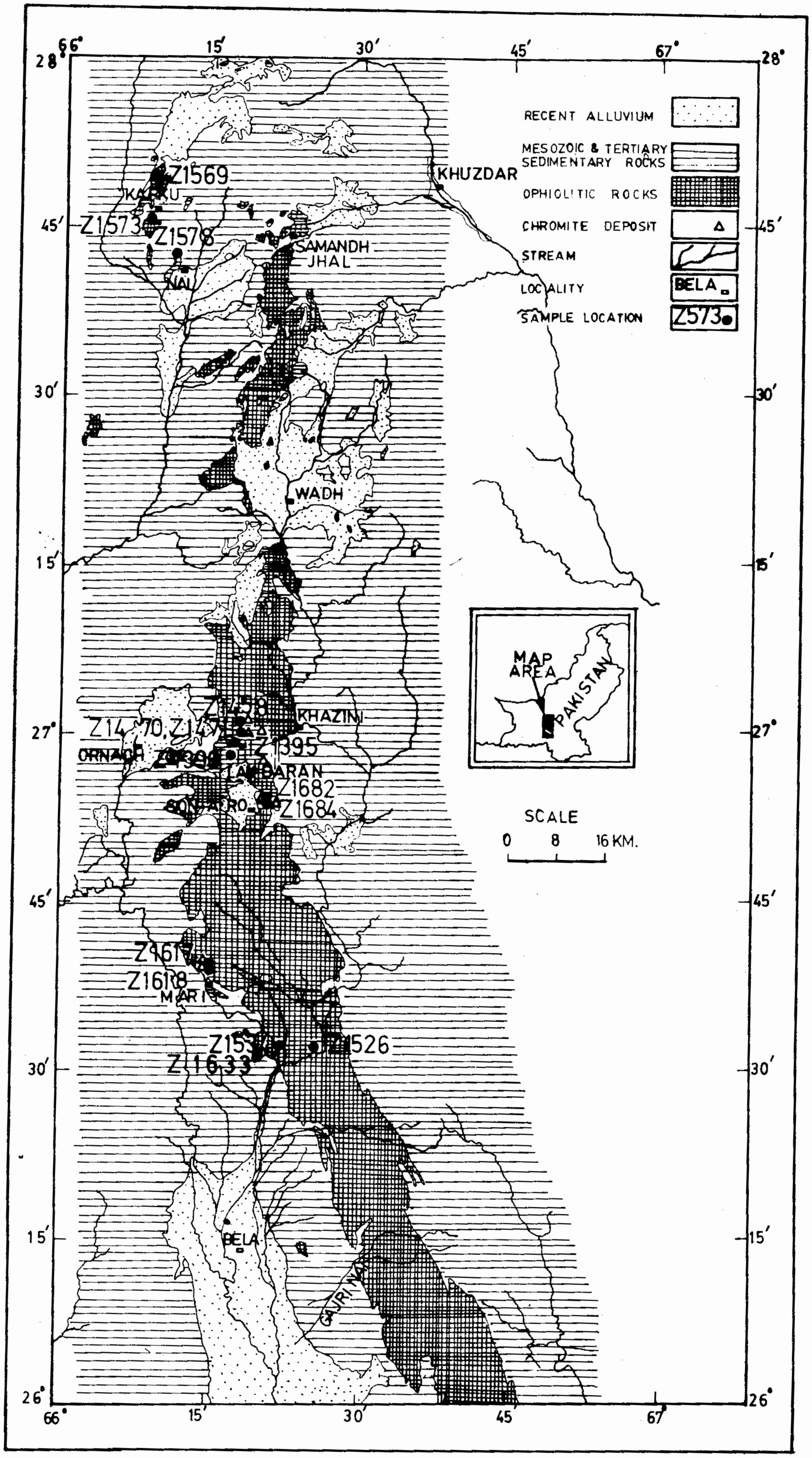

Fig. 1. Outcrop map of the northern half of the Bela ophiolite showing locations of rock samples included in this study. Position of the map area on the map of Pakistan is given in the inset.

Table 1. Location and description of chromitiferous rock samples from the Bela ophiolite, Khuzdar District.

	Sample No.	Latitude & Longitude	Locality	Descriptive Remarks
I.	**SEGREGATED CHROMITE:**			
(A)	**Disseminated to massive textured chrome Ore:**			
	Z 1569 66° 8' 29" E.	27° 48' 4" N; Jhal (Stream),	Upstream Karku	One of the most northerly chrome deposits of Bela ophiolite. Enclosed in cumulate dunite.
	Z 1458 66° 18' 24" E.	27° 1' 25" N; Bidrang),	Pahar Khan	Lenticular layer of chrome ore in cumulate dunite that overlies harzburgite.
	Z 1684	26° 53' 21" N; 66° 20' 46" E.	East of Sonaro	Hosted by dunite body within harzburgite (sample Z 1682).
	Z 1470	26° 59' 52" N; 66° 18' 7" E.	Lake Baran	Enclosed in the serpentinite envelope (sample Z 1471) in the lherzolite (sample Z 1395) host rock.
(B)	**Nodular chrome ore:**			
	Z 1618	26° 38' 57" N; 66° 15' 1" E.	Near Mari, upstream of Bora Jhal (stream),	Hosted by ultramafics underlying mafic rock ophiolitic sequence.
(C)	**Primary magnetite (non-chromitiferous) ore**			
	Z 1633	26° 30' 42" N; 66° 20' 5" E.	Jani Jhal, east of Jani peak.	
II.	**ACCESSORY CHROMITE :**			
(A)	**In Lherzolite:**			
	Z 1526	26° 31' 18" N; 66° 24' 27" E.	Junction of Hinami Jhal (stream) with Porali river.	
	Z 1390	26° 58' 2" N; 66° 17' 44" E.	Near Hinar Trikki, Lak Baran	
	Z 1395	26° 59' 50" N; 66° 17' 56" E.	Lak Baran.	
(B)	**In Clinopyroxene Harzburgite:**			
	Z 1682	26° 53' 28" N; 66° 20' 45" E.	East of Sonaro towards Tibbi Jhal.	
	Z 1561	27° 40' 9" N; 66° 10' E.	Nal town.	
(C)	**In Serpentinized – Harzburgite:**			
	Z 1471 66° 18' 7" E.	26° 59' 2" N;	Lak Baran	Hosts chrome deposit (sample Z 1470).
(D)	**In Wehrlite:**			
	Z 1534	26° 31' 54" N; 66° 22' 44" E.	East slope of Kohan Jhal.	Partly serpentinized.
	Z 1573	27° 45' 46" N; 66° 8' 5" E.	Karku mountain.	
(E)	**In Pyroxenite:**			
	Z 1617	26° 38' 58" N; 66° 15' 1" E.	Near Mari, upstream of Bora Jhal (stream).	Veins harzburgite.
(F)	**In Pillowed basalt:**			
	Z 1578	27° 42' 16" N; 66° 11' E.	Kumbi, near Nal town.	

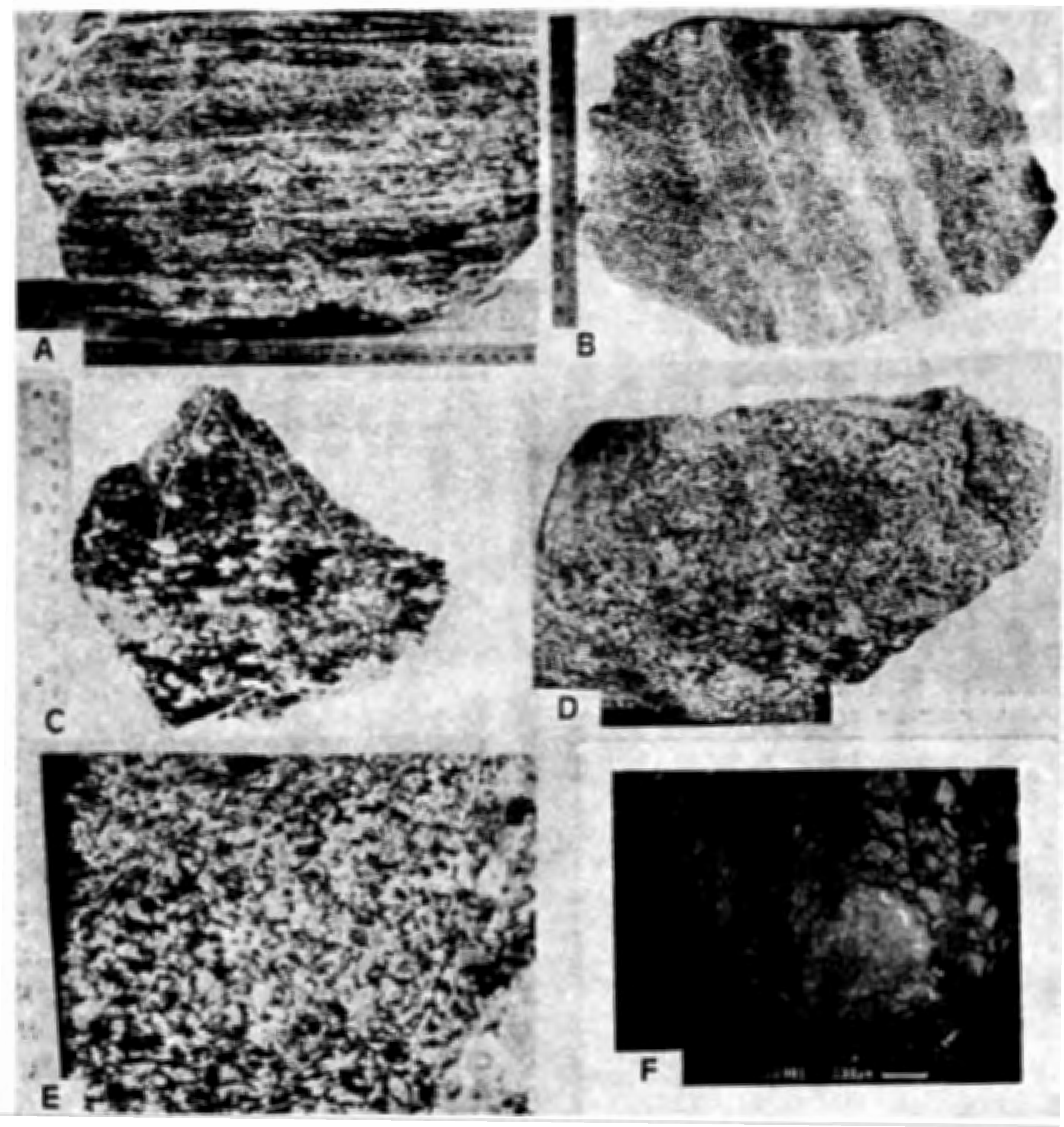

Fig. 2. (A to E) Hand specimen photographs taken with scale in cms, of the chrome ore from a mine of Lak Baran area displaying textures : (A) typical banded ore, (B) banded ore with some graded layers and layers containing the occluded silicate "eyes" in disseminated chromitite layers, (C) massive ore grading into occluded silicate ore, (D) chromite-net ore whose part is enlarged in (E). (F) Secondary electrons image taken by an SEM showing accessory chromite anhedra (bright) enclosed inside the margin of a coarser pyroxene grain (grey) of a wehrlite sample (Z1526).

the Macintosh computer programme MINTAB (Rock & Carroll, 1990) for the mineral formulae recalculations. The cation deficiencies are neglected as they are not significant in the natural plutonic chromites (Stevens, 1944; Thayer, 1964; Irvine, 1965).

The secondarily altered parts of chromian spinel grains appear optically distinct and are readily recognizable by the method of Ahmed & Hall (1981). The identifications of altered parts were confirmed under the microprobe; and analyses of such altered phases such as those shown in Fig.3, or as analysis 19 in Table 2, are avoided in the interpretations relating to primary chromian spinel.

Apart from the elements listed in Tables 2 and 3, chromite grains were also analyzed for their K, Na, Ba, Sr, Zr, Cl, P, which are found to be below detection levels.

Results

The compositional variation of primary chromian spinel is shown in Tables 2 & 3 and plots of analyses in the spinel compositional prism designed by Johnston (Jackson, 1969) are shown in Fig. 4. In the rectangular plots, the axis for trivalent cations are enlarged twice the length of the axis for divalent cations, because this corresponds to the spinel stoichiometry and because this convention is followed previously (e.g., Jackson, 1969; Dick & Bullen, 1984).

According to the classification of chromian spinels by Stevens (1944), these chromites belong to the aluminian chromite and chromian spinel fields, and many analyses plot in his metallurgical grade.

The analyses point to a strong chemical resemblance of the Khuzdar District chromites with the other podiform chromite deposits of the world which develop in alpine type peridotites of ophiolites. The chemical distinctions of such deposits have been studied by many workers including Thayer (1964, 1969, 1970), Irvine (1967), Dickey & Yoder (1972), Dickey (1975), Malpas & Strong (1975), Ahmed (1984) and Dick & Bullen (1984). The features noted in the Khuzdar chromites include the following:

1. Relative constancy of total iron content; independent of variation in Cr_2O_3 content.
2. A more magnesian character with total iron content lower than that of stratiform chromites. The MgO / FeO ratio for most analyses exceeds 1. The total iron content is below 20 %.
3. Constancy of Fe^{2+}/Mg ratio in chromites from individual occurrences or segregations, relative to stratiform complexes.
4. Low Fe_2O_3 content; most of the Fe being in the ferrous state.
5. Low TiO_2 content, and lack of any significant correlation between Ti and major elements.
6. A large range in the reciprocal Cr-Al variation with Fe^{3+} staying low and roughly constant. In the triangular plot of Cr-Al-Fe^{3+}, all analyses plot very close to the Cr-Al join (Fig. 4).
7. The Khuzdar District chrome ores are mostly of high Cr, low Fe (metallurgical) grade, with a lesser fraction (e.g., nodular ore) of high Al (refractory) grade. The chemical analyses presented here do not show high Fe (chemical grade) ores, except their secondarily altered parts which do not change the overall grade of the ore.
8. The elemental Cr/Fe ratio similar to that of the podiform deposits and ophiolitic peridotites.
9. Absence of continuous gradation in the segregated chromite composition, giving a bimodal Cr-Al distribution, as discussed by Thayer (1970) and Dickey (1975)

The composition of primary chromian spinel from different rock units of the Bela ophiolite is displayed in the spinel prism plots in Fig. 4. The accessory chromites show a consistent Fe^{2+} enrichment and Mg depletion compared to the associated segregated chromites, and plot separately in the spinel prism.

In the Cr- Al variation, the accessory chromites show a trend similar to the segregated chromites (Fig.4) but with a more limited variation range.

The Cr/(Cr + Al) values (called Cr #) range as follows: 0.6373-0.8089 in the segregated chromite, 0.4187-0.4216 in the nodular chromitite, 0.1711-0.7836 in the accessory chromite. The large range in accessory chromite corresponds to the

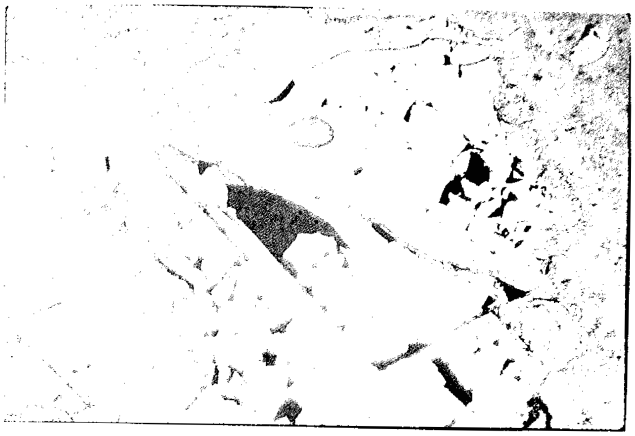

A

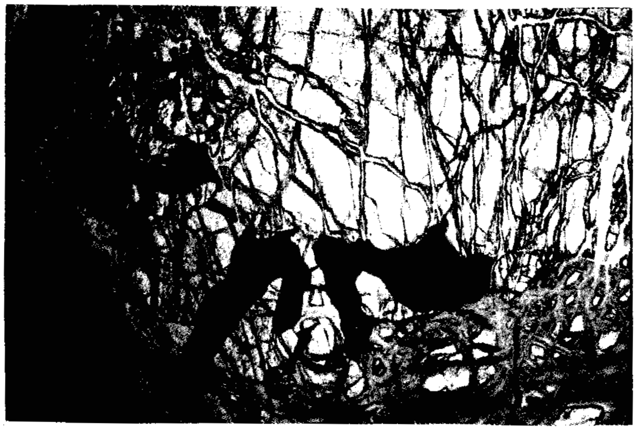

B

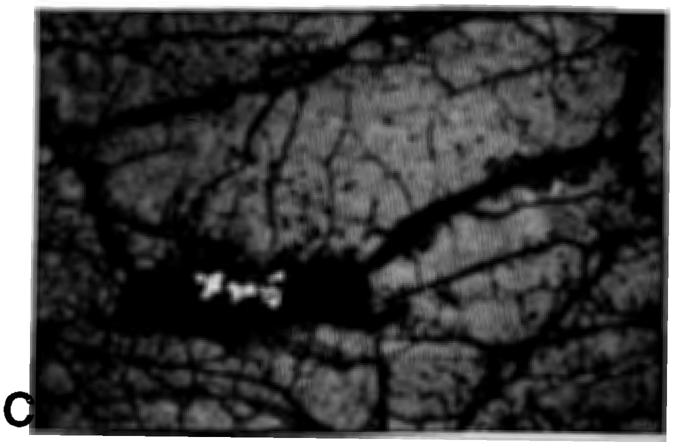

C

D

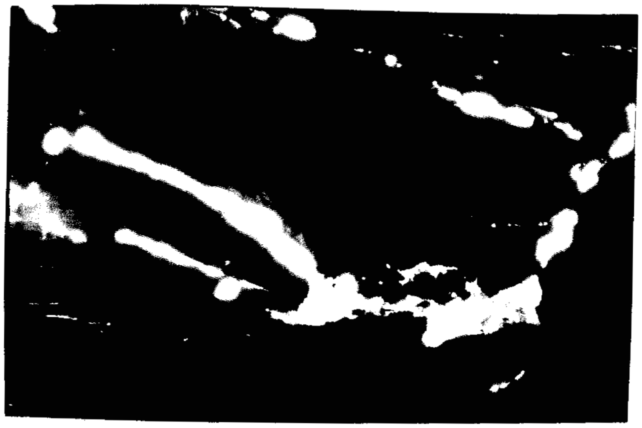

E

F

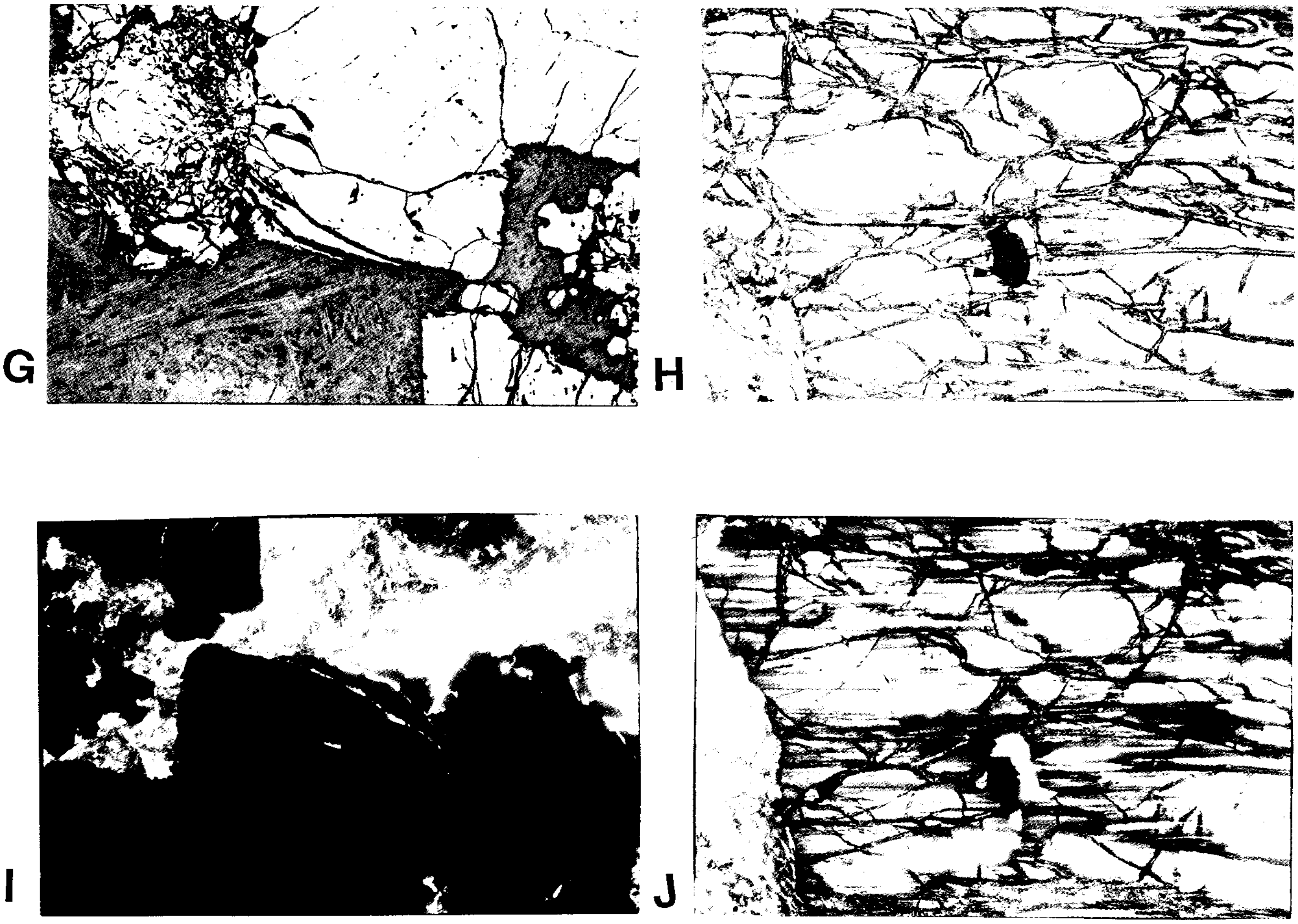

Fig. 3. Polished thin section photomicrographs showing the reflected light (RL); crossed-nicols (XL), or plane-polarized transmitted light (PL) images of Bela ophiolite samples. Each view measures 2.25 mm X 1.5 mm. **(A)** RL view of nodular chromitite sample (Z1618) shows unaltered chromite bordered by variable thickness of more pitted ferritchromite rim. The serpentine veinlet contains a bright speck of pentlandite. **(B)** XL view of lherzolite sample (Z1526) shows anhedral chromite within coarse clinopyroxene. **(C)** RL, **(D)** PL, and **(E)** XL views of chromitite sample (Z1470) with serpentine veinlets containing NiS specks. **(F)** RL view of wehrlite sample (Z1534) with anhedral chromite, brighter ferritchromite rim with cracks, and still brighter tiny sulphide specks and some magnetite. **(G)** RL and **(H)** XL views of magnetite sample (Z1633) showing better polished magnetite with another shattered grain which is not ferritchromit. Long flaky chlorite on one side is not so on the other corner. **(I)** XL, and **(J)** PL views of clinopyroxene -harzburgite sample (Z1561) an orthopyroxene grain at nearly extinction position containing inclusions of olivine and chromite and surrounded by olivine, serpentine and clinopyroxene.

Table 2. Selected analyses of segregated chromite.
1 to 15 = Disseminated to massive chromitite; 16 to 18 = Nodular chromitite; 19 = Ferritchromite.

Anal No.	1	2	3	4	5	6	7	8	9	10	11	12	13	14	15	16	17	18	19
Sample	Z 1684					Z 1458				Z 1569				Z 1470		Z 1618			
SiO_2	0.03	0.02	0.06	0.03	0.12	0.01	0.05	0.01	0.01	0.02	0.09	0.02	0.02	0.05	0.05	0.05	0.01	0.02	2.42
TiO_2	0.17	0.18	0.18	0.14	0.20	0.12	0.17	0.14	0.15	0.13	0.19	0.16	0.20	0.19	0.15	0.27	0.25	0.26	0.36
Al_2O_3	10.31	10.37	10.48	10.25	10.08	13.18	12.87	12.70	13.11	14.28	14.29	14.62	14.49	15.70	15.84	32.89	33.11	32.69	8.91
Gr_2O_3	63.76	63.76	63.34	62.97	63.50	57.46	57.28	57.16	54.70	57.63	56.65	56.86	56.99	53.55	51.99	35.55	35.99	35.54	45.91
V_2O_3	0.11	0.12	0.05	0.08	0.11	0.19	0.20	0.19	0.17	0.08	0.04	0.07	0.09	0.08	0.07	0.10	0.14	0.10	0.13
Fe_2O_3	0.00	0.00	1.02	1.75	0.79	3.40	3.48	3.48	4.46	1.80	1.97	2.19	1.85	0.77	3.99	3.31	3.40	4.35	8.45
FeO	11.50	11.45	10.43	9.68	10.80	12.41	12.48	13.47	10.85	13.03	13.90	12.46	13.14	15.35	13.09	11.32	10.51	10.21	23.11
MnO	0.23	0.22	0.10	0.09	0.17	0.17	0.22	0.30	0.26	0.22	0.24	0.27	0.25	0.21	0.32	0.15	0.23	0.08	1.15
MgO	13.84	14.22	15.49	15.71	15.14	14.37	13.97	13.41	14.65	13.92	13.37	14.37	13.94	12.04	13.51	17.05	17.66	17.82	7.65
NiO	0.25	0.16	0.14	0.30	0.15	0.10	0.16	0.04	0.15	0.08	0.11	0.09	0.05	0.13	0.14	0.17	0.19	0.17	0.09
CaO	0.02	0.00	0.00	0.01	0.00	0.00	0.01	0.00	0.00	0.03	0.03	0.00	0.00	0.00	0.00	0.00	0.00	0.02	0.04
ZnO	0.00	0.00	0.00	0.06	0.00	0.01	0.05	0.13	0.12	0.07	0.13	0.11	0.03	0.08	0.10	0.04	0.02	0.12	0.26
Total	100.22	100.50	101.29	101.07	101.06	101.42	101.30	101.03	98.63	101.29	101.11	101.22	101.05	98.15	99.25	100.95	101.51	101.38	98.48
Cations to 32 oxygens:																			
Si	0.01	0.01	0.02	0.01	0.03	0.00	0.01	0.00	0.00	0.01	0.02	0.01	0.01	0.01	0.01	0.01	0.00	0.00	0.66
Ti	0.03	0.03	0.03	0.03	0.04	0.02	0.03	0.03	0.03	0.02	0.04	0.03	0.04	0.04	0.03	0.05	0.04	0.04	0.07
Al	3.11	3.12	3.11	3.04	3.00	3.89	3.82	3.79	3.96	4.21	4.23	4.30	4.28	4.78	4.74	8.87	8.85	8.87	2.87
Cr	12.91	12.86	12.59	12.54	12.70	11.38	11.40	11.45	11.08	11.40	11.26	11.21	11.29	10.95	10.42	6.43	6.45	6.39	9.90
V	0.02	0.02	0.01	0.02	0.02	0.04	0.04	0.04	0.04	0.02	0.03	0.01	0.02	0.02	0.02	0.02	0.03	0.02	0.03
Fe^{3+}	0.00	0.00	0.19	0.33	0.15	0.64	0.66	0.66	0.86	0.33	0.37	0.41	0.35	0.15	0.76	0.57	0.58	0.74	1.73
Fe^{2+}	2.46	2.44	2.19	2.04	2.28	2.60	2.70	2.86	2.33	2.73	2.92	2.60	2.75	3.32	2.77	2.17	1.99	1.94	5.27
Mn	0.05	0.05	0.02	0.02	0.04	0.04	0.05	0.06	0.06	0.05	0.05	0.06	0.05	0.05	0.07	0.03	0.04	0.02	0.27
Mg	5.28	5.41	5.81	5.90	5.71	5.37	5.24	5.07	5.60	5.19	5.01	5.34	5.20	4.64	5.11	5.82	5.97	6.04	3.11
Ni	0.05	0.03	0.03	0.06	0.03	0.02	0.03	0.01	0.03	0.02	0.02	0.02	0.01	0.03	0.03	0.03	0.03	0.03	0.02
Ca	0.01	0.00	0.00	0.00	0.00	0.00	0.00	0.00	0.00	0.01	0.01	0.00	0.00	0.00	0.00	0.00	0.00	0.01	0.01
Zn	0.00	0.00	0.00	0.01	0.00	0.00	0.01	0.02	0.02	0.01	0.02	0.02	0.01	0.02	0.02	0.01	0.00	0.02	0.05
Cr#	80.59	80.48	80.19	80.49	80.89	74.53	74.90	75.13	73.67	73.03	72.69	72.28	72.51	69.61	68.73	42.03	42.16	41.87	77.53
Mg#	68.21	68.91	72.59	74.30	71.43	67.36	65.97	63.96	70.65	65.57	63.15	67.28	65.42	58.32	64.81	72.79	74.99	75.69	37.11

Cr = 100 x Cr/ (Cr+Al). Mg # = 100 x Mg/ $(Mg+Fe^{2+})$.

Table 3. Selected analyses of accessory chromite.

Anal. No.	1	2	3	4	5	6	7	8	9	10	11	12	13	14	15	16	17	18	19	20	21	22	23	24	25	26	27
Sample	Z–1526				Z 1395					Z 1390		Z 1682					Z 1471					Z 1573		Z 1534		Z 1617	Z 1578
SiO_2	0.01	0.00	0.01	0.05	0.00	0.01	0.04	0.02	0.01	0.00	0.03	0.02	0.00	0.01	0.03	0.03	0.04	0.04	0.02	0.00	0.00	0.05	0.08	0.08	0.02	0.02	0.07
TiO_2	0.04	0.04	0.00	0.03	0.01	0.04	0.04	0.06	0.06	0.07	0.05	0.06	0.09	0.10	0.09	0.10	0.06	0.01	0.02	0.04	0.04	0.08	0.09	0.00	0.05	0.12	0.24
$Al_2()_3$	31.64	32.58	34.26	30.94	24.48	22.08	25.23	22.29	22.87	51.74	52.47	17.99	17.33	18.43	17.22	16.93	17.71	17.88	17.01	18.76	17.46	31.78	28.65	43.84	48.59	13.59	10.83
Cr_2O_3	39.51	38.84	36.73	40.72	44.49	47.18	44.28	46.90	45.65	15.98	16.13	47.57	45.98	46.94	47.53	46.05	49.96	50.19	49.89	49.56	50.85	36.39	40.39	23.77	19.26	60.13	58.47
V_2O_3	0.22	0.22	0.21	0.18	0.23	0.22	0.27	0.21	0.23	0.12	0.00	0.35	0.37	0.40	0.36	0.34	0.27	0.22	0.23	0.29	0.27	0.24	0.22	0.11	0.13	0.09	0.05
Fe_2O_3	0.83	0.78	1.11	0.48	1.99	2.48	1.61	2.01	1.80	2.96	1.65	5.08	7.42	6.39	6.63	7.77	2.58	3.18	3.55	2.24	1.95	2.19	1.31	3.31	3.24	0.00	3.59
FeO	14.48	15.31	14.90	14.74	18.96	16.54	17.02	18.01	16.79	9.63	10.44	19.15	18.96	19.80	18.43	19.55	20.60	20.99	21.10	20.00	19.38	17.11	17.19	12.87	10.88	13.72	9.02
MnO	0.24	0.20	0.24	0.16	0.19	0.28	0.29	0.30	0.26	0.14	0.15	0.37	0.43	0.29	0.25	0.27	0.38	0.38	0.34	0.28	0.22	0.21	0.19	0.20	0.15	0.12	0.14
MgO	14.95	14.65	14.95	14.73	11.16	12.38	12.44	11.52	12.07	19.81	19.38	10.07	10.03	10.19	10.57	9.80	9.20	9.09	8.38	9.74	9.85	13.15	12.69	17.07	18.75	13.12	15.55
NiO	0.07	0.05	0.16	0.16	0.09	0.07	0.07	0.05	0.09	0.32	0.25	0.11	0.17	0.02	0.14	0.19	0.00	0.07	0.05	0.05	0.10	0.06	0.05	0.13	0.32	0.14	0.21
CaO	0.01	0.02	0.03	0.04	0.02	0.01	0.02	0.00	0.00	0.01	0.02	0.01	0.02	0.03	0.03	0.01	0.02	0.01	0.01	0.00	0.00	0.00	0.00	0.08	0.01	0.06	0.09
ZnO	0.10	0.16	0.16	0.19	0.18	0.13	0.11	0.12	0.10	0.14	0.11	0.19	0.18	0.14	0.14	0.14	0.19	0.22	0.17	0.20	0.18	0.15	0.09	0.15	0.19	0.01	0.00
Total	102.10	102.85	102.76	102.42	101.81	101.42	101.42	101.49	99.93	100.92	100.87	100.97	100.98	102.74	101.42	101.18	101.01	102.30	101.22	101.16	100.30	101.41	100.87	101.61	101.58	101.12	98.26
Cations to 32 Oxygens:																											
Si	0.00	0.00	0.00	0.01	0.00	0.00	0.01	0.00	0.00	0.00	0.01	0.01	0.00	0.00	0.01	0.01	0.01	0.01	0.01	0.00	0.00	0.01	0.00	0.02	0.00	0.01	0.02
Ti	0.01	0.01	0.00	0.01	0.00	0.01	0.01	0.01	0.01	0.01	0.01	0.02	0.02	0.02	0.02	0.02	0.01	0.00	0.00	0.01	0.01	0.01	0.02	0.00	0.01	0.02	0.05
Al	8.60	9.79	9.17	8.42	7.02	6.37	7.18	6.45	6.67	12.83	13.03	5.38	5.21	5.42	5.13	5.09	5.33	5.32	5.14	5.59	5.27	8.78	8.06	11.29	12.20	4.04	3.29
Cr	7.20	7.03	6.80	7.43	8.56	9.12	8.45	9.11	8.93	2.69	2.69	9.55	9.26	9.26	9.50	9.29	10.08	10.02	10.11	9.91	10.29	6.74	7.63	4.11	3.24	11.98	11.91
V	0.04	0.04	0.04	0.03	0.05	0.04	0.05	0.04	0.05	0.02	0.00	0.07	0.08	0.08	0.07	0.07	0.06	0.05	0.05	0.06	0.05	0.05	0.04	0.02	0.02	0.02	0.01
Fe^{3+}	0.14	0.13	0.19	0.08	0.36	0.46	0.29	0.37	0.33	0.47	0.26	0.97	1.42	1.20	1.26	1.49	0.50	0.60	0.68	0.43	0.38	0.39	0.24	0.55	0.52	0.00	0.70
Fe^{2+}	2.79	2.93	2.83	2.85	3.86	3.38	3.43	3.70	3.47	1.69	1.84	4.07	4.04	4.13	3.90	4.17	4.40	4.43	4.52	4.23	4.15	3.35	3.43	2.35	1.94	2.89	1.94
Mn	0.05	0.04	0.05	0.03	0.04	0.06	0.06	0.06	0.06	0.03	0.03	0.08	0.09	0.06	0.05	0.06	0.08	0.08	0.07	0.06	0.05	0.04	0.04	0.04	0.03	0.03	0.03
Mg	5.14	5.00	5.06	5.07	4.05	4.52	4.48	4.22	4.45	6.21	6.09	3.81	3.81	3.79	3.99	3.73	3.50	3.42	3.38	3.67	3.78	4.59	4.52	5.56	5.95	4.93	5.97
Ni	0.01	0.01	0.03	0.03	0.02	0.01	0.01	0.01	0.02	0.05	0.04	0.02	0.03	0.00	0.03	0.04	0.00	0.01	0.01	0.01	0.02	0.01	0.01	0.02	0.06	0.03	0.04
Ca	0.00	0.01	0.01	0.01	0.01	0.00	0.00	0.00	0.00	0.00	0.01	0.00	0.01	0.01	0.01	0.00	0.01	0.00	0.00	0.00	0.00	0.00	0.00	0.02	0.00	0.02	0.03
Zn	0.02	0.03	0.03	0.03	0.03	0.02	0.02	0.02	0.02	0.02	0.02	0.03	0.04	0.03	0.03	0.03	0.04	0.04	0.03	0.04	0.03	0.03	0.00	0.02	0.03	0.00	0.00
Cr#	45.77	44.44	42.58	46.88	54.94	58.88	54.06	58.55	57.24	17.17	17.11	63.97	63.99	63.08	64.94	64.60	65.41	65.32	66.30	63.94	66.13	43.43	48.63	26.69	20.98	74.78	78.36
Mg#	64.79	63.04	64.14	64.06	51.20	57.18	56.60	53.28	56.18	78.58	76.80	48.38	48.53	47.84	50.56	47.19	44.33	43.56	42.78	46.48	47.52	57.80	56.82	70.28	75.45	63.04	75.19

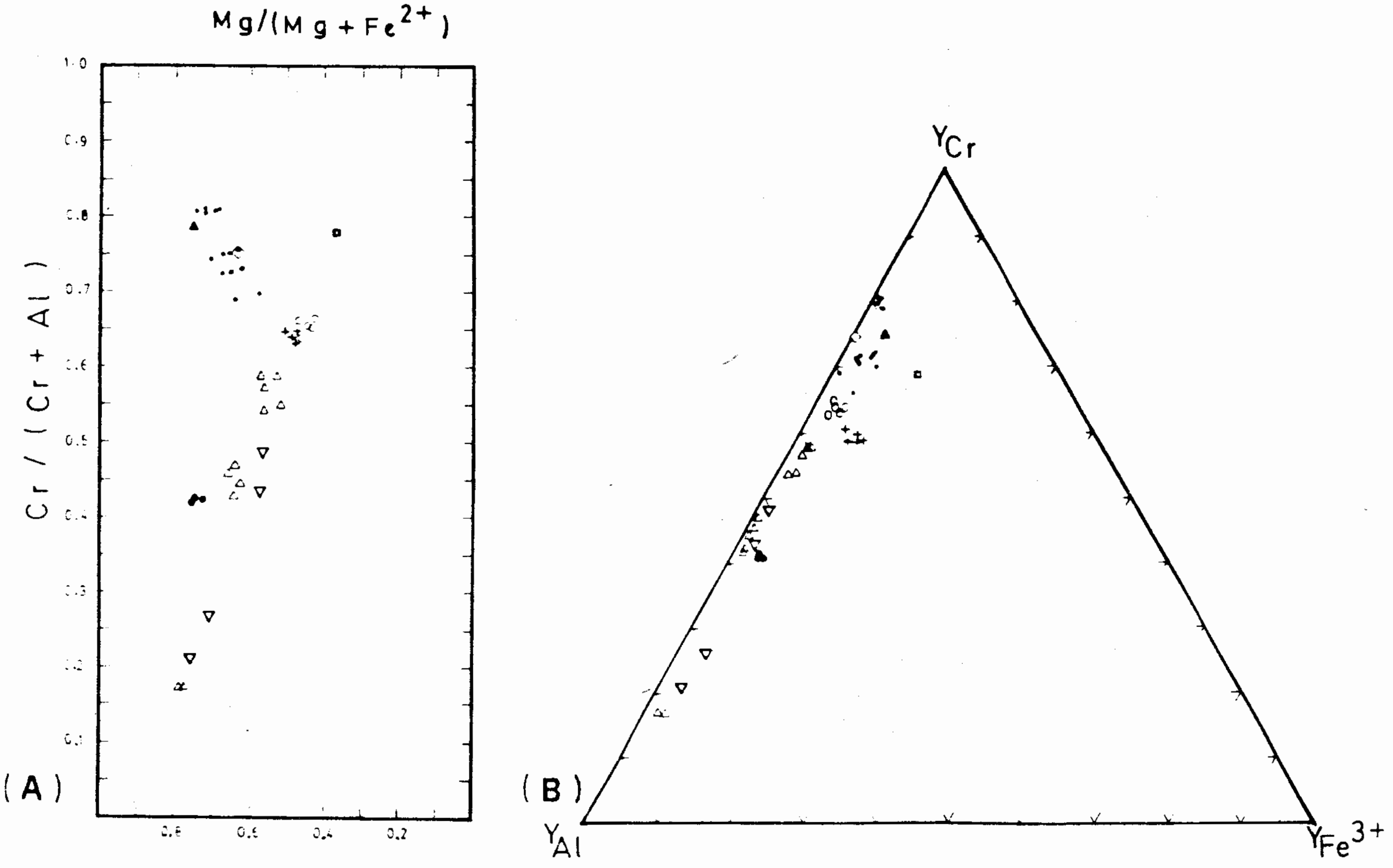

Fig. 4. Spinel prism plots of the Bela ophiolite chromian spinel microprobe analyses for the nodular segregated chromite (bigger dots), non-nodular segregated chromite (smaller dots); and accessory chromite from the lherzolites (triangles), clinopyroxene harzburgite (crosses), serpentinized harzburgite (open circles), wehrlites (inverted triangles), clinopyroxenite (diagonal square), and basalt (solid triangle). One analysis of secondary "ferritchromit" chromite is also plotted.

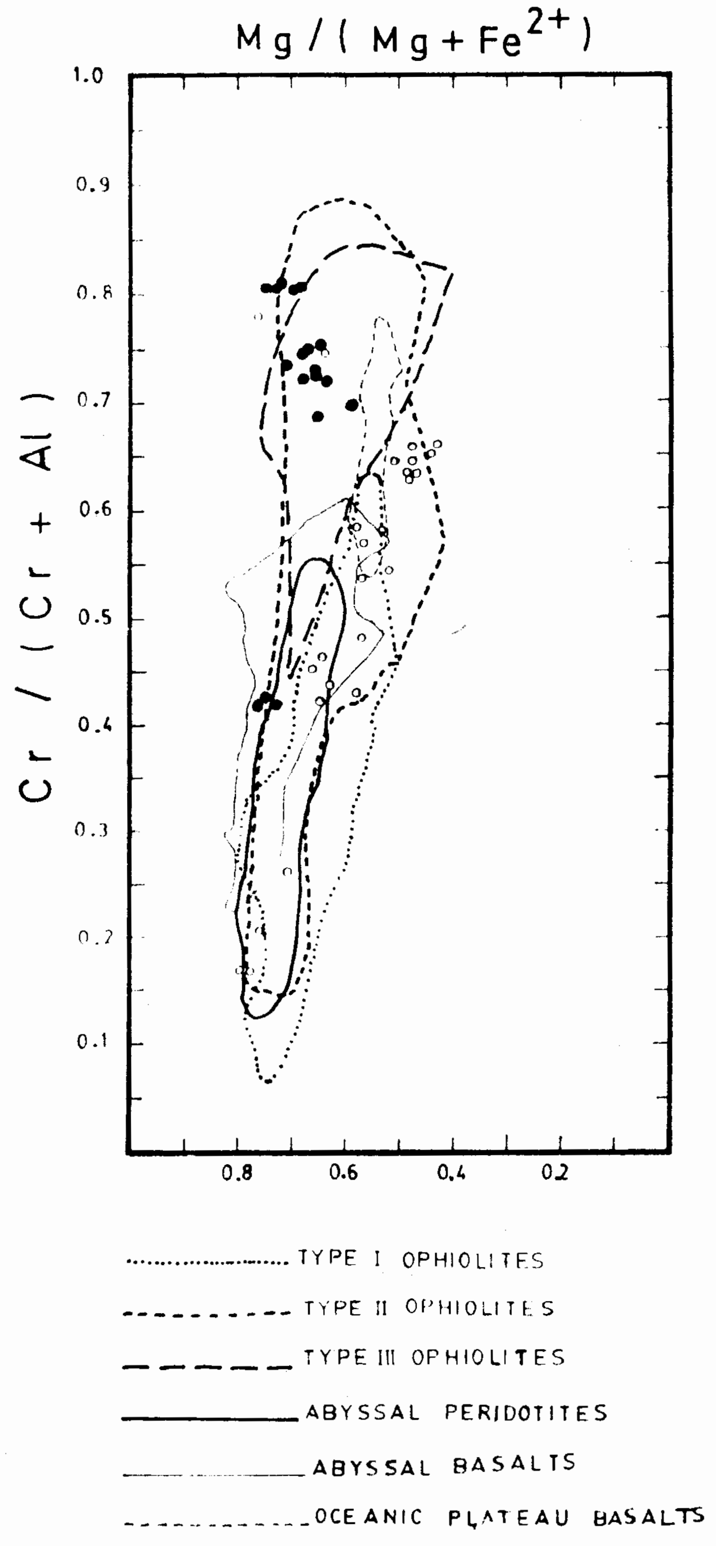

Fig. 5. Plot on the Cr/(Cr+Al) vs Mg/(Mg+Fe 2+) face of the spinel prism comparing the segregated (dots) and accessory (open circles) chromites of the Bela ophiolite with the compositional fields for the Type I (generated at mid-ocean ridge settings) ophiolites, Type II (transitional type) ophiolites, Type III (arc-related environment) ophiolites, abyssal peridotites, abyssal basalts and oceanic plateau basalts. The fields are plotted after the compilations of Dick & Bullen (1984) and Pober & Faupl e (1988).

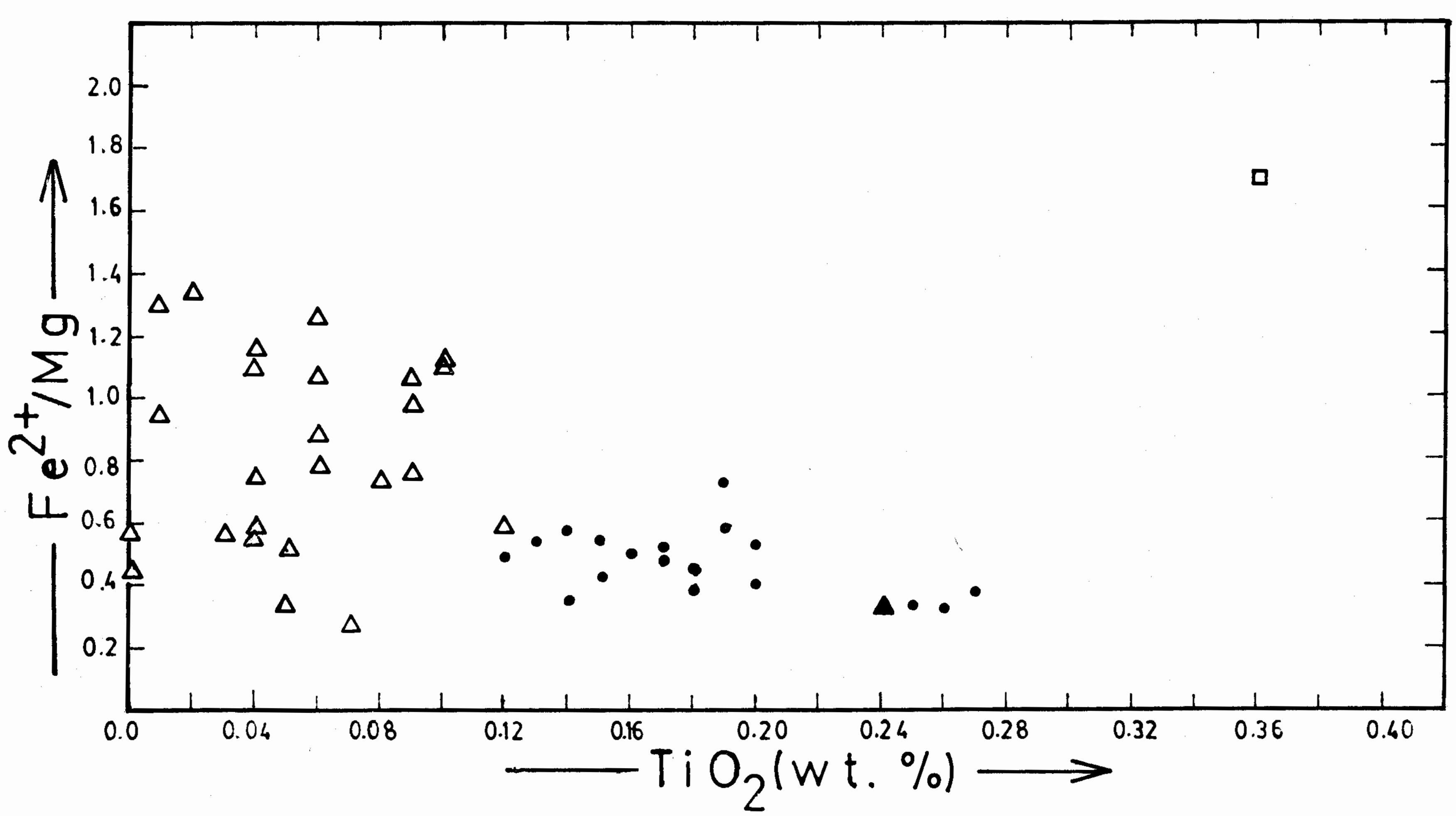

Fig. 6. Fe^{2+}/Mg vs TiO_2 wt.% plot for the Bela ophiolite chromites drawn after Dickey (1975). Due to low values of TiO_2, all points fall in the area where podiform and stratiform chromites overlap. Accessory chromites (triangles) plot separately from the segregated chromites (dots) except for the chromite from a basalt host rock (solid triangle). The isolated plot of "ferritchromit" (square) shows the trend of secondary alteration.

Type II alpine-type peridotites of Dick & Bullen (1984) which have composite origins with large variations in the degree and provenance of melting over relatively short distances.

The Khuzdar District chromites contain low TiO_2 contents (< 0.27 wt. %) which is even lower for accessory chromites. (< 0.12 wt. %) than for segregated chromites (0.12 to 0.27 wt. %).

The clinopyroxene-bearing peridotites, except pyroxenite, contain accessory chromite which plots more towards the low-Cr end compared to the plots of harzburgite spinel. This feature is parallel with the plots of abyssal peridotites (Fig. 5) given in Dick & Bullen (1984).

The spinel in basaltic pillow lava plots towards the Cr-rich end, and lies outside the range of abyssal peridotites and basalts. The composition falls within the range of podiform chromitites and seem to imply a genetic relationship. This high-Cr spinel is not found in the mid-ocean ridge basalts (Dick & Bullen, 1984).

In Fig. 5, the Khuzdar District deposits fall within the alpine field and follow a pronounced trend of Cr-Al substitutions typical of the alpine type.

The massive-disseminated chromite from the cumulate zone dunite and harzburgite-dunite contact zone fall entirely within the high-Cr area of stratiform field which overlaps the alpine field.

Tables 2 & 3 show relative Ti content of various chromite types from the Bela ophiolite samples. TiO_2 Values are higher for segregated than for accessory chromite; higher for nodular than for non-nodular ore; higher for basalt than for peridotitic rocks, higher for pyroxenite than for the rest of the ultramafic rocks, and the lowest values are for the harzburgite sample no. Z1471.

DISCUSSION

The chemical characteristics of chromite from Khuzdar District described above, are similar to those of the podiform chromites that occur in alpine type peridotites.

Dick & Bullen (1984) used the average Cr # of spinel as an index of the degree of melting. The large range in the Cr # of Bela ophiolite spinel and the large size of the Bela ophiolite may represent complex multistage melting histories in which the degree of partial fusion and melt removel varied greatly. Such alpine peridotites are not found at mid-ocean ridges. A part of this ophiolite may be similar to the present day abyssal peridotites as its spinel prism plot with Cr # < 60 overlaps with those peridotites. This part may be due to generation at a marginal basin ridge.

The higher Cr in harzburgitic spinels compared to the lherzolitic spinels may be a partial melting effect (Roberts, 1988).

The large volume of segregated chromite may be due to the supra-subduction zone setting of the host Bela ophiolite (Roberts, 1988), which may have formed in marginal basin environments (Ahmed, 1991).

The segregated chromites are mostly high-Cr type; but at least one mine in the western part of the outcrop, with nodular ore contains high-Al chromite.The latter is compositionally similar to the chromite from the present day abyssal peridotites. The high-Al chromite is restricted in occurrence relative to the high-Cr chromite; and occurs in a spatially distant and tectonically separated area from the area of high-Cr chromite. The high-Al chromites may reflect the primary melt composition and degree of partial melting for the mid-ocean ridge and marginal basin environments suggested by Dietrich et al. (1981).

The reciprocal variation in Cr-Al is a common feature of chrome ores and has been explained variously by different workers.

According to Rammlmair (1986), chromite ore of the central Palawan ophiolite, Phillipines, show increasing Cr # with depth in the ophiolite sequence.

At Kempirsaisky massif, USSR, the high-Cr chromitite occurs in another uplift part, away from the high-Al chromitite bodies. In the SE part of Kempirsaisky massif, USSR, the chromitites contain high-Al, low-Cr chromite. Their enclosing rocks also possess chromite with high-Al content. Moreover, the dunites contain chromite with higher Al and lower Cr than the harzburgites and troctolites. This indicates a syngenetic origin of chromitites and surrounding ultramafic rocks (Kravchencko & Grigoryeva, 1986). The high-Cr chromites in the SE part of the massif show, within individual bodies, higher-Cr and Mg chromite developed in their central parts with higher modal chromite and more constant grain size than their peripheral parts, with lesser modal chromite, and finer inequigranular ore.

In Yugoslavia, high-Cr and Mg chromites are associated with tectonites where dunites are abundant (in part with the transition zone in southern ophiolite belt) (Jankovic, 1986). The high-Al chromites occur in dunites within tectonites and / or cumulates near to gabbro contact or gabbroic differentiates where lherzolites and pyroxenites are abundant and dunites rarer.

At the Brezovica deposit, Sara Mountain, Yugoslavia, (Obradovic, 1986) Cr_2O_3 content is lower and Al_2O_3 higher in chromites from pyroxenites than in those from dunites. The chemistry of chromites does not depend on the distance from the cumulate level; but on the concentration of chromite. MgO decreases and FeO increases successively from massive, to banded to nodular and onto disseminated and poorly impregnated chromitites, and to accessory chromites in which FeO content is about twice as high as MgO.

In the chrome ores from Albanide ophiolites (Cina et al., 1986) , Mg / Fe^{2+} decreases from denser ores to banded and to accessory chromite. Cr # decreases from chromitites to accessory chromites, because of early separation.

The ophiolitic chrome deposits of Greece are divisible into an eastern belt with high-Cr chromite and cumulate sequence in the order olivine- clinopyroxene- orthopyroxene- plagioclase. (gabbronorite type) and a western belt with high-Al chromite and cumulate sequence in the order olivine - clinopyroxene - plagioclase (troctolite type).

In the Troodos ophiolite deposits of alpine type, Panayiotou et al. (1986) noticed composition of accessory chromite characterizes the rock types although there is considerable overlap in their fields.

The experimental work (Irvine, 1967) shows that the high-Al chromites are more likely to develop under higher pressures than high-Cr chromites, assuming a constancy in the bulk composition of the deposits.

In Oman, the chromitites within 100-200 m of gabbro contact are high-Cr chromites whereas the deposits within the lower parts of the metamorphic peridotite are high-Al chromites (Coleman, 1977).

Dick & Bullen (1984) divided the ophiolitic peridotites into three types on the basis of spinel composition. The variation of chromian spinels from the three ophiolite types is shown in Fig.5. The range of Cr # shown by the spinel peridotitic rocks of Khuzdar District not only span the range of Type I peridotites (< 0.6) of Dick & Bullen (1984) but also extends far higher. Thus , the Cr # of Bela chromites does not resemble that from the mid-ocean ridge ophiolites, abyssal peridotites and basalts. The Cr# range is similar to the Type II alpine peridotites of Dick & Bullen (1984), which include peridotites of Bay of Islands, Josephine, New Caledonia and Semail. This appears to preclude a mid-ocean ridge origin for the peridotitic rocks of Khuzdar which seem to represent a composite complex with possibly a multistage melting history in which the degree of partial fusion and melt removal varied greatly.

The Cr # in alpine peridotites as well as abyssal peridotites decreases with increasing Mg #, i.e., the ratio Mg / (Mg + Fe^{2+}), (Thayer, 1970; Dick & Bullen, 1984).

In the Khuzdar District samples, the trend of decreasing Cr # with increasing Mg # is observed for the spinel compositions with Cr # < 65. In chromites with higher Cr #, the trend is changed and displays a sympathetic increase in Cr # and Mg #. The samples which show this trend include majority of the analyzed chromitites in addition to the pyroxenite and basalt samples. The increased Mg # may be partly a reflection of higher Mg # of segregated chromites compared to that of the accessory chromites, shown by Sakhakot-Qila ophiolite (Ahmed, 1984), or Josephine peridotite (Dick & Bullen, 1984).

Low TiO_2 is a characteristic of chromite from ophiolites. Cumulates of higher levels are richer in Fe_2O_3 and TiO_2 (e.g., Pallister & Hopson, 1981) while residual spinels usually have very low TiO_2.

Fig. 6 shows a plot of Fe^{2+}/Mg versus weight percent TiO_2 drawn after Dickey (1975). Low values of both parameters are noticeable but typical trends of podiform or stratiform types are not obvious. The accessory chromites plot in separate field from the segregated chromites, except the chromite from basalt.

According to Sarwar (1992), the tectonic setting of the Bela ophiolite was that of an oceanic fracture zone which formed as a leaky transform during Cretaceous in the Tethyan basin along the western margin of the Indian plate, and was destroyed in Paleocene - early Eocene by processes of plate reorganization, oblique convergence and ophiolitic obduction. The variation in the chromite chemistry observed in the present study does not agree with this model as the fracture zone chromites would plot differently in the spinel prism (cf. Dick & Bullen, 1984; Kimball, 1990).

In the Zambales ophiolite, high-Cr ores of Acoje area are regarded as the initial stage, IAT-type ore; while Coto area contains high-Al ores of more advanced BABB stage, with MORB affinities. The dying rift of this basin is shown by the Palawan ophiolite (as noted above) and has both IAT and MORB affinities. The chromite chemistry has also been related to the degree of the partial melting and the tectonic setting. The high-Al chromite is present in the Coto block formed by 15-25 % partial melting (Hawkins & Evans, 1983). The Acoje block with higher Cr but high total Fe-bearing chromite, is formed by 35-45 % partial melting of a partly depleted mantle. For the Palawan ophiolite, > 50 % partial melting of primordial mantle is assumed to produce low total Fe, high-Cr chromite.

The problem of the origin of chromite is not yet unequivocally settled. It has been suggested that chrome ores in ophiolites may have formed in several ways and not under calm conditions. For example, in the Albanides ophiolites, Cina et al. (1986) suggest that scarce refractory chromite formed from only slight melting of more primitive upper mantle. In the tectonite harzburgite-dunite sequences, chromite forms by crystallization of accumulated ore melts fused from upper mantle. Some podiform deposits undergo plastic deformation to form pressed platy bodies which may be folded. The cumulate sequence contains deposits formed by stratiform type fractional crystallization. Some deposits in the transition zone may have features of both stratiform and podiform deposits. Later injection of ore melt is also evidenced, e.g., cementation of pyroxene by chromite (Cina et al., 1986).

Chromian spinel is very rare in basalts. In the mid-ocean ridge basalts, it may make upto 0.5 % by volume; and seems to be restricted to the most primitive olivine - rich basalts with picritic character and other Cr-rich primitive melts with high $Mg/(Mg+Fe^{2+})$ ratios which have not undergone significant magmatic fractionation (Pober & Fauple, 1988). The MORB spinels have higher Mg # than those of the mantle peridotites and cumulate rocks of ophiolites. This may be probably due to rapid cooling of basalts. The higher Mg # of the basalt sample in Fig. 4 probably represents its initial Mg/Fe ratio, less affected by later reequilibration.

CONCLUSIONS

Bela ophiolite is a site for abundant podiform type chrome ore. The chromite chemistry resembles that shown by podiform chromites of ophiolites in many respects such as reciprocal Cr-Al variation, bimodal Cr-Al distribution, low TiO_2 content and less variable and below 20% total iron content. The accessory chromites are consistently Fe-richer and Mg-poorer compared to the associated segregated chromites. In terms of the ophiolitic types of Dick & Bullen (1984), the chromite compositions span a range known from the type II (transitional) ophiolites which represent multistage melting histories under conditions different from those existing beneath mid-ocean ridges, as well as island arcs. This agrees with the idea that the Bela ophiolite does not represent a section of the main Tethyan oceanic crust; but is made of fragments from the crust of a marginal basin. The presence of deep sea sediments overlying basalts of the Bela ophiolite such as the Fe– and Mn– rich cherts, mudstones, shales and limestones may be due to a marginal basin.

The chromite found in a basalt sample is high in Cr and Mg. It seems to represent a composition of its initial crystallization little affected by reequilibration. On the spinel prism, it does not plot in the known fields of abyssal basalts and plateau basalts of ocean basins.

REFERENCES

AHMED, Z. (1984) Stratigraphic and textural variations in the chromite composition of the ophiolitic Sakhakot-Qila complex, Pakistan. Econ. Geol. **79,** (6), pp. 1334-1359.

_______ (1986) Ophiolites and chromite deposits of Pakistan. *In*: Petraschek, W., Karamata, S., Karavchenko, G.G., Johan, Z., Economou,M. & Engin, T. (eds.) Chromites, UNESCO's IGCP 197 Project, Metallogeny of Ophiolites. Theophrastus Publications, Greece, pp. 241-262.

_______ (1991) Basalt geochemistry and the supra-subduction zone origin of the Bela ophiolite, Pakistan. Acta Mineralogica Pakistanica **5,** pp. 83-98.

_______ **& HALL, A.** (1981)Alteration of chromite from the Sakhakot-Qila ultramafic complex, Pakistan. Chemie der Erde **40,** pp. 209-239.

CASSARD, D., NICOLAS, A., RABINOVITCH, M., MOUTTE, J., LEBLANC,M. & PRINZHOFER, A. (1981) Structural classification of chromite pods in Southern New Caledonia. Econ. Geol. **76,** pp. 805-831.

COLEMAN, R.G. (1977) OPHIOLITES —— ANCIENT OCEANIC LITHOSPHERE? Springer-Verlag, Berlin. pp. 130-134.

DICK, H.J.B. & BULLEN, T. (1984) Chromian spinel as a petrogenetic indicator in abyssal and alpine type peridotites and spatially associated lavas. Contrib. Mineral. Petrol. **86,** pp. 5-76.

DICKEY JR., J.R. (1975) A hypothesis for origin of podiform chromite deposits. Geochim. Cosmochim. Acta **39,** pp. 1061-1075.

_______ **& YODER JR., H.S.** (1972) Partitioning of chromium and aluminium between clinopyroxene and spinel. Carnegie Inst. Wash. Yearb. **71,** pp. 384-392.

DIETRICH,V. OBERHANSLI,R. & MERCOLLI, I. (1981) A new occurrence of boninite from the ophiolitic melange in the Pindus-Sub-pelagonian zone S.L. (Aegina island, Saronic gulf, Greece). Ofioliti **12,** pp. 83-90.

GARTZOS, E. MIGIROS, G. & PARCHARIDIS, I. (1990) Chromite from ultramafic rocks of northern Evia (Greece) and their geotectonic significance. Schweiz. Mineral. Petrogr. Mitt. **70,** pp. 301-307.

HAWKINS, J.W. & EVANS, C.A. (1983) Geology of Zambales Range, Luzon, Phillipine Islands: Ophiolite derived from an island arc-back arc basin pair. *In*: Hayes, D.E. (ed.) AGU, Washington, D.C., Geophys. Monogr. Ser. **27,** pp. 95-123.

HUNTING SURVEY CORPORATION LIMITED (1960) RECONNAISSANCE GEOLOGY OF PART OF WEST PAKISTAN. A Colombo Plan Cooperative Project, Government of Canada, Toronto. 550 p.

IRVINE, T.N. (1965) Chromian spinel as a petrogenetic indicator : Part 1, Theory. Can. J. Earth Sci. **2,** pp. 648-672.

_______ (1967) Chromian spinel as a petrogenetic indicator: Part 2, Petrologic applications. Can. J. Earth Sci. **4,** pp. 71-103.

JACKSON, E.D. (1969) Chemical variations in coexisting chromite and olivine in chromite zones of the Stillwater complex. Econ. Geol. Monog. **4,** pp. 41-71.

_______ **& THAYER, T.P.** (1972) Some criteria for distinguishing between stratiform, concentric and alpine peridotite-gabbro complexes. 24th Internat. Geol. Congr. Montreal, Section **2,** pp. 289-296.

KIMBALL, K.L. (1990) Effects of hydrothermal alteration on the composition of chromian spinels. Contrib. Mineral. Petrol. **105,** pp. 337-346.

MALPAS, J. & STRONG, D.F. (1975) A comparison of chrome spinels in ophiolites and mantle diapirs of Newfoundland. Geochim. Cosmochim. Acta **39,** pp. 104-1060.

POBER, E. & FAUPL, P. (1988) The chemistry of detrital chromian spinels and its implications for the geodynamic evolution of the Eastern Alps. Geologische Rundschau **77,** (3), pp. 641-670.

ROBERTS, S. (1988) Ophiolite chromitite formation: a marginal basin phenomenon? Econ. Geol. **83,** pp. 1034-1036.

ROCK, N.M.S. & CARROLL, G.W. (1990) A general-purpose mineral recalculation and tabulation program for Macintosh microcomputers. Am. Mineral. **75,** pp. 424-430.

STEVENS, R.E. (1944) Composition of some chromites of the Western Hemisphere. Am. Mineral. **29,** pp. 1-34.

THAYER, T.P. (1964) Principal features and origin of podiform chromite deposits and some observations on the Guleman-Soridag district, Turkey. Econ. Geol. **59,** pp. 1497-1524.

_______ (1969) Gravity differentiation and magmatic reemplacement of podiform chromite deposits. Econ. Geol. Monog. **4,** pp. 132-146.

_______ (1970) Chromite segregations as petrogenetic indicators. Geol. Soc. South Afr. Spec. Publ. **1,** pp. 380-390.

ZHOU, M. - F. & KERRICH, R. (1992) Morphology and composition of chromite in komatiites from the Belingwe greenstone belt, Zimbabwe. Can. Mineral. **30,** pp. 303-317.

Manuscript received October 20, 1992; accepted for publication December 10, 1992.

ACTA MINERALOGICA PAKISTANICA
VOLUME 6 (1992) PP. 21-29.

ISOTOPE COMPOSITION OF LEAD IN GALENAS FROM THE DUDDAR AND KHARRARI ZINC-LEAD-BARITE ORE BODIES, LASBELA DISTRICT OF BALOCHISTAN PROVINCE, PAKISTAN.

ARSHAD M. BHUTTA
Geological Survey of Pakistan, 68-D, Model Town, Lahore.

ABSTRACT : Ore samples, containing galena, from the Duddar North, Kharrari North and Kharrari South ore bodies of the Duddar area were analyzed to determine the isotopic composition of lead. Duddar and Kharrari Zn-Pb-Ba ore bodies are located on the southernmost part of the Lasbela-Khuzdar metallogenic belt in Balochistan Province. A series of such deposits are present within a sequence of shallow marine carbonate and terrigenous clasts belonging to the Shirinab Formation. The Shirinab Formation, divisible into three members, is predominantly composed of limestone, shale and sandstone of lower to middle Jurassic age. These miogeosynclinal continental-shelf type deposits are exposed on the western edge of the Indo-Pakistani plate represented by the Axial Belt. Sphalerite and galena are the principal ore minerals, and marcasite and pyrite are the principal sulphide gangue minerals present in the ore bodies.

The isotopic compositions of lead in galena from the Duddar deposits were determined by Teledyne Isotopes (New Jersey, USA) using triple filament solid sample thermal ionization mass spectrometry. A standard sample of known lead isotopic value was used for reliable analytical accuracy. The lead isotopic values showed a general consistency in atomic percentage values. The ^{204}Pb atomic percentage values match exactly, whereas slight variations exist in the ^{206}Pb, ^{207}Pb and ^{208}Pb atomic percentage values and yield a nearly constant set of ratios. The isotopic ratios of the lead in galena of the area vary between 18.475–18.487, 15.663–15.703 and 38.674–38.724 for ^{206}Pb/^{204}Pb, ^{207}Pb/^{204}Pb, and ^{208}Pb/^{204}Pb, respectively. These isotopic fractions when compared with the single stage growth curves by Holmes (1946) and Houtermans (1946) and two stage growth curves by Stacey & Kramers (1975) and others indicate that the modern model ages range from 150-175 m.y. for the leads incorporated in the Duddar ores. These modern ages suggest that the lead present in the Duddar ores is one of the youngest leads.

INTRODUCTION

A series of lead-zinc-barite occurrences are found in a narrow, northerly trending, metallogenic zone in the Bela-Khuzdar region of the eastern part of Balochistan province (Fig. 1a). The most significant deposits discovered to-date are : Gunga, Surmai, Malkhore and Sekhran in the Khuzdar area; and Duddar, exposed on the eastern flank of the Mor Range in the southernmost part of the Axial Belt (Fig. 1a, b). The Duddar deposits (latitude 26° 5' N and longitude 66° 55' E) consist of the Duddar North, Duddar South, Kharrari North and Kharrari South (Fig. 1c) bodies.

The mineralization occurs within a sequence of shallow, marine carbonate and clastic sediments belonging to the Shirinab Formation of lower-middle Jurassic age. The Shirinab Formation contains three distinct lithologic units and is predominantly composed of limestone, shale, sandstone and minor siltstone. Sphalerite, and galena are the principal ore minerals whereas marcasite and pyrite are the abundant gangue minerals. Barite, is widely exposed in Duddar ore bodies.

The source of the metalliferous brines and the time of mineralization and isotopic signatures of the ores are unknown because

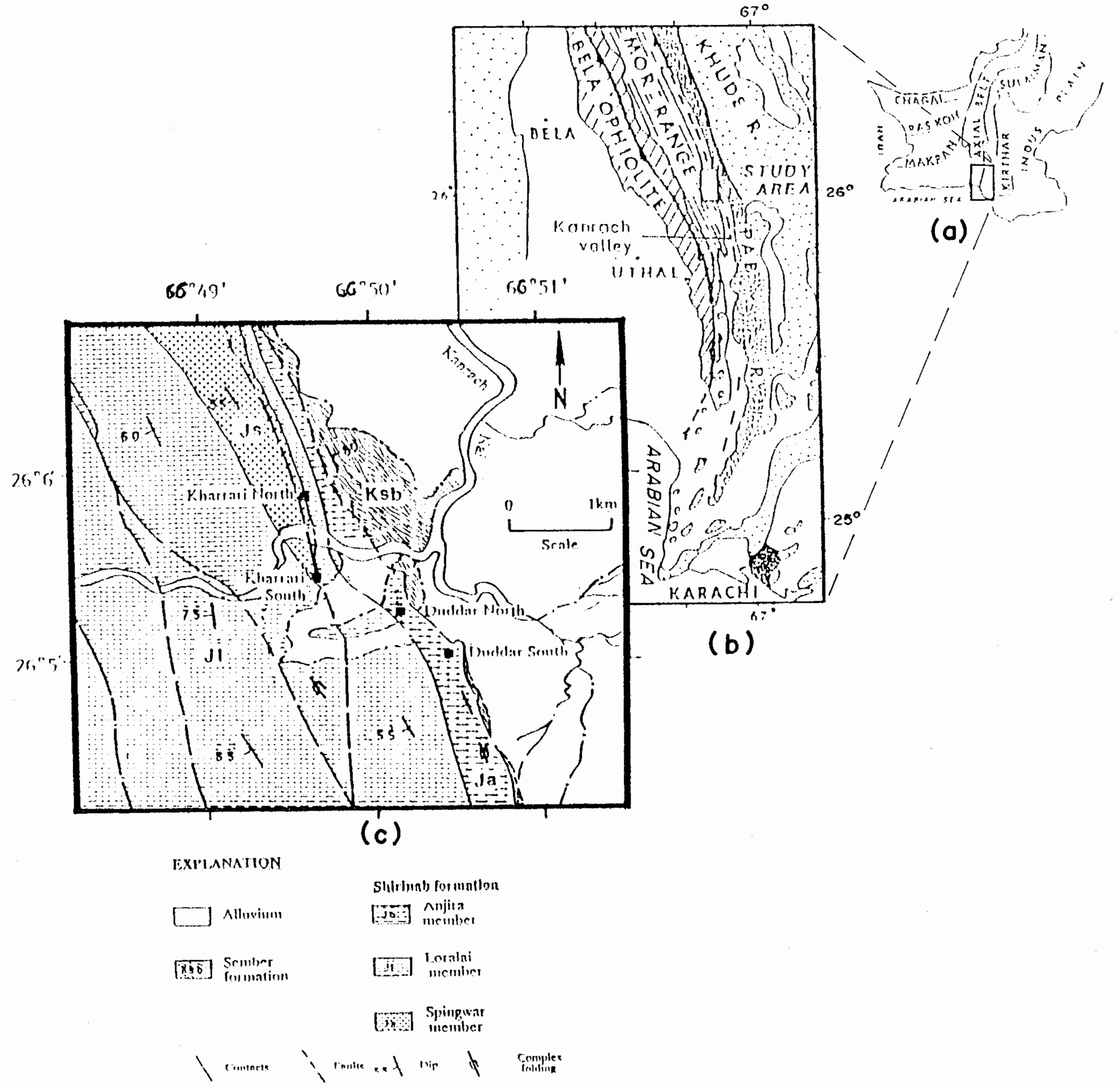

Fig. 1. Index map showing the location of the study area: (a) In the southern part of Axial Belt, south-eastern Balochistan; and, (b) On the eastern flank of Mor Range (small rectangle). (c) Regional geological map showing the relative positions of Duddar North, South, Kharrari North and South ore bodies.

of the lack of any previous isotopic data for the area.

GEOLOGICAL FRAMEWORK

A number of lead-zinc-barite deposits are present in the Mesozoic carbonates and terrigenous clastics widely distributed in the norrow northerly-trending Lasbela-Khuzdar metallogenic zone. These miogeosynclinal sediments are related to an early phase of Balochistan geosynclinal development ern (Shcheglov, 1969) and were deposited along the northwestern continental margin of the Indo-Pakistani shield from early Mesozoic to late Paleogene. The rocks are predominantly composed of reefoid, oolitic, pisolitic limestone with quartzose sandstone and shale. These are characteristic of shallow marine environments which are typical of platform type environment of early epicontinental seas (Jankovic, 1983). The continuation of the marine conditions enhanced the deposition of the carbonate sediments from early Jurassic through mid-Jurassic producing the rocks of the Shirinab Formation which are extensively exposed in the region.

The Shirinab Formation is divisible (Shah 1977) into the following three distinct lithostratigraphic units : (1) Spingwar member (lower), (2) Loralai member (middle) and (3) Anjira member (upper) (Fig. lc); briefly described below.

Spingwar member (Js) :Light brown to rusty brown on weathering, thinly-bedded, well-laminated, orthoquartzitic, ferruginous sandstone with intercalated thin-bedded calcareous shales.

Loralai member (Jl) :Dark grey, medium-to thick-bedded, massive fine-grained, argillaceous, mottled, fossiliferous with interlayered shales.

Anjira member (Ja) : Alternating sequence of thin-bedded, olive grey to dark grey, fine-grained, sublithographic limestone and splintery shales.

The Mesozoic shallow marine continental-shelf type carbonate and clastic sediments belonging to Shirinab Formation are the host rocks for the zinc-lead-barite mineralization in the area (Fig. lc). They are monotonously exposed in the rugged elevated terrain of the Mor range, on the eastern flank of which the study area lies (Fig. lb), and extend northward until they terminate in the Khuzdar Knot.

The top of the Shirinab Formation is marked by a post-Bajocian unconformity which resulted from a temporary emergence at the end of mid-Jurassic. The area was resubmerged from late Jurassic to early Cretaceous causing the deposition of the shaly and silty Sember formation (Ksb) (Fig. lc) which constitutes the outer eastern part of the Mor Range. The Bela ophiolites, emplaced during Paleocene, lie west of Mor Range marking a tectonically sheared oblique crush zone. The Jurassic - Cretaceous sequence generally has a north - south strike with moderate to steep dips.

The regional tectonics and close proximity to the thrust boundary, the Chaman and Ornach-Nal fault systems, which originated from the collision of the Indo-Pakistan and Eurasian plates, have subjected the area to great structural complexities. The initial tectonic phases, resulting from the collision of the converging plates developed early folding and thrusting; the later tectonic pulses caused thrusting and refolding of the pre-existing structures. the north-west trending thrust faults, strike-slip faults and vertical faults are all nearly parallel to the regional tectonic boundaries.

DUDDAR AND KHARRARI ORE BODIES

The ore bodies of the Duddar area alongwith many other lead, zinc, and barite deposits compose the Lasbela-Khuzdar metallogenic belt, which is a segment of the oroclinal Axial Belt.

The Duddar North is the most promising ore body of all these four ore bodies. It has a NW trend, about 285 m long and 35 m wide, and is enclosed within the steeply eastward dipping rocks of the Anjira member of the Shirinab Formation. The Duddar South, separated from the Duddar North by 370 m wide stretch of alluvium, is about 265 m long and 30 m wide and has the same NW trend. The development of a dard black to orange silicified gossan over the Duddar South ore body is a distinguishing feature. The Kharrari South ore body is located 0.65 km north of the Duddar North ore body. The Kharrari North ore body is separated by the 185 m wide Kharrari Nai (Nai = stream) from the Kharrari South ore body. Both the Kharrari ore bodies are located in rough terrain of moderate to steep north-trending linear ridges and narrow valleys.

Host Rocks and Mineralization

In the Duddar North and Duddar South ore bodies the mineralization is restricted to the alternating sequence of thin-bedded, fine-grained limestone and calcareous, splintery shales of the Anjira member (Bhutta, 1991). The mineralization of the Kharrari South is found in the thick-bedded to massive limestone of the Loralai member and the orthoquartzitic thinly-bedded sandstone of the Spingwar member. The mineralization of the Kharrari North is hosted by the Loralai and the Spingwar members which are the northward extensions of the same lithologies from the Kharrari South.

The observed structural deformation in the Duddar North is reflected by severe faults, fractures and folds present in the ore body and the adjoining rocks (Bhutta, 1991). A vertical northwest-trending fault, following the bedding attitude has sheared the carbonaceous and other contact rocks. Barite exposed in the open pit mines shows mostly tight asymmetrical folds which commonly trend N 45°W, plunging 45°-65° NW. The structural deformation is less pronounced in the Duddar South where faults and folds are minor. The structures in the Kharrari ore bodies are more strongly developed than those in the Duddar ore bodies. The structural components comprise the thrust faults, strike-slip faults, fractures, shear zones and narrow folds.

Sphalerite and galena are the principal ore minerals and marcasite and pyrite are the principal sulphide gangue minerals associated with the Duddar deposits. Barite is mineralized in various morphological forms and patterns in all the ore bodies and is abundantly exposed in the Duddar North. Limonite, goethite, jarosite and other mixed hydrous oxides are present in the gossans and the oxide zones; rare cerussite alterations are also observed in the oxide zones. Quartz, gypsum and siderite are common in the gangue. Development of maroon to dark desert-varnished, siliceous gossans is a characteristic feature of the ore bodies. The mineralization is observed in the regular pattern, nearly concordant to the general bedding trends in the Duddar North and South, but has an irregular distribution along faults, fractures and related structural features.

GALENA SAMPLES FROM THE DUDDAR DEPOSIT

The isotopic studies of the Duddar area were carried out by isotopically analyzing lead from galena to determine the isotopic composition of lead present in galena. The galena is occasionally exposed as coarse crystals on the surface, in gossans, or in veins in the Duddar ore bodies. Three samples containing crystalline galena, one each from the Duddar North, Kharrari North and Kharrari South ore bodies, were collected and analyzed. The host rock lithology, mineralogy and locations of these galena samples are shown in Table 1. A galena sample from the Bleiberg mine in Austria was analyzed as a standard sample alongwith these samples.

Sample AB-258 (Kharrari Ore Body)

Sample AB-258 was collected from the ferruginous zone exposed in a small anticlinal structure in the Spingwar member of the Shirinab Formation of the Kharrari North body. The galena crystals, are associated with weathered and oxidized barite in a 0.5 cm thick vein. The galena-bearing barite exhibits deeply leached cavities (after sulphides) marked with yellowish brown and maroon oxides. Finely developed boxwork, commonly of cubic shape signifying leaching of pyrite/marcasite, are frequently developed. A cellular texture with calcite, gypsum, altered oxides and sulphides prevails extensively. Hematite in fine clusters and mixed with gypsiferous flakes and veins is common.

Sample AB-295 (Kharrari South Body)

The galena sample Ab-295 was collected from the Loralai member of the Shirinab Formation. The dard grey, medium-bedded limestone with minor shales is extensively fractured and is poorly exposed under the veneer of colluvial fragments. The rare crystals of galena are associated with extensively weathered barite in the limestone. Hematite veinlets and small globules on the oxidized surface are observed.

Sample AB-269 (Duddar North Body)

The galena sample AB-269 was collected

Table 1. Mineralogy, host rock lithology and description of the galena samples, used for isotopic analyses, from the Duddar area.

S.No.	Location	Host Rocks	Host Sequence	Mineralogy	Sample Description
AB-258	Kharrari North	Thin-medium bedded sandstone, minor shale.	Spingwar member; Shirinab Formation.	Galena, barite, oxides, gypsum.	Crystalline galena in vein in barite having leached cavities
AB-295	Kharrari South	Medium-thick bedded limestone, minor shale.	Loralai member; Shirinab Formation.	Galena, barite & oxides.	Crystalline galena in extensively weathered barite, limestone
AB-269	Duddar North	Medium bedded limestone, minor shale.	Loralai member; Shirinab Formation.	Galena, barite & minor oxides.	Large specks of coarse crystalline galena in unaltered limestone
SAB-4*	Bleiberg, Austria+	Green marl (Tuffs?), breccias, calcarenites	Cordevolian substage, Wetterstein carbonate. Mid-Triassic series	Galena, traces of oxides, gypsum.	Finely crystalline to massive galena

* Reference sample.

+ Brigo et al.. (1977).

from the west part of the Duddar North body. Galena is present mostly as large irregular crystals in the dark grey, medium- to thick- bedded, unweathered limestone of the Loralai member. Minor galena mineralization is associated with barite which is exposed as thin layers and veins but mostly as radiating rossets. Fracture- filled barite veins, containing galena crystals, indicate a paragenetic sequence of later precipitation of galena in barite.

LEAD ISOTOPES

Analytical Techniques

The ore samples were manually extracted and crushed into small fragments for separation of crystals of galena from the host rock. Galena was hand picked under binocular microscope.

The lead isotopic compositions of three galena specimens from these samples, were analyzed by Teledyne Isotopes (new Jersey, USA) using triple filament solid sample thermal ionization mass spectrometry. The isotopic ratios were normalized to a lead standard of National Bureau of Standards, NBS SRM-981, which was purified to 99.9% purity. Mixtures of ^{208}Pb and ^{206}Pb ratio, prepared from high-purity separated isotope, were used as comparison standards.

A sample of galena from the Bleiberg lead-zinc mine in Austria, with known isotopic values was included with the three samples from the Duddar area as a standard sample (Table 1) to control the reliability of the analytical measurements. The deposit at Bleiberg is regarded as of alpine-type or Mississippi - Valley Type (Maucher and Schneider, 1967, p.274)

Lead Isotopic Data

The lead isotopic data indicating the isotopic compositions of the leads present in the galenas from the Kharrari North,Kharrari South and Duddar North for ^{204}Pb, ^{206}Pb ^{207}Pb and ^{208}Pb in atomic percentage values is presented in Table 2. The ^{204}Pb atomic percentage values are exactly the same for all the ore bodies. However, the ^{206}Pb atomic percentage values range from 25.115 to 25.032, the ^{207}Pb atomic per centage values range from 21.207 to 21.262 and the ^{208}Pb atomic percentage values range from 52.364 to 52.432. The atomic percentage values for the standard sample (SAB-4) are also given in the Table 2.

The lead isotopic ratios, derived from the atomic percentage values of ^{206}Pb, ^{207}Pb and ^{208}Pb are shown in Table 3. The lead isotopic ratios for the area vary between 18.475 - 18.487, 15.663 - 15.703 and 38.674 - 38.724 for ^{206}Pb/ ^{204}Pb, ^{207}Pb/ ^{204}Pb and ^{208}Pb/ ^{204}Pb, respectively.

Lead Isotopic Pattern of the Duddar and Kharrari Ore Bodies

The lead isotope values are compared with various growth curves to determine the isotopic pattern and the model ages of the leads. The model ages of lead from galena of the Duddar ore deposits were estimated by comparing their isotopic values with the single-stage model of Holmes (1946) Houtermans (1946) and two-stage model by Stacey & Kramers (1975).

Comparison with a Single-Stage Model

The interpretation for the model ages for the leads from the galena of the Duddar ore bodies was done with the help of the often used Holmes-Houtermans model for single-stage common lead (Fig. 2) (Holmes, 1946; Houtermans, 1946; Faure, 1986, p. 310). This model comprises the uranogenic growth curves having μ values ranging between 8 and 10 and the isochrons and the geochron originate from the primeval lead of 4.55 b.y. The lead isotopic values of ^{207}Pb/ ^{204}Pb versus ^{206}Pb/ ^{204}Pb were plotted on this model and the data points clustered close to the intersection of the growth curve having an initial ratio of μ = 9 and the slope of the geochron as determined by Patterson (1953).

The comparison with the Holmes-Houtermans model (Fig. 2) of single-stage growth curves, for lead isotopic values of ^{207}Pb/ ^{204}Pb versus ^{206}Pb/ ^{204}Pb, yielded a model age of 150-175 m.y. i.e., late Jurassic (early Tithonian) to middle Jurassic (late Bajocian).

Comparison with a Two-Stage Model

The isotopic data from Duddar and Kharrari ore bodies was compared with the model (Fig. 3) proposed by Koppel & Grunenfelder (1979, p. 134-142), based on the two-stage growth curves by Stacey & Kramers (1975) and Cumming and Richards (1975). This model was constructed on the isotopic data derived from the various world known stratabound deposits with established isotopic values. The data points were plotted for ^{207}Pb/ ^{204}Pb versus ^{206}Pb/ ^{204}Pb and ^{208}Pb/ ^{204}Pb versus ^{206}Pb/ ^{204}Pb in this model. The plot of the isotopic values indicates model ages ranging from 150-175 m.y. characterized by two stage development. The values fall close to the fields of the Alpine-type ore depsits of Halls Peak, Australia, and the stratiform deposits of the Bathrust mines of Canada (Ostic et al., 1967, p. 259).

CONCLUSIONS

The paucity of the present isotopic data, consisting of merely one isotopic measurement for each ore body greatly hampers the precise and conclusive evaluation of the area. However, based on the single-element isotopic data of only three samples, the following conclusions are derived :

The lead isotopic values from the galenas of the Duddar area are characterized by a limited range, uniformity, and consis-

Table 2. Atomic % values of lead isotopes from the Duddar and Kharrari ore bodies.

S.No.	**Ore Body**	**^{204}Pb**	**^{206}Pb**	**^{207}Pb**	**^{208}Pb**
AB258	Kharrari North	1.354	25.015	21.262	52.369
AB295	Kharrari South	1.354	25.032	21.250	52.364
AB269	Duddar North	1.354	25.016	21.207	52.432
*SAB-4	*Bleiberg, Austria	1.356	25.006	21.288	52.350

Analyses performed by Teledyne Isotopes, Westwood, New Jersey.
* Reference Sample from Bleiberg Mine, Austria.

Table 3. Lead isotopic ratios of the Duddar and Kharrari ore bodies.

Sample #	**locality**	**^{206}Pb/^{204}Pb**	**^{207}Pb/^{204}Pb**	**^{208}Pb/^{204}Pb**
AB258	Kharrari North	18.475	15.703	38.677
AB295	Kharrari South	18.487	15.694	38.674
AB269	Duddar North	18.476	15.663	38.724
*SAB-4	*Bleiberg, Austria	18.441	15.699	28.606

* Reference sample

tency in their isotopic characters. Comparison of the isotopic ratios with the Holmes-Houtermans model (Fig. 2) and with the growth curves of Stacey-Kramers and Cumming-Richards (Fig. 3), ranks the lead present in the galenas of the Duddar area with a model age of 150-175 m.y. as one of the youngest known model ages. The isotopic values are close to the isotopic values of the Bleiberg, Austria; Halls Peak, Australia and Bathrust-Canada, but are distinctly younger.

The observed model ages of 150-175 m.y. are late Jurassic (early Tithonian) or Middle Jurassic (early Bajocian) and are contemporaneous or younger than the host rocks characterizing the ore bodies in the area.

Though the isotopically analyzed leads from galena in the area represent ores hosted in different statigraphic horizons (i.e., the Spingwar member, the Loralai member and the Anjira member) their isotopic ratios are

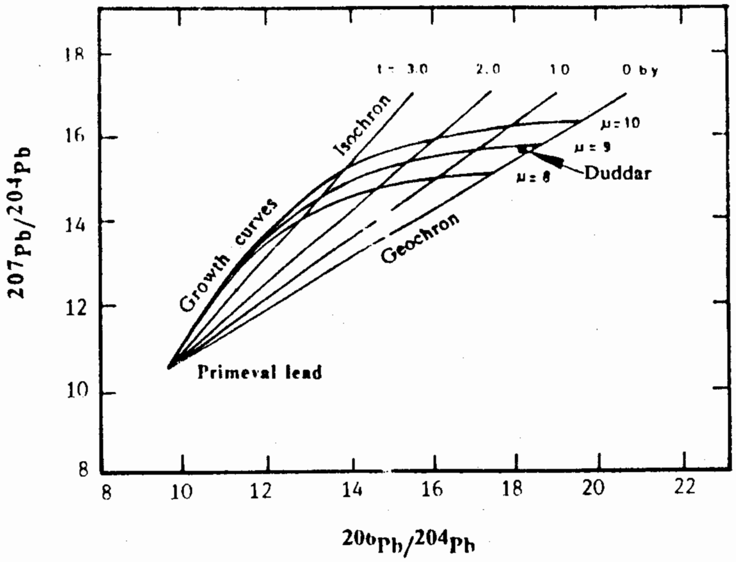

Fig. 2. The lead isotopic plot showing that values of the Duddar area fall close to the intersection of the growth curve of $^{238}U/^{204}Pb$ ratio (μ) equal to 9 and the geochron of zero value, in the Holmes-Houtermans model. The age of the Earth is taken as 4.55 b.y.

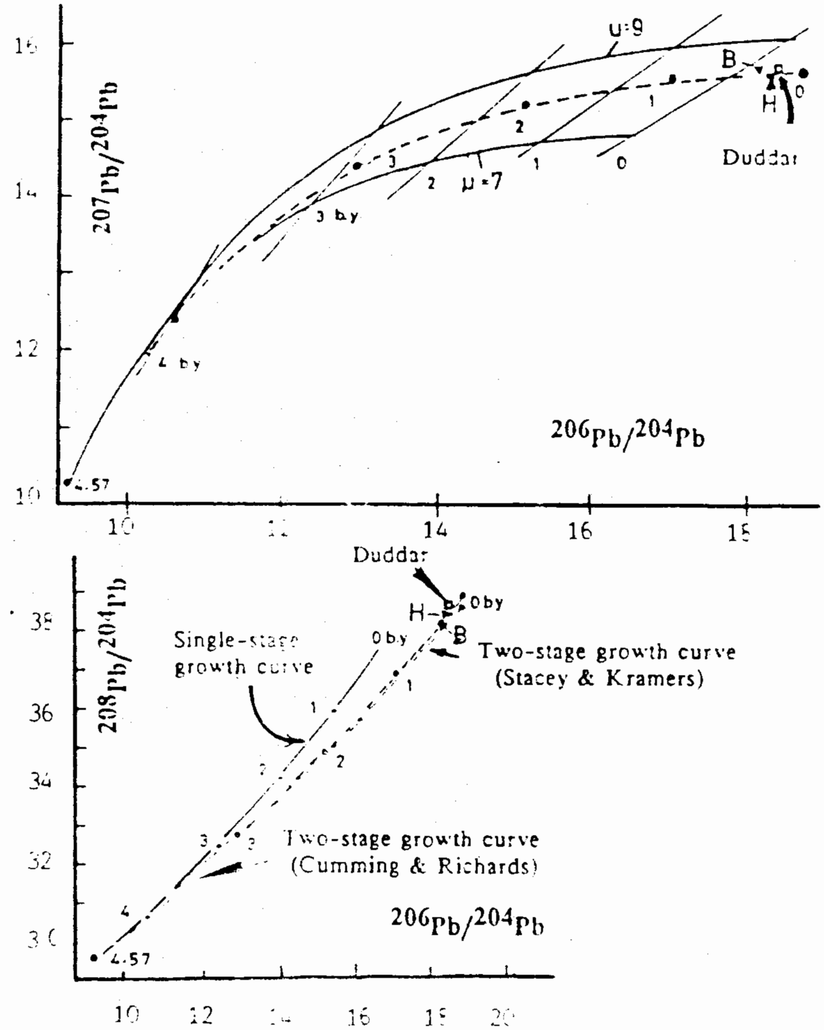

Fig. 3. The plots of the lead isotopic values of the Duddar area on the two-stage growth curves of Stacey-Kramers (1975) and Cumming-Richards (1975), shown by broken lines. Single stage growth curve is shown by the solid line.

constant. This suggests that mineralization might have come from the same source since it carries the same model age.

ACKNOWLEDGEMENTS

Thanks are due to the U.S. Agency for International Development for providing funds for the analytical work. The Natural History Museum of Smithsonian Institution in Washington is greatly acknowledged for providing one sample of galena, from the Bleiberg mine, Austria, to use as a standard sample for the isotope studies. The author is thankful to Mr. G. Sarwar Alam, Director, Geological Survey of Pakistan, for his useful comments to improve the paper.

REFERENCES

BHUTTA, A.M. (1991) Zinc -Lead-Barite mineralization in the Duddar and Kharrari Area, Lasbela District of Balochistan, Pakistan. M.S. thesis, University of South Carolina, USA.(Unpublished).

BRIGO, L., KOSTELKA, L., OMENETTO, P., SCHNEIDER, H. -J., SCHROLL, E., SCHULZ, O., STRUCL, I. (1977) Comparative reflections on four Alpine Pb-Zn Deposits. *In:* Klemm, D.D., & Schneider, H.-J. (eds.) TIME-AND STRATA-BOUND ORE DEPOSITS. pp. 273-293.

CUMMING, G.L., & RICHARDS, J.R. (1975) Ore lead isotopes ratios in a continuously changing earth. Earth Planet. Sci. Lett. **28,** pp. 155-171.

FAURE, G. (Ed.) (1986) PRINCIPLES OF ISOTOPE GEOLOGY, 2nd edition. John Wiley & Sons Inc., New York, pp.309-340.

HOLMES, A. (1946) An estimate of age of earth. Nature **157,** pp. 680-684.

HOUTERMANS, F.G. (1946) The isotopes ratios in natural lead and the age of Uranium. Naturwissenschaften **33,** pp. 185-186.

JANKOVIC, S. (1983) Exploration and preliminary evaluation of the lead-zinc-barite deposits, Lasbela-Khuzdar district, Balochistan, Pakistan. Final Report, Pak/79/026, UNDTCD/UNDP, **158** p. (Unpublished).

KOPPEL, V. & GRUNENFELDER, M. (1979) Isotopic geochemistry of lead. *In:* Jagger, E., and Hunziker. J.C. (eds.) LECTURES IN ISOTOPIC GEOLOGY, pp. 132-153.

MAUCHER, A. & SCHNEIDER, H. -J. (1967) The Alpine lead ores. Econ. Geol. Mon. **3,** pp. 71-89.

OSTIC, R.G., RUSSEL, R.D. & STANTON, R.L. (1967) Additional movements of the isotopic composition of lead from stratiform deposits. Can. J. Earth Sci. **4,** pp. 245-269.

PATTERSON, C.C. (1953) The isotopic compositions of meteoritic, basaltic and oceanic leads and the age of the Earth. Proc. 1st Conference on Nuclear Processes in Geological Setting, pp. 36-40.

SHAH, S.M.I. (ed.) (1977) STRATIGRAPHY OF PAKISTAN. Mem. Geol. Surv. Pakistan, **12,** 138 p.

SHCHEGLOV, A.D. (1969) Main features of endogenous metallogeny of the south part of West Pakistan. Mem. Geol. Surv. Pakistan, **7,** pp. 3.

STACEY, J.S. & KRAMERS, J.D. (1975) Approximation of terrestrial lead isotope evolution by a two stage model. Earth Planet. Sci. Lett. **26,** pp. 207-221.

Manuscript received on November 12, 1992; accepted for publication on December 31, 1992.

ACTA MINERALOGICA PAKISTANICA
VOLUME 6 (1992) PP. 30-36.

FIRST REPORT ON THE DISSEMINATED COPPER-NICKEL-IRON SULPHIDES AND AWARUITE FROM THE OPHIOLITIC ROCKS OF KHUZDAR DISTRICT, PAKISTAN.

ZULFIQAR AHMED
National Centre of Excellence in Mineralogy, University of Balochistan,
G.P.O. Box 43, Quetta, Pakistan.

ABSTRACT: Accessory opaque mineral assemblage comprising Cu-Ni-Fe sulphides and awaruite occurs in the Bela ophiolite; mostly in its ultramafic rocks but rarely in the mafic rocks as well. Microprobe analyses are given here for awaruite from chromitites; pentlandite from chromitites, lherzolite and wehrlite; pyrrhotite from clinopyroxenites, and chalcopyrite from clinopyroxenites and a coarse-grained dolerite. The data suggests differences between rock types due to magmatic differentiation. Ni-rich earlier paragenesis is found in olivine-rich rocks and cupriferous and ferriferous phases are developed in the later paragenesis of clinopyroxenites and some mafic rocks.

INTRODUCTION

This article is the first report on occurrence of disseminated Cu-Ni-Fe sulphides and awaruite in the rocks of Bela ophiolite in Pakistan. Similar accessory minerals are known to occur disseminated in many other ophiolites, such as the Sakhakot-Qila complex, Pakistan (Ahmed & Bevan, 1981; Ahmed & Hall, 1982), Limassol Forest plutonic complex of the Troodos ophiolite, Cyprus (Panayiotou, 1980), Samari area, Greece (Sideris et al., 1980) and the Ballantrae complex, Scotland (Stone et al., 1986).

The assemblage is generally regarded as magmatic although modification during secondary alteration, tectonism and metamorphism is observed in most cases (e.g., Panayiotou, 1980; Ahmed & Hall, 1982;). These processes may result in the modification of the phase distribution; or the enhancement of its variety by alteration (Shiga, 1987).

This study describes and attempts to explain the chemical compositional variations of the sulphides and awaruite from various rock units of the Bela ophiolite.

OCCURRENCE OF SULPHIDES AND AWARUITE

Location of rock samples from Bela ophiolite that were found to contain sulphides or awaruite are given in Table 1. These samples are from the northern part of the Bela ophiolite exposed in the Khuzdar District, and comprise mostly weakly serpentinized ultramafic rocks. Pentlandite and awaruite are present in chromitites and peridotites with possible presence of millerite in one sample. Clinopyroxenite and mafic rocks contain dominantly chalcopyrite. The sulphides and awaruite occur in disseminated forms as displayed in Fig.1.

PHASE CHEMISTRY

Method

Mineral phases in the carbon-coated polished thin sections were analyzed by the Jeol Superprobe 733 model electron probe microanalyzer, set up at the California Institute of Technology (Caltech), U.S.A. Standard procedures of wavelength dispersive technique were followed, combined with qualitative determinations on the EDS spectra.

Results

Awaruite analyses from the chromitite sample (no. Z1569) show negligible differences in composition between grains that make inclusions in chromite (analysis no. 28, Table 2) and those which occur in serpentinous areas (analysis 27, Table 2). In this sample, Ni : Fe ratio varies between 2.69 : 1 and 2.75: 1. The awaruite contains more Co than Cu. Awaruite from other chromitite samples (e.g., Z1458) shows higher Fe and lower Ni contents, but analyses are not reported because of larger uncertainty. Millerite analyses from chromitite sample Z1470 are not reported but its presence is indicated. Pentlandite occurs in ultramafic rocks only and exhibits large compositional variation. Pentlandite from the nodular chromitite sample (Z1618) is, in general, higher in Ni and Co, and lower in Fe than that in other ultramafic rocks. The clinopyroxenite sample Z1617 contains a large variety of sulphides and shows strong variation in its pentlandite shown by its Cu-rich pentlandite. It also exhibits a good development of cupriferous (chalcopyrite) and ferriferous (pyrrhotite) sulphides. One chalcopyrite is exceptionally Ni-rich (analysis 9, Table 2). However, sample Z1617 is not representative of all clinopyroxenites. The olivine-clinopyroxenite sample (Z1475) does not exhibit strong variation in sulphide composition and contains troilite as the only sulphide mineral.

Among mafic rocks, the sulphides are dominantly Cu-bearing. Thus, chalcocite is present in gabbronorite and chalcopyrite in dolerite (sample Z1583); although one exceptional analysis yielded a Co-rich pentlandite composition (analysis 11, Table 2).

Massive sulphides or sulphides of spreading-centre hydrothermal processes are not yet found in the Bela ophiolite. The basalt sample Z1715 showed rare presence of a Zn-Co phase, but is not reported here due to analytical uncertainty. Also, the chlorite schist at ophiolite contact near Sonaro showed specks with 95.4 % zinc. However, such rare unconfirmed analyses do not support the spreading-centre activity.

The crystallization of nickeliferous opaque minerals is related to olivine crystallization. Rocks deficient in olivine are depleted in Ni, e.g., clinopyroxenite, gabbronorite, dolerite, basalt, which tend to contain Cu instead of Ni.

The clinopyroxenite dyke (Z1617) contains Cu-rich pentlandite and Ni-rich chalcopyrite compositions.

The high Ni content in pyrrhotite of clinopyroxenite sample Z1617 corresponds to its magmatic activity (cf. Campbell & Ethier, 1984, Fig.2). However, this high level of Ni in pyrrhotite is not maintained in the other sample of clinopyroxenite (Z1475).

The sulphide minerals present in various rock types include awaruite, pentlandite, ?millerite, chalcopyrite, troilite, pyrrhotite, chalcocite, Co-rich and Cu-rich Fe-Ni sulphide, Ni-rich chalcopyrite, and unconfirmed Zn and Co-Zn minerals. The mineral assemblage comprises Ni-rich at the basal parts to Cu-rich towards upper parts of the ophiolitic sequence. Thus nickeliferous assemblage (awaruite, pentlandite) belongs to an earlier paragenesis and cupriferous one to the later paragenesis.

The iron sulphide in the earlier paragenesis tends to contain more Fe than S (e.g., troilite in sample no. Z1475) and in the later paragenesis contains more S than Fe (e.g., pyrrhotite in sample no. Z1617).

DISCUSSION

The samples of the Bela ophiolite do not exhibit the seafloor hydrothermal mineralization which frequently ensues at the seafloor spreading centres (e.g., Rona, 1988).

Within the igneous rock types, the copper-rich sulphides are localized towards upper levels of ophiolitic sequence, in the clinopyroxenite, gabbronorite and dolerite samples. The nickeliferous opaque minerals are localized towards lower levels of ophiolitic sequence, i.e., in the chromitite, lherzolite and wehrlite.

The clinopyroxenite sample Z1617 contains a variety of Cu-rich, Ni-rich and Fe-rich sulphides in coexistence (Tables 1 & 2). Probably there was an earlier sulphide melt with high Ni:Cu ratio which deposited sulphide by primary precipitation; and a later Cu-enriched magmatic fluid, that may have deposited sulphides by replacement.

Co-rich pentlandite is rare and occurs in the gabbronorite (sample Z1445). Similar Co-rich pentlandite is known from other occurrences (e.g., from the disseminated magmatic sulphides in the mafic metagabbro of the Thierry Mine,


A


B


C


D

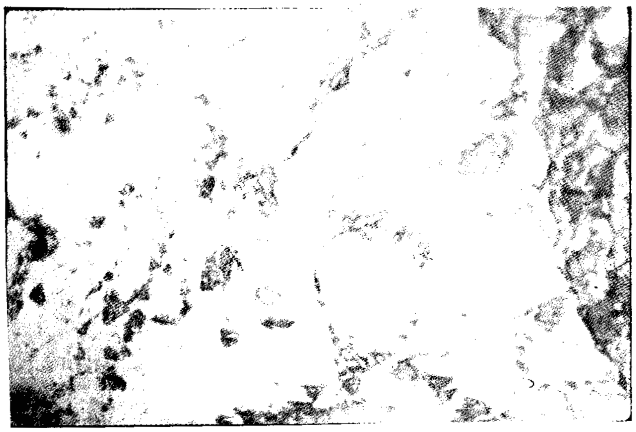
E

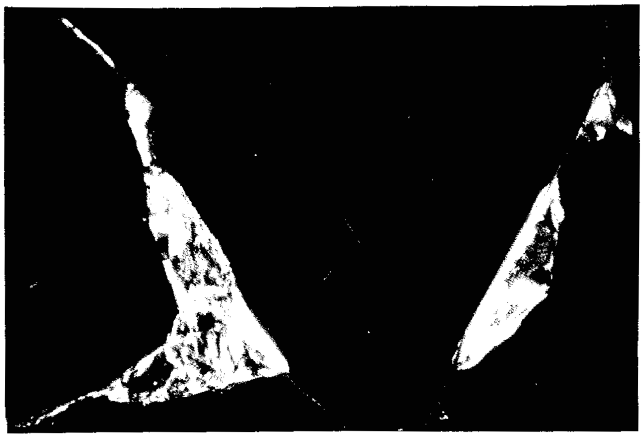
F

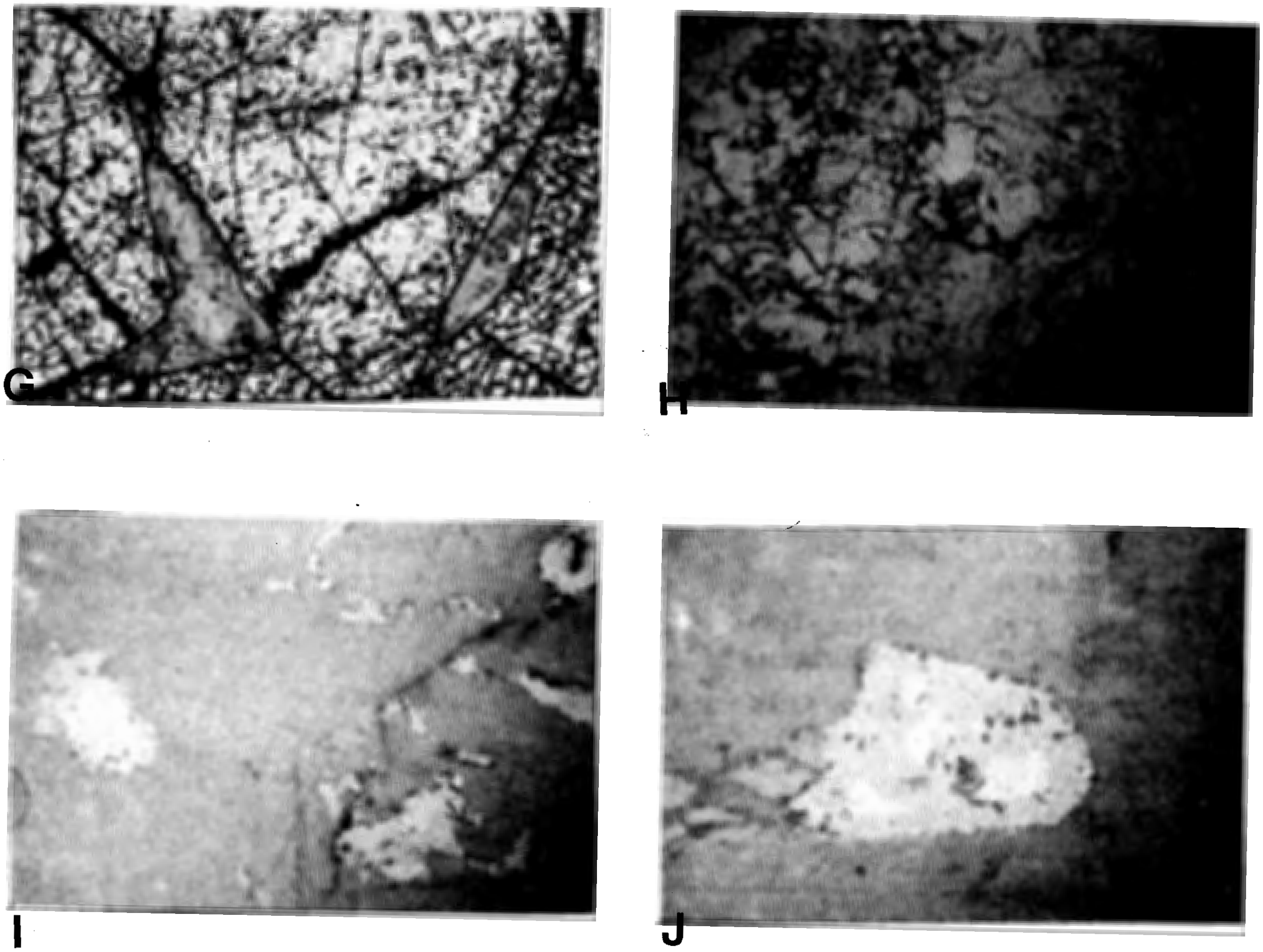

Fig. 1. Photomicrographs from polished thin sectionsof the Bela ophiolite samples listed in Table 1. **(A,B)** Reflected light views from clinopyroxenite sample (Z1617) showing anhedral chalcopyrite inside the cleaved clinopyroxene grains. **(C)** Crossed nicols transmitted light view of the same area as in **(B)** showing a larger opaque area due to alteration halo around chalcopyrite. Each of **A,B,** and **C** views measure 1.13 mm X 0.75 mm. **(D,E)** Reflected light views from clinopyroxenite (Z1617) showing high reflectance pentlandite grains with pyrrhotite intergrown in D and making a minute speck in E. Each view measures 0.23 mm X 0.15 mm. **(F)** Transmitted light view , 2.25 mm X 1.5 mm, of chromitite sample Z1458 showing flaky chlorite developed along cleavage cracks of opaque chromite. Minute dark speck in chlorite area near its contact with chromite is awaruite which shows up brighter in the reflected light view of the same area represented in **(G)**. **(H)** Reflected light view, 0.57 mm X 0.38 mm, of high reflectance pentlandite in lherzolite sample Z1390. **(I,J)** Reflected light views, each 0.23 mm X 0.15 mm, from wehrlite sample (Z1534), showing brighter pentlandite remnants inside magnetite.

Table 1. Location and description of ophiolitic rock samples. All chromitite samples are collected from mine faces.

Sample No.	Latitude & Longitude	Locality	Rock Name	Minerals Examined
Z 1715	26° 30' 50" N; 66° 24' 22" E.	Haji Mohammad Khan Bent.	Basalt	? Co-Zn mineral
Z 1583	26° 35' 29" N; 66° 19' 48" E.	Hund Jhal	Coarse dolerite.	Chalcopyrite
Z 1445	28° 12' 12" N; 66° 21' 2" E.	S.E. of Purwait Bhut	Gabbronorite lens in serpentinite.	Chalcocite, Co-rich pentlandite
Z 1617	26° 38' 58" N; 66° 15' 1" E.	Near Mari, upstream Bore Jhal (stream).	Clinopyroxenite dyke in harzburgite	Pyrrhotite-chalcopyrite, chalcopyrite, Ni-rich chalcopyrite, Cu-rich pentlandite.
Z 1475	27° 1' 13" N; 66° 20' 13" E.	Pahar Khan Bidrang.	Olivine clinopyroxenite dyke.	Troilite (inclusions in clinopyroxene)
Z 1534	26° 31' 54" N; 66° 22' 44" E.	Kohan Jhal.	Wehrlite.	Pentlandite.
Z 1390	26° 58' 2" N; 66° 17' 56" E.	Near Hinar Trikki, in Lak Baran area.	Lherzolite.	Pentlandite.
Z 1569	27° 48' 4" N; 66° 8' 29" E.	Upstream Karku Jhal (stream).	Chromitite.	Awaruite.
Z 1458	27° 12' 5" N; 66° 18' 24" E.	Pahar Khan Bidrang	Chromitite.	Awaruite.
Z 1470	26° 59' 52" N; 66° 18' 7" E.	Lak Baran.	Chromitite.	? Millerite.
Z 1618	26° 38' 57" N; 66° 15' 1" E.	Near Mari peak, upstream Bora Jhal.	Nodular chromitite.	Pentlandite.

NW Ontario as described by Patterson & Watkinson, 1984).

The Co-rich pentlandite with 12.08 to 43.50 atomic percent cobalt without systematic stoichiometric relation, is known to occur in the upper zone of western Bushveld complex, South Africa (Merkle & Von Gruenewaldt, 1986). This was explained by Ni depletion due to olivine crystallization which resulted in high Co/Ni ratio in the sulphide melt.

The rarity of sulphides is generally limited in unaltered ultramafic rocks and typically comprises pyrrhotite, pentlandite and chalcopyrite. A much larger variety of minerals is observed with greater serpentinization and talc-carbonate alteration (e.g., Shiga, 1987).

The sulphide assemblage from Bela rocks is similar to that found in relatively less altered ultramafic rocks generally, i.e., pyrrhotite -pentlandite- chalcopyrite.

CONCLUSIONS

Accessory opaque mineral assemblage comprising Cu-Ni-Fe sulphides and awaruite occurs widely distributed in the Bela ophiolite. Such minerals and their chemical compositions exhibit

Table 2. Analysis of Sulphides awaruite from Bela ophiolite

Anal. No.	**1**	**2**	**3**	**4**	**5**	**6**	**7**	**8**	**9**	**10**	**11**	**12**	**13**	**14**
Sp.No.	Z 1617	Z 1475	Z 1445	Z 1617	Z 1617	Z 1617	Z 1583	Z 1617	Z 1617	Z 1617	Z 1617	Z 1445	Z 1617	Z 1617
S	36.74	35.92	21.32	32.55	34.28	34.47	34.42	33.74	34.07	33.01	33.54	31.41	33.32	33.21
Cu	0.19	0.01	76.65	33.48	35.59	34.52	34.96	24.83	30.85	8.13	11.59	1.74	0.19	1.25
Fe	63.86	64.21	0.91	32.84	32.24	31.72	31.78	32.14	31.95	34.67	34.28	20.51	36.58	36.88
Ni	0.36	0.07	0.00	0.16	0.05	0.07	0.00	8.32	3.28	25.32	21.96	32.08	31.04	30.53
Co	0.02	0.03	0.00	0.06	0.00	0.05	0.06	0.12	0.03	0.23	0.28	13.58	0.43	0.28
Zn	0.00	0.17	0.00	0.03	0.02	0.03	0.04	0.02	0.02	0.00	0.03	0.00	0.02	0.00
Total	101.17	100.41	98.88	99.12	102.18	100.86	101.26	99.17	100.20	101.43	101.68	99.32	101.58	102.15
Atomic Percents:														
S	49.85	49.26	35.23	47.57	48.43	49.12	48.92	48.66	48.82	46.51	47.09	45.54	46.53	46.23
Cu	0.13	0.01	63.91	24.69	25.37	24.82	25.07	18.07	22.30	5.78	8.21	1.27	0.13	0.88
Fe	49.74	50.55	0.86	27.55	26.15	25.95	25.93	26.61	26.28	28.04	27.63	17.07	29.32	29.47
Ni	0.27	0.05	0.00	0.13	0.04	0.05	0.00	6.56	2.57	19.49	16.84	25.41	23.68	23.21
Co	0.01	0.02	0.00	0.04	0.00	0.04	0.05	0.09	0.02	0.18	0.21	10.71	0.33	0.21
Zn	0.00	0.11	0.00	0.02	0.01	0.02	0.03	0.01	0.01	0.00	0.02	0.00	0.01	0.00

Anal. No.	**15**	**16**	**17**	**18**	**19**	**20**	**21**	**22**	**23**	**24**	**25**	**26**	**27**	**28**
Sp.No.	Z 1617	Z 1617	Z 1617	Z 1534	Z 1390	Z 1390	Z 1390	Z 1390	Z 1618	Z 1618	Z 1618	Z 1618	Z 1569	Z 1569
S	33.12	33.40	33.01	31.75	32.37	31.96	31.66	32.61	32.87	32.72	32.98	33.15	0.00	0.00
Cu	0.16	2.54	0.44	0.01	0.11	0.03	0.00	0.06	0.00	0.00	0.00	0.06	0.12	0.22
Fe	36.63	36.96	36.77	30.70	35.29	34.73	37.08	37.68	30.69	29.12	30.70	30.02	26.17	25.99
Ni	32.37	30.02	32.49	37.47	31.96	30.25	31.32	30.51	38.81	39.17	37.43	38.00	73.97	74.98
Co	0.43	0.36	0.33	0.98	0.87	0.91	1.35	0.89	1.09	1.02	0.88	1.09	o.57	0.66
Zn	0.04	0.01	0.02	0.02	0.03	0.03	0.03	0.03	0.00	0.06	0.04	0.00	0.03	0.03
Total	102.75	103.29	103.06	101.03	101.44	98.13	101.69	101.78	103.37	102.09	102.03	102.32	100.86	101.88
Atomic percents:														
S	45.90	46.07	45.67	45.11	45.83	46.35	44.72	45.65	45.48	45.81	46.09	46.19	0.00	0.00
Cu	0.11	1.77	0.31	0.00	0.08	0.02	0.00	0.04	0.00	0.00	0.00	0.04	0.11	0.20
Fe	29.14	29.27	29.20	25.04	28.68	28.92	30.06	30.28	24.37	23.41	24.63	24.01	26.92	26.47
Ni	24.50	22.62	24.56	29.08	24.72	23.97	24.16	23.33	29.33	29.96	28.58	28.93	72.39	72.67
Co	0.32	0.27	0.25	0.76	0.67	0.72	1.04	0.68	0.82	0.78	0.67	0.83	0.56	0.64
Zn	0.03	0.00	0.01	0.01	0.02	0.02	0.02	0.02	0.00	0.04	0.03	0.00	0.03	0.03

1= Pyrrhotite. 2 = Troilite 3 = Chalcocite 4–7 = Chalcopyrite. 8-9 = Ni-rich Chalcopyrite. 10–11 = Cu-rich pentlandite.
12 = Co-rich pentlandite. 13–26 = Pentlandite. 27–28 = Awaruite.

variations according to their host primary rock types. The samples from the Bela ophiolite included in this study show nickeliferous phases (pentlandite and awaruite) belong to an earlier paragenesis, being formed in olivine-rich residual and earlier–crystallized rocks. These are succeeded by the cupriferous and ferriferous phases (chalcopyrite) in the later paragenesis of clinopyroxenites and some mafic rocks. The awaruite has average Ni / Fe ratio of 2.7 and has Co as its third element rather than Cu as reported from other similar awaruite occurrences (e.g., Ahmed & Bevan, 1981). Pentlandite in the nodular chromitite has higher Ni and Co and lower Fe than that in the other rocks. One clinopyroxenite dyke has more variety and abundance of Ni-Cu-Fe sulphides.

REFERENCES

AHMED, Z. & BEVAN, J.C. (1981) Awaruite, iridian awaruite and a new Ru-Os-Ir-Ni-Fe alloy from the Sakhakot-Qila complex, Malakand Agency, Pakistan. Min. Mag. **44**, pp. 225-230.

AHMED, Z. & HALL, A. (1982) Nickeliferous opaque minerals associated with chromite alteration in the Sakhakot-Qila complex, Pakistan, and their chemical variation. Lithos **15**, pp. 39 -47.

CAMPBELL, F.A. & ETHIER, V.G. (1984) Nickel and cobalt in pyrrhotite and pyrite from the Faro and Sullivan ore bodies. Can. Mineral. **22**, pp. 503-506.

MERKLE, R.K.W. & VON GRUENEWALDT, G. (1986) Compositional variation of Co-rich pentlandite: Relation to the evolution of the upper zone of the western Bushveld complex, South Africa. Can. Mineral. **24**, pp. 529-546.

PANAYIOTOU, A. (1980) Cu-Ni-Co-Fe sulphide mineralization, Limassol Forest, Cyprus. *In*: Panayiotou, A. (ed.) OPHIOLITES: Proceedings International Ophiolite Symposium, Cyprus, 1979. Geological Survey Department,Cyprus. pp. 102-116.

PATTERSON, G.C. & WATKINSON,D.H. (1984) Metamorphism and supergene alteration of Cu-Ni sulfides, Thierry Mine, Northwestern Ontario. Can. Mineral. **22**, pp. 13-21.

RONA, P.A. (1988) Hydrothermal mineralization at oceanic ridges. Can. Mineral. **26**, pp. 431-465.

SHIGA, Y. (1987) Behaviour of iron, nickel,cobalt and sulfur during serpentinization, with reference to the Hayachine ultramafic rocks of the Kamaishi mining district,northeastern Japan. Can. Mineral. **25**, pp. 611-624.

SIDERIS,C., SCOUNAKIS,S. & ECONOMOU, M. (1981) The ophiolite complex of Edessa area and the associated mineralization. *In*: Augustithis, S.S. et al. (eds.) UNESCO International Symposium on Metallogeny of mafic and ultramafic complexes, I.G.C.P. Project no.169, National Technical University, Athens, Greece, Vol. 3, pp. 142-153.

STONE, P., GUNN, A.G., COATS, J.S. & CARRUTHERS, R.H. (1986) Mineral exploration in the Ballantrae complex, southwest Scotland. *In*: Gallagher, M.J., Ixer, R.A., Neary, C.R. Prichard, H.M. (eds.) METALLOGENY OF BASIC AND ULTRABASIC ROCKS. The Institution of Mining & Metallurgy, London. pp. 265 -278.

Manuscript received on October 14, 1992; accepted for publication on November 19, 1992.

ACTA MINERALOGICA PAKISTANICA
VOLUME 6 (1992) pp. 37-43.

FACIES ANALYSIS AND DEPOSITIONAL PROCESSES OF THE BANNISDALE SLATES, LAKE DISTRICT, NORTHWEST ENGLAND

ABDUL SALAM KHAN
Department of Geology, University of Balochistan, Quetta, Pakistan.

ABSTRACT : Bannisdale Slates consist of mudstones, siltstones and subordinate fine sandstones. Five different facies, i.e., laminated siltstones, homogeneous mudstones, ripple cross-laminated siltstones, bioturbated mudstones and sandstones, are recognized based on lithology and sedimentary features identified from study of polished slabs, X-radiographs and thin sections. Possible depositional processes of each facies are described . Sedimentary features observed in the Bannisdale Slates suggest that various mechanisms, e.g., dominantly low velocity, low-density turbidity currents, accumulation through flocculation and bottom current reworking with less frequent dense turbidty currents, were involved in the deposition of these sediments.

INTRODUCTION

Bannisdale Slates occupy the greatest area of the Silurian rocks in the Lake District, northwest England (Fig. 1) and constitute the thickest sequence of the fine-grained sediments in the Wenlock and Ludlow succession (Late Silurian). Due to folding and faulting, it is difficult to estimate its thickness. However, in the eastern part of the area it is believed to be 1450 m thick (Furness et al., 1967). This Formation is generally poorly exposed and detailed measurements are rarely possible. However, the New road cut (on the A590T) near Lindale (SD417808) and the stream section near Killington Bridge (SD622907) provide a good opportunity for detailed study.

METHODS OF STUDY

Field studies were confined to several sections because of the lack of continuous outcrop in the studied area (Fig. 1) Rock sequences were examined in detail which include measurements of bed thickness, sedimentary structures, lithologic variation and extensive sampling. In mudstone- dominated sequences, sedimentary features are rarely discernible in the field. Therefore, each sample was slabbed perpendicular to the bedding. Slabs were polished and examined for structures and textures. Selected parts of the salbs were thin sectioned for further detailed inspection of microstructures, textures and composition. Slabs displaying vague or no obvious sedimentary structures were X-radiographed.

FACIES DESCRIPTIONS

Bannisdale Slates are composed dominantly of mudstones and siltstones with minor sandstones. Bannisdale Slates can be divided into 5 facies on the basis of rock types and sedimentary structures. These include laminated siltstones, homogeneous mudstones, siltstones / mudstones, bioturbated mudstones and sandstones.

1. Facies 1 (Laminated Siltstones)

This facies is characterized by regular alternations of silt and mud laminae. Silt laminae consist of quartz and feldspar grains with subordinate mica and are 0.5 to 1.5mm thick. There is no systematic vertical variation in thickness and grain size in the laminated units (Fig. 2a), but the individual laminae are slightly graded. These laminae are generally undulatory in geometry with no obvious erosion and no flame structures. Mud laminae are generally very thin, rarely

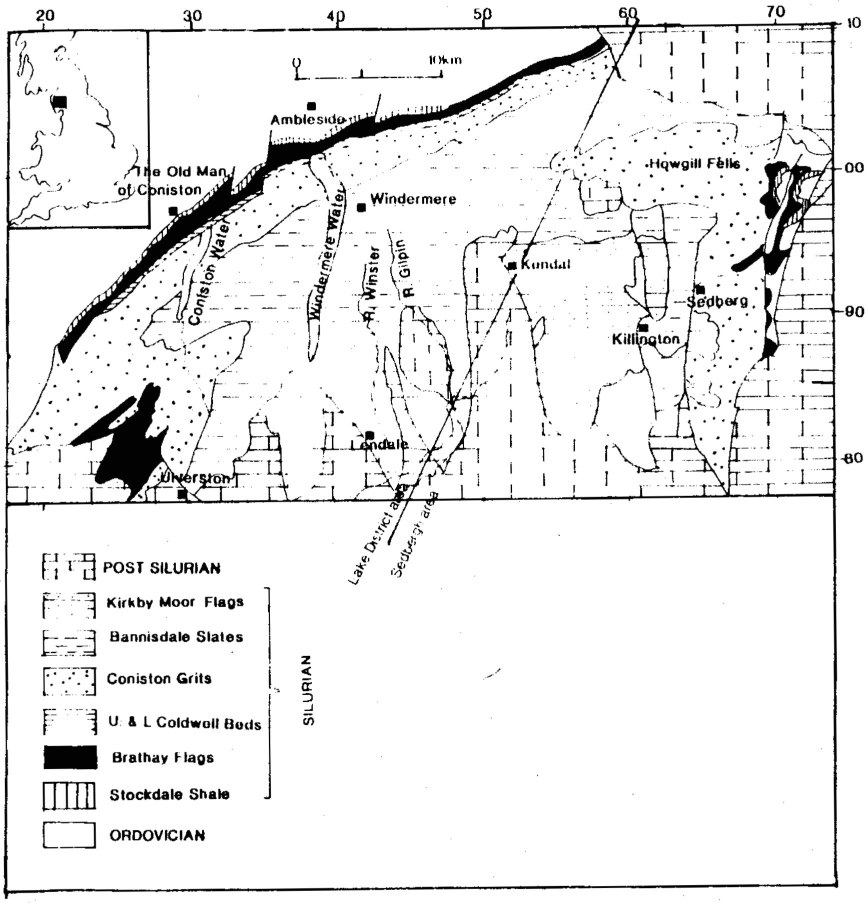

Fig. 1. Geological map showing distribution of the Wenlock and Ludlow strata in the Lake Distric (simplified from Geological Survey Sheet No. 54N).

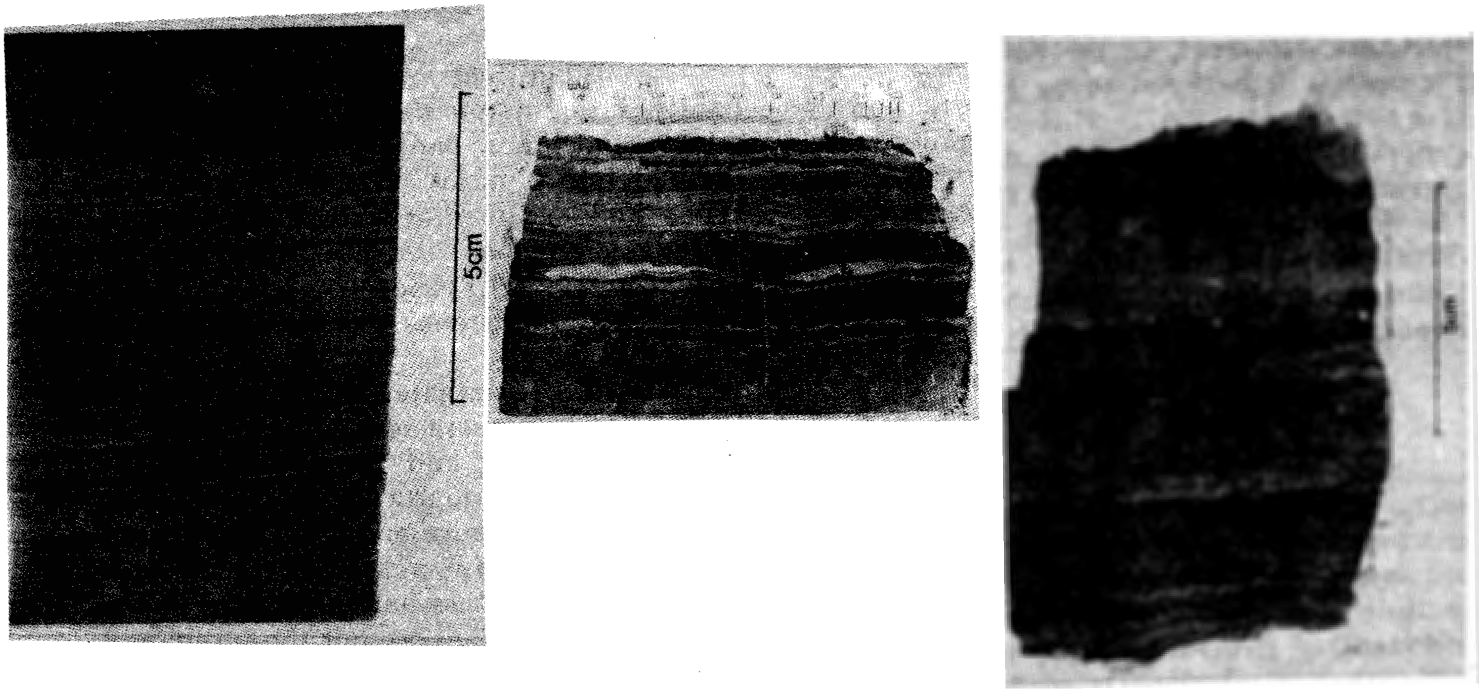

Fig. 2. (a) X-radiograph of laminated siltstone (facies 1) and homogeneous mudstone (facies 2). (b) Photograph of polished slab showing discontinuous, lenticular and partially bioturbated silt laminae. (c) Photograph of polished slab showing high degree bioturbation (facies 4) which has destroyed most of the sedimentary structure.

reaching upto 0.3mm in thickness and consist of clay with some films of carbonaceous material.

The thickness of individual laminated units ranges from a few mm to 35 cm and are commonly less than 5 cm. These units are laterally continuous and constant in thickness with sharp, non-erosive bases and sharp tops.

2. Facies 2 (Homogeneous Mudstones)

This facies is characterized by 1 to 5 cm thick beds of uniform mudstones, regularly interbedded with facies 1 (Fig. 3a). In polished slabs, X-radiographs and thin sections, these units appear homogeneous and structures (Fig.2a) with minor bioturbation in some examples. These units are well sorted and rarely graded under microscope.

3. Facies 3 (Rippled Cross-laminated Siltstones)

This facies is characterized by rippled, wavy or lenticular siltstones (Fig. 2b), ranging in thickness from a few mm to 5cm. They are composed of silt-grade siliciclastic material that are well sorted. Starved ripples are quite common which show internal lamination. Both lower and upper contacts are sharp and gradational.

4. Facies 4 (Bioturbated Mudstones)

Bioturbation is the dominant feature of this facies, and has destroyed or modified much of the original sedimentary structures. In some cases, bioturbation is so intense that only vague traces of primary sedimentary structures remain (Fig. 2c). Bioturbation can easily be observed in X-radiographs and thin sections. Bioturbation seems to be continuous process with irregular fluctuations that are evident from partial to complete distortion of the primary depositional features. Specific trace fossils are difficult to be identified, but small rounded, oval and horizontal burrows filled with silt grade material may be *planolities*, and tiny black spot-like features are more likely be *chondrites*.

5. Facies 5 (Sandstones)

This facies is sporadically present at some horizons, and ranges in thickness from less than 10 cm upto 175 cm. These sandstones are medium to fine grained and usually graded, displaying Bouma (1962) Tabcde, Tbcde and Tcde divisions. However, some beds seems to be ungraded or graded only at the very tops. Thinner bed are usually rippled cross laminated.

FACIES ASSOCIATIONS

Two distinct facies associations are recognised in the Bannisdale Slates, dominated by one or more than one facies described above. These facies associ-ations are (i) striped beds, and (ii) mottled beds.

(i) Facies Association 1 (Striped Beds)

This facies association is characterized by a regular alternation of facies 1 (laminated siltstones) and facies 2 (homogeneous mudstones), with less frequent interbeds of facies 5 (Fig. 3a). It occurs as pockets varying in thickness from a few metres to a few tens of metres.

(ii) Facies Association 2 (Mottled Beds)

This facies association consists dominantly of facies 4 (bioturbated mudstones) and facies 3 (rippled cross laminated siltstones) (Fig. 3b). This facies association froms packets ranging in thickness from 1 m upto hundreds of metres, and are interbedded with facies association 1.

FACIES VARIATIONS

There is a significant downcurrent facies change in the Bannisdale Slates. Facies association 1 is dominated in the proximal sequences of the Bannisdale Slates, while facies association 2 predominates in the distal part of the succession.

The thickness and grain size of the laminated siltstones (facies 1) decrease downcurrent, while the thickness of interbedded homogeneous mudstones (facies 2) increases downcurrent. This variation in bed thickness and grain size is responsible for the observed changes in the proportion

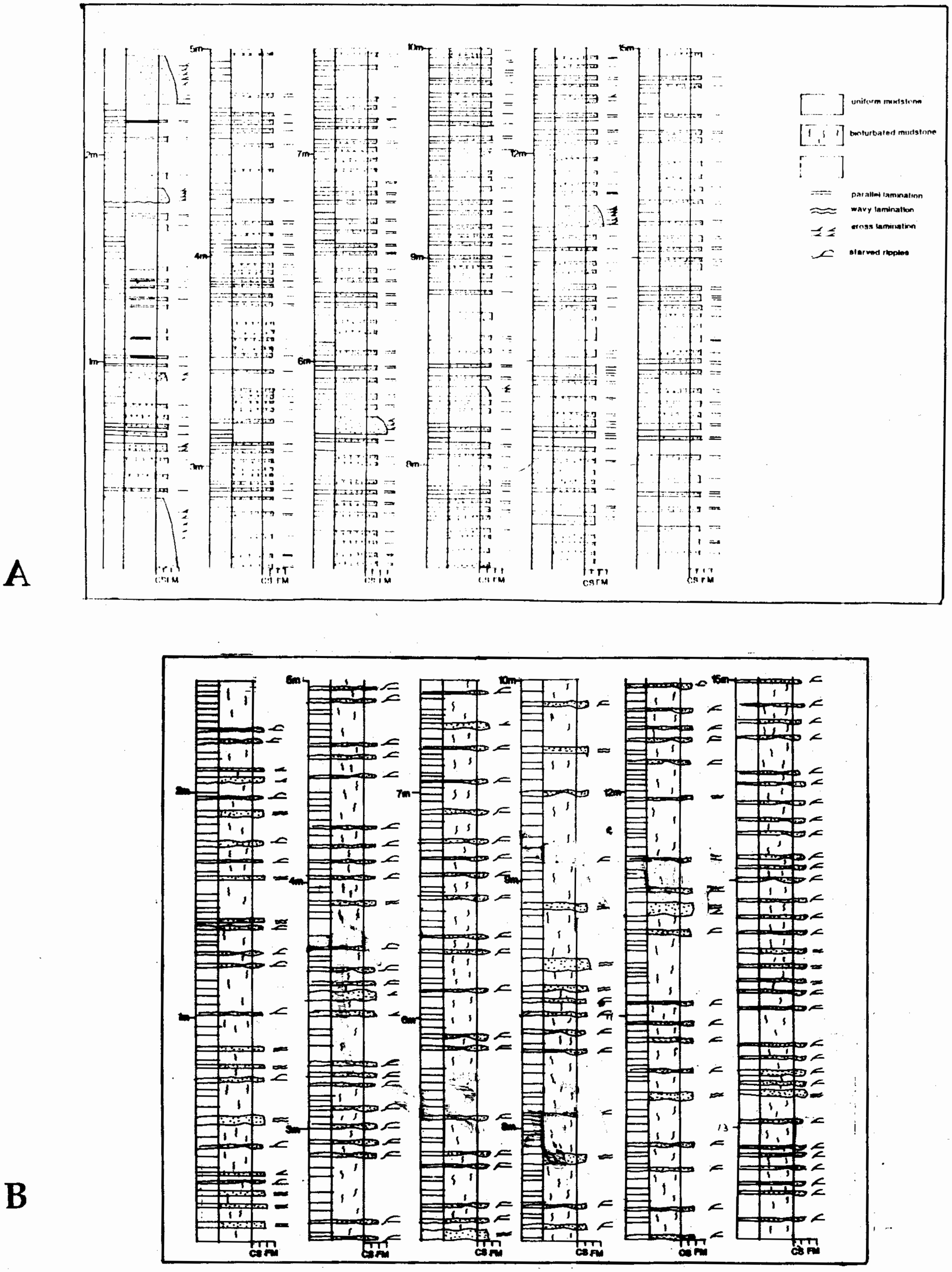

Fig. 3. Sedimentary logs of (a) facies association 1 (striped beds), comprising laminated siltstone and homogeneous mudstone with less frequent sandstone. (b) facies association 2 (mottled beds) comprising bioturbated mudstone and starved ripple siltstone.

of the component facies. For example, facies association 1 in the proximal part of the sequence is dominated by facies 1 (laminated siltstones). The thickness of these laminated siltstone beds usually is greater than 10 cm and the grain size mostly is coarse silt to very fine sand. In the distal sequences, facies association is dominated by facies 2 (homogeneous mudstones) with thin (generally less than 2cm) interbeds of facies 1 (laminated siltstones).

Units of facies association 2 are coarser grained and poorly sorted in the proximal sequences, while in the distal sequences theses units are fine grained (mudstone dominated).

Facies 5 (sandstones) is more common, thicker and coarser-grained in the proximal sequences, but there is no systematic decrease in bed thickness and grain size distally.

DISCUSSION AND INTERPRETATIONS

There is no detailed published study of the sediment transport and deposition of the Bannisdale Slates. Furness et al. (1967) interpreted these sediments as "the deposits of low velocity turbidity currents". Detailed examination of these rocks in polished slabs, X-radiographs and thin sections has revealed that most of the features are not consistent with normal turbidites.

In ancient sequences, it is very difficult to distinguish between various types of fine grained deep sea deposits (e.g., hemipelagites, turbidites and contourites) because they show some similar depositional features (Stow & Piper, 1984). Criteria have been proposed for the distinction of these deposits from one another (Stow & Piper, 1984), but it is very rare to find a complete set of features in every fine grained deep sea deposit.

Hemipelagites usually show no current induced sedimentary structures due to lack of sediment transport as a bed load and are thoroughly bioturbated due to continuous reworking by benthonic animals (Chough et al., 1984).

Fine grained turbidites are the most common deep-sea deposits that can be indentified by making use of the sedimentary features as proposed by several authors (Rupke & Stanley, 1974: Hesse, 1975: Piper, 1978: Stow & Shanmugan, 1980 and Stow & Piper, 1984).

Contourites are deposits resulting from bottom currents. Bottom currents can erode, deposit or simply rework deep sea sediments (Hollister & Heezen, 1972: Stow, 1979). No standard sequence of sedimentary structures has been recognised for contourites yet, which show high degree of variability in sedimentary structures (Stow & Piper, 1984). These deposits range from highly mottled (Chough & Hesse, 1985) to highly laminated (Stanley, 1987) and may not be easily distinguished from bioturbated hemipelagites and turbidites respectively.

The majority of the sedimentary features observed in the Bannisdale Slates distinguish them from typical mud turbidites. For example :

1. Fine grained turbidites show a standard usually partial sequence of sedimentary structures with a progressive upward decrease in grain size indicative of waning energy conditions. No. such sequence of sedimentary structures is recognised in majority of the facies of the Bannisdale Slates.

2. In turbidites, the sedimentary structures are usually preserved due to rapid deposition, and bioturbation is restricted to the tops of the units, whereas most of the sedimentary structures in facies 4 have destroyed or modified by syn-depositional bioturbation.

3. In turbidites, parallel laminated intervals generally are graded, showing systematic upward decrease in grain size thickness and frequency of the silt laminae, whereas laminated siltstone (facies 1) of the Bannisdale Slates show no systematic upward decrease in grain size, thickness and frequency of the silt laminae.

4. In turbidites, laminated intervals have gradual transition into the overlying mud interval, whereas there are sharp contacts between facies 1 and facies 2.

The deposition of the Bannisdale Slates cannot readily be explained by single mechanism. More than one mechanisms were involved in the deposition of these sediments. The graded, non-erosive nature of the silt laminae of the facies 1 (laminated siltstones) suggest that this facies was deposited from repetitive, weak and dilute turbidity flows and the thinness of the mud laminae indicates that the time interval between two successive flows was not enough for the suspended mud fraction to be settled completely. During calm periods (when turbidity flows ceased), the finer (dominantly clay) suspension settled down in the form of flocs (Kranch, 1975) forming homogenous mudstone layers (facies 2), interbedded with laminated siltstone layers, thus producing the observed sequence of alternating beds of laminated siltstone and homogeneous mudstones of facies association 1 (Fig. 3a).

Sediments of facies 3 and 4, which are dominant in the distal part of the succession seem to have been reworked by bottom currents. The association of current-induced features (facies 3) and bioturbation (facies 4) can best be explained by bottom currents reworking which renewed the bottom water, allowing re-colonization of benthonic organisms and at the same time winnowed the sediments, producing discontinuous ripple cross laminated siltstones (facies 3).

A close association of mud turbidites, hemi-pelagites and contourites is common in deep-sea environments, and a continuum may exist between their processes of deposition (Stow & Lovell, 1979; Stow & Piper, 1984). Low velocity, low density turbidity currents are most susceptible to modification by bottom currents (Stow & Lovell, 1979). In such circumstances it may be difficult to distinguish between mud turbidites and muddy contourites because they may show similar hydraulic sorting and depositional features (Hesse, 1975).

Sediments of facies 3 and 4 may not be true contourites, but most of the sedimentary features observed in this facies association are characteristic of reworking by the bottom currents. Evidence for bottom current reworking comes from the wavy, lenticular, discontinuous lamination, the abundance of starved ripples with common gradational bases and sharp tops and disruption of the sedimentary structures by benthic animals. It is believed that sediments were delivered initially by low velocity and low density turbidity currents to a region (probably lower slope and rise) where bottom currents were active. After immediate emplacement, most of the sediments were reworked and displaced.

Sandstone beds (Facies 5) which display sedimentary structures characteristic of sand turbidites were delivered by thick turbidity currents (Lowe, 1982) which may not have allowed the sediments to become organized and sorted to produce grading and other sedimentary structures.

ACKNOWLEDGEMENTS

This study was carried out as part of the Ph. D project under the tenure of a scholarship, sponsored by the Ministry of Science & Technology, Government of Pakistan; and is gratefully acknowledged. Many thanks are due to Professor Gilbert Kelling for his supervision and guidance during this research, and other staff members of the Geology Department, Keele University, England, for their help.

REFERENCES

BOUMA, A.H. (1962) SEDIMENTOLOGY OF SOME FLYSCH DEPOSITS : A Graphic Approach to Facies Interpretation. Elservier, Amsterdam, **168** p.

CHOUGH, S.K. & HESSE, R. (1985) Contourites from Eirik Ridge, south of Greenland. Sed. Geol **41**, pp. 185-200.

CHOUGH, S.K., LEE, G.H., PARK, B.K. & KIM, S.W. (1984) Fine structures of turbidite and associated muds in the Ulleung (Tsushima) basin, East Sea (Sea of Japan. J. Sed. Petrol.

54, pp. 1212-1220.

FURNESS, R. R., LLENWELLYN, P. G., NORMAN, T.N. & RICKARD, R.B. (1967) A review of the Wenlock and Ludlow Stratigraphy and sedimentation in the northwest England. Geol. Mag. **104**, pp. 132-147.

HESSE, R. (1975) Turbidite and non-turbiditic mudstone of Cretaceous Flysch sections of the East Alps and other basins. Sedimentology **22**, pp. 387-416.

HOLLISTER, C. D. & HEEZEN, B. C. (1972) Geological effects of ocean abottom currents : western North Atlantic. *In :* Gordon, A. L.(ed), STUDIES IN PHYSICAL OCEANOGRAPHY. Gordon Breach Scientific Publication **2**, pp. 37-66.

KRANCH, K. (1975) Sediment deposition from flocculated suspensions. Sedimentology **22**, pp. 111-123.

LOWE, D. R. (1982) Sediment "Gravity Flows : II Depositional models with special reference to the deposits of high density turbidity currents. J. Sed. Petrol. **52**, pp. 279-297.

PIPER, D. J. W. (1978) Turbidite mud and silts on deep sea fans and abyssal plains. *In :* Stanley, D.J. & Kelling, G. (eds.), SEDIMENTATION IN SUBMARINE CAYONS, FANS AND TRENCHES, pp. 163-176. Dowden, Hutchison and Ross, Strousdburg.

RUPKE, N. A. & STANLEY, D. J. (1974) Distinctive properties of turbiditic and hemipelagic mud layers in Algero-Balearic Basin, West Mediterranean. Smithsonian Contr. Earth Sci. **13**, pp. 1-40.

STANLEY, D. J. (1987) Turbidite to current reworked sand continuum in Upper Cretaceous rocks, US, Virgin Islands. Mar. Geol. **78**. pp. 143-151.

STOW, D. A. V. (1979) Distinguishing between fine-grained turbidites and contourites on the Nova Scotian deep water margin. Sedimentology **26**, pp. 371-387.

STOW D. A. V. & LOVELL, J. P. B. (1979) Contourites : their recognition in modern and ancient sediments. Earth Sci. Rev. **14**, pp. 251-291.

STOW D. A. V. & PIPER, D. J. W. (1984) Deep water fine-grained sediments : facies models. *In:* Stow, D.A.V. & Piper, D.J.W. (eds.). DINE GRAINED SEDIMENTS : Deep water Processes and Facies. Geol. Soc. London. Spec. Publ. **15**, pp. 611-646.

STOW D. A. V. & SHANMUGAN, G. (1980) Sequences of structures in fine-grained turbidites : comparison of recent deep-sea and ancient flysch sediments. Sed. Geol. **25**, pp. 23-42.

Manuscript received on October 16, 1992; accepted for publication on December 31, 1992.

ACTA MINERALOGICA PAKISTANICA
VOLUME 6 (1992) pp. 44-54.

GEOCHEMICAL SAMPLING OF LAKE BOTTOM SEDIMENTS FROM LOKKEN AREA, CENTRAL NORWAY

KHALIL A. MALLICK,
SHAHID NASEEM,
SHAMIM A. SHEIKH
&
NADEEM A. KHAN
Department of Geology, University of Karachi, Karachi, Pakistan.

ABSTRACT: Frozen lake bottom core sediments have been collected from Lokken area, Norway, by designing and fabricating new samplers. The results are encouraging both in the instrumentation and the study of minor elements as tools in the geochemical exploration of ore deposits in glaciated terrains. Concentration of Cu in the sediment samples is described as an illustration.

INTRODUCTION

Most of the work done todate by exploration geochemists has been on rocks, stream sediments, marine sediments, waters soils and vegetation. On lake bottom sediments and waters relatively less work has appeared. The problems in sampling of sediments are increased when the area is dominated by disorganized drainage and glacial lakes. Less attention paid to the study of lake sediments is attributed to the problems in the collection of samples. The lake sediment geochemistry can be used as an indicator of mineralization in reconnaissance-level exploration, especially in areas of glacial overburden having indefinite and disorganized drainage where conventional geochemical exploration techniques involving sampling and analysis of sediments have limited application (Allan & Timperley, 1975; Nichol, et al., 1975).

Schmidt (1956) studied the adsorption of Cu, Pb and Zn on common rock-forming minerals and its effects on lake sediments of New Brunsvick and Quebec, Canada. Arnold (1970) studied the concentration of metals in lake water and sediments of the lakes associated with mineralization in the Flin Flon and Lac La-Range areas in Saskatchewan, Canada.

A well documented example of the use of lake sediment geochemistry in mineral exploration was that of Allan (1971) in the Copper Mine River Area of North Western Territories, Canada, where he used helicopter for access to the sample site. Dyck (1971) carried out a geochemical survey of Beaverlodge, Saskatchewan region by using helicopter. In Bear and Slave Provinces of the Canadian Shield, Allan et al. (1972) used fixed wing aircraft for the collection of water and sediment samples by using conventional samplers.

Fredricksson and Qvarfort (1973) used boat and Livingstone sampler to study the Hg content of sediments from the lakes in Dalarna, Sweden. In the Superior Province of Canada, Coker & Nichol (1974) used boat and Ekman-Birge dredge sampler for the collection of lake sediments. While working in Western Newfoundland, Canada, Devenport et al. (1974) used helicopter and hollow pipe with valve at the lower end for the collection of lake bottom sediments. Likewise Timperley and Allan (1974) used both the fixed wing aircraft and boat for the collection of lake sediments from Red Lake and Uchi Lake areas of Canada. They used Ekman-Birge bottom dredge equipment for sampling. The same method was used in the Sudbury area, Canada by Allan & Timperley (1975). Coker & Nichol (1975) preferred fixed wing aircraft and Ekman-Birge Bottom Dredge for the collection of lake sediments from some of the lakes of southern shield, Canada.

Some work on the collection of lake sediments and water samples has been done in Norway and Sweden mainly for the limnological and pollution research (Fredrickasson & Quarfort, 1973; Lag & Bolviken, 1974).

The present paper attempts to find out an easier and less expensive method for the collection of lake bottom sediments from the desired sites. A new sampler fabricated in the workshop of the Geological Survey of Norway is introduced for geochemical exploration of ore deposits in gla-

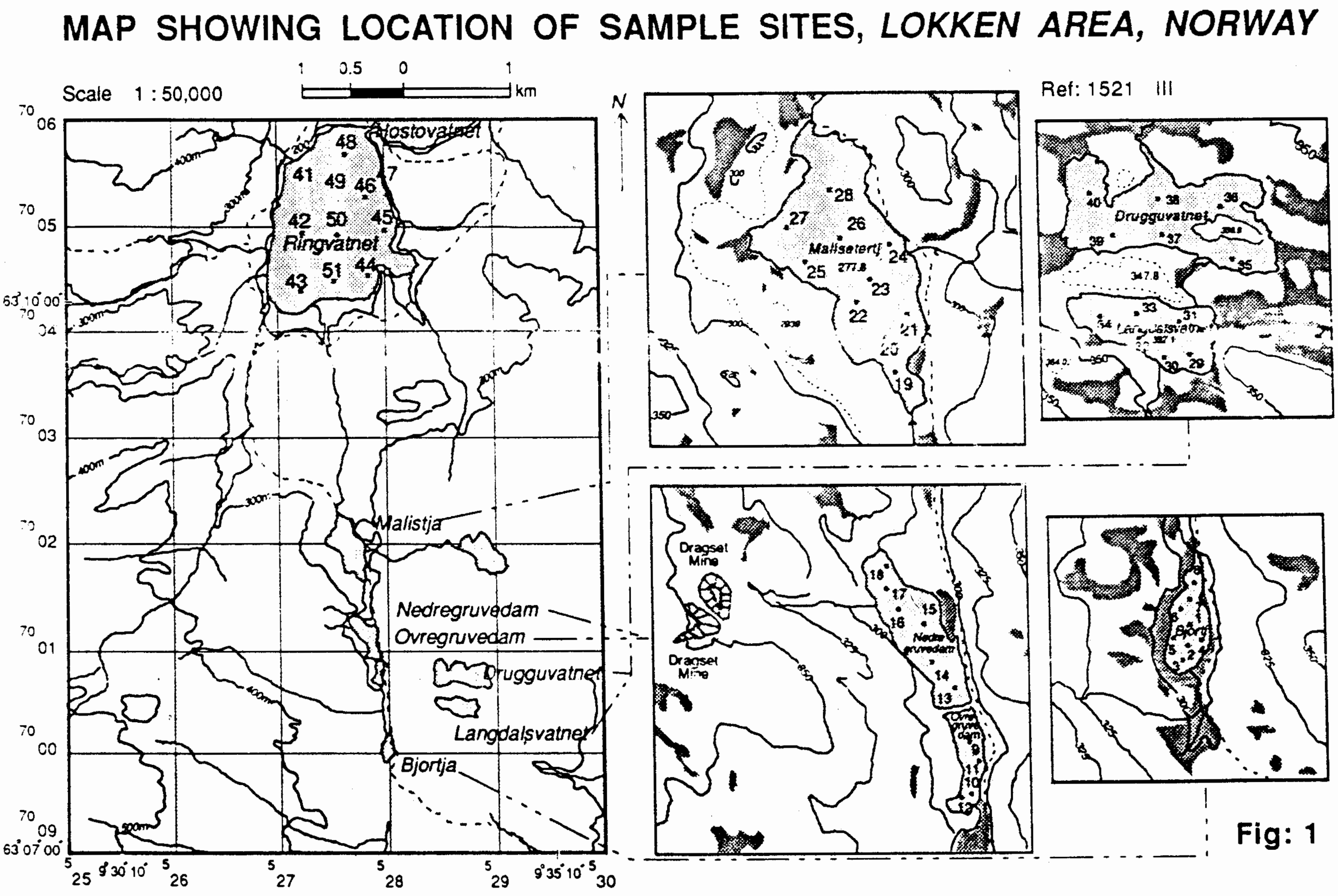

Fig. 1. Map showing location of sample sites, Lokken area, Norway.

ciated terrains having abundant lakes and poor bed rock exposures. The Lokken area, known for it mineralization of Cu, Pb and Zn is selected to determine the suitability of sediment geochemistry as a tool for exploration of ore deposits in glaciated terrains (Fig. 1).

GENERAL GEOLOGY

The area selected, to study the effectiveness of the method and interpretation of geochemical data, is known as Lokken (Fig.1). It is 70 km SE of Trondheim at an elevation of 300 m. There are three main valleys with N-S trend and dense vegetation of pine trees. The rocks exposed in this area are of Roros Group, Storen Group, and Hoven Group, in chronological order. The Roros Group mainly consists of mica schist, amphibolites and gneisses. The rock is older than upper Cambrian. The rocks of Storen Group are mainly basic lavas, pyroclasts and acidic rocks of upper Cambrian age. The copper-rich pyritic ores containing 0.9 to 2% copper are found in the basic lava. The copper ore had been under active mining from A.D. 1646 to 1946. The cupriferous pyrite is also accompanied by lead and zinc. The rocks comprise greenstone spread over all the glacial lakes area. The copper mine known as Dragset mine is in the western valley trending N-S. The rocks of Hoven Group of middle Ordovician age are mainly conglomerates, shales, sandstones and limestones. The whole area is below treeline and is covered by dense vegetation of pine trees in which marshy land and the lakes of varying sizes are common (Chaplow, 1968).

METHOD OF STUDY

In Lokken area, some of the lakes are thought to be affected by the abandoned mining activities for Cu, Pb and Zn from the massive sulphides of the Caledonides. Other lakes of the same area apparently have no drainage from the known mineralized areas. Such lakes were taken as virgin or non-contaminated lakes. The virgin lakes were sampled to work as background lakes and to have a comparative account of the degree of contamination. The geochemical data is also expected to help in evaluation of possible mineralized localities.

The lakes chosen for the present study were sampled during the winter when the surface water of the lakes was frozen and it was possible to walk on and to drill holes in the ice to collect bottom sediment samples from the desired sites in the lakes.

During field work the snow scooter was used to approach the desired sample sites on the lakes. The winter season was considered the most suitable time for sampling because of minimum upwelling effects in the lake water and less disturbance in the chemical stratification of the water. The inlet streams also would not be having any pronounced effects on the lake water and the sediments due to frozen condition. In this set up the sediments collected from the mouth of the streams would be more representative of the stream sediments and their influence on the minerals and mineralization at the lake bottom.

To evaluate the suitability of the method adopted for geochemical exploration, copper content has been selected to describe the degree and depth of contamination. Quantitative estimation of copper was made in the sample fractions obtained through coning and quartering. The sample solutions were run on Perkin Elmer atomic absorption spectrometer in the geochemical laboratory of the Geological Survey of Norway at Trondheim.

The lakes selected for the present study, from S to N were Bjortja, Ovre Gruvedam, Nedre Gruvedam, Malistja and Ringvatnet. They are interconnected.

SAMPLING TECHNIQUE

The available core samplers with a suction valve above the sampling tube are not able to prevent the slipping out of loose deposits. Ekman's Sampler (1905) with a slip valve is relatively better but very often the slip valve closes when the tube is still penetrating the mud to reach the more compact layers. The sampler designed by Strom (1934) could be used to collect core samples from the lake bottom if provision is made to get the sample in glass or plastic tube fitted inside the sampler tube. The use of glass or plastic tubes of ample diameter would minimize the friction between sediment and inner tube wall of the sampler. Since. Strom's sampler is made of stainless steel and brass, it would be a source of contamination for Cr, Ni and Cu.

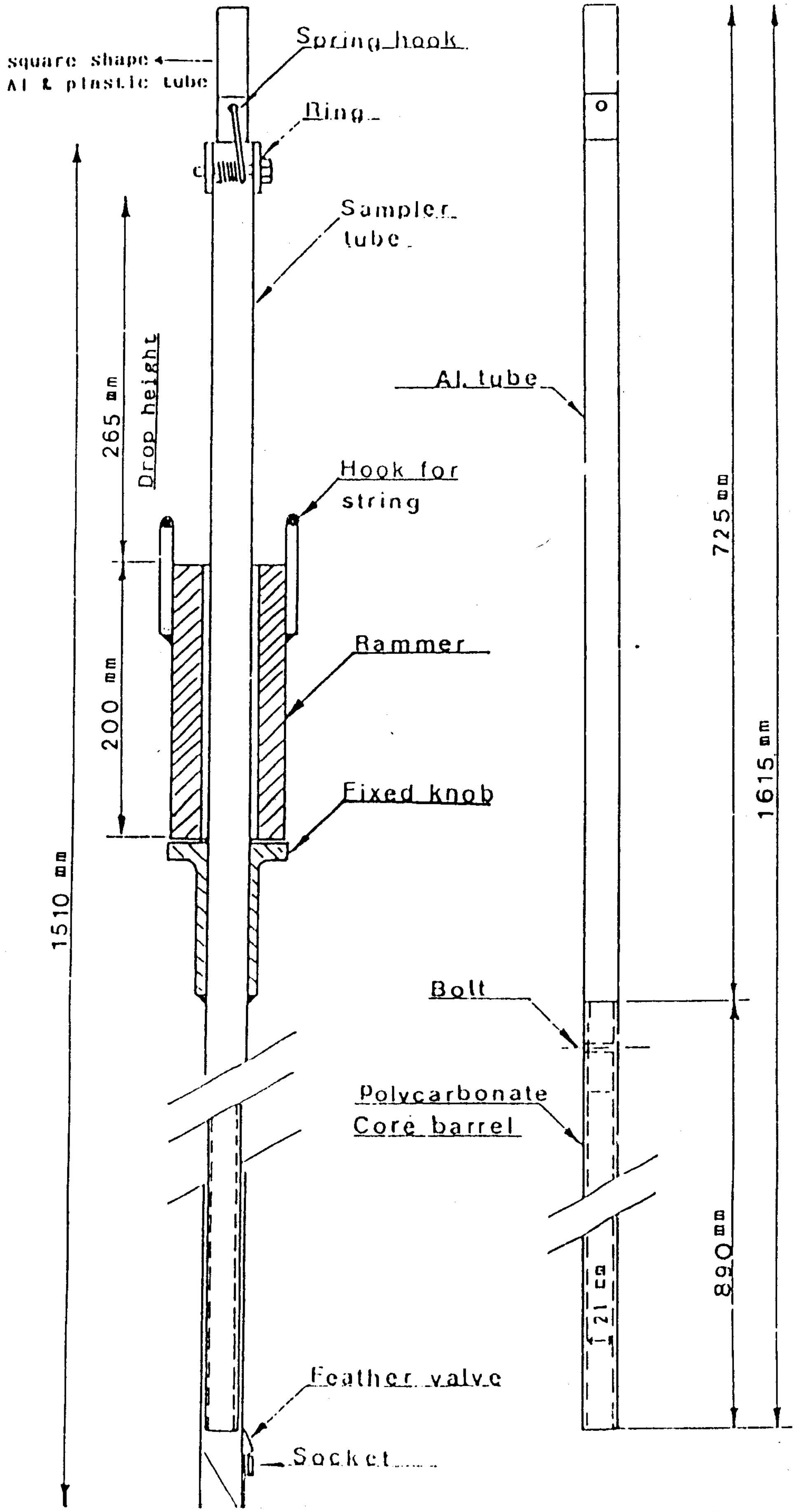

Fig. 2. Details of lake sediments sampler no. 1 fabricated at the Geological Survey of Norway.

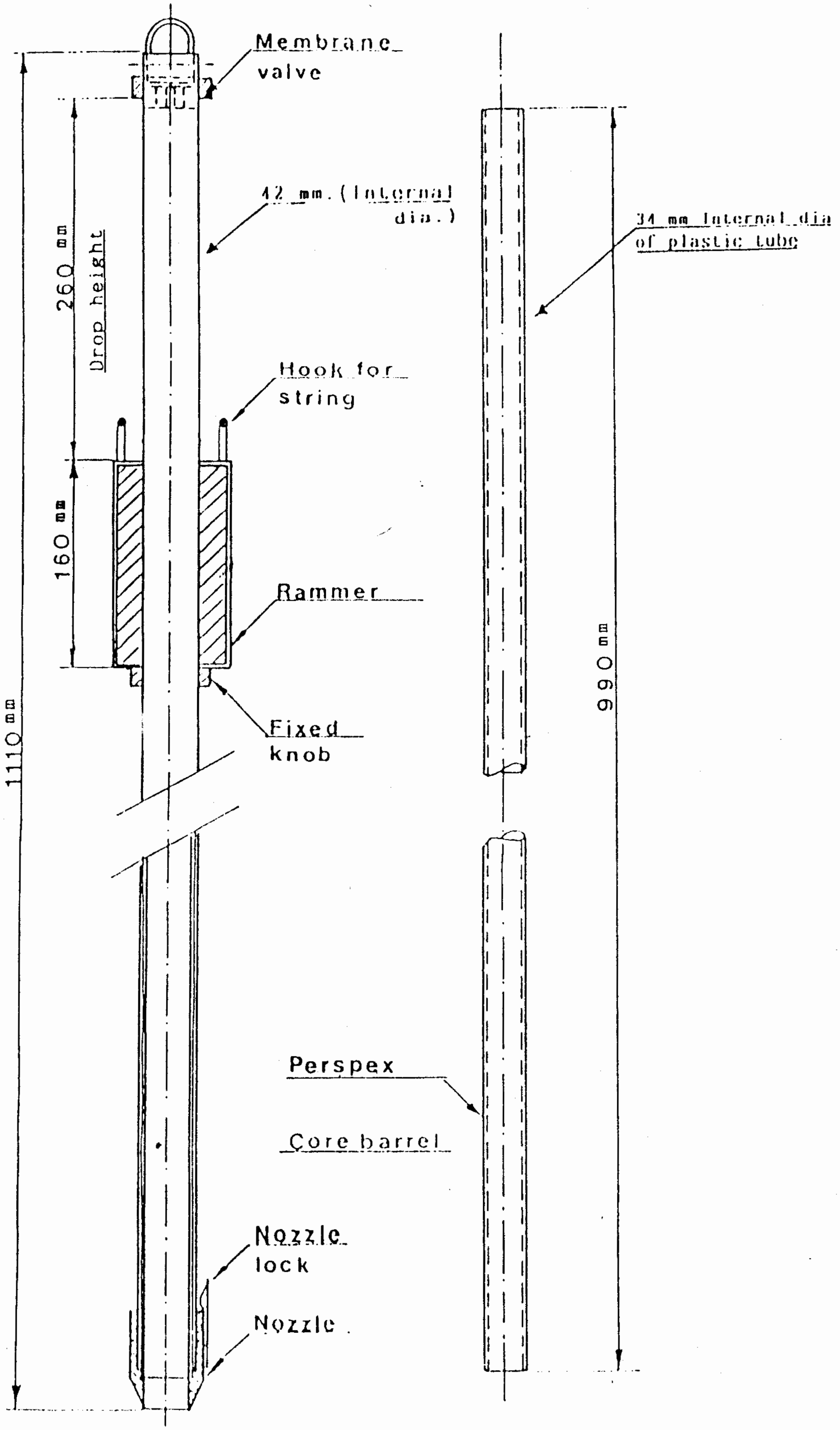

Fig. 3. Details of lake sediments sampler no. 2 fabricated at the Geological Survey of Norway.

To avoid complications, unnecessary weight and contamination, a new sampler was designed and constructed in the workshop of the Geological Survey of Norway to collect lake bottom sediments with least disturbance of sediment column. The sampler was found to be satisfactory for the collection of profile lake bottom sediments and their geochemical studies. Two different types of samplers having same basic functions were designed with the following details:

Two versions of the sampler are shown in Figs. 2 and 3, respectively. The sampler is made of either a hollow square/circular steel tube of 1510 or 1110 mm length, respectively. The internal diameter of the sampler tube is 27mm/42mm in which the square shape/cylindrical plastic tube with an internal diameter of 21mm/34mm is fitted for the preservation of sediment samples. The plastic tube known as sample tube or core barrel is 890mm / 990mm long and it is bolted at the top to keep the barrel in fixed position (Figs. 2 & 3). The sample tube or barrel is replaceable and so the sample can be stored in the tube for laboratory studies by putting caps at the two ends (Fig. 4). There are two fixed knobs on the sampler tube which help in raming the sampler tube into the sediment column. The rammer is cylindrical and moves up and down between the rimmed top of the sampler and the knob. The rammer is 200/160mm long and 6 kg in weight. The two hooks at the upper end of the rammer are to fix the string that hangs the whole sampler in water. The cylindrical shape of the rammer helps in uniform raming of the sample tube into the lake bottom sediments. The low end of the sampler is fitted with a strip of iron which works as a valve. The valve is replaceable in the socket made at the lower end of the sampler. A slight push from the lower end of the sampler removes the valve and the sediments entering the sample tube is locked in. A wooden square / circular rod 100 cm in length just penetrating the tube is used as a piston to push out the sample from the sample tube. The sampler has the following advantages as compared to other sampler already used for sampling of lake sediments.

1. It is easier to operate, lighter in weight and inexpensive.
2. It does not contaminate the sample by any other metal except Fe and Cr.
3. The friction between sediment and the inner wall of the plastic sample tube is very small and so the sample is preserved with its original structure.
4. The study of physical properties of sediments such as colour, lamination and relative textures of different laminae is made without pushing the sample out of the plastic tube.
5. The valve is simple and replaceable and it works properly even in sandy clay and mud.
6. The presence of raming device helps in penetrating the sampler tube in the sediments column to a maximum.

RESULTS AND DISCUSSION

The plot of copper concentration versus depth of sediments is expected to reveal the depth of contamination and also the dispersion pattern in the lake sediments of Nedra Gruvedam and interconnected Bjortja, Ovre Gruvedam, Malistja and Ringvatnet lakes which extend from south to north downstream.

These plots are also expected to reveal the depth of contamination of lake bottom sediments and thus indirectly would help in determining the rate of sedimentation in the lakes. The plots should also prove helpful in differentiating between contaminated and uncontaminated lakes. Any deviation from the background value of Cu in the lake sediments would further facilitate in the determination of sources of contamination and thus would help in locating unknown mineralization in the surroundings. This is based on the assumption that the lake-bottom sediments represent the average chemical composition of the rocks in the surroundings and any deviation from the average chemical composition is a reflection of contaminating sources like mining activities or an indication of some unknown mineralization in the area. Although the complex situation in nature and the type of mineral deposits will not make the assumption rigorously true for all cases, the overall effect as judged from many samples may give a good indication of the concentration of the element under study. For this purpose, the sediment samples from the top 0 to 3cm depth level were not taken into consideration to avoid complexities arising due to redox potential and other related factors.

"Standard average" means the average con-

Fig. 4. Core of lake bottom sediments in plastic barrel of the sampler.

centration of the element with reference to the value of Cu concentration given in Rose et al. (1979).

The lake sediments showing average Cu concentration equal to the "standard average" of soils (av. 20 ppm; range 2-100 ppm) at the sediment-water interface or an increase with depth may represent non-contaminated lakes.

Lakes showing higher and variable Cu concentration at and below sediment-water interface at certain depth, but nearly uniform Cu concentration in the deeper parts of the sediment column, have been considered as contaminated lakes. The lakes getting stream water directly from the mine area or flow of water from the contaminated lake into the adjacent lake have also been considered as contaminated lakes of varying degrees.

It appears from the study of the plots (Fig. 5) that the Cu mining activities which were operating in Dragset area about fifty years ago could not effect the sediments of some of the lakes like Bjortja and Ringvatnet which form the true ends of the chain in contaminated lakes. Same non-contaminated conditions for Cu concentration in the sediments of Langdalsvatnet and Drugguvatnet are also observed (Fig.5). Perhaps the wind direction and intensities were not competent to blow the particles from the mining wastes to these lakes at higher altitudes.

Copper in the sediments of lake Bjortja does not show any significant variation with depth and the concentration is slightly higher than the "standard average" value (40-100 ppm). The sediments from different parts of this lake do not show any sign of appreciable change in Cu content. On the

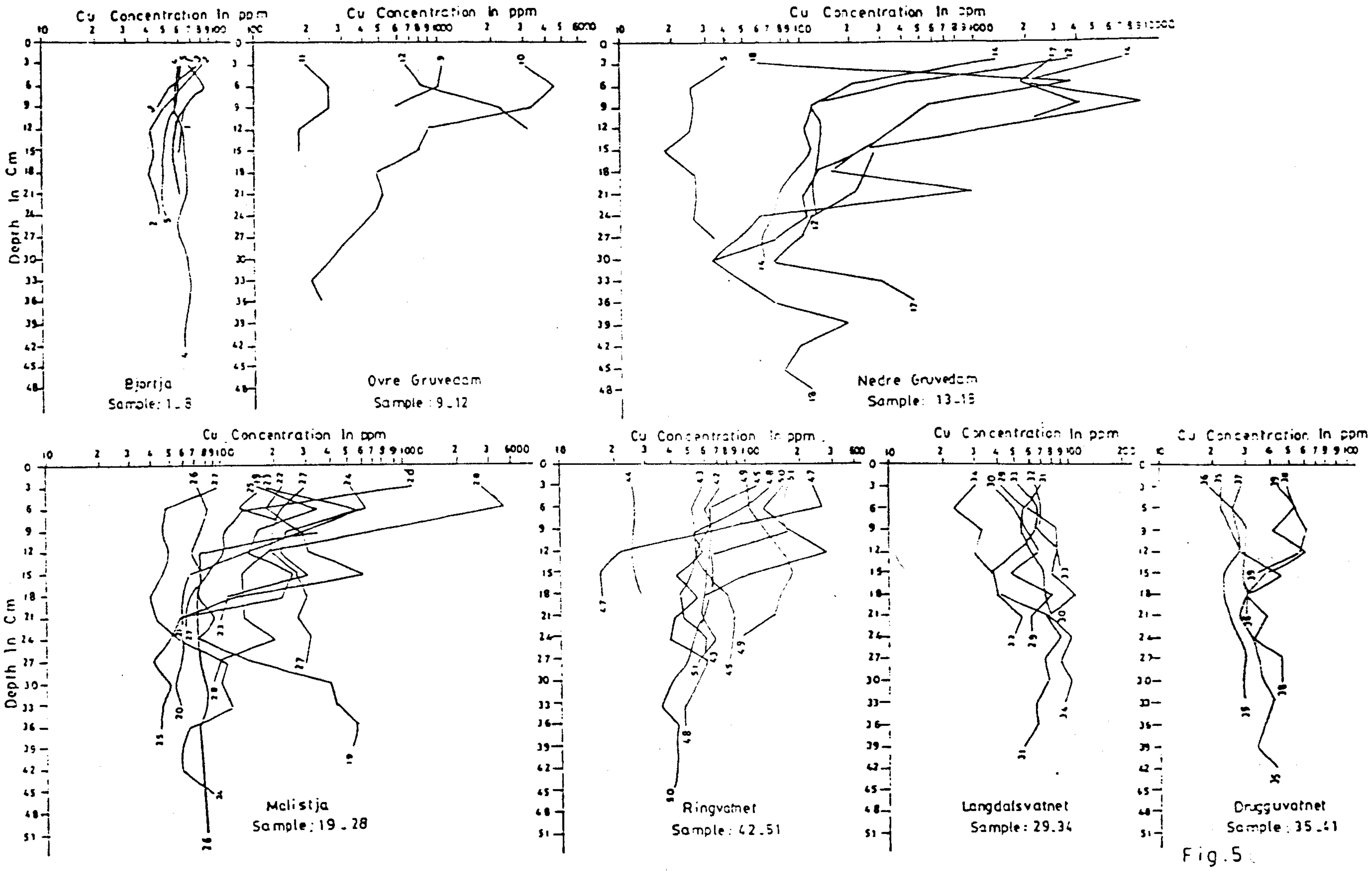

Fig. 5. Profiles of Cu content in contaminated and uncontaminated sediments of Lokken area, Norway.

contrary, the sediments of lake Langdalsvatnet which is further east of the abandoned copper mine show more variation in concentration of copper as compared to Bjortja (ca. 20-100 ppm). The concentration of copper in the sediments of Drugguvatnet lake is less than that in Langdalsvatnet lake which is a neighbouring and connected lake.

Apparently, Ovre Gruvedam lake does not have any feeding stream from the mine area and the water of Lake Bjortja pours into it. This lake shows radical and diverse changes in Cu concentration with depth at different sample sites. The Cu content in sediment sample of site 11 is nearly equal to the "standard average" concentration. The variation in copper concentration at different sample sites is probably due to varying degree of contamination in different parts of this lake. This condition of Cu enrichment and depletion at different sites may be due to incipient drainage. The higher value of Cu concentration in deeper parts of sediment colum (ca. 200-350 ppm) of site 10 may be attributed to some local mineralization around the sample site.

Nedre Gruvedam has incoming streams directly from the abandoned Dragset Mine area. Copper in the sediments of different sites of this lake shows a general decrease in its concentration with increase in depth of sediments. Sample site 13 of lake Nedre Gruvedam is not far from the adjacent lake Ovre Gruvedam which feeds the bulk of its water to this lake, but very high concentration of copper as compared to site 14 and 15 of the same lake can be observed. The effect of contamination is more pronounced in the upper 15 cm thickness of the sediments except in the samples of site 15 which show copper concentration nearly equal to the "standard average". The samples from the sediment-water interfaces of different sites of this lake show some major irregularities in Cu content but with increase in depth, a general decrease in Cu concentration can be observed. A depth of about 21 cm in lake-bottom sediment column appears as a turning point in the concentration level of copper. No effect of copper contamination was found in the sediment column below the depth of 21 cm even in the known contaminated lakes. This depth of contamination decreases to 18 cm in Lake Malistja. The decrease in depth of contamination is probably because of dilution of copper by greater bulk of water and less quantity of fine sediments and copper ions transported from one lake to the other. The depth of contamination in sediment column helps in recomputing the rate of sedimentation. Organic matter present in the lake water and sediments could be an important factor in irregular distribution of copper in lake-bottom sediments.

Site 17 in Lake Nedre Grubedam is not far from the incoming stream from the mine locality but the sediments do not show any higher Cu concentration as compared to sites 13, 14 and 16, probably due to movement of water towards the deeper part away from the inlet stream.

Lake Malistja receives the bulk of its water from the contaminated Nedre Gruvedam lake. In addition to the streams from the western side, no sign of any stream coming from the mine area into this lake is observable. The higher concentration of copper in the upper 12 cm thickness of the sediment column of sample site 28 is quite prominent. The concentration decreases with depth and reaches to average at 21 cm depth level from each site except site 19. Wide concentration and dispersion of copper is prominent in the sediments of this lake, but the degree of dispersion is less erratic than at Nedre Gruvedam.

Lake Ringvatent has its water supply mainly from Lake Malistja but there are 2 streams from the western side not far from the sample sites 41 and 43. There are also 2 incoming streams from the eastern side which fall in the lake near sites 45 and 47. The thickness of sediment at sites 40 and 41 are very shallow and are not plotted in Fig. 5.

Copper in the sediment samples of sites 40, 41 and 44 is exceptionally low and shows invariable distribution. Other sample sites show variation in concentration with depth in the upper 18cm thickness of the sediment column which is probably due to variable dilution of the contamination coming in the water from Lake Malistja.

CONCLUSIONS

1. The method devised for sampling appears simple and less expensive as compared to the methods previously adopted.

2. To get sediment column exactly from the desired site of the lake, it is better to work on lakes while frozen.
3. The column sample of sediments is obtainable without any disturbance of physical characteristics of sediments.
4. The sediments contamination is limited upto 21 cm depth-level of lake bottom.
5. The down-core variations of Cu concentration from the contaminated and uncontaminated lakes under study showed encouraging results for using this technique for geochemical exploration of ore deposits in glaciated terrains.

ACKNOWLEDGEMENTS

The senior author is very much indebted to Norwegian Agency for International Development (NORAD) for offering postdoctoral fellowship and financial assistance which made the work possible. We have deep sense of gratitude to late Professor Dr. Chr. Oftedhal, Director, Institute of Geology, Technical University of Norway and Dr. B. Bolviken, Director, Chemical Division, Geological Survey of Norway, Trondheim, for their interest, encouragement, and providing facilities during the work. Our thanks are also due to Eng. Rolf Nelsen and his colleagues who cooperated and assisted in the field during collection of samples and field data in severe winter season of Central Norway. The chemical analyses of minor elements were carried out in the Geochemical Laboratories of Geological Survey of Norway which is acknowledged with thanks and gratitude.

REFERENCES

ALLAN, R.J. (1971) Lake sediments: A medium for regional geochemical exploration of the Canadian Shield. Can. Inst. Min. Metall. Bull. 64, (715), pp. 43-59.

——— **, CAMERON, E.M. & DURHUM, C.C.** (1972) Lake Geochemistry- a low sample density technique for reconnaissance geochemical exploration and mapping of the Canadian Shield. Geochem Expl. Proc. pp. 131-160.

——— **& TIMPERLEY, M.H.** (1975) Prospecting using lake sediments in areas of industrial heavy metal contamination Congr. Prospecting in Glaciated Terrain, Geol. Surv. Canada, **3**, pp. 87-111.

ARNOLD, R.G. (1970) The concentration of metals in lake waters and sediments of some Precambrian lakes in the Flin Flon and La Ronge areas, Circ. Geol. Div. Sask. Re. Council **4**, p.1-30.

CHAPLOW, R. (1968) The geology of Lokken Area of Central Norway with particular reference to Dragset area. M.Sc. Thesis. Imperial College London. (Unpublished), 179 p.

COKER, W.B. & NICHOL, I. (1974) Metal dispersion in lake sediments related to mineralization and its role in reconnaissance in the Southern Canadian Shield. Geochemical Exploration Sp. Publ. **2.**, pp. 549-553.

——— & ——— **(1975)** The relation of lake sediment geochemistry to mineralization in the north-western Ontario region at the Canadian Shield. Econ. Geol. **70**, pp. 202-217.

DEVENPORT, P.H., HORNBROOK, E.H.W. & BUTTLER, A.J. (1974) Regional lake sediment geochemical survey of Zn mineralization in western Newfoundland. Geochem. Expl. Sp. Publ. **2**, pp. 555-578.

DYCK, W. (1971) Lake sampling vs stream sampling for regional geochemical surveys. Ge ol. Surv. Canada Pap. **71-1 (B)**, pp. 70-71.

EKMAN, V.M. (1905) An apparatus for the collection at bottom samples. Public de circonstance **27**, pp.1-6.

FREDRICKSSON, I. & QVARFORT, U. (1973) The mercury content of sediments from two lakes in Dalarna, Sweden. Geol. For. Stock. month. **92.** (2), pp. 237-242.

LAG, J. & BOLVIKEN, B. (1974) Some naturally heavy metal poisoned areas of interest in prospecting, soil chemistry and geomedicine. Norges Geologiske Undersokelse **304**, pp. 73-96.

NICHOL, I., COKER, W. B. & JACKSON, R.G. (1975) Relation of lake-sediment composition to mineralization in different limnological environments in Canada. Trans. Inst. Min. Metall. London, pp. 112-124.

ROSE, A.W., HAWKES, H.E. & WEBB, J.S. (1979) GEOCHEMISTRY IN MINERAL EXPLORATION (2nd ed). Academic Press, London, 657 p.

SCHMIDT, R.C. (1956) Adsorption of Cu, Pb, and Zn, on some common rock forming minerals and its effect on lake sediments. Ph.D. Thesis, McGill University, Montreal, Canada (Unpublished), 359 p.

STROM, K.M. (1934) A new sampler lead. Norsk. Geologisk. Tids. **14**, pp. 162-166.

TIMPERLEY, M.H. & ALLAN, R.J. (1974) The formation and detection of metal dispersion halos in organic lake sediments. J. Geochem. Expl. **3**, pp. 167-190.

Manuscript received on October 20, 1992; accepted for publication on December 31, 1992.

ACTA MINERALOGICA PAKISTANICA
VOLUME 6 (1992) pp. 55-64.

MINERAL CHEMISTRY OF A MANGANIFEROUS PEGMATITE FROM SITASAONGI BHANDARA DISTRICT, MAHARASTRA, INDIA

M. QASIM JAN
NCE in Geology, University of Peshawar, Peshawar
&
S.A. BILGRAMI
68/2, 21st St. Phase V, Defence Society, Karachi 75500

ABSTRACT: The Chikla area is made up of Late Proterozoic schists and gneisses metamorphosed to kyanite grade. Associated with these are gondites and related rocks containing manganese ore bodies which are locally cut by thin pegmatites. One of these contains abundant manganiferous xenoliths. Four samples of the pegmatite studied here contain pure albite, Na-K feldspar (An $_{0.4}$, Ab$_{85.5}$, Or$_{14.1}$), brain feldspar (Cn $_{10.5\text{-}26.7}$, Or $_{87.6\text{-}46.8}$, Ab $_{1.9\text{-}31.5}$ An $_0$), quartz, manganoan pholgopite (Mn_2O_3 1.1-1.5 wt. %), manganoan aegirine augite (MnO 2.3-2.8%), piemontite (Mn_2O_3 12.3-14.8%, Fe_2O_3 9.8-11.6%, SrO ~ 1.0%), braunite (Fe_2O_3 3.8-4.6 and 10.7-12.5%), and hollandite (Fe_2O_3 10.0-10.4%). Calcic amphibole, (MnO < 0.3%), albite, epidote (Mn_2O_3 10.0-10.4%). Calcic amphibole, (MnO < 0.3%), albite, epidote ($Mn_2O_{3\,=}$ 2.3%), manganoan aegirine augite (MnO = 2.5-2.7%), sphene and chlorite (MnO < 0.2%) were also studied in the country rock to pegmatite. The unusual mineral assemblage in the pegmatite may be due to incorporation of the country rock material.

INTRODUCTION

The manganese ore bodies at Chikla, Sitasaongi and Dongri Buzurg area of Bhandara District, Maharashtra, constitute one of the richest horizons of syngenetic manganese ores of India. The ore bodies are closely associated with gondites (metamorphosed maganiferous silicate rocks). The ore bodies occur in a terrain of Late Proterozoic schists, gneisses, calc-silicate granulites and quartzites metamorphosed to kyanite grade (Bilgrami, 1955; Mitra, 1964a; Roy, 1966). These rocks are cut by pegmatites containing abundant enclaves of the country rocks. The ore bands in Saitasaongi are 2.5 to 6m thick, strongly folded and faulted, and the entire area has passed through a complex tectono-metamorphic history (Mitra, 1964a).

The first detailed reference to the occurrence of manganese minerals in South India was made by Fermor (1909). Since then many workers have presented data on the physical properties, mineral chemistry and parageneses of these minerals (for details see Roy, 1966, 1981). Bilgrami (1951, 1955, 1956) and Mitra (1964b) described many minerals from a 200 m long and 1-3 m thick pegmatite in the Sitasaongi mine. This pegmatite, cutting the manganese ore band, quartzite, gondite, pelitic schists and gneisses at the 60-feet level of the mine, has been carefully mapped by Mitra (1964b). The pegmatite has a sharp contact with the country rocks but at places it appears to "replace" the ore body. It contians abundant, irregularly distributed xenoliths of the country rocks, especially at margins (Fig. 1).

Following array of minerals has been reported from the pegmatite: albite, alurgite, apatite, barite, biotite, blanfordite, braunite, greenovite, juddite, lepidolite, manganophyllite, microcline, microperthite, orthoclase, piemontite, quartz, sericite, sphene, rhodonite, tirodite, tremolite and winchite, with some of the mica books reaching 8 cm in size (Bilgrami, 1951). Mitra (1964b) has added bixbyite, cryptomelane, hollandite, manganite and pyrolusite to this list, and we have identified barian feldspar as an additional phase. Many of the minerals, especially those rich in Mn, are resticted to the xenoliths, but others

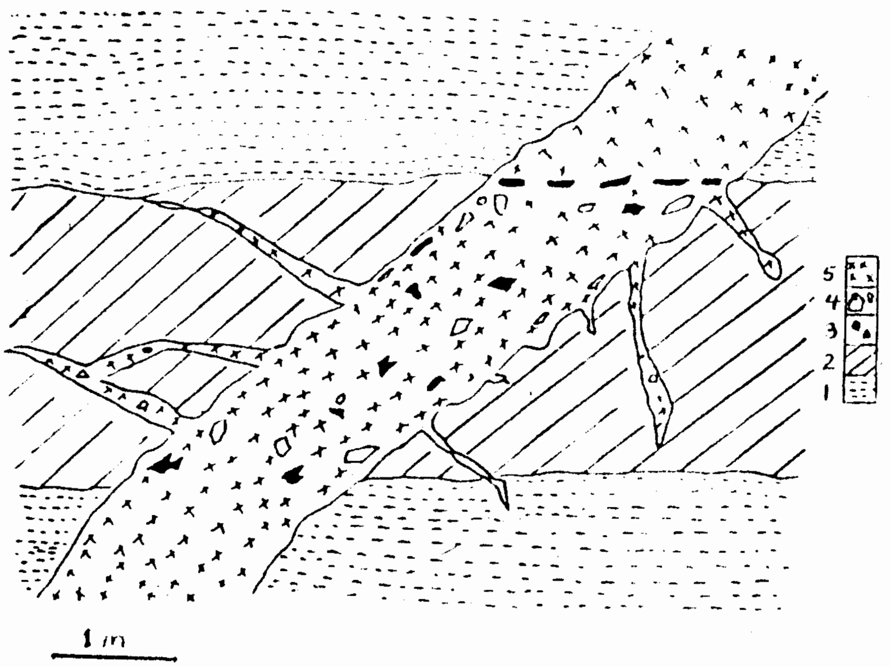

Fig. 1. Plan at the 60-feet level of the Sitasaongi mine, Chikla, showing the pagmatite cutting through the country rocks. (1) muscovite schist, (2) manganese ore band,(3) ore xenoliths, (4) Mn-silicate minerals, (5) pegmatite (modified after Bilgrami, 1955).

appear to have crystallized from the pegmatite melt, suggesting the assimilation of the country rocks.

Bilgrami (1955, 1956) presented bulk mineral analyses of Mn amphiboles (juddite, winchite, tirodite, chiklite), pyroxenes (blanfordite, rhodonite), micas (alurgite, manganophyllite) and piemontite. In this paper we present microprobe analytical data on some minerals of the pegmatite. Our work is restricted to limited material which consisted of a rock sample (B), a mica flake (M) and two powder concentrates (J and R) from the pegmatite, and powder of a gneissose country rock (W). The pegmatite sample contains large crystals of piemontite (up to 3 cm long) in a matrix of feldspars, quartz, piemontite, and dusty braunite and hollandite. Textural and petrographic features of the minerals in the pegmatite have been described at length by Bilgrami (1951) and Mitra (1964b), so the present study is restricted to mineral chemistry. Analyses were performed with electron probe microanalyser, using suitable minerals and synthetic oxides as standards.

MINERAL CHEMICAL DATA

Piemontite

Manganese epidotes were analysed in one pegmatite sample (B) and the country rock (W). Representive analyses, recalculated on 12.5 oxygen-basis, are presented in Table 1. All iron and manganese was considered to occur in trivalent form. The recalculated analyses are quite close to ideal formula Ca_2 $(Mn^{3+}, Fe^{3+} Al)_3$ O. $[Si_2O_7]$ $[SiO_4]$, ignoring OH.

The coarser epidote (some > 2.5 cm in length) in the pegmatite is uniform in composition, with only a slight increase in Fe_2O_3 with or without

Table 1. Representative microprobe analyses of piemontite

	1	2	3	4	5	6
SiO_2	35.77	35.77	35.67	36.06	35.58	37.17
TiO_2	0.01	0.01	0.00	0.01	0.01	0.11
Al_2O_3	15.24	16.36	15.36	15.49	14.45	22.08
Fe_2O_3	10.10	9.92	10.10	10.38	11.55	14.40
Mn_2O_3	14.13	12.90	13.48	13.34	13.09	2.38
MgO	0.08	0.06	0.07	0.05	0.02	0.11
CaO	21.42	21.57	21.45	21.23	21.45	23.05
Na_2O	–	–	0.02	–	0.01	0.04
K_2O	–	–	0.01	–	0.00	0.00
SrO	–	–	1.13	–	–	–
BaO	–	–	0.08	–	–	–
TOTAL	96.75	96.59	97.37	96.56	96.16	99.34
Number of cations based on 12.5 oxygens:						
Si	2.998	2.986	2.991	2.975	3.010	2.952
Ti	0.000	0.000	0.000	0.000	0.000	0.006
Al	1.506	1.610	1.518	1.550	1.442	2.068
Fe^{3+}	0.637	0.623	0.637	0.663	0.736	0.861
Mn^{3+}	0.902	0.820	0.861	0.862	0.843	0.144
Mg	0.010	0.007	0.008	0.006	0.003	0.013
Ca	1.924	1.929	1.927	1.931	1.945	1.962
Sr	–	–	0.055	–	–	–
Ba	–	–	0.003	–	–	–

1,2,3: Peimontite spot analyses in the central and middle parts of a large phenocryst in sample B (pegmatite).
4: Margin of above.
5: Groundmass piemontite in B1.
6: Piemontite from country rock sample W (gneiss).

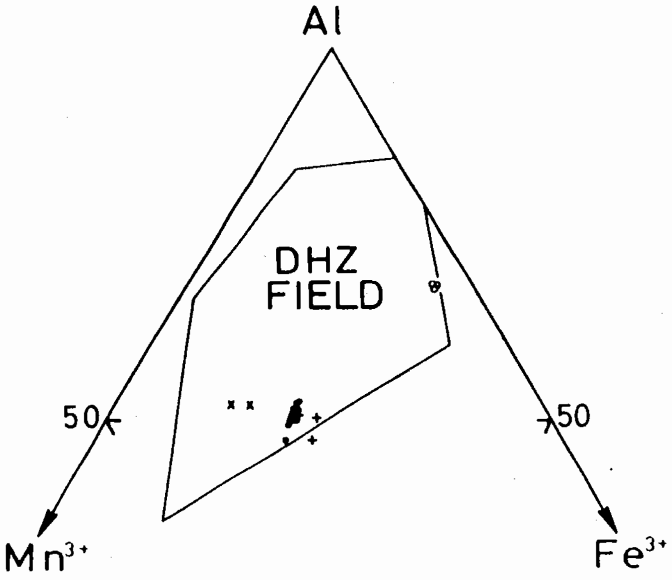

Fig. 2. Al-Fe-Mn plots of the piemontite analyses compared with the compilation of Deer et al. (1986) "DHZ field". Analyses of the "phenocrystic" (•) and groundmass (+) piemontite in pegmatite sample B are much more enriched in Mn than those of the gneissose country rock W (o). Also shown are the two analyses reported in Bilgrami (1956) (X).

a decrease in Mn_2O_3, in some marginal parts. Such margins bridge the gap towards the fine-grained piemontite which contains a little higher Fe_2O_3 and lower Mn_2O_3 than the cores of the coarse crystals. The noteworthy features of the pegmatite piemontites are high Mn_2O_3 (12.3 to 14.1 wt%) and SrO (1.1%), and the presence of BaO (the latter two analysed in only one of the 22 spots). The Al-Fe^{3+} -Mn^{3+} plots of the analyses from the two rocks are compared with piemontites reported in Deer et al. (1986) in Fig. 2.

Bilgrami (1956) presented chemical analyses of two piemontites from the pegmatite, and of a bulk- sample of schist from the Chikla area. The present analyses are very similar to the one from the schist, but his pegmatitic piemontite is enriched in Mn_2O_3 and impoverished in Fe_2O_3. There is no evidence to suggest that his piemontite concentrate contained impurities of a Mn-rich phase. Both sets of analyses are reliable because the proportions of cations fulfill the stoichiometric requirements. This suggests that the Mn^{3+}: Fe^{3+} intake of the piemontite in the pegmatite varies from place to place and may depend on the environment, i.e., chemical composition of the xenoliths. It may be worth mentioning that Bilgrami's (1956) piemontite analysis from the pegmatite is amongst the most Mn-enriched so far reported.

The analyses of the manganoan epidote from the country rock sample contain higher Al_2O_3 and Fe_2O_3, and much lower Mn_2O_3 than those from the pegmatite. The amount of Mn^{3+} + Fe^{3+} cations in the clinozoisite-pistacite series seldom exceeds unity, whereas in the piemotite it is commonly above unity (Deer et al., 1986). The present analyses are border-line cases in this respect, with $Fe^{3+} + Mn^{3+} \sim 1.0$ Although displaying light hue, the piemontite in the country rock is also strongly pleochroic (yellow to deep pink) due to its appreciable manganese. The pegmatite piemontite is peppered with Mn ore and deep -coloured, with brownish and violet pink to ruby red pleochroism.

Manganoan Ca-Na Pyroxene

Pink to blue pleochroic clinopyroxene, containing 2.3 to 2.8 wt.% MnO, occurs in two of the four pegmatite samples (J and R) and the country rock (W). Representative analyses are shown in Table 2. Despite taking all the iron as Fe^{3+}, there is a slight excess of Na in the analyses, although the recalculated analyses approach the ideal formula (Na, Ca) (Fe^{3+}, Mn Mg, Al) [Si_2O_6]. According to IMA nomenclature (Morimoto et al., 1988), the analyses classify as manganoan aegirine-augite. A number of analyses plot above the Q-J tie line (Fig. 3), possibly due to a slight overestimation of Na_2O or underestimation of Al_2O_3.

Table 2. Representative analyses of clinopyroxenes.

	1	2	3	4	5
SiO_2	53.54	53.34	53.82	53.69	53.03
TiO_2	0.45	0.45	0.46	0.47	0.44
Al_2O_3	0.59	0.61	0.62	0.63	0.64
Fe_2O_3	22.81	20.56	19.14	20.16	19.99
MnO	2.71	2.33	2.50	2.80	2.71
MgO	4.55	4.42	6.02	5.84	5.21
CaO	6.09	7.69	7.76	8.15	7.94
Na_2O	10.64	8.28	9.35	9.67	10.35
K_2O	0.00	0.00	0.00	0.00	0.00
Total	101.38	97.68	99.67	101.41	100.31
Calculation of atoms based on 6(O):					
Si	1.964	2.012	1.994	1.968	1.970
Ti	0.013	0.013	0.013	0.013	0.012
Al	0.026	0.027	0.027	0.027	0.028
Fe^{3+}	0.700	0.649	0.593	0.618	0.621
Mn	0.084	0.074	0.078	0.087	0.085
Mg	0.249	0.248	0.332	0.319	0.288
Ca	0.239	0.311	0.308	0.320	0.316
Na	0.757	0.606	0.681	0.687	0.746

1: Manganoan aegirine-augite from country rock W.

The analyses display fairly consistent composition within the demain of a thin section, and sample to sample variation is limited (Fig.3). All are characterized by having low TiO_2 and Al_2O_3, and Na_2O in excess of CaO. Their manganese content is fairly uniform, but the country rock pyroxene contains higher Fe_2O_3 and Na_2O and lower CaO and MgO than the other two. When compared with the two blanfordite analyses reported in Bilgrami (1956), the present analyses are enriched in Fe_2O_3, CaO and MgO, and impoverished in MnO and, especially, Al_2O_3 (10 to 14 times). However, similar analyses have been reported in the literature (cf. Deer et al., 1978).

Amphibole

Unusual manganoan amphiboles (winchite, tirodite, and chiklite) have been reported in

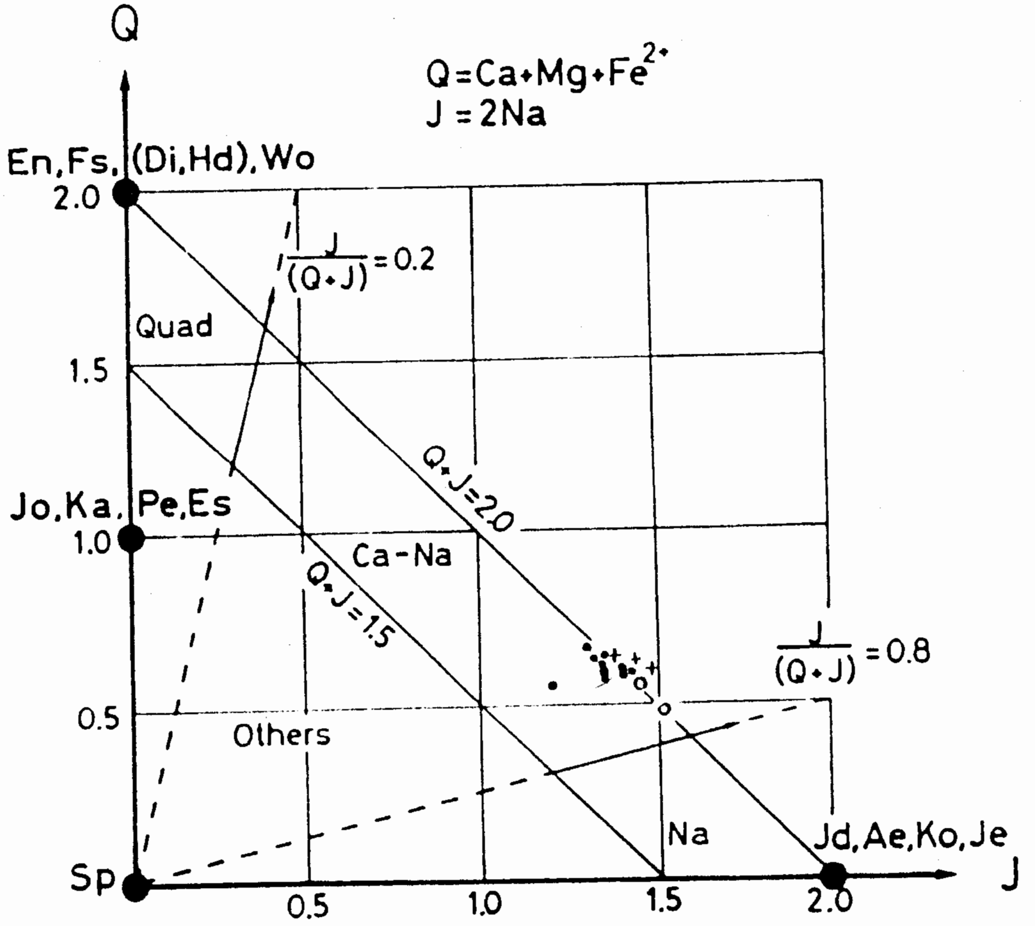

Fig. 3. Plots of the manganoan aegirine augite analyses according to the IMA nomenclature (Morimoto et al., 1988). Crosses and dots represent analyses from pegmatite samples J and R, respectively and open circles are from country rock W.

manganese-rich rocks (e.g., Bilgrami, 1955). The samples investigated during the present work are apparently devoid of manganoan amphibole. Calcic amphibole, however, is present in the country rock. Several probe analyses reveal that it ranges in composition from magnesio-horblende to actinolite through actinolitic hornblende (cf. Leake, 1978). All the analyses (Table 3) are typically depleted in MnO (<0.3%). The actinolite (anal. 3) is odd: it has a total vacancy in A site and has insufficient occupancy in C and B sites. This is possibly due to overestimation of SiO_2.

Manganoan Phlogopite

In the Chikla pegmatite, Bilgrami (1956) reported that alurgite (manganoan phengite) and manganophyllite (mangnoan phlogopite) books reach up to 8 cm in size. Several analyses were here performed on a 1 cm broad mica flake from the pegmatite. All are similar in composition and can be classified as manganoan phlogopite. They are broadly similar to the bulk analysis of manganoan phlogopite from the pegmatite (Bilgrami, 1956) except for their lower iron and higher magnesium contents. The lower K_2O and Na_2O in our analyses (Table 4) probably reflect understimation of these components.

Chlorite

Grains of a yellow micaceous mineral occur in the country rock sample. Three analyses of the flakes suggest that these are chlorite (Table 4). They are depleted in MnO (<0.2%) and classify as diabantite according to Hey's (1954) classification. An analysis of the yellowish mica contains 6% K_2O and is intermediate (? mixed) between chlorite and biotite. There is, thus, a possibility that the chlorite is a retrograde product of biotite.

Sphene

Its analysis from a country rock sample. (Table 4) is devoid of manganese.

Feldspar

Table 3. Representative amphibole analyses from the country rock sample W.

Weight Percentages				*Number of Cautions per 23(O):*			
	1	2	3		1	2	3
SiO_2	49.26	49.76	59.52	Si	7.050	7.245	8.306
TiO_2	0.60	0.47	0.00	Ti	0.065	0.052	0.000
Al_2O_3	5.79	4.00	1.36	Al	0.977	0.686	0.224
Fe_2O_3	6.73	6.35	0.00	Fe^{3+}	0.725	0.696	0.000
FeO	9.95	7.83	11.13	Fe^{2+}	1.191	0.954	1.299
MnO	0.25	0.22	0.11	Mn	0.030	0.027	0.013
MgO	13.89	15.40	14.40	Mg	2.963	3.341	2.995
CaO	12.22	12.23	11.48	Ca	1.874	1.908	1.717
Na_2O	0.95	0.63	0.21	Na	0.263	0.178	0.057
K_2O	0.32	0.16	0.00	K	0.58	0.030	0.000
Total	99.96	97.05	98.21				

Analyses are recalculated to 13.00 cations on Ca, Na, K–free basis.
Iron is partitioned on the basis of charge–balance.

Table 4. Representative mica, chlorite and sphene analyses.

Weight percentage:				*Numbers of cations:*			
	1	2	3		1	2	3
SiO_2	40.83	34.16	30.08	Si	5.897	6.845	4.000
TiO_2	1.31	0.10	35.82	Ti	0.142	0.015	3.582
Al_2O_3	16.75	16.23	1.19	Al	2.851	3.834	0.186
FeO_t	4.21	21.10	1.89	Fe^{2+}	0.508	3.536	0.189
MnO	1.63	0.10	0.00	Mn	0.200	0.017	0.000
MgO	19.04	16.30	0.03	Mg	4.098	4.868	0.005
CaO	0.00	0.37	27.13	Ca	0.000	0.079	3.866
Na_2O	0.20	0.06	0.11	Na	0.056	0.024	0.028
K_2O	8.81	0.12	0.00	K	1.623	0.031	0.000
Total	92.78	88.54	96.25				

* 1. Manganoan phlogopite from the pegmatite sample M, recalculated on the basis of 22 oxygens.
2. Chlorite from country rock W, recalculated on 28 oxygen basis.
3. Sphene from sample W, recalculated to 4 Si atoms. Total iron as Feo.

The amphibole-bearing country rock sample contains only one type of feldspar, i.e., very pure albite (Ab 99.8 mole%). In the pegmatite sample R there are two types of feldspar: Na-(Ca) and K-Ba-(Na). The former is mostly pure albite (Ab=99 mole %), but one analysis gives the composition An $_{4.3}$, Ab $_{95.4}$, Or $_{0.2}$. This is the most clacic of the feldspars in the samples analysed during the present course of investigation. The barian feldspar (two analyses) has the composition Cn $_{14.2\text{-}14.3}$, Or $_{84.0\text{-}81.4}$ Ab $_{1.8\text{-}4.3}$.

There is a substantial variation in the composition of feldspars from the pegmatite sample B. These can be grouped into Na–, Na–K–, and K–Ba–Na–types (Table 5, anal. 1–6). The Na–

Table 5. Representative analyses of feldspar

	1	2	3	4	5	6	7	8	9	10
SiO_2	70.16	67.53	60.20	56.47	52.99	53.46	69.07	70.04	68.78	57.19
TiO_2	–	–	–	–	–	–	0.01	0.03	0.01	0.22
Al_2O_3	20.33	17.59	19.13	18.61	21.33	20.85	19.50	20.09	20.57	18.00
Fe_2O_3	–	–	0.07	–	0.14	0.12	0.07	0.53	0.08	0.43
MnO	–	–	0.03	–	0.03	0.00	0.00	0.02	0.00	0.00
MgO	–	–	0.00	–	0.00	0.00	0.01	0.00	0.00	0.00
CaO	0.13	0.08	0.00	0.00	0.00	0.00	0.01	0.02	0.80	0.00
Na_2O	10.66	8.86	0.21	3.48	0.85	0.34	11.44	10.09	9.80	0.47
K_2O	0.04	2.21	14.82	8.40	9.66	11.11	0.02	0.11	0.04	13.44
BaO	–	–	5.75	10.65	15.36	13.79	–	–	–	7.70
SrO	–	–	0.11	–	0.00	0.02	–	–	–	–
Total	101.32	96.27	100.32	97.61	100.36	99.69	100.13	100.93	100.08	97.45
End member composition:										
Cn	–	–	10.5	19.3	30.1	26.7	–	–	–	14.3
Or	0.3	14.1	87.6	49.5	61.6	70.0	0.1	0.0	4.3	81.4
Ab	99.0	85.5	1.9	31.2	8.2	3.3	99.8	99.3	95.4	4.3
An	0.7	0.0	0.0	0.0	0.0	0.0	0.0	0.7	0.2	0.0

1-2: Albite and oligoclase, 3-6 barian feldspars from sample B.
4: Host to exsolved compositions represented by 5 and 6.
7: Albite from country rock W.
8-9: Albite and barian feldspar from pegmatite sample R.

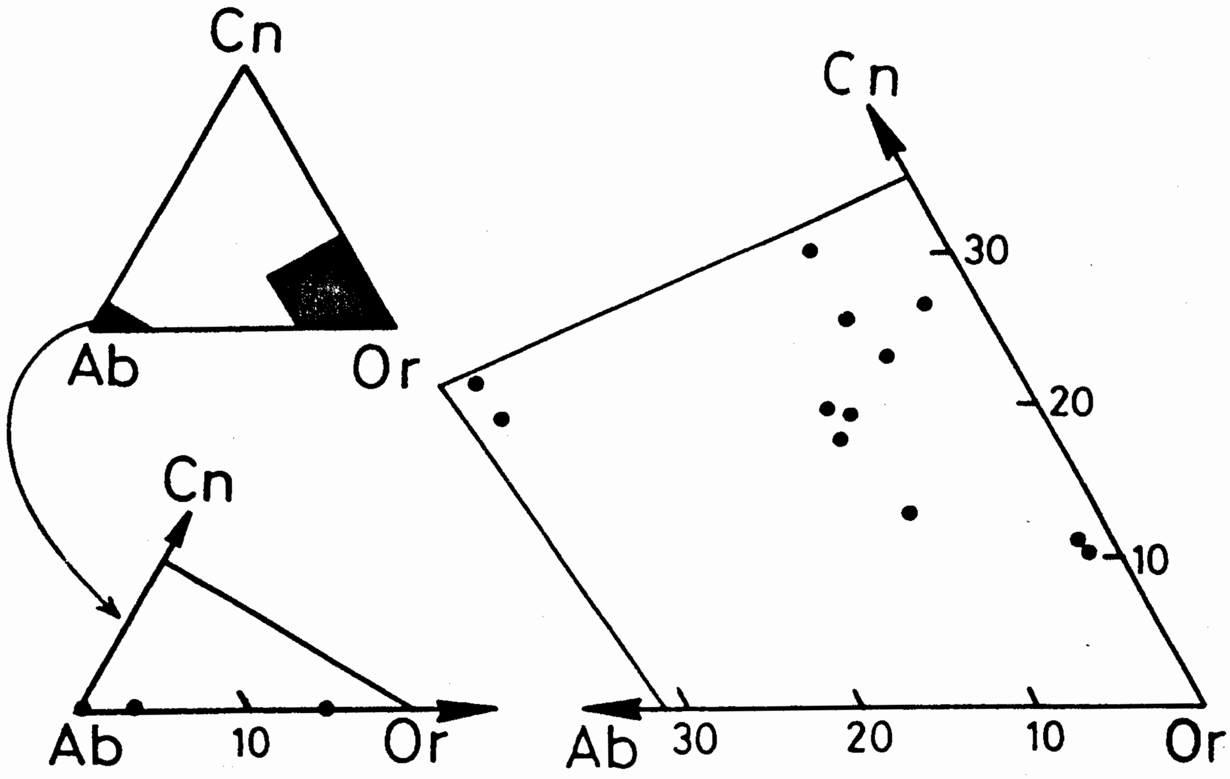

Fig. 4. Composition of the feldspar analyses from pegmatite sample B in terms of orthoclase-celsian-albite end-members.

Table 6. Representative analyses of braunite recalculated on 12(O) basis

Weight percentages:						Number of cations:					
	1	2	3	4	5		1	2	3	4	5
SiO_2	9.79	9.64	9.51	9.70	9.72	Si	0.985	0.964	0.958	0.974	0.987
TiO_2	0.00	0.02	0.00	0.06	0.05	Ti	0.000	0.002	0.000	0.005	0.004
Al_2O_3	0.14	0.21	0.15	0.03	0.02	Al	0.017	0.025	0.018	0.004	0.002
Fe_2O_3	11.54	12.40	10.67	3.86	4.65	Fe^{3+}	0.874	0.932	0.809	0.292	0.356
Mn_2O_3	66.85	66.60	67.87	74.85	73.12	Mn^{3+}	5.128	5.069	5.209	5.726	5.654
MnO	8.67	8.06	8.65	10.09	10.39	Mn^{2+}	0.739	0.682	0.738	0.858	0.894
MgO	1.23	1.52	1.11	0.78	0.51	Mg	0.184	0.226	0.167	0.116	0.077
CaO	0.72	1.14	1.16	0.32	0.26	Ca	0.077	0.122	0.126	0.034	0.028
Na_2O	–	0.00	0.00	0.01	0.01	Na	–	0.000	0.000	0.002	0.002
K_2O	–	0.00	0.00	0.00	0.00						
BaO	–	0.00	0.00	–	–	X	1.00	1.03	0.98	0.98	0.99
SrO	–	–	0.00	–	–	Y	6.00	6.00	6.02	6.02	6.01
Total	98.94	99.59	99.12	99.70	98.73	Z	1.00	0.99	1.03	1.01	1.00

1,2,3 from pegmatite sample B; 4,5 from pegmatite sample R.

Table 7. Representative analyses of hollandite from pegmatite sample B, recalculated on 16(O) basis.

Weight Percentages:				Number of Cations:			
	1	2	3		1	2	3
SiO_2	0.00	0.02	0.05	Si	0.000	0.003	0.007
TiO_2	0.00	0.00	0.00	Ti	0.000	0.000	0.000
Al_2O_3	0.65	1.15	0.96	Al	0.110	0.190	0.159
Fe_2O_3	10.04	10.42	10.99	Fe^{3+}	1.082	1.111	1.158
MnO_2	64.30	64.29	64.18	Mn^{4+}	6.362	6.295	6.214
MnO	3.00	2.80	5.00	Mn^{2+}	0.364	0.336	0.593
MgO	0.00	0.01	0.00	Mg	0.000	0.002	0.000
CaO	0.00	0.03	0.02	Ca	0.000	0.004	0.003
Na_2O	0.04	0.07	0.02	Na	0.010	0.019	0.005
K_2O	0.07	0.05	0.03	K	0.012	0.008	0.005
BaO	19.68	19.58	18.10	Ba	1.101	1.087	0.993
SrO	0.15	0.05	0.04	Sr	0.012	0.004	0.003
Total	97.93	98.47	99.39				

type is again pure albite (Ab_{99}), whereas the Na–K variety (only one analysis) is made up of $An_{0.4}$, $Ab_{85.5}$ Or $_{14.1}$. No unmixing is apparent in this grain. The associated barian feldspar shows a considerable compositional variation and exsolution on a fine scale. One host grain has the composition Cn $_{19.3}$ Or $_{49.5}$, Ab $_{31.2}$, with exsolved component consisting of Cn $_{26.7-31.1}$, Or $_{70.0-61.6}$, Ab $_{3.3-8.2}$. All the feldspar analyses in the sample B are characteristically impoverished in CaO. The albites contain up to 1.1 mole% An (averaging 0.4 mole%), whereas the barian feldspars are totally devoid of CaO. The analyses are also impoverished in MnO and SrO depsite a probable abundance of Mn in the rocks due to assimilation/ absorption. Viswanathon and Kielhorn (1983) reported considerable amounts of Fe^{3+} (related to Al) in their analyses of barian feldspars, but those of Sitasaongi are substantially impoverished in this component also.

The compositions of the feldspar in terms of orthoclase (microcline) - celsian-albite components is plotted in Fig. 4. The Ce content of the barian feldspars shows an overall range of 10.5 to 30.1 mole %. Barian feldspars form a complete solid solution at high temperature, but miscibility gaps occur in those formed at low temperature. Possible imscibility gaps have been reported in the ranges Cn_{21} to Cn_{29} (Viswanathan and Kielhorn, 1983), Cn_{10} to Cn_{30} and Cn_{60} to Cn_{80} (Gay and Ray, 1988), Cn_{15} to Cn_{25}, Cn_{30} to Cn_{40} and Cn_{47} to Cn_{65} (Pan & Fleet, 1991). Our data on feldspar from the Chikla pegmatite show a gap between Cn_{14} and Cn_{18}.

Braunite

Braunite is a common mineral in manganese deposits. In the Sitasaongi pegmatite sample B, fine-grained braunite and hollandite are closely associated matrix minerals. They occur in clusters or may be scattered, and as inclusions in other minerals. Braunite also occurs in sample R of the pegmatite. Representative analyses from the two are shown in Table 6. All iron has been assumed as Fe_2O_3 and manganese has been portioned into Mn_2O_3 and MnO so as to conform to ideal formula 3 $(Mn^{3+}, Fe^{3+})_2O_3$ Mn^{2+} SiO_3 or R^{2+} R^{3+}_6 SiO_{12}.

Common braunite contains about 9-10 % SiO_2 but the so-called braunite-II, reported from the Kalahari manganese ore field (Villiers, 1965), contains less than half as much silica. Muan (1959) emphasised an extremely strong stabilizing effect of silica on Mn^{2+} in braunite structure. The presence of silica in the mineral has been attributed to coupled substitution Mn^{3+} Mn^{3+} = Mn^{2+} Si^{4+} (Moore & Araki, 1976). A considerable amount of Fe_2O_3 can substitute for Mn_2O_3 (Villiers & Herbstein, 1967), and ferrian braunites with more than 23% Fe_2O_3 have been analysed (Roy, 1981).

The braunites analysed in the two rocks from Sitasaongi pegmatite differ considerably in Fe_2O_3, Mn_2O_3, CaO and MgO contents. In braunite of sample B Fe_2O_3 ranges from 10.7 to 12.5% and in sample R it is only 3.9 to 4.6%. Both groups of analyses show some solid solution towards $CaMn^{3+}{}_6[Si_4/O_8]$ end members. In sample B, these components range from 7.5 to 1.22 and 15.9 to 22.6 mole %. and in sample R from 2.8 to 3.4 and 7.4 to 12.2 mole %, respectively. Again, the vairation suggests environmental control on the composition of the mineral which might be xenocrystic.

Hollandite

This mineral was first reported by Fermor (1909) from Kajlidongri manganese ore deposits of India. Since then, it has been described from many other localities in India and elswhere (Roy, 1966, 1981). Of the samples studied here, it was found only in the pegmatite sample B as a matrix (probably xenocrystic or xenolithic) mineral in association with braunite. The approximate composition of hollandite is $BaMn_8O_{16}$ (Turner & Busseck, 1979). It belongs to a group of minerals forming an isostructural series with a general formula $A_{1\text{-}2}$ $(Mn, Fe)_8O_{16}$. XH_2O, where A may principally be Ba (hollandite), K (cryptomelane, some analyses of which contain > 5% ZnO), Na (manjiroite), or Pb (coronadite).

Three electron microprobe analyses of the hollandite are given in Table 7. All the iron has been assumed to be Fe_2O_3 and the partitioning of manganese into MnO and Mn_2O_3 has been carried out such that A=1 formula unit on 16 oxygen basis. Despite taking most of the manganese as Mn_2O_3, the number of atoms in A exceeds 1 formula unit in the first two analyses, suggesting an overestimation of BaO. These analyses are quite similar to those from Kajlidongri except for slightly higher amounts of BaO. Compared to hollandite analyses from other areas reported in Roy (1966, Table 14; 1981, Table 2), the Sitasaongi hollandites contain lower amounts of Mn oxides, SiO_2 and alkalis, but considerably higher Fe_2O_3 and BaO.

PARAGENESIS

An unusually large numbr of minerals is present in the pegmatite. Some of the minerals, such as quartz and feldspar, are the usual minerals found in granitic pegmatites and represent crystallization from fluid/volatile-rich silicate "melts". The paragenesis of the Mn oxides in the pegmatite is similar to that of metamorphosed Mn ores of the area (Roy & Mitra, 1964); these must have been incorporatd as xenoliths and xenocrysts in the pegmatite. The Mn bearing silicates (pyroxene, amphibole, mica, epidote) are unusual for granitic pegmatites. These may be xenolithic in origin; formed by the reaction of the pegmatite melt with "higher" oxides of Mn (e.g., pyrolusite, cryptomelane) of the ore body or due to assimilation. The Mn-silicates are well-crystallised and have no reaction rims, favouring the last possibility. The "lower" oxides such as braunite, bixbyite, etc., whose structure is stable at high temperature (Mitra, 1964b), may not have played much role in the production of the manganese silicates.

ACKNOWLEDGEMENT

The analytical work for this paper was performed at the Universities of Peshawar and South Carolina. We are thankful to Jim Witke, John Shervais and M. Barkatullah for their advice during the probe analyses.

REFERENCES

BILGRAMI, S.A. (1951) The mineralogy and petrology of the manganese bearing rocks of Chikla area (Bhandara district, M.P.). M.Sc. thesis, Indian School of Mines, Dhanbad (Unpublished).

——— (1955) Manganese amphiboles from Chikla, Bhandara district, India. Min. Mag. **30**, pp. 633-644.

———(1956) Manganese silicate minerals from Chikal, Bhandara district, India. Min. Mag. **31**, pp. 236-244.

DEER, W.A., HOWIE, R.A. & ZUSSMAN, J. (1978) ROCK-FORMING MINERALS, Vol.2A. Longman, Essex.

———, ——— & ——— (1986) ROCK-FORMING MINERALS, Vol.1B. Longman, Essex.

FERMOR, L.L (1909) The manganese-ore deposits of India. Mem. Geol. Surv. India. **37**, pp. 68-77.

GAY, P. & ROY, N.N. (1968) The mineralogy of the potassium-barian feldspar series. III. Subsolidus relationships. Min. Mag. **36**, pp. 914-932.

HEY, M.H (1954) A review of the chlorites. Min. Mag. **30**, pp. 277-292.

LEAKE, B.E. (1978) Nomenclature of amphiboles. Min. Mag. **42**, pp. 533-563.

MITRA, F.N. (1964a) Structure and tectonics of the area around Dongri Buzurg, Chikla and Sitasaongi, Bhandara District, Maharastra. Proceeding National Institute of Science, India, **30**, pp. 253-281.

—— (1964b). Manganese minerals in a clac-alkaline pegmatite vein cutting across the mangenese ore band, Sitasaongi mine, Bhandara district, Maharastra. Indian Mineralogist **5**, pp.1-16.

MOORE, P.B. & ARAKI, T. (1976). Braunite: its structure and relationship to bixbyite, and some insights on the genealogy of fluorite derivative structures. Am. Mineral. **61**, pp. 1226-1240.

MORIMOTO, N., FABRIES, J., FERGUSON, A.K., GINSBURG, I.V., ROSS M., SEIFERT, F.A., ZUSSMAN, J., AOKI, K. & GOTTARDI, G. (1988) Nomenclature of pyroxenes. Am. Mineral. **73**, pp. 1123-1133.

MUAN, A. (1959) Phase equibilria in the system manganese oxide-SiO_2. Am. J. Sci. **257**, pp. 297-315.

PAN, Y. & FLEET, M.E. (1991) Barian feldspar and barian- chromian muscovite from the Hemlo area, Ontario. Can. Mineral. **29**, pp. 481-498.

ROY, S. (1966) Syngenetic Manganese Formations of India. Jadavpur Univ., Calcutta **32**, 219 p.

——— (1981) MANGANESE DEPOSITS. Academic Press, New York, 458 p.

——— **& MITRA, F.N.** (1961) Genesis of the manganese ore bodies in Chikla-Sitasaongi, Bhandara district, Maharastra. Proc. Indian Science Congr. (Abs), **48**, 192 p.

TURNER, S. & BUSECK, P.R. (1979) Manganese oxide tunnel structures and their intergrowths. Science, **203**, pp. 456-458.

VILLIERS, P.R., DE. (1945). Some minerals occurring in South African manganese deposits. Trans. Geol. Soc. Afri. , **54**, pp. 89-98.

——— **& HERBSTEIN, F.H.** (1967) Distinction between two members of the braunite group. Am. Mineral. **52**, pp. 20-30.

VISWANATHAN, K., & KIELHORN, H.-M. (1989). Variations in the chemical compositions and lattice dimensions of (Ba, K, Na)- feldspars from Otjosondu,Namibia and their significance. Am. Mineral. **68**, pp. 112-121.

ACTA MINERALOGICA PAKISTANICA
VOLUME 6 (1992) PP. 65-73.

MANGANESE OCCURRENCES IN OPHIOLITIC ROCKS OF KHUZDAR DISTRICT, PAKISTAN.

ZULFIQAR AHMED
National Centre of Excellence in Mineralogy, University of Balochistan, G.P.O.Box 43,
Quetta, Pakistan.

ABSTRACT: Various kinds of Mn mineralizations occur at a few scattered localities in Khuzdar District, Pakistan, associated with layes 1 and 2 of the Bela ophiolite and associated ophiolitic mélange. Nodulous Mn deposits of small size and of diagenetic - hydrogenous origin occur in the Karku Jhal area, north of Nal town. In the low hills situated in the immediate NE of Kargaz peak, NNW of Wadh town, low grade Mn deposits occur. These are formed by precipitation in the fracture system of bedded cherts of a large outcrop of mélange.

Chemical and mineralogical data has been obtained on samples from an old working in the Kohan Jhal canyon near Koraro, Khuzdar District. This deposit appears to have a hydrothermal origin and the major Mn mineral is a slightly disordered pyrolusite. This is determined by studies on polished thin sections by microscope and electron microprobe in addition to the X-ray powder diffractometry and infra-red spectroscopy.

INTRODUCTION

Manganese occurs worldwide in layers 1 and 2 of typical ophiolitic sequences (e.g., Halbach et al., 1992; Skarpelis et al., 1992) and exhibits different geneses (e.g., Huebner & Flohr, 1990). The mélange and ophiolitic rocks of the Bela ophiolite in SW Pakistan outcrop in a belt that exceeds 450 km in length and stretches from Gadani beach area on the Arabian Sea coast (lat. 25° 6' 30" N; long. 66° 43' 12" E) near Karachi in the south, to Sange Siah (lat. 28° 9′ N; long. 66° 18' E) in Kalat District in the north. Mining of Mn from these outcrops has been done on a very small scale by the local population. The deposits exhibit a variety of field relations and appear to have formed by different processes during various stages in the evolution of surrounding ophiolitic rocks. Fossil nodules, stratiform, lenticular and disseminated mineralization as well as discordant veins of Mn ore minerals occur locally associated with bedded and non-bedded chert and basalts of the Bela ophiolite. Observations on three such localities are included in this study as a preliminary report on the nature of deposits. Detailed mineralogical and chemical characterization of the ore at one of the mines is included.

OPHIOLITIC ROCKS

The Bela ophiolitic rocks form certain large coherent massifs which expose intact ophiolitic sequence, such as the Lak Baran massif; in addition to their frequent occurrence as tectonic slices and nappes. A nearly complete ophiolitic sequence is present in the Lak Baran massif. The tectonic slices are usually bounded by thrust faults, often carrying sheared material alongside, and are made of portions from the ophiolitic sequence. The mélange generally forms low hills and exceeds the other ophiolitic rock outcrops in areal extent. The ophiolitic rock sequence broadly conforms to the general features of the harzburgite subtype of Jackson & Thayer (1972).

It has been indicated by earlier work (Ahmed, 1991) that the Bela ophiolite was not generated at a major ocean basin spreading centre, but in a suprasubduction zone environment at convergent margin. The oceanic lithosphere source of the Bela ophiolite might have formed in a marginal basin peripheral to the Tethys ocean. Presence of products of spreading axis activity at marginal basin floor are indicated at many places.

Volcanic rocks of the Bela ophiolite appear to belong to more than one rock suite. In and around Margh area (lat. 26° 48′N, long. 66° 18' E), typically ophiolitic and thoroughly pillowed basaltic rocks contain red cherts in their upper parts and are overlain by bedded red chert and limestone strata. In and around Kandaro area (lat. 26° 40' N, long. 66° 19′E), basalts show lesser development of pillows, and largely occur as flows. These basalts possess interbeds of argillite, black to dark grey coloured shales and

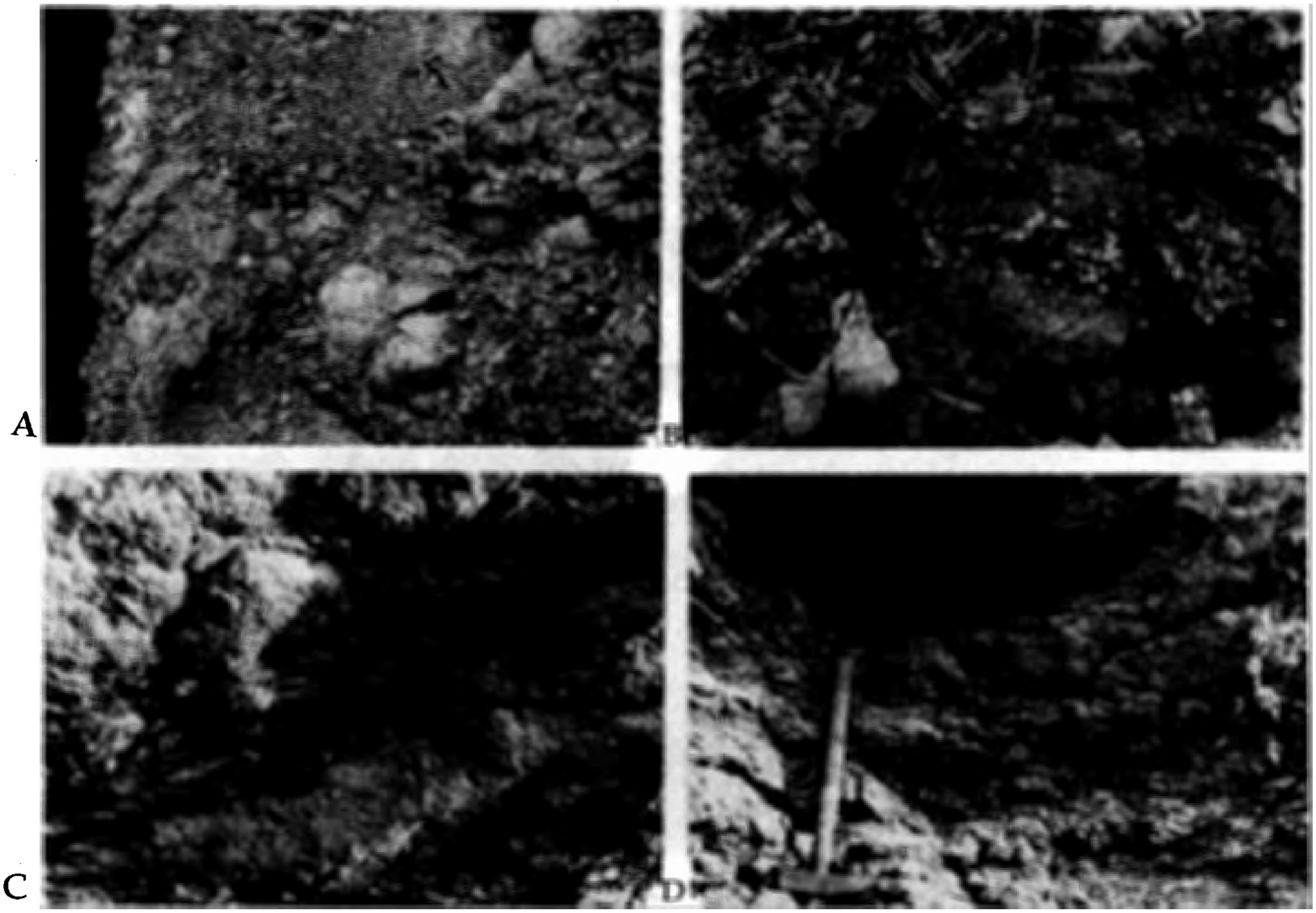

Fig. 1. **(A)** Photograph from Karku Jhal mine shows nodules of Mn collected from the hematitic sheared red mudstone that overlies the pillowed basalt. **(B)** Photograph from Kargaz peak (Goth Shafi) area showing a breccia with hematitic matrix and blocks of greenish dolerite. The solid rock around the breccia is also brecciated but the texture is not prominent in the photograph, and is seen on one rock face. **(C, D)** Photograph showing veins of manganese ore at the Kohan Jhal mine.

white limestone. Where pillowed, the basalts often possess green cupriferous cherts in between pillow lobes.

MANGANESE OCCURRENCE

Manganese deposits are known from the northern half of the Bela ophiolite belt (Ahmed, 1991) and occur mainly within the administrative District of Khuzdar. Manganese deposits occur scattered at many localities associated with the ophiolitic outcrops. The deposits are developed at local scale and are generally associated with massive or bedded chert and jasper bodies embedded in basalts of the Bela ophiolite.

Hunting Survey Corporation Limited (1960) reported the occurrence of Mn deposits from the following areas of Bela ophiolite: Siro Dhora, Khabri, Mohammad Khan Bent, Khan Kheo Nai, Kohan Jhal and Gadani. The host rocks of the deposits were identified as thin jasperoid layers (chert) immediately above the pillowed lavas and below shales. Their formation was speculated to be due to the hydrothermal replacement of marine sediments by solutions of volcanic derivation and rich in Fe, Si and Mn.

This study shows that fossil nodules, stratiform and fracture-fill mineralizations, as well as discordant veins of Mn ore minerals occur locally associated with bedded and non-bedded chert, mudstones and basalt. Three deposit types, as described below, are observed to occur; other types may also be present and require prospecting.

(a) *Nodulous Deposits*: Deposits of this type are examplified by the manganese deposits of Karku Jhal area where the extreme northerly outcrops of the Bela ophiolite are found. In this area, north of Nal town, pillowed basalts occur well developed. Western upper part of these basaltic outcrops is overlain by hematitic, sheared and incompact red mudstone and deep sea sediments which contain loose lumpy manganese nodules with considerable amount of associated goethite and limonite. The lumpy Mn nodule- bearing bed at one pit trends N 4°E, and dips 62° W. The nodules exhibit diameters from 3 to 7 cms. The deposits is apparently of hydrogenous origin.

(b) *Joint - fillings and Crusts of Mn on Chert*: The low-hills area (lat. 27° 34' 11" N; long. 66° 23' 16" E) just NNE of the Kargaz peak (lat. 27° 32' 36"N; long. 66° 22' 54" E) near Goth Shafi village, comprises ophiolitic mélange.The cherts, well bedded, have Mn deposits of small tonnage and low grade. The chert block has associated basalt and limestone. Oxidized manganese is concentrated on joints and open spaces in chert. Some black, sooty wad is also present. Adjacent to chert, an outcrop of breccia occurs. Breccia contains hematitic matrix and blocks of greenish mafic igneous rock. Breccia veins are seen cutting the solid rock which is also brecciated but does not show up due to lack of hematitic matrix. Breccia forms sheets and has red hematitic and chert content in the matrix. Mostly it is dolerite (ca. 95 %) with small amounts of red matrial healing the cracks. The brecciation of dolerite had occurred after its solidification. The overlying limestone occurs westwards and is also intensely brecciated. The brecciation may probably be due to submarine volcanism.

(c) *Vein Forming Mn*: At the Kohan Jhal Mn mine, hydrated oxides of Mn and Fe form interlayers in sediments of cherty and hematitic- limonitic chert. Some goethite is associated. Mudstones and siltstones are present nearby.

Mn may be produced from hydrothermal fluids coming up and precipitating oxides and hydroxides of Mn and Fe. The likely source of Mn is the abundant basalt surrounding the deposit. The deposit resembles the high temperature hydrothermal deposits.

The hydrothermal activity is indicated by the presence of quartz and high degree of crystallinity of pyrolusite, its occurrence in veins that are now parallel to the sedimentary layering, small lateral extent and presence of volcanic bedrock. The ore boundary (Fig.1C) is sharp and distinct and vein-like. The crystallinity of pyrolusite could be produced by aging and recrystallization of initially amorphous oxides (Nicholson, 1992) but this does not hold in the Kohan Jhal mine where the surrounding rocks do not exhibit signs of alteration and metamorphism.

The pyrolusite may have been deposited by the fluids moving along the veins and channels either beneath or above the seafloor that contained Mn and Fe.

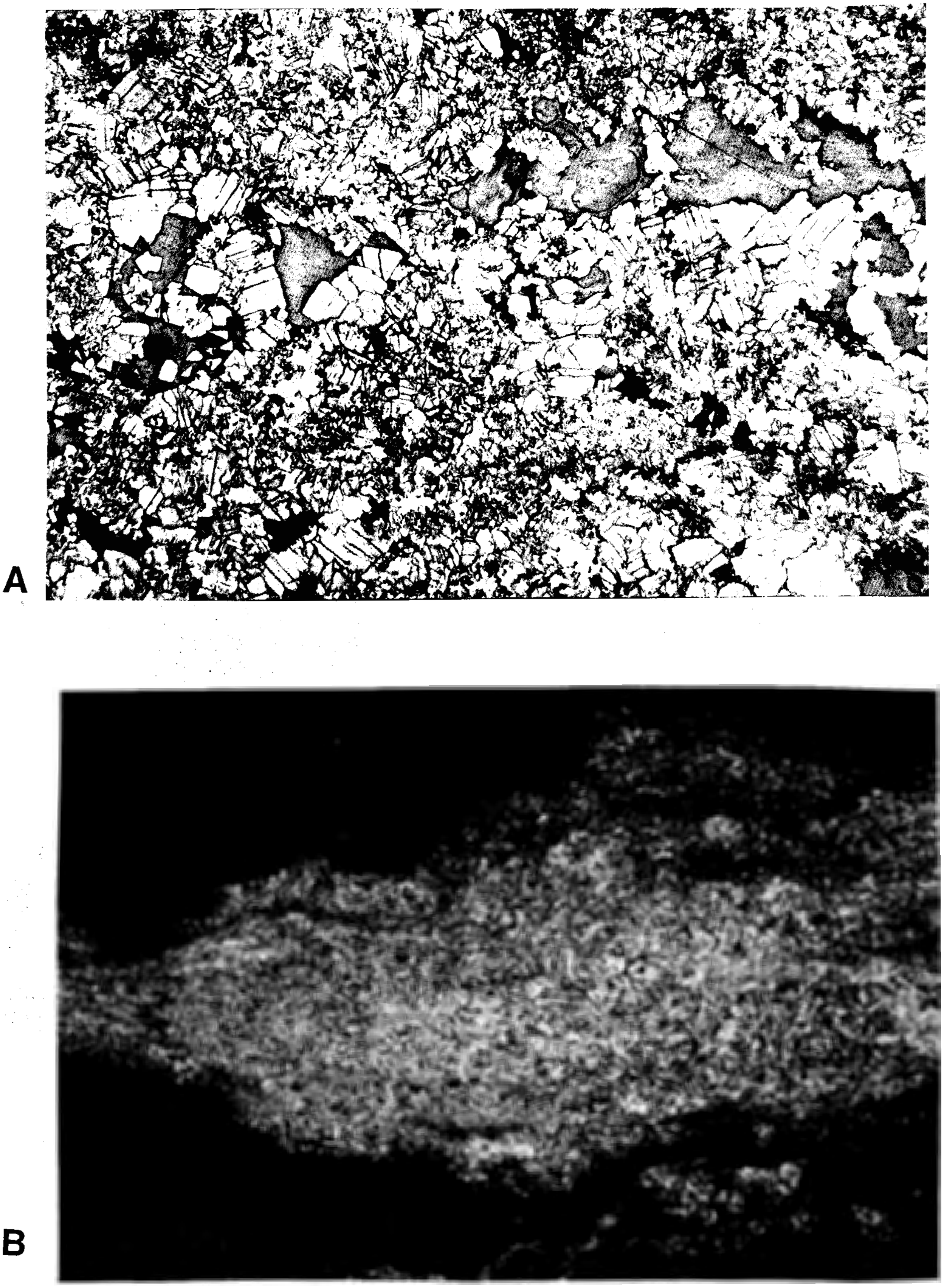

Fig.2. Reflected light photomicrographs from sample no. Z1591 showing : (**A**) pyrolusite (higher reflectance crystals) lining the vugs; (**B**) a veinlet with pyrolusite segregation.

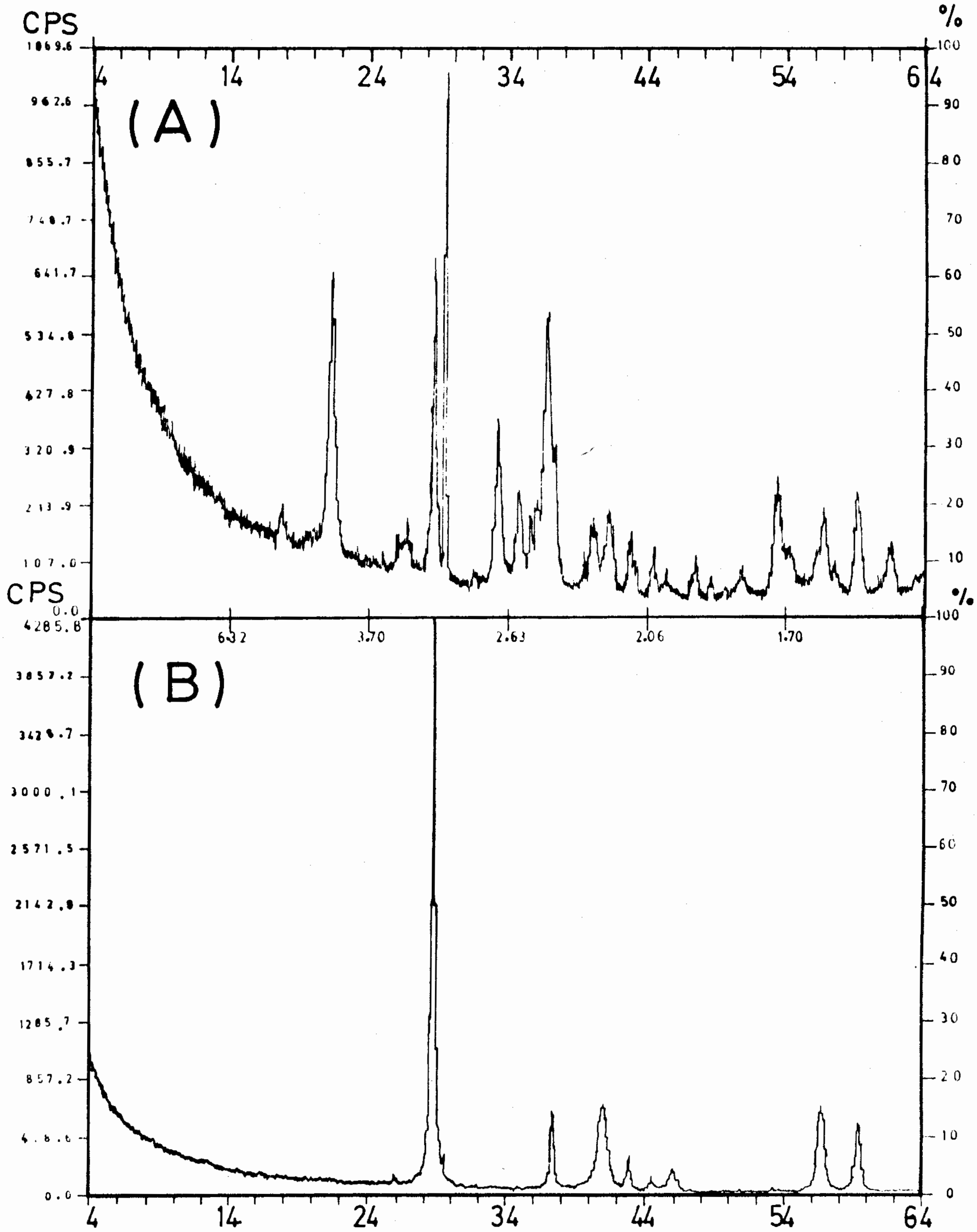

Fig. 3. X-ray powder diffraction traces for the altered mafic rock (sample Z1592; trace A) that hosts Mn ore (sample no. Z1591, trace B). Scale bars for the 2θ and *d* values are given on horizontal axes.

MINERALOGY AND CHEMISTRY

Methodology

Data were obtained by using transmitted and reflected light optical microscopy, X-ray powder diffractometry (XPD), electron microprobe analysis (EMP) and infra-red spectroscopy (IR).

Samples were run on a Scintag X-ray diffractometer set up at the Illinois State Geological Survey, U.S.A., by Duane M. Moore, by generating X-rays at 40kV voltage and 30 mA current, and by using the Cu K∝ radiation.

The infrared spectroscopy was carried out in the laboratory of George R. Rossman at the California Institute of Technology (Caltech), U.S.A., using the standard procedure as detailed by Potter & Rossman (1979). Electron microprobe analyses were performed employing the JEOL 733 SUPERPROBE instrument set up at the Caltech, U.S.A. Standard procedures for wavelength-dispersive analyses were employed to acquire high quality data. Analyzed compositions were compared with the respective energy-dispersive spectra to determine any missed out element.

Results

The ore sample Z1591 collected from the Kohan Jhal mine contains quartz and goethite, but the main constituent is slightly disordered pyrolusite. This has been confirmed by the chemical composition (Table 1), X-ray diffraction pattern (Fig. 3) and infra-red absorbance spectra (Fig. 4). MnO_2 is present in the associated goethite structure as well. Pyrolusite shows well developed cleavage, higher reflectance. Goethite occurs more in veinlets cutting the pyrolusite concentrations.

Sample Z1592 is from the host rock of the ore and contains Mn-bearing goethite , pyrolusite and calcite as exhibited by the X-ray diffraction pattern (Fig.3). The XPD patterns of goethite and Mn-goethite are similar in their *d*-values (Manceau et al., 1992, Fig.5)

Representative microprobe analyses of the pyrolusite are given in Table 1. The goethite analyses (Table 1) show considerable SiO_2 due to admixture and impurity in the samples. Some Mn^{3+} is present as well, substituting for Fe^{3+}. In addition to the elements reported in Table 1, the analyses were performed for certain other elements including Ba, Sr, S, Cl, Zr, Co, Cu and Y; but nil values were found.

X-ray powder diffraction traces for sample Z1591 (Fig. 3) shows the 100–intensity peak of pyrolusite at 3.14 Å. The peak at 2.113 Å is very close in position to the 2.13 Å peak of pyrolusite. The peak at ca. 41° 2θ is too broad and intense for pyrolusite and indicates either the structural disorder, or the presence of some other phase in small amounts. The latter possibility is also apparent from the additional peaks that show up on expanding the scale. These appear at 21.2° (4.21 Å) and 33.24° (2.69 Å). The traces for sample Z1592 (Fig. 3A) shows the presence of pyrolusite, goethite and calcite.

The infrared absorbance spectrum of sample no. Z1591 (Fig. 4) closely resembles curve no. 6 of Potter & Rossman (1979, Fig. 3). For typical well-ordered pyrolusites, two characteristic peaks occur in the wave-number range 300 - 400. The sample under study does not transmit light in this range and those peaks are not seen. However, in the wavenumber range 400 - 500, the curve closely matches that given by Rossman (1979) for typical pyrolusite. The spectrum in Fig.4 displays a peak at ca. 570 wavenumber and a shoulder at ca. 670 wavenumber. The spectrum shows that the sample is structurally neither a well-ordered pyrolusite nor a strongly disordered one, but only a slightly disordered pyrolusite.

DISCUSSION

Generally three kinds of processes are recognized that deposit and redistribute Mn at the ocean floor. These are hydrogenous, diagenetic and hydrothermal processes. These may operate singly or combined, but produce deposits with features characteristic of each process (Huebner & Flohr, 1990). Different views have been presented for certain Mn deposits. For example, Mn mineralizations in cherts and jaspers of the Nicoya ophiolite complex are regarded both as primary sedimentary early diagenetic as well as volcanic exhalative deposits formed when Mn-rich hydrothermal solutions penetrated the siliceous ooze and reached the ocean floor (Halbach et al., 1992). The fossil manganese nodules occur in the pelagic successions in western Sicily as distal members of hydrothermally supplied precipitates (Jenkyns, 1970). Such nodules also occur in the slowly -deposited neo-Tethyan margin environment (Halbach et al., 1992).

Table 1. Composition of pyrolusite (columns 1-7), manganese goethite (column 8) and impure (silica - rich) hydrous iron oxide (columns 9 -12) from the Kohan Jhal deposit, Khuzdar District, Pakistan.

	1	**2**	**3**	**4**	**5**	**6**	**7**	**8**	**9**	**10**	**11**	**12**
SiO_2	0.76	1.03	0.89	0.35	0.57	0.76	0.72	4.29	8.86	8.62	16.45	11.15
TiO_2	0.01	0.00	0.00	0.00	0.00	0.00	0.00	0.04	0.03	0.07	0.03	0.02
MnO_2	97.75	94.27	97.75	97.70	94.58	96.70	94.18	4.14	4.03	3.52	3.36	7.82
Al_2O_3	0.21	0.55	0.53	0.40	0.31	0.29	0.19	0.97	1.94	1.75	2.53	2.50
Cr_2O_3	0.00	0.03	0.02	0.00	0.01	0.05	0.00	0.00	0.03	0.00	0.00	0.00
V_2O_3	0.01	0.04	0.02	0.00	0.01	0.02	0.02	0.02	0.01	0.05	0.00	0.02
Fe_2O_3	0.08	0.06	0.12	0.14	0.07	0.01	0.04	74.47	49.17	50.92	49.88	52.53
MgO	0.17	0.19	0.16	0.19	0.21	0.15	0.15	1.09	1.75	1.76	2.20	1.91
NiO	0.02	0.06	0.06	0.01	0.00	0.04	0.04	0.00	0.06	0.03	0.00	0.00
CaO	0.66	0.88	0.63	0.76	0.68	0.64	0.74	0.34	0.42	0.81	0.34	0.30
ZnO	0.00	0.00	0.00	0.00	0.00	0.00	0.00	0.03	0.04	0.06	0.02	0.06
Na_2O	0.07	0.10	0.01	0.06	0.08	0.06	0.07	0.07	0.15	0.18	0.15	0.03
K_2O	0.00	0.00	0.04	0.02	0.12	0.04	0.06	0.00	0.71	0.63	1.94	1.24
Total	99.74	97.21	100.23	99.63	96.64	98.76	96.21	85.46	67.18	68.40	76.90	77.58

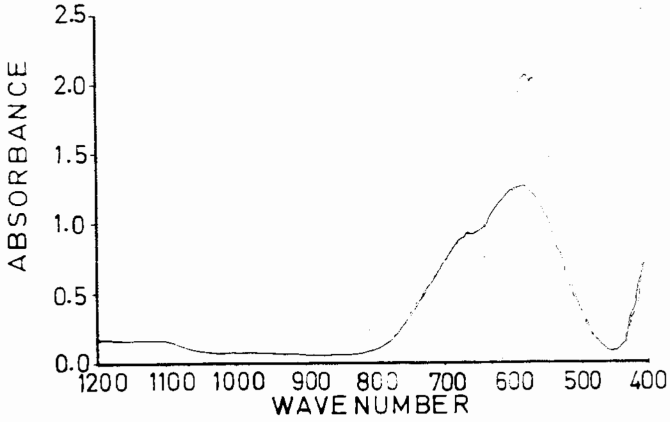

Fig. 4. Infrared absorbance spectrum of pyrolusite separated from Mn ore sample (no. Z 1591) from the Kohan Jhal mine.

The Karku Jhal deposits are nodulous and may be hydrogeneous; being derived by precipitation and gravity settling of particulates through a stationary fluid above the sea floor.

Hydrogeneous deposits form by precipitation and settling of Mn and Fe oxyhydroxides directly from cold seawater onto the top of the sediments (Huebner & Flohr, 1990). Purely hydrogeneous, nodulous deposits are rare in geological record as they tend to alter diagenetically or get subducted. At the Karku Jhal deposit, since there are no sulphides or Mn carbonates, the deposit was probably formed under oxic conditions. The deposits are not laminated. They are enclosed in unlaminated mudstones, they differ from purely hydrogeneous deposits.

The mineral pyrolusite is known from a wide range of environments of manganese genesis, although it is common in the supergene marine environment of Nicholson (1992). In the Mn nodules from the Nicoya ophiolite complex, NW Costa Rica (Halbach et al., 1992), pyrolusite is the youngest Mn- phase which formed probably below 100° C and under oxidizing conditions. Pyrolusite is also known as a supergene alteration product of braunite (Halbach et al., 1992). However, the source of Mn at the Kohan Jhal deposit is indicated as hydrothermal.

The Bela ophiolite interpreted as the old marginal basin basement (Ahmed, 1991) could be a favourable site for such Mn mineralizations. The association of Mn-rich lithologies with chert and basalts is consistent with deposition of host sediments in a rifting environment such as a marginal basin (e.g., Flohr, 1992).

The paleodepositional settings of the Mn deposits cannot yet be unambiguously identified Ahmed, 1991; Sarwar, 1992). The association of manganiferous sediments with chert and basalts may possibly indicate a marginal basin. Such an environment would provide the heat source necessary to drive a circulating hydrothermal system and provide pathways for transport of seawater and mineralizing fluids (Flohr, 1992). Recent submarine Mn crusts are thought to have a hydrothermal source originating from small or large hydrothermal convective cells (e.g., Crerar et al., 1982).

CONCLUSIONS

The manganese deposit at Kohan Jhal is mainly composed of slightly disordered pyrolusite which occurs associated with goethite and calcite. The deposit is apparently of hydrothermal origin.

Nodules of Mn oxides and hydroxides occur at Karku Jhal. The deposit seems to be of diagenetic-hydrogeneous origin.

The bedded cherts that occur widely in the melange zone contain Mn as later fracture fillings as examplified by the deposits of low hills near Kargaz peak.

REFERENCES

AHMED, Z. (1991) Basalt geochemistry and suprasubduction zone origin of the Bela ophiolite, Pakistan. Acta Mineralogica Pakistanica **5**, pp. 83-98.

CRERAR, D.A., NAMSON, J., SOCHY, M., WILLIAMS, L. & FEIGENSON, M.D. (1982) Manganiferous cherts of the Franciscan assemblage: I. General geology, ancient and modern analogues and implications for hydrothermal convection at ocean spreading centres. Econ. Geol. 77 (3), pp. 519-540.

FLOHR, M.J.K. (1992) Geochemistry and origin of the Bald Knob manganese deposit, North Carolina. Econ. Geol. **87**, pp. 2023-2040.

HALBACH,P., GURSKY, H.-J., GURSKY, M.M., SCHMIDT-EFFING, R. & MARESCH, W.V. (1992) Composition and formation of fossil manganese nodules in Jurassic to Cretaceous radiolarites from the Nicoya ophiolite complex (NW Costa Rica). Mineral. Deposita **27**, pp. 153-160.

HUEBNER, J.S. & FLOHR, M.J.K. (1990) Microbanded manganese formations: Protoliths in the Franciscan complex, California. U.S. Geol. Surv. Prof. Pap. **1502**, pp. 72p.

HUNTING SURVEY CORPORATION LIMITED (1960) RECONNAISSANCE SURVEY OF PART OF WEST PAKISTAN. A Colombo Plan Cooperative Project, Government of Canada, Toronto. 550p

JACKSON, E.D. & THAYER, T.P. (1972) Some criteria for distinguishing between stratiform, concentric and alpine peridotite - gabbro complexes. 24th Internat. Geol. Cong. Montreal, Section **2**, pp. 289-296.

JENKYNS, H.C. (1970) Fossile manganese nodules from the west Sicilian Jurassic. Eclogae Geol. Helv. **63**, pp. 741-774.

MANCEAU, A., GORSHKOV, A.I. & DRITS, V.A. (1992) Structural chemistry of Mn, Fe, Co and Ni in manganese hydrous oxides : Part II. Information from EXAFS spectroscopy and electron and X-ray diffraction. Amer. Mineral. **77**, pp. 1144-1157.

NICHOLSON, K. (1992) Contrasting mineralogical- geochemical signatures of manganese oxides: Guides to metallogenesis. Econ. Geol. **87**, pp. 1253-1264.

POTTER, R.M. & ROSSMAN, G.R. (1979) The tetravalent manganese oxides : identification, hydration and structural relationships by infrared spectroscopy. Am. Mineral. **64**, pp. 1199-1218.

SARWAR, G. (1992) Tectonic setting of the Bela ophiolite, southern Pakistan. Tectonophys. **207**, pp.359-381.

SKARPELIS, N., HATZIPANAGIOTOU, K. & KAISERLOGLOU, M. (1992). Manganiferous cherts in siliceous sediments overlying the Koziakas ophiolite, Western Thessaly, Greece. Can. Mineral. **30**, pp. 415 - 421.

Manuscript received on October 20, 1992; accepted for publication on November 14, 1992.

ACTA MINERALOGICA PAKISTANICA
VOLUME 6 (1992) pp. 73-84.

PETROLOGY AND CHEMISTRY OF THE ULTRAMAFIC ROCKS FROM THE ALLAI KOHISTAN SECTION OF THE INDUS SUTURE ZONE IN HAZRA, N. PAKISTAN

MOHAMMAD TAHIR SHAH
National Centre of Excellence in Geology, University of Peshawar, Peshawar.
&
MOHAMMAD MAJID
Department of Geology, University of Peshawar, Peshawar.

ABSTRACT: Rocks of the Shergarh Sar area, a part of the Allai Kohistan are divisible into three petrotectonic units: (1) Kohistan island arc sequence, (2) Indus suture zone, and (3) Indo-Pakistan subcontinent sequence. The Indus suture zone in this area comprises an elongated belt of ultramafic rocks, pillow lavas, greenschists, blueschists and metasediments that have been obducted onto the Indo-Pakistan plate. Ultramafics (clinopyroxenite, peridotite and serpentinite) exhibit strong shearing or cataclasis. Clinopyroxene and olivine are the dominant primary phases and are partially or completely altered to serpentine, fibrous amphibole, chlorite, magnetite and chromite. Among serpentine, both antigorite and chrysotile of syntectonic and posttectonic behaviour have been distinguished. The effects of serpentinization on the whole-rock chemistry is indicated by the release and introduction of certain elements during the process. The constituent rocks are comagmatic and probably represent a dismembered ophiolite suite.

INTRODUCTION

In accordance with the model of evolution of the Himalayas through the continental collision processes between Asia and Indo-Pakistan; the Main Karakoram Thrust (MKT) in the north and the Main Mantle Thrust (MMT) in the south are regarded as the tectonic fingerprints of the past subduction zone. Both are characterized by the ophiolitic melanges. In addition, blueschists and high-P garnet granulites are also associated with MMT. These faults are the result of bifurcation of the Indus Zangbo Suture (IZS) in Ladakh and Kohistan. This suture is considered to be the northern limit of the Indian continent. Both the MMT and MKT enclose the Kohistan-Ladakh island arc and separate it from the Indian plate in the south and Karakoram plate in the north. The Shergarh Sar area (Fig. 1) occupies northern part of the Allai Kohistan in Hazara division and marks an ideal section of the collision zone between the Kohistan island arc and the Indo-Pakistan plate (Fig. 1). The rocks of the area are predominantly composed of amphibolites, ultramafics, lavas with associated metachert and limestone, greenschist, blueschist facies metagraywacke, schist, crystalline limestone and granite gneiss. These are described in a north to southward stratigraphic succession as (a) The Kohistan arc sequence (b) Indus suture zone (3) Indo-Pakistan subcontinent sequence.

The Indus suture zone constitutes an intervening zone between the Indo-Pakistan plate and the Kohistan Island arc block. It records suturing of the Kohistan arc to the Indo-Pakistan subcontinent. Complexities within the structure and types of rocks in the Indus suture zone were first recognized by Tahirkheli et al. (1979) and Bard (1983). Within the Mangora-Shangla section of the suture zone in Swat Kohistan, Lawrence et al. (1983) and Kazmi et al. (1985) recognized a variety of rocks, i.e., ultramafics (ophiolitic melange), metabasites (greenschist melange) and blueschists occurring as separate slices. Occurrences of ultramafic rocks in Indus suture zone have also been reported in the Jijal area of Swat Kohistan by Jan (1979) and Jan & Howie (1981).

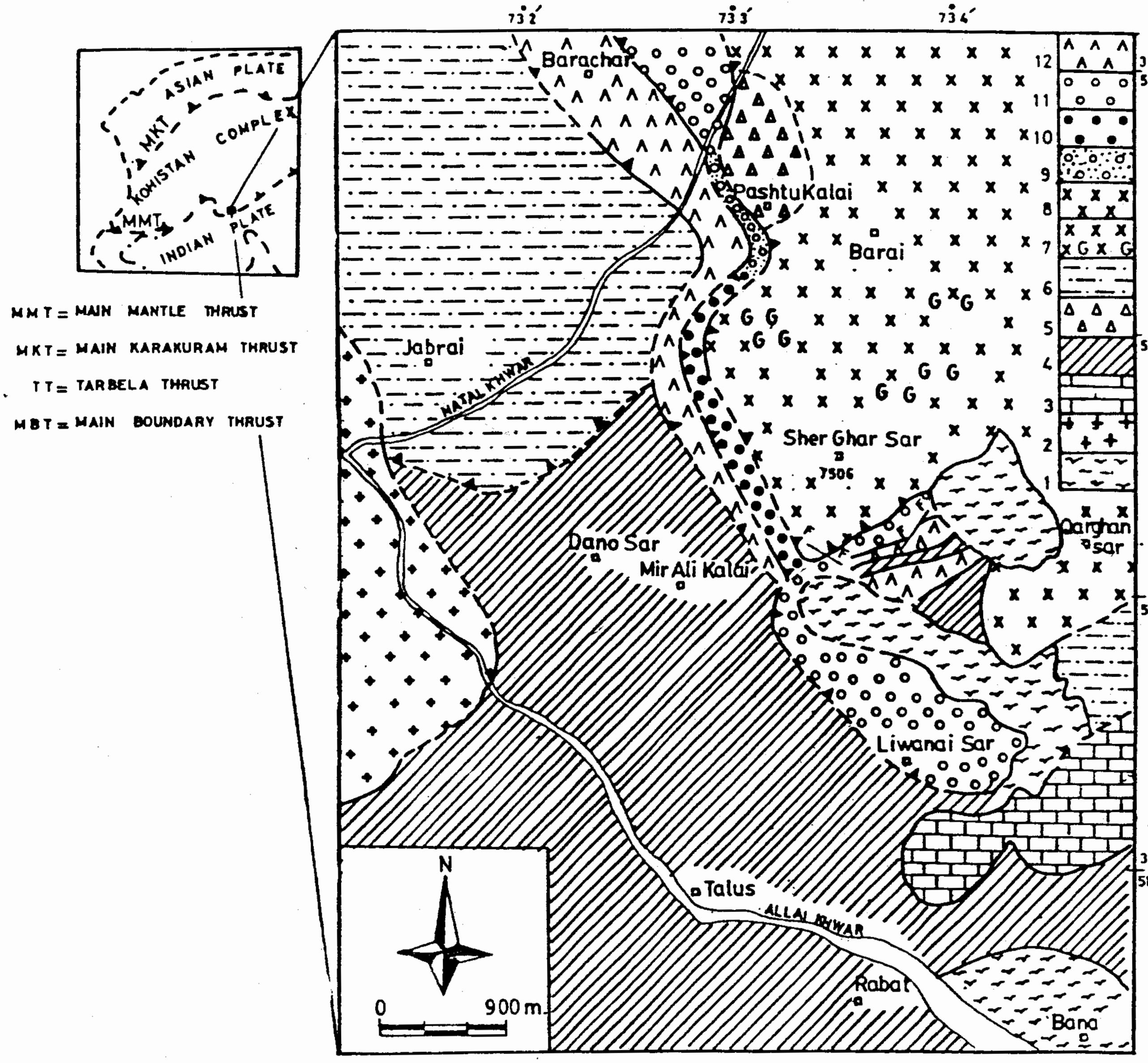

Fig. 1. Geological map of the Shergarh Sar area, Allai Kohistan. N. Pakistan. 1. Overburden; 2. Granite gneiss; 3. Limestone; 4. Schist; 5. Brecciated zone; 6. Greenschist; 7. Garnet-epidote-amphibolite; 8. Epidote-amphibolite; 9. Serpentinite; 10. Peridotite; 11. Clinopyroxenite; 12 Lavas. Heavy solid line shows thrusted contact; the dashed where inferred.

Shah & Majid (1985) identified a chaotically arranged stack of thrust slices and tectonic wedges of ultramafic rocks, lavas, green schists, metasediments and to lesser extent metachert and blue schist facies metagraywacke in the Indus suture zone of Shergarh Sar area, Allai Kohistan. Petrochemical indices of the lavas and blueschist facies metagraywacke have been discussed in a genetic context elsewhere (Majid & Shah, 1985; Shah & Majid, 1985).

In this paper, the field characteristics and petrochemistry of the ultramafic rocks of a SE-NW trending belt (approx. 4 km in length and 200 m maximum width) stretching between Liwanai Sar to Pashtu village (Fig. 1) within the suture zone, are described. Analyses of the clinopyroxenite and serpentinite which are the dominant rock types, are compared with equivalent composition from different tectonic regions and also with average mantle data.

FIELD ASPECTS

The ultramafic rocks are hard, massive and fine- to medium-grained with variation in color from greenish grey to dark-grey. Contacts between various units are not clear because major portion of the ultramafics is covered with overburden and vegetation. These rocks are highly fractured and sheared. Partial serpentinization is ubiquitous along shear zones. At some places (i.e., at Liwanai Sar and in the stream section west of Pashtu village) the serpentinization is so intense that the rocks grade to serpentinites. The development of talc is conspicuous within the body of serpentinite at Liwanai Sar. The clinopyroxenites are very well exposed at the base of Shergarh Sar near Mir Ali Kalai and also near Richarai. These have a thrusted contact with the overlying amphibolites and underlying lavas and greenschists.

The ultramafics are, in places, highly fractured, brecciated and granulated. The Pashtu village is located over such a brecciated zone. In the Natal Khwar section, the brecciated zone consists of blocks and angular to subangular fragments of ultramafics (mostly serpentinites) and volcanics, set in a matrix of magnesite, silica, carbonate and granulated serpentinite typical of melange. The brecciated zone is about 300 m thick and 1/2 km wide. Knobby outcrops of brecciated zone are typical within the exposed section.

PETROGRAPHY

Clinopyroxenites

The clinopyroxenites are hard, massive, medium- to coarse-grained rocks having light greenish grey to dark-grey color in hand specimen. The rocks are generally serpentinized in parts. The microveins of oxidized iron have been noticed in a few specimens.

The primary mineral constituents are clinopyroxene and olivine, while serpentine, fibrous amphibole, chlorite, talc, calcite and iron ores are the secondary alteration products. Clinopyroxene (40-95%) and olivine (< 3%) occur as anhedral to rounded grains set in a matrix dominantly composed of serpentine, chlorite, fibrous tremolite-actinolite, talc, carbonate and magnetite. On the basis of optical properties, clinopyroxene is classified as diopsidic augite and olivine as Mg-rich variety. Both the porphyroclasts of clinopyroxene and olivine are fractured and corroded at the margins. Some exhibit kink banding, laminar twinning and exsolution lamellae. In addition, clinopyroxene and olivine indicate partial to complete alteration to serpentine (generally antigorite with some chroysotile), chlorite and fibrous amphibole. Serpentinization is dominant over chloritization but chlorite is frequently present in majority of the clinopyroxenites. Microveins of carbonate material cross cutting the clinopyroxene grains, have also been noticed in some thin sections. Fine grained magnetite seems to be a byproduct of serpentinization in these rocks.

Reaction rims with cores of clinopyroxene, middle rims of fibrous amphibole and outer rims of chlorite are a common feature of these rocks. In some cases the middle rim may be missing, while in other sections the clinopyroxene core has turned cloudy. The texture of the rocks clearly shows that these have undergone severe shearing and cataclasis, for example, flexion structures shown by serpentine and magnetite surrounding olivine and clinopyroxene and also the drastic reduction in grain size of both these minerals.

Serpentinites

Serpentinites occur in the form of lenses and elongated masses in the area (Fig. 1). There are fine and coarse-grained types. The fine-grained variety is a compact rock with grey to dark-grey color having white coating of magnesite on the weathered surfaces. The coarse-grained variety is of greenish-grey color. These have laths of serpentine up to 1 cm in length which can be identified easily in hand specimens. A weakly-defined preferred orientation is shown by these laths.

In thin sections, serpentine (75-95%) is the dominant mineral occurring together with variable proportions of chlorite, talc and opaque grains (magnetite with some chromite) with relics of clinopyroxene and olivine. In extreme cases no relic grains of olivine and clinopyroxene are, however, observed. The overall texture of the serpentinite is lenticular to fibrous but locally developed ribbon, mesh and spherulitic textures are also common.

Two habits of serpentine (dominantly antigorite with some chrysotile) have been noticed: (a) an earlier syntectonic long-fibre and cross-fibre variety, accurring in occordance with general fabric of the rock; (b) post-tectonic coronas of serpentine, developed in a radial pattern at the expense of olivine and syntectonic serpentine. The absence of any Ca-bearing minerals in serpentinite indicates that Ca, released from the alteration of clinopyroxene, has probably been lost during serpentinization (Coleman, 1967).

Peridotites

In handspecimen, peridotites from Shergarh Sar area are indistinguishable from the clinopyroxenites. Samples collected near Richarai, when studied in thin section, have olivine and clinopyroxene as the major mineral constituents. Olivine and clinopyroxene occur as rounded, anhedral grains and constitute 70% by volume of these rocks, while serpentine, chlorite, spinel and magnetite represent the secondary alteration products and occur as fine-grained matrix. Olivine grains vary from 0.5 mm to 4 mm in diameter but show a decreasing tendency in diameter wherever they occur in association with the clinopyroxene. On the basis of optical properties, olivine and clinopyroxene correspond to those of the clinopyroxenite and are thus classified as forsterite and dioside, respectively. Both olivine and clinopyroxene are generally kinked and corroded at margins.

In most thin sections, olivine is partially altered to srpentine and magnetite along fractures and margins but complete alteration to serpentine has also been noticed. The roundness of olivine and clinopyroxene grains seems to have a direct relation with the degree of serpentinization. Severely serpentinized parts of peridotite have isolated clusters of olivine and clinopyroxene occurring in serpentine mass. Serpentine is dominantly antigorite while cross-fibers of chrysotile also exist.

Anhedral to euhedral grains mostly magnetite, occur is association with serpentine replacing olivine. A thin zone of green to light-green chlorite surrounding chromite grains is conspicuous in sections Alk 132A and Alk 140A. Spinel occurring in asociation with magnetite has also been noticed in sections 132A and 142A.

From the textural evidences in the ultramafic rocks from Shergarh Sar area, it appears that the antigorite + chlorite + fibrous amphibole assemblages have been produced by the partial alteration of clinopyroxene and olivine. High proportions of antigorite in the ultramafic rocks indicate metamorphic conditions close to the boundary of epidote-amphibolite facies and greenschist facies (Evans and Trommsdroff, 1970, 1972). The deformational features observed in the ultramafic rocks suggest that the original texture of these rocks are completely obscured by later tectonic deformation.

CHEMISTRY

Clinopyroxenites, serpentinites and peridotites were analysed for major and trace elements. The chemical analyses along with C.I.P.W norms of the selected samples are presented in Tables 1 & 2. Both the instrumental and classical methods were used for chemical analyses. The IUGS standards (BCR-1 & PCC-1) were used for reference. SiO_2 was determined gravimetrically; AL_2O_3, P_2O_5, and TiO_2 colorimetrically; FeO by ammonium metavanadate method (Wilson, 1955, 1960). The remainder major elements were determined by atomic absorption spectrophotometer. The H_2O^+ and CO_2 were determined as ignition loss at about 1000°C. Trace elements in all the rock samples were analyzed by XRF, using pressed powder tablets.

The clinopyroxenite and peridotite are mildly to strongly serpentinized as is indicated by their petrographic study and also by the greater loss on ignition in these rocks. The average values of the loss on ignition for the clinpyroxenite, peridotite and serpentinite are 3.54, 2.26 and 9.74 respectively. According to Malakhov (1965) the loss on ignition is a better measure of the degree of serpentinization than the "bivalent Fe/total Fe" ratio in such rocks. All the analyses for these rocks are, therefore, recalculated on H_2O– and CO_2 – free basis and the selected samples are reported in Table 2. This anhydrous data has been used for further interpretations.

Variations in the values of SiO_2, CaO and MgO from clinopyroxenite to serpentinite have been noticed. The higher contents of Ni, Cr and Co in peridotite relative to clinopyroxenite are distinct (Table 1). This has already been noted for Ni and Co by several authors (Fomin & Kozak, 1971). Clinopyroxenites have relatively high V contents. Few samples of clinopyroxenites have exceptionally high Cu contents (124-984

Table 1. Chemical analyses of the clinopyroxenites, serpentinites and peridotites from Shergarh Sar area, Allai Kohistan.

	Pyroxenites:						*Serpentinites:*					*Peridotites:*		
	Alk67A	**Alk77A**	**Alk70A**	**Alk73a**	**Alk75A**	**Alk138A**	**Alk12**	**Alk38A**	**Alk137A**	**Alk122A**	**Alk121A**	**Alk132A**	**Alk140A**	**Alk142A**
SiO_2	46.22	45.34	49.26	49.74	48.38	42.80	39.38	37.32	41.01	38.70	42.33	42.72	43.37	43.89
TiO_2	0.45	0.54	0.48	0.09	0.72	0.05	0.00	0.12	0.04	0.37	0.03	0.14	0.18	0.16
Al_2O_3	2.55	1.30	1.33	1.22	2.10	2.02	1.95	1.20	1.32	1.89	2.69	2.67	1.98	2.11
Fe_2O_3	8.42	3.14	5.04	4.20	3.32	4.54	2.18	8.26	7.67	6.37	5.33	3.78	3.37	2.98
FeO	3.65	3.27	2.91	3.86	4.32	0.62	3.45	2.64	2.92	4.32	4.86	5.12	6.12	6.32
MnO	0.18	0.21	0.14	0.14	0.18	0.11	0.11	0.15	0.14	0.15	0.12	0.16	0.15	0.15
MgO	20.69	28.55	25.13	25.87	23.04	26.70	38.21	40.30	39.02	39.51	38.98	39.23	39.89	40.10
CaO	16.15	14.27	14.19	13.79	11.54	16.98	0.39	0.00	0.45	0.19	0.40	2.97	1.51	2.12
Na_2O	0.37	0.38	0.44	0.52	0.24	0.37	0.59	0.37	0.32	0.24	0.31	0.18	0.32	0.26
K_2O	0.00	0.00	0.00	0.01	0.00	0.00	0.00	0.00	0.00	0.00	0.00	0.03	0.02	0.03
P_2O_5	0.01	0.02	0.02	0.02	0.03	0.01	0.08	0.02	0.02	0.00	0.01	0.04	0.18	0.13
H_2O	0.10	0.03	0.17	0.14	0.11	0.08	0.41	0.10	0.22	0.13	0.12	0.21	0.13	0.00
L.O.I.	1.42	3.57	0.88	1.86	6.32	5.54	12.35	8.10	7.57	8.48	6.41	2.13	2.42	2.22
Total	100.21	100.62	99.99	101.46	100.30	99.82	99.10	98.58	100.70	100.35	101.59	99.38	99.64	100.47

Trace element (in ppm):

	Alk67A	Alk77A	Alk70A	Alk73a	Alk75A	Alk138A	Alk12	Alk38A	Alk137A	Alk122A	Alk121A	Alk132A	Alk140A	Alk142A
Ni	214	238	242	163	138	352	2533	2200	1872	2442	2044	1831	1870	1918
Cr	1684	3708	1435	1437	2346	2517	4525	5531	5132	4111	4678	4732	4810	4772
Sr	44	21	12	24	19	25	12	6	9	10	11	11	9	10
Co	0	22	36	20	36	45	115	135	127	105	100	120	135	130
Rb	8	5	5	5	5	4	5	10	7	9	4	3	2	3
Y	16	2	2	15	15	1	2	17	3	2	0	6	3	2
Ba	0	0	0	0	0	20	138	39	168	102	139	24	18	16
Cu	0	0	948	249	0	0	0	0	0	0	0	58	49	52
Zn	41	2	3	54	53	12	30	35	38	32	32	40	32	30
Zr	1	9	9	1	0	9	15	1	13	14	13	6	8	9
V	56	69	200	100	1	74	40	70	0	0	11	53	52	50
Ce	13	10	0	34	49	6	0	47	24	0	20	23	26	21
Cs	2	0	0	2	1	0	0	1	0	0	0	0	0	0
Nb	6	0	0	4	3	0	0	11	0	0	4	5	0	10

Table 2. Major elements and C.I.P.W. norms of clinopyroxenites, serpentinites and peridotites from Shergarh Sar area (recalculated to 100 on anhydrous basis).

	Pyroxenites:							*Serpentinites:*					*Peridotites:*		
	Alk67A	Alk77A	Alk70A	Alk73A	Alk75A	Alk138A	Alk131A	Alk12	Alk38A	Alk137A	Alk1224A	Alk121A	Alk132A	Alk140A	Alk142A
SiO_2	46.83	46.73	49.79	50.01	51.54	45.44	54.14	45.61	41.29	44.14	42.18	44.53	44.02	44.67	44.67
TiO_2	0.46	0.56	0.49	0.09	0.77	0.05	0.05	0.00	0.13	0.04	0.40	0.03	0.14	0.19	0.16
A^2O_3	2.58	1.34	1.34	1.23	2.24	2.14	1.91	2.26	1.33	1.42	2.06	2.83	2.75	2.04	2.15
F_2O_3	8.53	3.24	5.09	4.22	3.54	4.82	1.52	2.52	9.14	8.26	6.94	5.61	3.90	3.47	3.03
FeO	3.70	3.37	2.94	3.88	4.60	0.66	2.67	4.00	2.92	3.14	4.71	5.11	5.28	6.30	6.43
MnO	0.18	0.22	0.14	0.14	0.19	0.12	0.11	0.13	0.17	0.15	0.16	0.13	0.16	0.15	0.15
MgO	20.96	29.43	25.40	26.01	24.54	28.34	18.91	44.26	44.59	42.00	43.07	41.01	40.43	41.09	40.81
CaO	16.36	14.71	14.34	13.86	12.29	18.03	20.34	0.45	0.00	0.48	0.21	0.42	3.06	1.56	2.16
Na_2O	0.37	0.39	0.44	0.52	0.26	0.39	0.23	0.68	0.41	0.34	0.26	0.33	0.19	0.33	0.26
K_2O	0.00	0.00	0.00	0.01	0.00	0.00	0.10	0.00	0.00	0.00	0.00	0.00	0.03	0.02	0.03
P_2O5	0.01	0.02	0.02	0.02	0.03	0.01	0.01	0.09	0.02	0.02	0.00	0.01	0.04	0.19	0.13

C.I.P.W. Norms:

	Alk67A	Alk77A	Alk70A	Alk73A	Alk75A	Alk138A	Alk131A	Alk12	Alk38A	Alk137A	Alk1224A	Alk121A	Alk132A	Alk140A	Alk142A
Or	-	-	-	0.06	-	-	0.59	-	-	-	-	-	0.18	0.12	0.18
Ab	3.17	-	3.76	4.42	2.16	-	1.95	5.78	3.46	2.91	2.21	2.76	1.57	2.79	2.24
An	5.36	1.88	1.67	0.97	4.95	3.85	3.89	1.64	-	2.26	1.03	2.02	6.58	4.02	4.58
Ne	-	1.78	-	-	-	1.7	-	-	-	-	-	-	-	-	-
Ac	-	-	-	-	-	-	-	-	-	-	-	-	-	-	-
C	-	-	-	-	-	-	-	0.53	0.65	0.02	1.25	1.55	6.53	1.95	4.14
Di	58.90	55.08	53.98	52.95	43.76	62.56	76	-	-	-	-	-		24.98	22.49
Hy	6.92	-	16.11	14.3	35.18	-	14.6	21.91	18.25	32.21	24.61	33.34	60.58	60.35	61.38
Ol	12.75	35.49	16.13	20.97	7.3	26.53	0.64	66.27	65.27	50.95	60.06	52.12	5.65	5.03	4.40
Mt	11.19	4.67	7.39	6.12	5.13	2.22	2.21	3.66	9.57	10.49	10.07	8.13	-	-	-
Hem	0.81	-	-	-	-	3.02	-	-	2.54	1.02	-	-	0.27	0.35	0.31
Il	0.87	1.05	0.92	0.17	1.46	0.1	0.1	-	0.25	0.08	0.77	0.06	0.09	0.40	0.29
Ap	0.02	0.04	0.04	0.04	0.07	0.02	0.02	0.20	-	0.05	-	0.02	0.02	0.01	0.02
S.I.	62.45	80.79	74.97	75.07	74.51	82.84	80.71	86.00	78.15	78.15	78.78	78.78	81.15	80.23	80.70
Mg#	0.77	0.89	0.86	0.86	0.85	0.91	0.89	0.93	0.88	0.88	0.88	0.88	0.89	0.89	0.89

Table 3. The comparison of ultramafic rocks of the Shergarh Sar area with similar rocks of the ophiolitic complex from lesewhere in the world & with the estimated mantle composition.

	1	2	3	4	5	6	7	8	9
SiO_2	48.02	45.67	44.46	45.87	50.32	43.35	41.92	44.71	46.63
TiO_2	0.25	0.09	0.16	0.19	0.15	0.18	0.13	0.16	0.34
Al_2O_3	1.66	2.44	2.31	2.31	2.30	2.86	2.86	2.46	3.02
Fe_2O_3	4.17	5.89	3.47	5.35	0.27	9.29*	8.72*	9.06*	1.00
FeO	2.97	3.88	6.00	3.77	5.76	-	-	-	9.63
MnO	0.14	0.15	0.16	0.16	0.12	0.11	0.02	0.18	0.18
MgO	25.69	40.91	40.78	39.08	25.13	39.19	41.02	41.00	34.23
CaO	16.73	0.45	2.26	2.60	15.25	2.35	4.02	2.42	4.79
Na_2O	0.33	0.42	0.26	0.37	0.15	0.20	0.19	0.29	0.15
K_2O	0.02	0.04	0.03	0.04	0.02	0.00	0.02	Tr	0.03
P_2O_5	0.04	0.06	0.12	0.06	0.10	0.00	0.12	0.00	0.00

1. Average clinopyroxenite (this report).
2. Average serpentinite (this report).
3. Average peridotite (this report).
4. Average ultramafic rocks of the studied area. The calculation take into consideration the volume proportions the three rock types and therefore is not a simple arithmatic mean.
5. Olivine clinopyroxenite from Jijal Complex, Pakistan (Jan & Howie, 1981).
6. Average lherzolite from Lanzo, Tethyan ophiolites (Boudier, 1978).
7. Serpentinite from Dras area "Indus ophiolite belt", Ladakh, India (Prasad et al., 1979).
8. Estimated upper mantle composition (Maaloe and Aoki, 1977).
9. Average peridotitic komatiite, Barberton area, South Africa (Viljeon & Viljoen, 1969).

* = Total iron as Fe_2O_3.

ppm). Considering the C.I.P.W. norms, the proportion of ol varies with di in clinopyroxenite and with hy in serpentinite and peridotite. Ne also appear in the norms of these clinopyroxenites. Both serpentinites and peridotites have corundum in their norms, indicating the higher proportions of Al_2O_3 over CaO, possibly due to loss of Ca during serpentinization.

Fig. 2 (a-e) shows selected oxides (SiO_2, Fe_2O_3 + FeO, MgO, CaO, Al_2O_3) plotted against Solidification Index (SI=100 MgO/MgO+Fe_2O_3+ FeO+Na_2O+K_2O, after Kuno (1960). Apart from Fig. 2a & 2e where the analyses show considerable scatter, the data points on the other diagrams constitute two distinct variation trends which evidently reflect the fractionation control of various mineral phases (probably olivine and clinopyroxene). At a given Solidification Index the samples of peridotite-serpentinite series show comparatively high MgO, low CaO and SiO_2 than those in the clinopyroxenite series. P_2O_5, Al_2O_3, TiO_2, and K_2O+Na_2O variations are complex and patternless (not shown).

Distribution pattern of the chemical data

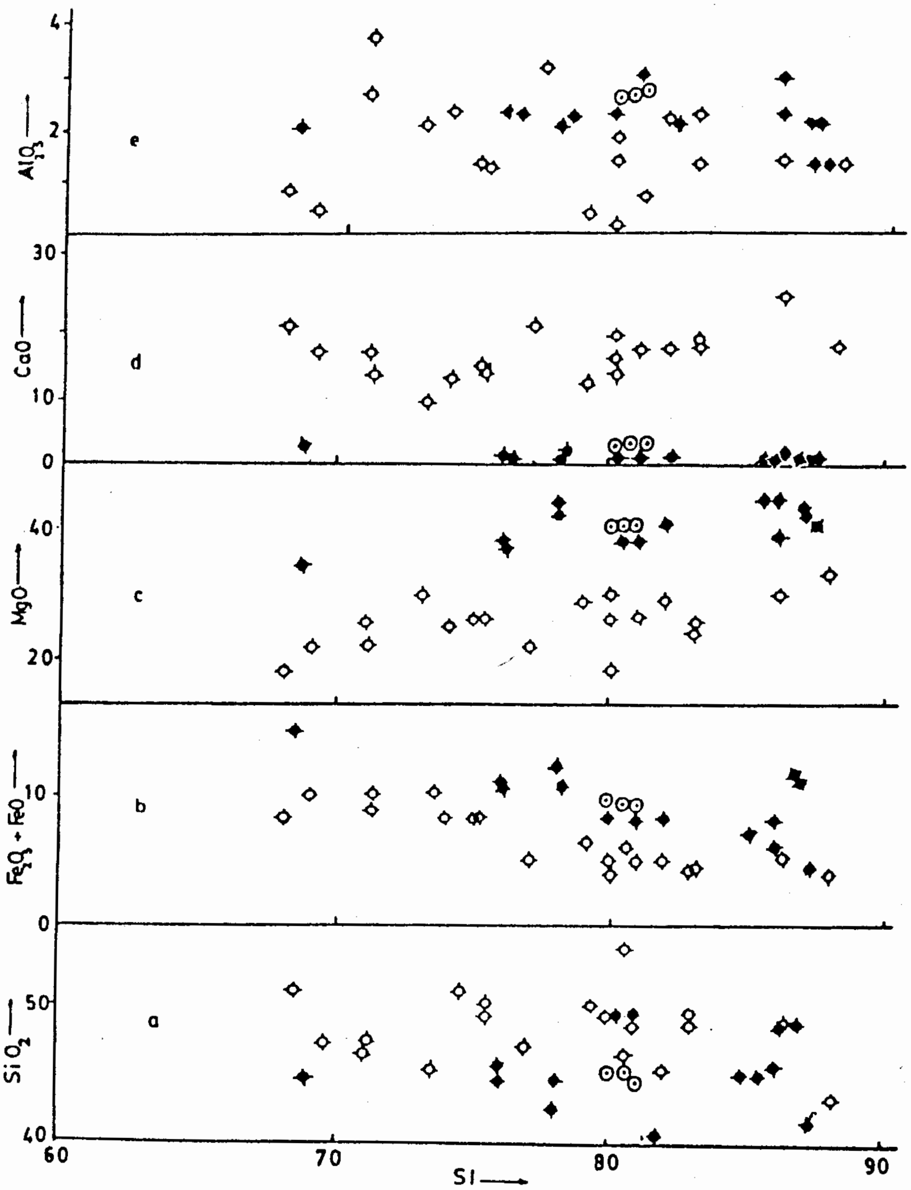

Fig. 2. Various oxides plotted against solidification index (S.I.) for the clinopyroxenites (open circles with crosses); peridotites (circles with dots); and serpentinites (solid circles with crosses) from the Shergarah Sar area.

of ultramafic rocks within the C.M.A.S. model (Cox et al., 1979) shows clustering close to the Enstatite (En) apex, and approaches the clinopyroxene position parallel to the En-Wol join in a projection from Qtz into En-Wol plane (Fig. 3). This suggests a dominant control of olivine and clinopyroxene fractionation from the parental magma. The fractionation control of olivine and clinopyroxene is further corroborated by the trace elements variation diagram (Fig. 4).

Nickel has a very regular positive correlation with MgO (Fig. 4) in the ultramafic rocks under discussion. It exhibits a marked decrease with MgO (45-35%) in the peridotite and serpentinite than in the clinopyroxenite. The average Ni contents (1876 ppm) of peridotites and serpentinites are lower than those of the peridotite, from mid-ocean ridges (about 2300 ppm, Vinogra dov, 1962; Bonatti, 1968). The Ni contents in the ultramafics from the area under discussion are not affected by serpentinization.

Cobalt (Co) which is generally insensitive to the degree of serpentinization (Steuber & Goles, 1967), exhibits constant variation with MgO in peridotite, serpentinite and also in clinopyroxenite. Similarities in the Co contents in serpentinite and peridotite (Tabe 1) indicate close relationship of the former with the latter type of rock than to the clinopyroxenite.

Chromium (Cr) also displays positive correlation with MgO (Fig. 4) similar to that of Ni. The higher concentration of Cr in peridotite and serpentinite reflects, in addition to olivine, the fractionation of clinopyroxene in the early stages of crystallization.

DISCUSSION

The chemical behavior of the ultramafic rocks from Shergarh Sar area suggests the derivation of serpentinite from peridotite by the alteration process. The H_2O_+ contents of the altered ultramafic rocks is a measure of the intensity of serpentinization and signify the completion of the peridotite to serpentinite conversion when it is about 11% (Thayer, 1966). The serpentinites listed in Table 1 are, therefore, true serpentinites in this sense. Considering the effects of serpentinization on the rock chemistry, it is clear from Table 3 that there was some loss of CaO during serpentinization of peridotite from the studied suite. Viljoen & Viljoen (1969) have also reported the loss of Ca during serpentinization of ultramafic komatiites of South Arica. The SiO_2 contents of the serpentinites (Table 3) are on the average about 1% higher than the peridotites which appears to support Sobolev's (1959) conclusion that serpentinization involves introduction of silica (Challis, 1965). The average higher amount of Na_2O in serpentinite relative to peridotite indicates its introduction during the process of serpentinization.

The trace elements such as Ba, K, Rb, and Cu in these ultramafic rocks, especially in peridotite and serpentinite were most likely affected by serpentinization. The Cr, Ni, Sr, Co contents have similarity among themselves and other types of ultramafic rocks and thus support the relatively insensitive nature of the elements to serpentinization processes.

The average anhydrous major oxides data for ultramafics (clinopyroxenite, peridotite and serpentinite) from the studied area are compared in Table 3 with compositions of ultramafic rocks developed in similar geographic/tectonic regions and with estimated mantle compositions. The average clinopyroxenite (column 1), serpentinites (column 2) and peridotites (column 3) match well in composition with similar rocks from ophiolitic complexes of Leka (column 6), (column 5), Lanzo (column 7) and Dras area (column 8). The average serpentinite of the studied area, however, has high SiO_2 than that of the Dras area, while the clinopyroxenite has slightly lower SiO_2 as compared to that of the Jijal complex. The average of 36 analyses (based on volume proportions) of ultramafic rocks from Shergarh Sar area (Table 3, column 4) is similar in terms of most of the oxide abundances to the estimated upper mantle composition (column 9) of Maaloe Aoki (1977).

The ultramafic rocks from the study area when plotted on the Mg-Fe-alk diagram (Fig. 5), show concentration within the limits suggested by Weedon (1970) for alpine type ultramafic rocks. Similar behaviour is also indicated by the clinopyroxenite on Ca-Mg-Fe diagram (Fig. 6) of Weedon (1970) whereas the peridotites are partially confined to the Bushveld field. The serpentinite analyses have not been plotted because of the considerable loss of CaO during serpentinization.

The molar MgO/(MgO+FeO Total +MnO) for the alpine type peridotites varies from 0.90 to 0.92 (Coleman & Keith, 1971; Himmelberg & Loney, 1973). The average molar ratio of peridotite (0.89) and serpentinite (0.90) of the studied area compares well with that of the alpine type peridotites.

The occurrence of ultramafics as separate masses in the neighborhood of lavas and greenschist facies rocks of basic composition and blue schist facies metagraywacke in the Main Mantle Thrust (MMT) zone signifies their non-sequential alpine type ophiolitic character (Miyashiro, 1973, p. 95). Abundances of clinopyroxenite among these ultramafics, however, discriminate them from the common alpine type ultramafic complexes, where periodotite and dunite are the dominant rock types (cf. Jackson & Thayer, 1972). The ultramafic rocks of the studied area appear to have a complex history like other alpine type peridotites (Wyllie,

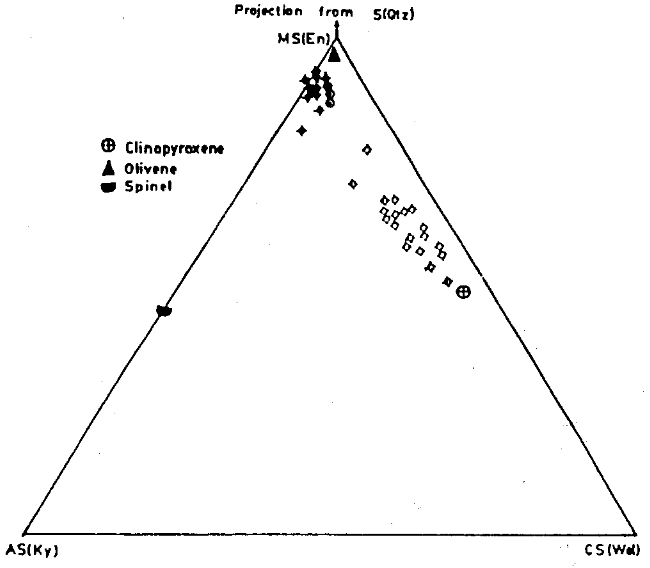

Fig. 3. Projection from Qtz into En-Ky-Wol plane for the ultramafics from Shergarh Sar area in C.M.A.S. model. Keyas for Fig. 2.

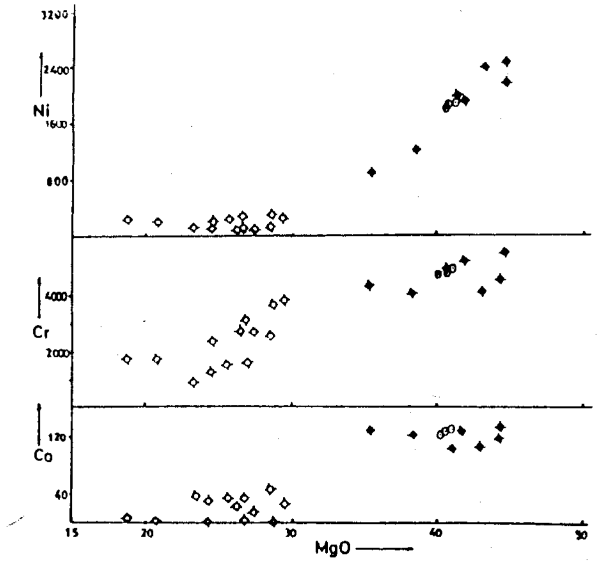

Fig. 4. Ni, Cr, Co, vs MgO plot for the ultramafic rocks from Shergarh Sar area. Key as in Fig. 2.

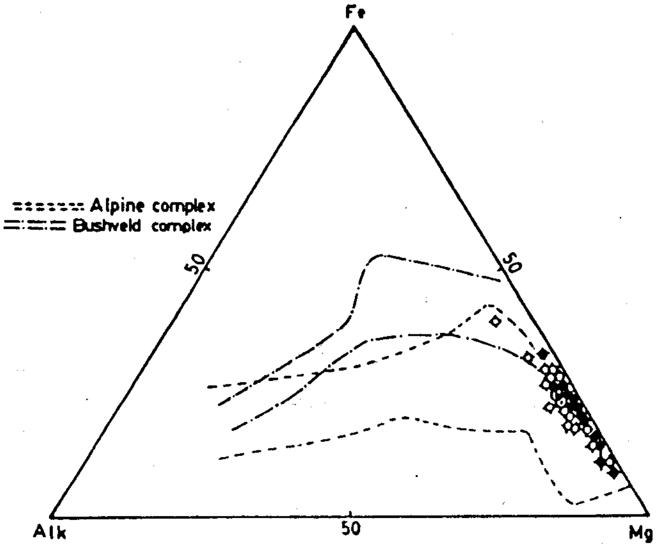

Fig. 5. Cation proportion of Fe, Mg, alkalies for the ultramafics from Shergarh Sar area, as compared to the trend in Alpine and Bushveld Complexes (after Weedon, 1970). Key as for Fig. 2.

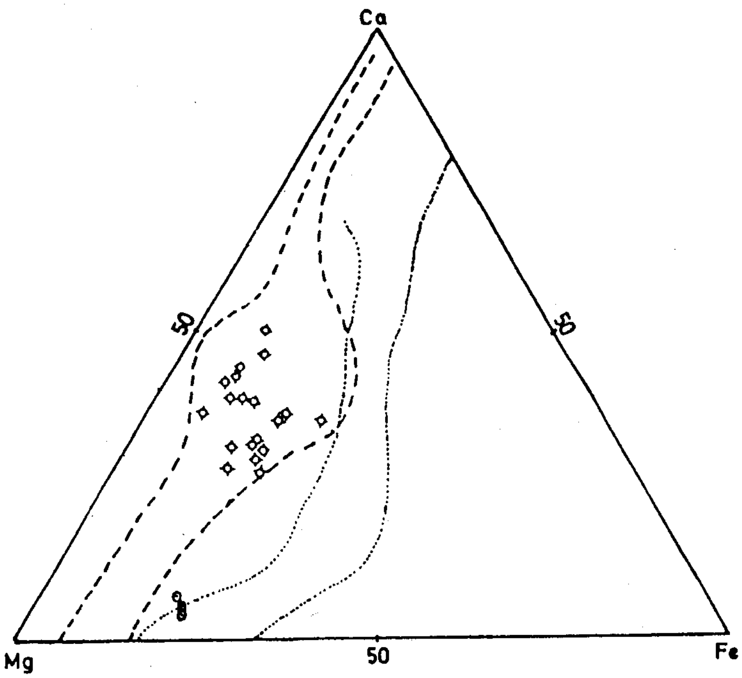

Fig. 6. Plot of Fe: Ca: Mg: (cation percent) for the clinopyroxenite and peridotite from Shergarh Sar area (after Weedon, 1970).

1969). These rocks were then probably tectonically emplaced in solid state from deeper zone into the upper crust along the MMT.

REFERENCES

BARD, J.P. (1983) Metamorphic evolution of an obducted island arc: Example of the Kohistan sequence (Pakistan) in the Himalayan collided range. Geol. Bull. Univ. Peshawar **16**, pp. 105-183.

BONATTI, E.. (1968) Ultramafic rocks from the Mid-Atlantic Ridge. Nature (London) **219**, pp. 363-364.

BOUDIER, F. (1978) Structure and petrology of the Lanzo peridotite massif (Piedmont Alps). Geol. Soc. Amer. Bull. **89**, pp. 1574-1591.

CHALLIS, G. (1965) The origin of Newzealand ultramafic inclusions. J. Petrol. **6**, pp. 322-364.

COLEMAN, R.G. (1967) Low-temperature reaction zones and alpine ultramafic rocks of California, Oregon, and Washington. U.S. Geol. Surv. Bull. **49**, pp. 1247.

——— **& KEITH, T.E.** (1971) A chemical study of serpentinization; Burro Mountain, California. J. Petrol. **12**, pp. 311-328.

COX, K.G., BELL, J.D. & PANKHURST, R.J. (1979) INTERPRETATION OF IGNEOUS ROCKS. George Allen & Unwin Ltd., London, 450p.

FOMIN, A.B. & KOZAK, S.A. (1971) Distribution of Cr, Co, and Ni in ultramafic rocks of the Middle Bug region. Geochem. Int. **8** (6), pp. 878-884.

HIMMELBERG, G.R. & LONEY, R.A. (1973) Petrology of the Vulcan Peak alpine-type peridotite, southwestern Oregon. Bull. Geol. Soc. Amer. **84**, pp. 1585-1600.

JACKSON, E.D., & THAYER, T.P. (1972) Some criteria for distinguishing between stratiform, concentric alpine peridotite-gabbro complexes. 24th Int. Geol. Congr. **2**, pp. 289-296.

JAN, M.Q. (1979) Petrology of the obducted mafic and ultramafic metamorphites from the southern part of the Kohistan Island arc sequence. Geol. Bull. Univ. Peshawar **13**, pp. 95-107.

——— **& HOWIE, R.A.** (1981) The mineralogy and geochemistry of the metamorphosed basic and ultrabasic rocks of the Jijal complex, Kohistan, NW Pakistan. J. Petrol. **22**, pp. 85-126.

KAZMI, A.H., LAWRENCE, R.D., DAWOOD, H., SNEE, L.W. & HUSSAIN, S.S. (1985) Geology of the Indus suture zone in the Mingora-Shangla area of Swat, Northern Pakistan. Geol. Bull. Univ. Peshawar **17**, pp. 127-143.

KUNO, H. (1960) Origin of Cenozoic petrographic provinces of Japan and surrounding areas. Bull. Volcanol. Ser. II, pp. 37-76.

LAWRENCE, R.D., KAZMER, C. & TAHIRKHELI, R.A.K. (1983) The main mantle thrust: a complex zone. Geol. Soc. Amer. Abs. with progr. **15**, p. 624.

MAJID, M. & SHAH, M.T. (1985) Mineralogy of the blue schist facies metagraywacke from Shergarh Sar area, Allai Kohistan, N. Pakistan. Geol. Bull. Univ. Peshawar **18**, pp. 41-52.

MALAKHOV, I.A. (1965) Criteria of degree of serpentinization of ultramafic rocks. Geochm. Int. **2** (4), p.678 (abstract).

MAALOE, S. & AOKI, K.I. (1977) The major element composition of upper mentle estimated from the composition of lherzolites. Contrib. Mineral. Petrol. **63**, pp. 161-173.

MIYASHIRO, A. (1973) METAMORPHISM AND METAMORPHIC BELTS. George Allen & Unwin Ltd., London, pp. 249-304.

PRASAD, U., SINGH, B., VENKATRAMAN, K. & GHOSH, D.B. (1979) Petrochemical characteristics of basic and ultrabasic rocks of Dras area, "Indus ophiolite belt" Ladakh India. *In*: Panayiotou, A. (ed.) "OPHIOLITES" Proceedings International Ophiolite Symposium, Cyprus, pp. 444-453.

SHAH, M.T. & MAJID, M. (1985) Major and trace element variation in the lavas of Shergarh Sar Area and their significance with respect to the KohistanTectonic Anomaly. Geol. Bull. Univ. Peshawar **18**, pp. 163-188.

SOBOLEV, N.D. (1959) Contribution to the petrochemistry of ultrabasic rocks. Geochemistry (English translation from Russian) No. **8**, pp. 839-864.

STEUBER, A.M. & GOLES, G.G. (1967) Abundances of Na, Mn, Cr, Sc and Co in ultramafic rocks. Geochim. Consmochim. Acta **31**, pp. 75-93.

TAHIRKHELI, R.A.D., MATTAUER, M., PROUST, F. & TAPPONNIER, P. (1979) The India Eurasia suture zone in northern Pakistan some new data for an interpretation at plate scale. *In*: Farah, A. & De Jong, K.A. (eds.) GEODYNAMICS OF PAKISTAN, Geol. Surv. Pakistan, Quetta, pp. 125-130.

THAYER, T.P. (1966) Serpentinization considered as a constant volume metasomatic process. Am. Mineral. **51**, pp. 685-710.

VILJOEN, M.J. & VILJOEN, R.P. (1969) The effects of metamorphism and serpentinization on the volcanic and associated rocks of the Barberton region. Geol. Soc. Af. Spec. Publ. **2**, pp. 29-53.

VINOGRADOV, A.P. (1962) Average contents of chemical elements in the principle types of igneous rocks of the earth crust. Geochem., pp. 641-664.

WEEDON, D.S. (1970) The ultrabasic/basic igneous rocks of the Huntly region. Scot. Jour. Geol. **6**, pp. 26-40.

WILSON, A.D. (1960). The micro determination of ferrous iron in silicate minerals by a volumetric and colourimetric method. Analyst. **85**, p. 823.

WILSON, N.D. (1955) A new method for the determination of ferrous iron in rocks and minerals. Bull. Geol. Surv., G.B., **9**, p. 56.

WYLLIE, P.J. (1969) The origin of ultramafic and ultrabasic rocks. Tectonophys. **7**, pp. 437-455.

Manuscript received on December 10, 1992;
accepted for publication on December 31, 1992.

ACTA MINERALOGICA PAKISTANICA
VOLUME 6 (1992) pp. 85-92.

DASHTE-KAIN PORPHYRY COPPER-MOLYBDENUM PROSPECT OF CHAGAI, BALOCHISTAN: AN INDUCED POLARIZATION STUDY

M. ANWAR UDDIN AHMAD
Geological Survey of Pakistan, P.O. Box 15, Quetta, Pakistan.
NAYYAR ALAM ZAIGHAM
Geological Survey of Pakistan, R-42, Block 6, PECHS, Karachi, Pakistan.
&
M. HAFEEZ BUTT
Geological Survey of Pakistan, 83-D, Model Town, Lahore, Pakistan.

ABSTRACT: In 1975, the Dasht-e-Kain porphyry copper - molybdenum prospect was discovered in Chagai District after an aerial reconnaissance survey of Chagai massif. Subsequently, detailed geological mapping and geophysical exploration were carried out. An induced polarization(IP) study has been found to be useful in the evaluation of sulphide mineral prospect. The IP anomalies show a definite correlation with the geology and the geochemical anomalies. The IP results clearly demarcate the zones of mineralization and their distribution in depth.

INTRODUCTION

At Dashte-Kain (latitude 29° 33' N and longitude 64°39' E), characteristic alteration favourable for porphyry sulphide mineralization was identified during an aerial reconnaissance survey (Sillitoe, 1975, 1981). The detailed geological mapping and geochemical prospecting by the Geological Survey of Pakistan indicated the presence of porphyry copper molydenum sulphide mineralization (Ahmed et al., 1981; Butt et al., 1985).

For the study of subsurface distribution of the sulphide mineralization, the IP time-domain exploration technique was applied.

GEOLOGICAL SETTING

In Dasht-e-Kain area, an alteration zone elongated in NE-SW direction, occurs in a composite stock emplaced in andesitic Sinjrani volcanic rocks of Cretaceous age (Fig. 1). Geologically the area may be divided into southwestern and northeastern portions on the basis of alteration characteristics (Sillitoe, 1975). In the south-western portion, a tonalite porphyry has undergone potassium silicate alteration which is surrounded by sericitic alteration zone. Numerous dykes of both late - and post - mineralization transect the area, trending northwards and range in composition from dacite porphyry to diorite porphyry, andesitic porphyry and andesite (Ahmed et al., 1981).

In the northeastern portion the most dominating geological feature is the hydrothermal breccia pipe surrounded by a body of equigranular granodiorite. The breecia is post-mineralization. It contains mineralized rock fragments and has undergone weak potassium silicate alteration.

GEOCHEMICAL ANOMALIES

In the geochemical anomaly map (Fig. 2), two separate mineralized or potassic zones are clearly discernible. The concentration of copper mineralization is higher in northeastern portion of the prospect area than in southwestern.

INDUCED POLARIZATION (IP) MEASUREMENTS

Method

The IP measurements were made along eleven selected profiles of 450 to 900 feet length and dipole-dipole field array was adopted. The scintrex time-domain transmitter IPC 7/15 kw and receiver IPR-8 were used. The IP scanning was done upto pseudo-depth of n5(450 feet) using the electrodes separation of 150 feet. The chargeability (millisecond) and the resistivity (ohm meter) values were obtained (Table 1) and used for constructing

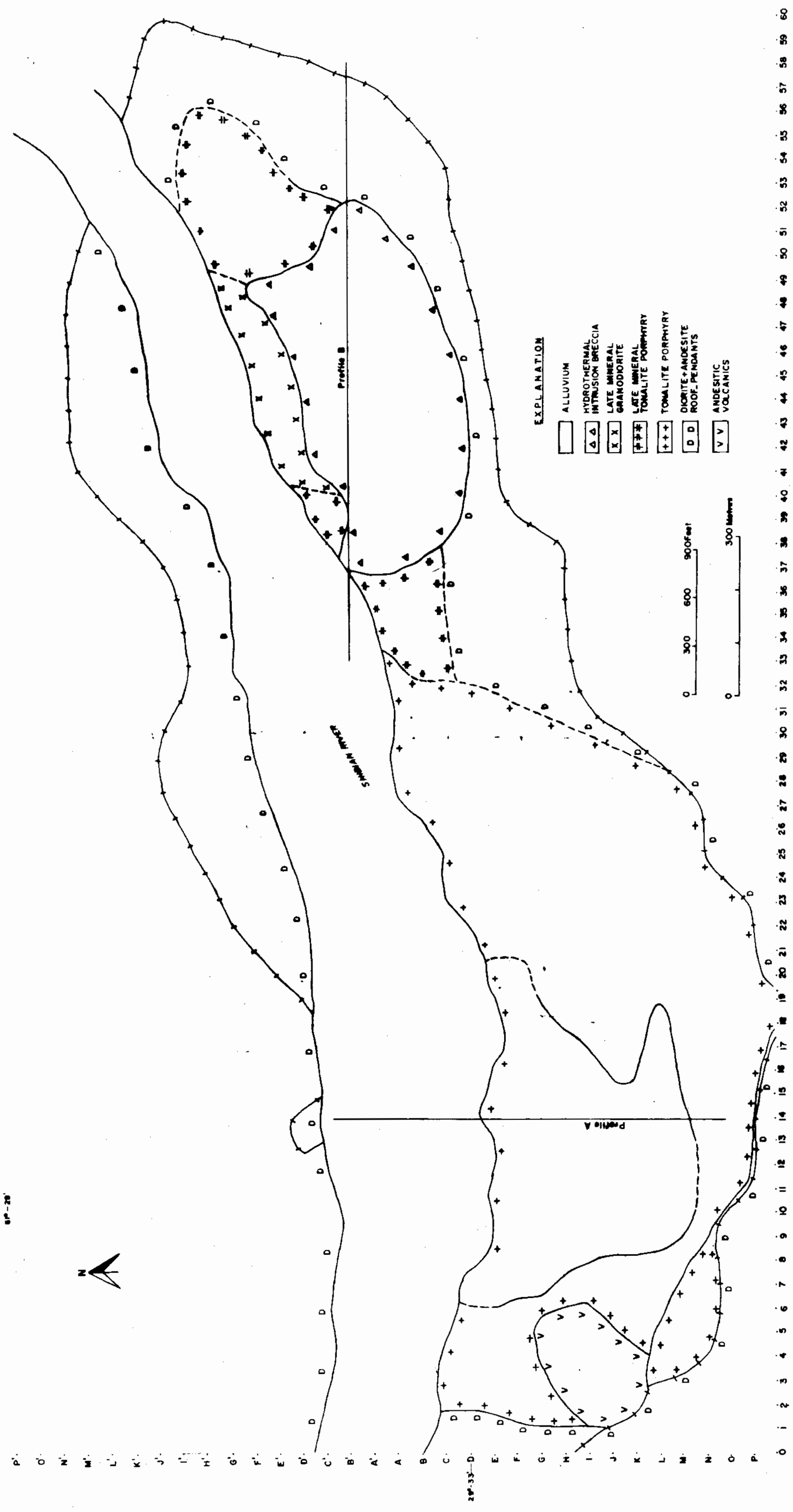

FIG. I.

Fig. 1. General geological map of Dasht Kain, Chagai District, Balochistan (after Ahmad & Siddiqui, 1989). Numbers and letters on the margins represent grids drawn for location reference. Distance between any two successive grid numbers or letters is 150 feet.

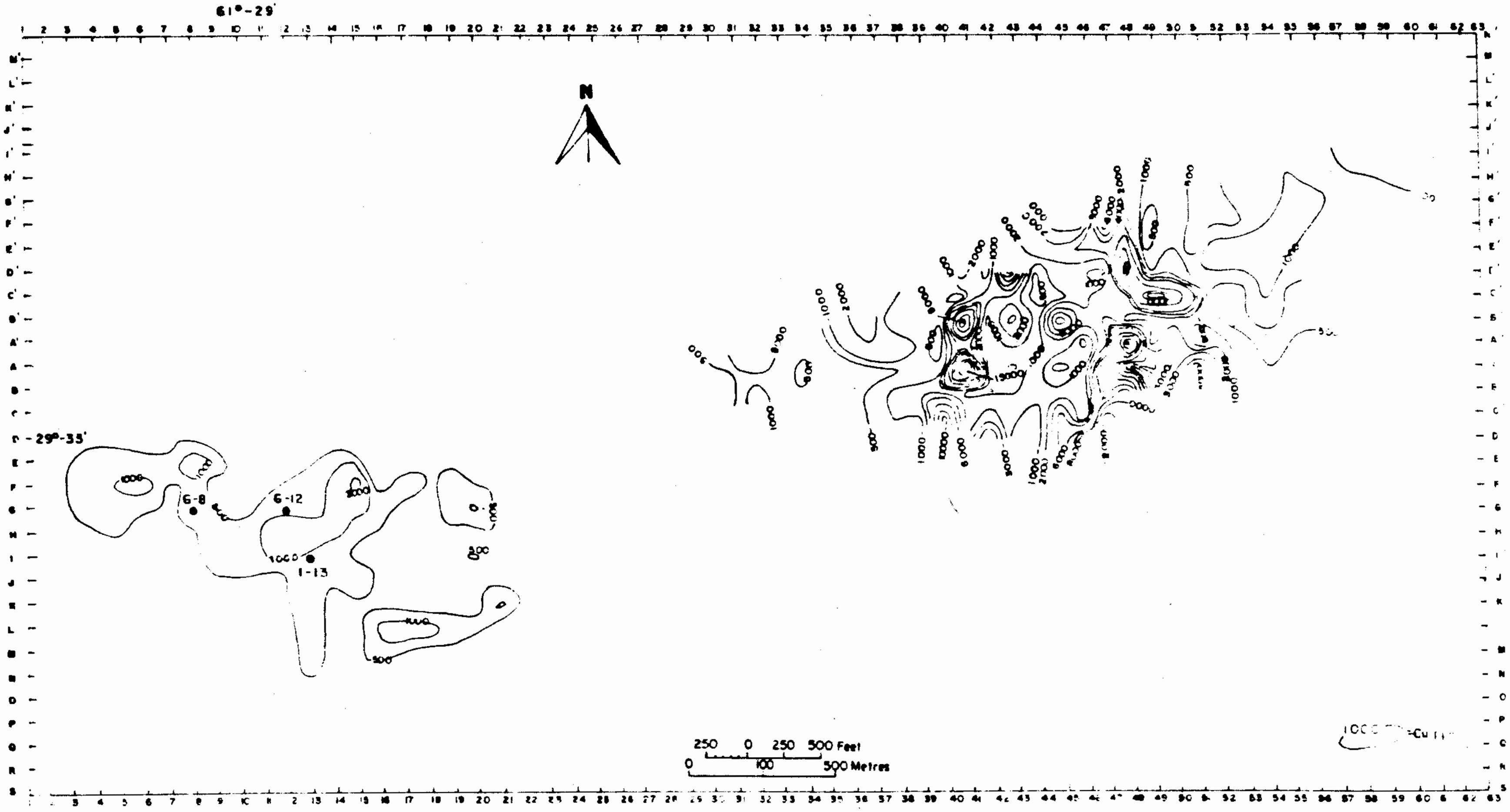

Fig. 2. Map showing geochemical concentration of copper in soil and location of test bore holes. The numbers and letters on outer frame are as in Fig. 1.

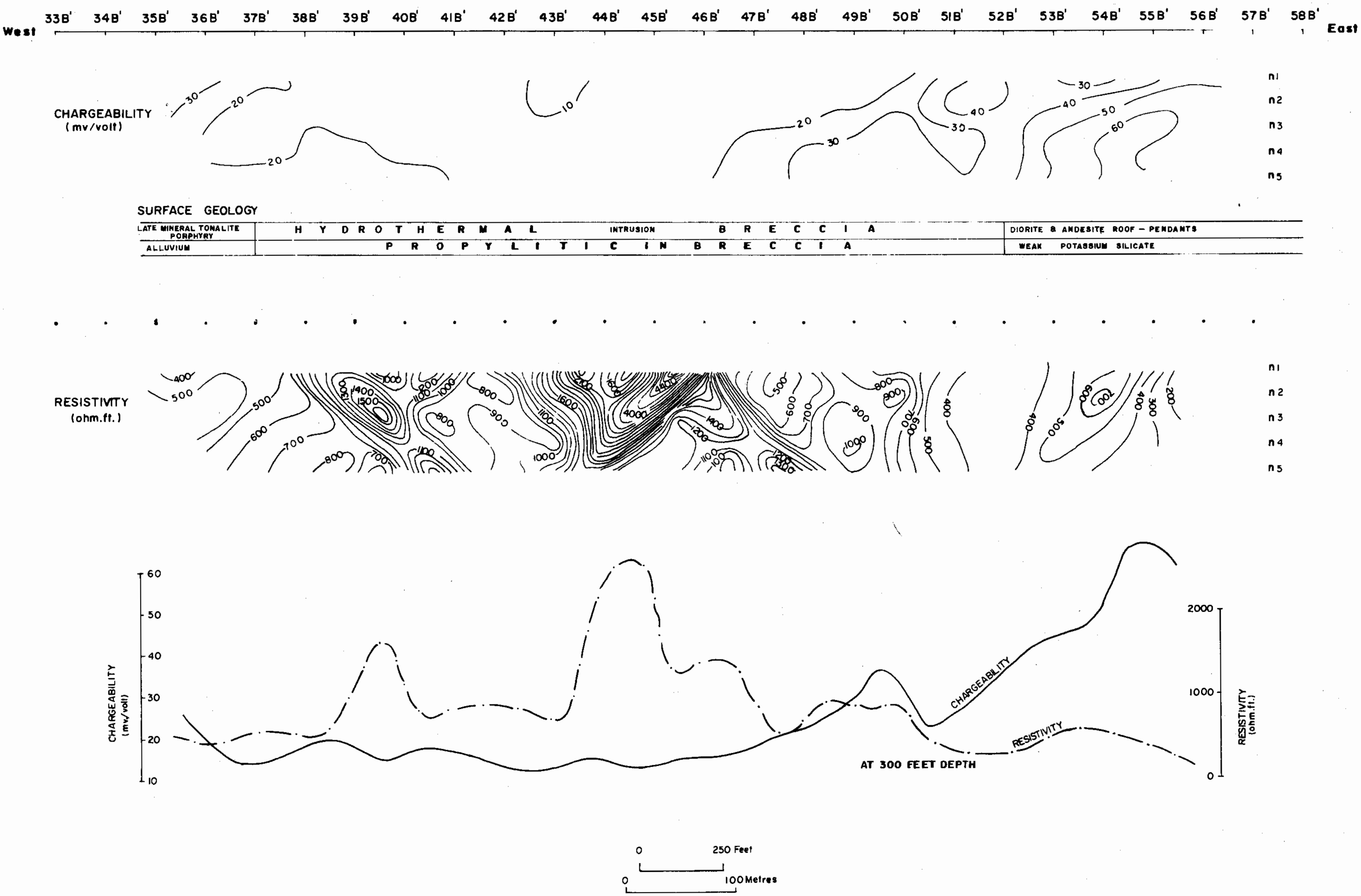

Fig. 3. Pseudo-sections of chargeability and resistivity along profile A and B which are indicated by straight lines in Fig. 1. The numbers and letters on outer frame are as in Fig. 1.

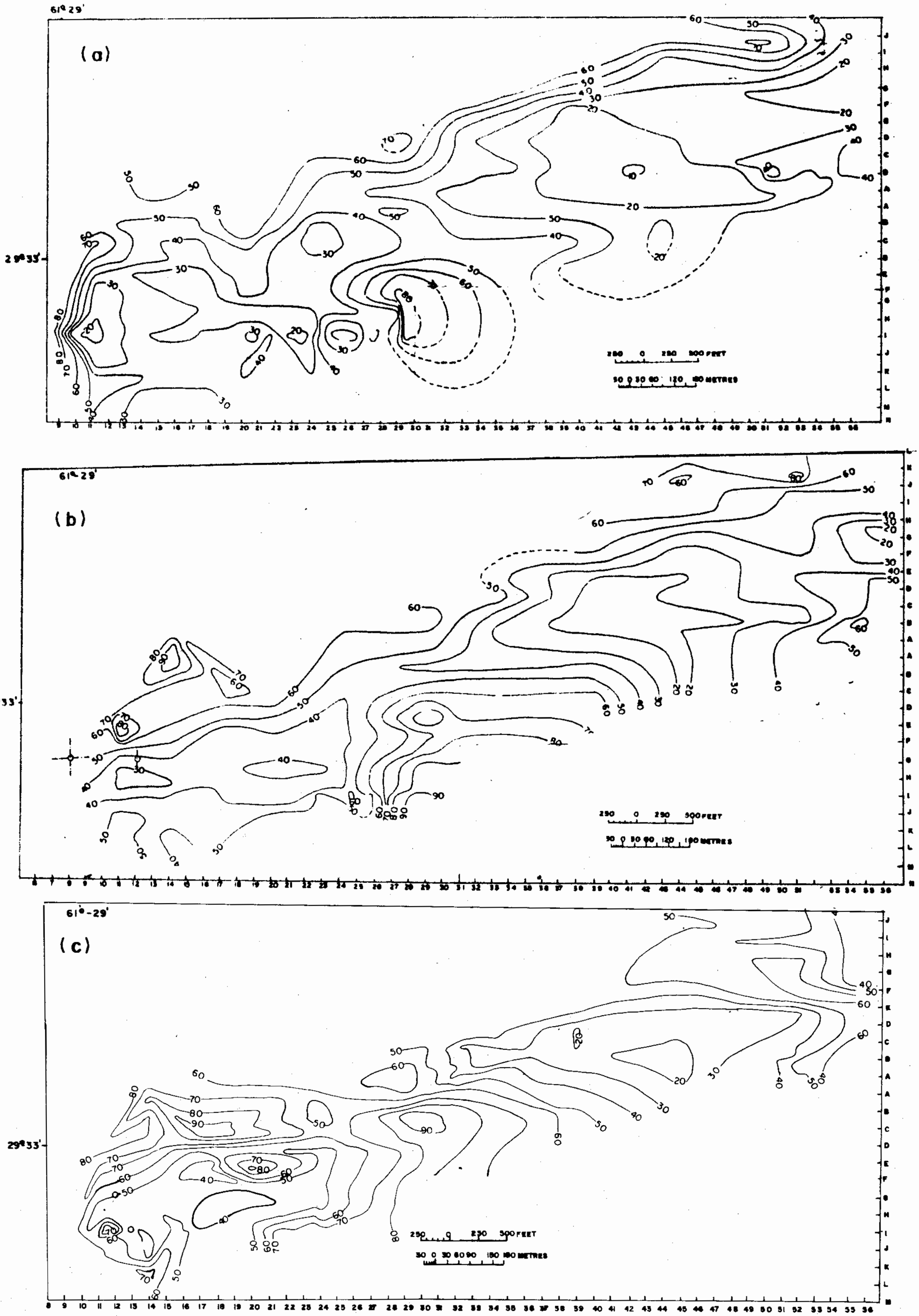

Fig. 4. Plan maps of chargeability at pseudo-depth (a) 150 feet, (b) 300 feet, and (c) 450 feet. The numbers and letters on outer frame are as in Fig. 1.

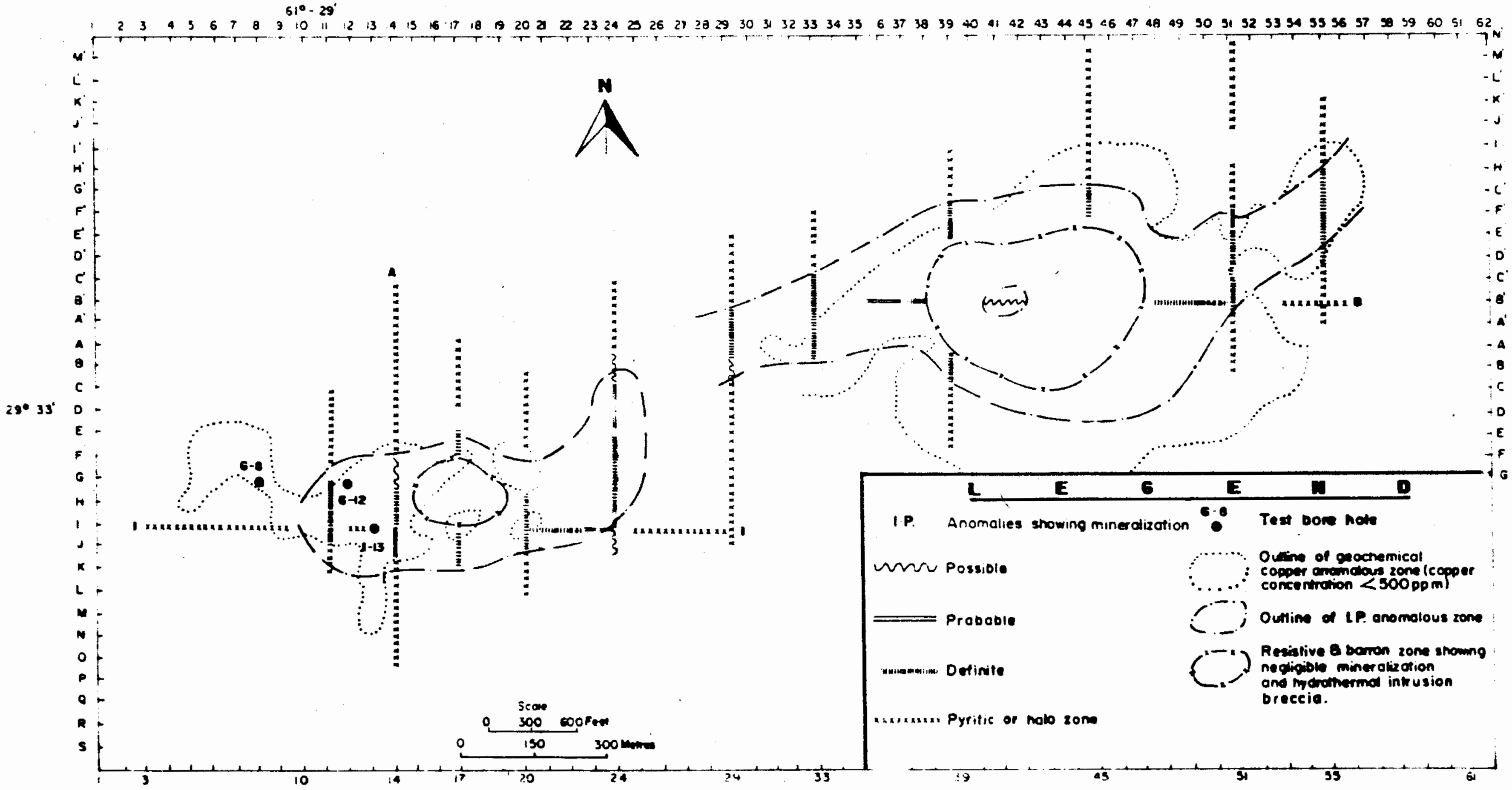

Fig. 5. Map showing the comparison between IP and geochemical anomalies and location of test bore holes. The numbers and letters on outer frame are as in Fig. 1.

pseudo-sections and plan maps of different depths (Figs. 3 & 4).

IP Data

The results of IP measurements have been interpreted in terms of concentration of sulphides. A disseminated ore is generally composed of metallic minerals scattered in the form of specks or veinlets in the host rock, representing less then 20% of the total volume.

IP Pseudo-Sections :

(i) *Pseudo-section – A*: It crosses the southwestern zone of the prospect. The chargeability values are increasing in depth consistently, whereas the resistivity pattern is quite complex, indicating alteration of varying degree. The comparison of chargeability and resistivity pattern indicates almost vertical attitude of the mineralized zone. The central portion of the section having moderate chargeability and resistivity is the most promising part of the mineralized zone. The extreme southern and northern portions have high chargeability and low resistivity anomalies indicating pyritic halos associated with phyllic zone. Mid-southern and mid-northern portions have low chargeability and moderate to high resistivity indicating relatively poor mineralization in the sericitic zone.

(ii) *Pseudo-Section – B:* It crosses the northeastern body of the prospect. On this section, the general pattern of chargeability and resistivity anomalies is quite different in comparison with that of southwestern zone. The attitude of the mineralized zone. The central portion of the section having moderate chargeability and resistivity is the most promising part of the mineralized zone. The extreme southern and northern portions have high chargeability and low resistivity anomalies indicating pyritic hales associated with phyllic zone. Mid-southern and mid-northern portions have low chargeability and moderate to high resistivity indicating relatively poor mineralization in the sericitic zone.

(ii) Pseudo-Section-B: It crosses the northeastern body of the prospect. On this section, the general pattern of chargeability and resistivity anomalies is quite different in comparison with that of southwestern zone. The attitude of the mineralized zone along this section appears to be moderately dipping. The section indicates interesting features of varying degree of alteration and resultant mineralizations. The IP effects on extreme eastern portion of the section indicate predominantly pyritic mineralization in dioritic-andesitic suite of rocks. The mid-eastern portion having moderate chargeability and resistivity is the promising zone. The central and mid-western portions have high resistivities and low chargeability with minor variations. Probably this entire portion consists of lean mineralization or "dry zone". The extreme western portion appears to be mineralized.

Plan Maps of Chargeability

The plan maps of chargeability at 150, 300 and 450 feet depth indicate the pattern of mineralization (Fig. 4).

In the western portion of the map two separate zones of mineralization with limited extent are noted. The contour pattern suggests that mineralized zone is elliptical-shaped and vertical in attitude. The overall IP response of this zone indicate fair to good mineralization of limited extent.

The eastern anomalous zone appears to be comparatively quite large. The central portion seems to be poorly mineralized having funnel-like pattern, pinching out in depth. The area surrounding the poorly mineralized zone is better mineralized. The aerial extent of mineralized zone suggests good prospect which extends towards NE in a narrow zone. The intervening zone seems to be pyritic in depth.

Comparison of IP Results with the Geochemical Anomalies and Drilling Information.

In the southwestern zone, the geochemical anomalies are rather weak. Moreover, the anomalous area appears to be of limited aerial extent. If these anomalies are compared with the IP results, a striking similarity is observed.

Fig. 5 shows on overlay of geochemical anomalous zone of 500 ppm copper concentration, over the IP results. The definite IP anomalies of economic significance lie within the zone of geochemical anomalies. The IP anomalies extend in NE direction, but since no geochemical sampling was done in that area, the comparison between IP and geochemical anomalies could not be made. The IP anomalies have been qualitatively interpreted in terms of probability of mineralization. In the central portion a dry zone with lean mineralization is discernible where no geochemical anomaly appears.

In the northeastern anomalous area the IP and geochemical anomalies correlate reasonably well. The definite IP anomalies lie within the geochemically anomalous zone. The IP anomalies

Table 1. Ranges of chargeability and resistivity values and their correlation with the concentration of sulphide mineralization.

Chargeability Mv/volt.		Resistivity Ohms ft.		Correlation*	Remarks
Range	*Grade*	*Range*	*Grade*		
10 to 20	Very low to low.	1500 to 3000.	Moderate to high.	Almost negligible mineralization.	Non-mineralized fresh rock or hydrothermal intrusion or post mineralized dykes.
20 to 30	Low to moderate.	600 to 1500%	Low to moderate.	Small quantity of chalcopyrite bornite & molydendum; negligible pyrite.	Indicating the mineralized zone being near and above the fresh intrusive.
30 to 40	Moderate to high.	600 to 1500 :	Low to modrate	Chalcopyrite 0.8% to 18% with 1% pyrite.	Indicating sulphide mineral concentration in K zone.
40 to 80	High to very high.	600 to 100.	Low to very low.	Fyrite more than 10% with negligible chalcopyrite less than 2%.	Indicating pyritic halo-associated with phyllic or sericitic zone.

* = Correlation of resistivity and chargeability with the concentration of mineralization.

follow the trend of geochemical anomalies towards E and W. The central portion has lean mineralization since the geochemical anomalies in this zone are not intense (Fig. 5).

The objective comparison of these two techniques suggests that the correlation of IP & geochemical techniques provides guidance for locating drill holes judiciously in the area for further exploration and evaluation of the prospect.

The bore holes G-8 to G-12 (vertical holes) and I-13 (inclined 45° towards east) were drilled in southwestern zone and did not yield very promising results. The reason of poor to fair mineralization encountered in these bore holes is obvious from the IP and geochemical results since these holes were located at the margin of definite IP anomalies and away from the zone of strong geochemical anomalies.

Three test bore holes were drilled, namely G-8, G-12 and I-13 (Figs. 2&5), in the southwestern part of the Dash-e-Kain prospect.

Based upon the bore holes information, an attempt has been made to establish a relationship of chargeability and resistivity ranges with the percentage of chalcopyrite, chalcocite and pyrite (Table 1).

CONCLUSION

The IP technique in combination with geochemical technique is found to be a powerful tool in delineating the promising zones of mineralization in Dashte Kain area. The IP results have provided information regarding possibilities of mineralization in depth.

REFERENCES

AHMAD, M.U. (1980) Alteration pattern, geochemistry & petrology of Dasht-e-Kain porphyry copper molybdenum prospect, Chagai District, Baluchistan, Pakistan. Inf. Rel. Geol. Surv. Pakistan **137**, 24p.

——, **CHAUDHERY, M.A. & SIDDIQUI, R.H.** (1981) Hydrothermal alteration and geochemistry of Dashte Kain porphyry copper molybdenum prospect, Chagai District, Baluchistan, province, Pakistan. Rec. Geol. Surv. Pak., **55** (in press).

BUTT, M.H., KHURSHID, A., & NAQVI, S.W.H. (1985) Induced polarization survey of sulphide mineral prospect in Dashte Kain area, Chagai District, Baluchistan, Province, Pakistan. Inf. Rel. Geol. Surv. Pakistan. **155**.

SILLITOE, R.H (1975) U.N.D.P. Report on prospect of metallic minerals in Chagai area. (Unpublished).

—— **(UNPUBLISHED) (1981)** Evaluation of Mineral Prospects and suggestions for exploration in Baluchistan, Pakistan UN. Report (Unpublished).

Manuscript received on October 30, 1992;
accepted for publication on December 30, 1992.

ACTA MINERALOGICA PAKISTANICA
VOLUME 6 (1992) pp. 93-100.

GEOLOGY OF THE KIRANA AREA, DISTRICT SARGODHA, PUNJAB, PAKISTAN

GHULAM SARWAR ALAM,
ASAD JALEEL
&
RASHEED AHMAD
Geological Survey of Pakistan, Lahore, Pakistan.

ABSTRACT: Metasedimentary and igneous Precambrain rocks are present in the Kirana, Chiniot, Shahkot and Sangla hills of Punjab, Pakistan. The area consists of two geomorphic features, viz., scattered hills and flat alluvial plains. The metasedimentary rocks include quartzites and slates, with layers of lava, tuff and volcanic breccia. These rocks are intruded by a number of basic dykes, sills and a few felsic dykes. The rocks of the Kirana area have been divided into five lithological units. Three units, namely, Asianwala, Taguwali and Hachi Formations have been included in Kirana Group. A new Sharaban Group has been proposed, comprising two units, namely calcareous conglomerate and sandstone. There are indications of iron mineralization in the form of hematite veins along fractures and joints, but as yet no significant deposit has been reported. However, drilling on the basis of the geophysical anomaly in Chiniot area promises encouraging results.

INTRODUCTION

The Kirana hills are the outliers of shield rocks in the Punjab plains, present in the Kirana, Chiniot, Shahkot and Sangla areas (Fig. 1). The rocks are of Precambrian age. The area consists of two geomorphic features, viz., scattered hills and flat alluvial plains.

Heron (1913) prepared a reconnaissance map of the area. Shah (1973) gave a brief description of the stratigraphy of the Kirana group. Alam (1987) carried out detailed geological mapping of the area. Alam and Ahmad (1990) grouped the Kirana rocks into three categories on the basis of suitability as aggregate resource.

This paper gives details of various lithounits in a new sub-division of the Kirana Group. Brief description is also given regarding the petrology of various formations, along with their age and correlation status.

GENERAL GEOLOGY

The Precambrian outcrops are composed of metasedimentary and igneous rocks (Fig. 2). The metasedimentary rocks are represented by quartzites, slates and phyllites; the igneous rocks include diabase, tuffs and lava. Metasedimentary rocks are interlayered with tuffs, volcanic breccia and lava flows of mainly acidic composition and are intruded by basic sills and dykes.

The rocks of Kirana area have been divided into five units on the basis of rock types, as shown in Table 1 (Alam, 1987).

Table 1. Stratigraphic sequence of the Precambrian basement rocks in Kirana area, reproduced from Alam (1987).

GROUP	FORMATION	DESCRIPTION
SHARABAN	Sharaban Formation	Conglomerate, dull rusty brown containing pebbles of quartzites, slate & limestone, embedded in calcareous matrix. 119 m thick..
	Hadda Formation	Quartzites, dull rusty brown, fine - grained, calcareous, typical of shallow marine or deltaic origin; containing minor conglomerate beds, rare lava flows. 372 m thick.
KIRANA	Asianwala Formation	Quartzites, light grey to dirty white, mottled brown, medium- to coarse - grained, cross-bedded, ripple-marked, contain minor intercalations of slate. 248 m thick.
	Taguwali Formation	Phyllite, light grey, minor intercalations of quartzites. Lower part fine-grained quartzite, cross-bedded. 1190 m thick.
	Hachi Formation	Slates, minor quartzites, with abundant tuff and lava flow. 404 m thick at the type locality.

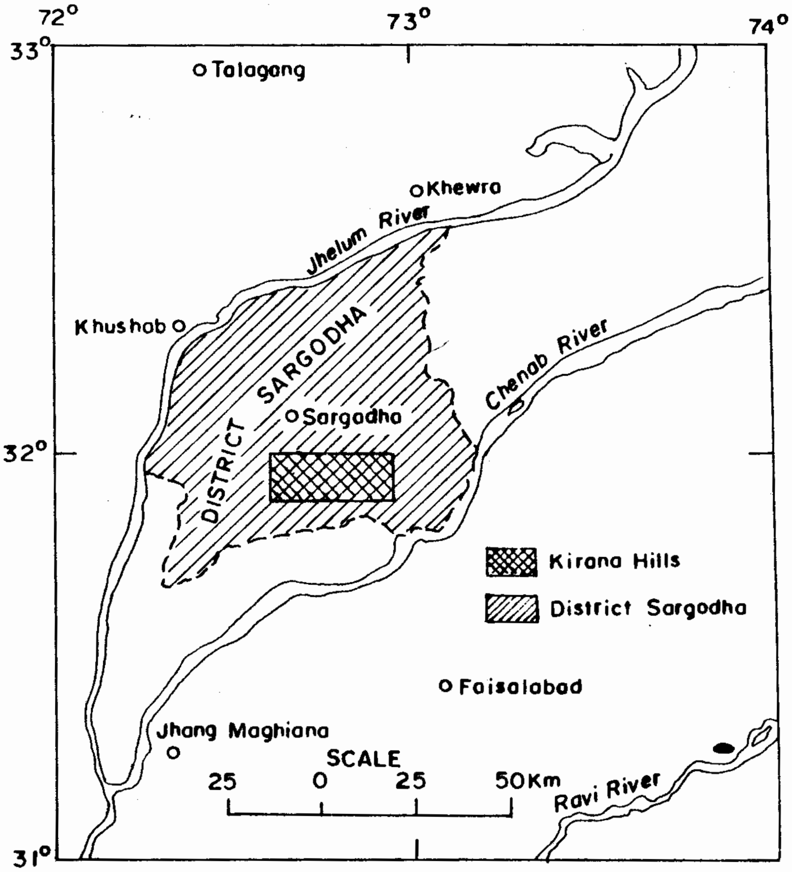

Fig. 1. Location map of Kirana Hills, District Sargodha.

Three units, namely the Asianwala, Taguwali and Hachi Formations are included in the Kirana Group. The Sharaban group has been proposed, comprising two units, namely Sharaban and Hada (Fig. 2). These units have not been included in the Kirana Group because no where in the area, there direct contact and relationship with the Kirana Group is found. The rocks of these units are exposed only in an isolated hill called Sharaban. These units are considered to be younger than the Kirana Group, on the basis of the regional trend in the Kirana area.

STRATIGRAPHY

The stratigraphic sections along hills south and north of Chak 123 S.B., Buland Hill, Hachi Hill and Sheikh Hill were measured and the columnar sections of the same are depicted in Fig. 3. The detail of the different formations is as follows.

HACHI FORMATION

The Hachi Formation is named after Hachi Hill located at latitude 31° 54' 12" N, longitude 72° 41' 58" E; north of Sikhanwali Railway Station. Nowhere in the mapped area has its full thickness been found. The Hachi and Sheikh hills are the type localities.

The characteristic lithology of the Hachi formation consists of quartzites, slates, phyllites, tuffs and lava flows present in variable proportions. This formation is exposed at Buland Hill, Hachi Hill, Sheikh Hill, Hundawali Hill and Chiniot Hill. In Buland Hill, lava and tuff are dominant. In the Chiniot area, a small hill located in Chiniot town is composed entirely of rhyolitic lava.

The quartzites are light- to medium- grey, and medium-grained and composed mostly of subrounded to rounded grains of quartz, with sericite and clay minerals.

Tuffs and volcanic breccia are present throughout in this formation, the best exposure of this rock is at Hachi Hill. The tuffs and volcanic breccia are light grey and present at different stratigraphic levels, interlayered with lava and metasediments. The volcanic breccia is rhyolitic with abundant rock fragments and large phenocrysts of feldspar and quartz, set in a fine-grained matrix. The tuffs are interlayered with quartzites and slates. In general the bedding is not distinct in these beds, but at places clear bedding is present. The rocks are slightly metamorphosed but retain their original texture. The slates interbedded with tuffs seem to have been derived from volcanic ash and other fine volcanic material. Thin section study of 15 rock samples from different beds shows that phenocrysts make 15 to 25% of the rock.

The groundmass is fine-grained and is made up of small grains of quartz, microlites of quartz and feldspar and partly devitrified glass. The abundance of phenocrysts is quartz 15-50%, feldspars (mostly perthite) 20-45%, and glass and rock fragments 5-10%. Quartz occurs both as phenocrysts and groundmass, is angular to subrounded, and has sharp boundaries with the groundmass.

The feldspar phenocrysts are mostly perthite and orthoclase; a few grains of magnetite and biotite are also present. The mineralogical composition of tuffs suggests that they have been derived from magma of acidic composition. Lava is interlayered with the metasediments. It is very difficult to study the nature of contact. However, it seems to be chilled. Pillow structure has not been found in the lava flows. Mostly the lava is acidic and is represented by such rocks as rhyolite, dacite and minor andesite. Lava of rhyolitic composition is present in Chiniot Hill, Hachi Hill, Sheikh Hill and Taguwali Hill.

In Hachi Hill, rhyolite is medium grey and made of quartz and feldspar phenocrysts (15%) set in fine, glassy matrix. A sample of dacite from Sheikh Hill gave the following mineral content: quartz 35-50%, feldspar (mostly albite), 45-55% and chlorite, 2-5%.

Andesite is present in Hundawali Hill. It is a dark grey, massive rock with holocrystalline, fine-grained, porphyritic texture. The phenocrysts of feldspar are set in groundmass of oligoclase, orthoclase and quartz. The percentage composition of the rock is: oligoclase, 45-50%; orthoclase 40-55%, hornblende (altered to chlorite), 5-7%, ilmenite; 7-9%; with accessory quartz and biotite.

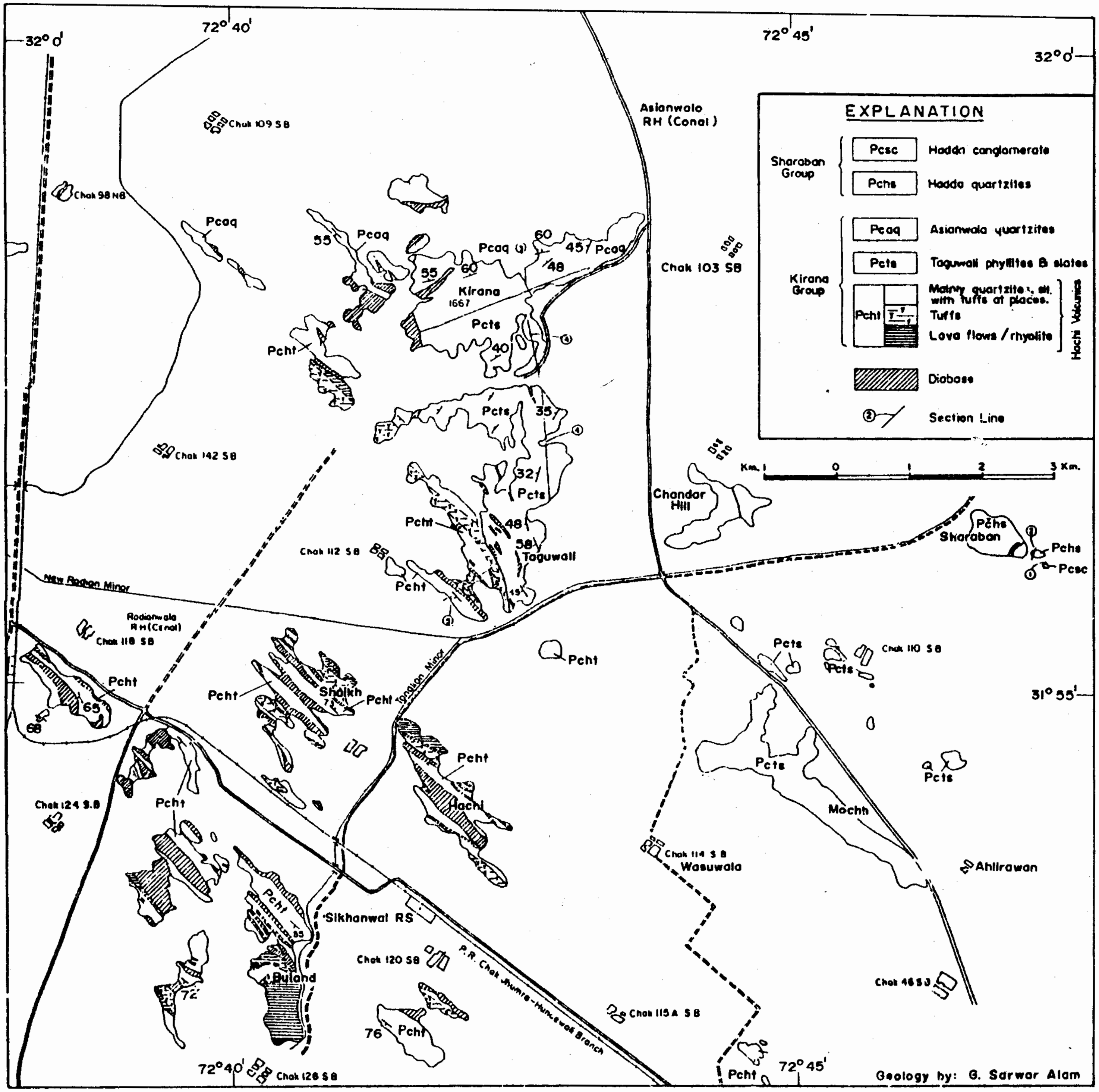

Fig. 2. Geological map of Kiran a Hills, Sargodha District, Pakistan.

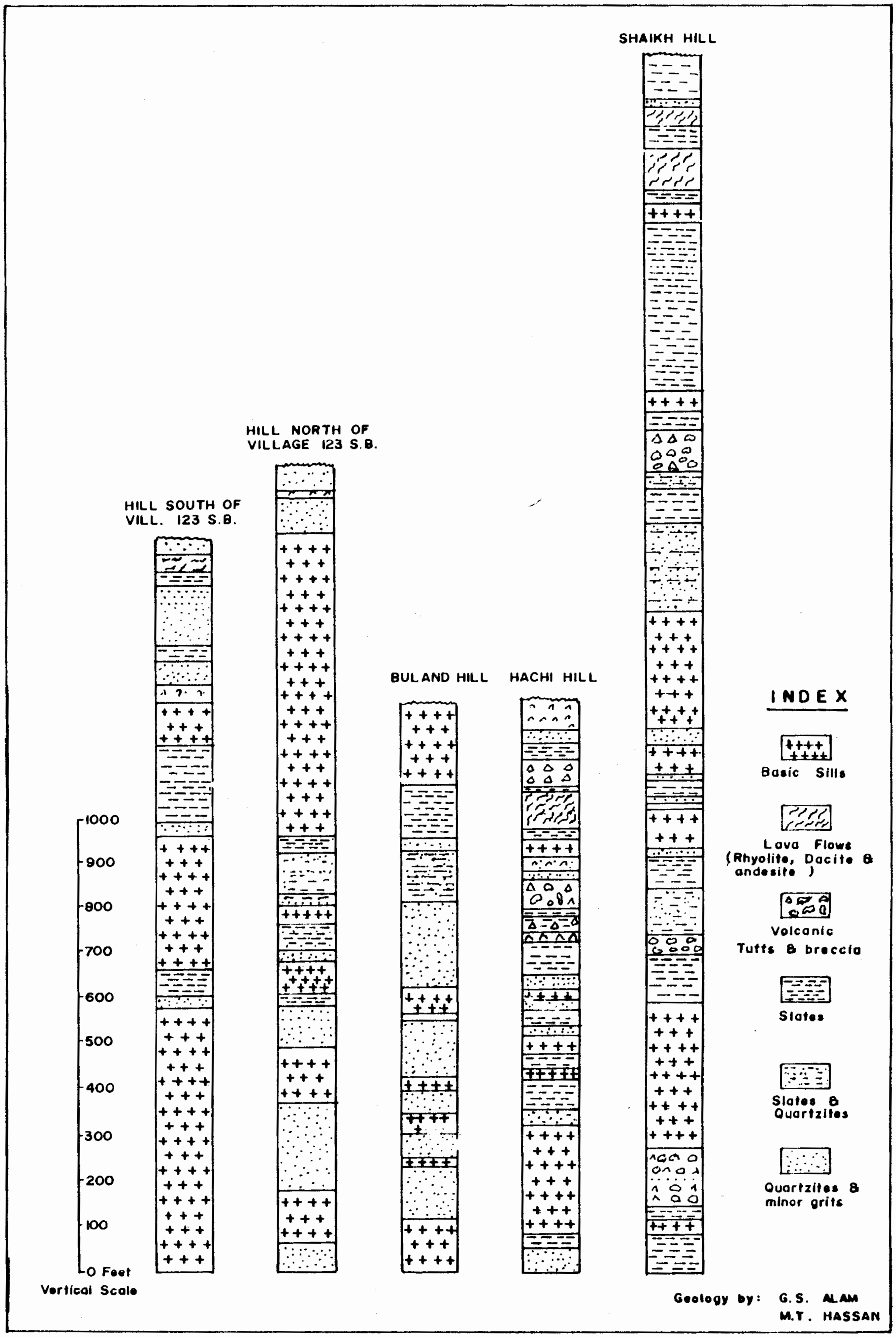

Fig. 3. Columnar section of hills north and south of village 123 S.B. and Buland Hill, Hachi Hill, Shaikh Hill, Kirana Hills, Punjab, Pakistan.

Age and Correlation

The lower contact of the formation is concealed under alluvium. The upper contact, with the Taguwali Formation, is also obscure. But the field relationship suggests that it represents the oldest formation in the Kirana area.

Discontinuity of the Precambrian outcrops of Pakistan and India and the altered nature of the rocks have renderd the correlation of these outcrops very difficult. No fossil or any trace or organic remains is found in the Kirana Group.

Heron (1913) placed these rocks as equivalent to the Malani rhyolite series of western Rajasthan. Davies & Crawford (1971, p.244) made age determination of six rock samples, collected from Buland Hill. The suite gave an isochron age of 870 ± 40 m.y.; hence the correlation by Heron with the Malani rhyolite series having an isochron age of 745 ±10 m.y. must now be abandoned.

The Buland Hill rocks are considered to be representative of the Hachi formation. On the basis of the above results, the rocks of the Hachi Formation probably lie within the time range of Vindhyan System, with its base at about 1400 m.y.

TAGUWALI FORMATION

The name has been assigned after Taguwali at latitude 31° 56' 15" N, logitude 72° 42' 36" E. The type locality and type section of this formation are on southern part of the Kirana Hill, at latitude 31° 58' 3" N, longitude 72° 42' 10"E.

The characteristic lithology of this formation is phyllite, slate and finer textured quartzites in the lower part. Phyllites are light silver grey, fine-grained, and may show cross-bedding. In the upper part of the formation, phyllite is the dominant rock type with minor slate. The middle part is composed of slate with slight sheen on the surface. One slate sample was found to contain quartz (60-70%), silt and clay (20-25%) and sericite (10-15%). The sericite has some preferred orientation.

This formation is quite widespread in the area. Besides its type locality in Kirana Hill, it is exposed in Chandar Hill where it is represented by fine grained quartzite. In Mochh Hill, 4 km SE of Taguwali, it is mostly represented by fine-grained and thin-bedded phyllite.

In Chiniot-Rabwah area, this formation is represented by fine-grained quartzites and thin-bedded slates. In Chiniot area, a small hillock of quartzite represents this formation.

The upper contact of this formation is with the Asianwala Formation and is gradational. The lower contact with the Hachi Formation is nowhere clear. The thickness of this formation in the type locality has been measured as 1189 m.

In the Rabwah and Shahkot areas, only small thicknesses of this formation are exposed.

ASIANWALA FORMATION

Asianwala Canal Rest House is located on the Sargodha–Faisalabad Road, 11 km from Sargodha. This name has been assigned after a subdivision of the Kirana Group. The main Kirana Hill is the type locality of this unit. The type section is along the road, which goes to the top of the Kirana Hill, and is about 4 km from Asianwala Rest House (latitude 31° 59' 38'N, longitude 72° 43' 42" E).

The characteristic lithology of the Formation is quartzite with minor intercalations of slate. The quartzite is generally coarse-grained, partly pebbly at places, dirty white to light grey, mottled brown and thick-bedded. It is cross-bedded and ripple-marked. At places, joints and fractures are filled with brown hematitic material.

The dirty white, coarse-grained quartzite is composed of well-sorted, subrounded to rounded grains of quartz (90-95%), with few particle of iron oxide and silt. The quartzite is derived from arenite formed under shallow water.

The interbedded light grey slates occur as thin layers in the thick beds of quartzite.

This Formation is exposed in the Chiniot, Sangla Hill and Shahkot areas. In the Sangla area, only one isolated hill represents the Precambrian rocks. This exposure is of medium to coarse-grained, thick-bedded quartzite, which can probably be correlated with the Asianwala Formation. In

Shahkot area, this Formation is exposed about one km west of Shahkot Town, and is represented by light grey, medium bedded and coarse-grained quartzite.

In the type locality, the upper contact of this Formation is with alluvium. The lower contact is gradational and passes into the Taguwali Formation. The thickness at the type section at Kirana Hill is ≥ 248 m.

Organic remains are not found in this formation. Being a younger Formation of the Kirana Group, it can be assigned age around 870 m.y., which is the isochron age of the older Hachi formation.

HADDA FORMATION

The Hadda Formation is named after the Canal Rest House Hadda located about 20 km ESE of Sargodha and about 10 km NE of Sharaban Hill.

The main rocks of the Hadda Formation are quartzites, slates, conglomerate and lava flows. Quartzites dominate the other rock types, and are finegrained and rusty brown. Quartzite is in places cross-bedded and shows complex contorted layering due to slumping before consolidation. Quartzites are marine or deltaic in origin.

Quartzite is fine-grained and composed of sub-angular quartz (65-75%) set in fine calcareous matrix with iron oxide, calcite and fine clay particles.

Conglomerate occurs in the upper part of the Formation interbedded with quartzite ranging in thickness from 1 to 2.5 m. The conglomerates are similar to those in the Sharaban Formation, and are composed of quartzite, slate, with minor limestone; veins of quartz and jasper are set in fine calcareous matrix of rusty brown colour. The pebbles are flattened and are arranged with their long axes parallel to the bedding.

The middle part of the Formation is composed of quartzite, which is light grey to brownish grey, fine-grained, thin-bedded, and partly phyllitic. Green-grey lava flows are present within the quartzite beds. The lower part of the Formation is represented by quartzites of light grey colour, highly ferrugineous at places. Some hematite-rich parts are being mined for use as pigment.

The upper contact is with the Sharaban Formation and the lower contact is concealed under alluvium. The formation is exposed in the type locality as an isolated hill without any connection with the older rocks. In the type locality, the thickness of the formation is 372 m.

No fossil record has been found in this formation. On the basis of the regional trend and structure, this formation is thought to be lying above the rocks of the Kirana Group. This assumption places this formation above the Asianwala Formation.

SHARABAN FORMATION

This formation is exposed in the southern end of Sharaban Hill. The only outcrop of this formation is present as an isolated, low-lying exposure adjoining Sharaban Hill; it is at least 119 m thick in the type locality. The upper contact of the formation is with alluvium.

The characteristic lithology of the formation is conglomerate, with minor stringers of fine-grained quartzite. The conglomerate contains flattened and elongated pebbles of quartzite, slate, limestone and a few veins of quartz and red jasper. The beds are 5 to 10 m thick. The quartzite and slate pebbles are similar to the rocks exposed in the area. The pebbles are generally 1-3 cm in diameter, and these constitute 80 to 85% of all the pebbles. The rest (10-15%) of the pebbles are in the range of 3 to 10 cm. The matrix is rusty brown, fine-grained and calcareous. The pebbles are flattened due to stress and are arranged with their long axes parallel to the bedding. A visual estimate suggests that 80-85% of the pebbles are of quartzite and slate.

The limestone pebbles present in the conglomerate are interesting as nowhere in the area limestone beds have been found in these Precambrian rocks. The limestone is light grey, fine-grained and microcrystalline.

Thin beds of rusty brown quartzite are intercalated with the conglomerate The quartzite is fine-grained and calcareous, and is similar to the matrix present in the conglomerate bed.

The Sharaban Formation is exposed only at the type locality. The top of this formation is not exposed and the base passes conformably into the Hadda Formation. The exposed thickness of the Formation is estimated at 118 m.

No fossil or any trace of organic remains has been found in this formation. This formation stratigraphically overlies all the other four formations of the Precambrain rocks of Kirana area.

ECONOMIC GEOLOGY

The rocks of the Kirana area bear no significant mineral deposits. Minor showings of a few minerals, which are described below, are present.

Hematite mineralization is present in the northern part of Kirana, Hundawali, Buland, Moch, Sharaban and Chiniot Hills. A deposit of hematite and magnetite ore also exists under the alluvium in the Precambrian basement rocks of the Punjab Plain near Chiniot. Hematite mineralization in the area occurs in thin quartz veins and as thin ferruginous layers interbedded with slate. The Fe_2O_3 content varies from 10 to 94%.

Gold content of up to 6 ppm in altered basic igneous rocks of a dyke in Kirana Hill was reported earlier (Shah, 1973). However, no indication was found by the present study.

Oxides of iron and other minerals are present in the Kirana area. Ochres of reddish brown and yellow colour are present.

The area yields important construction stone which is being used in buildings, bridges, highways and rail roads (Alam & Ahmad, 1990a).

CONCLUSIONS

The Kirana area comprises metasedimentary and igneous Precambrain rocks which have been intruded by basic dikes and sills.

A new Sharaban Group has been proposed, comprising calcareous conglomerate and sandstone.

A deposit of hematite and magnetite ore exists under the alluvium in the Precambrian basement rocks in the Punjab Plain near Chiniot at a minimum depth of 91.56 metres.

REFERENCES

ALAM, G.S. (1987) Geology of Kirana Hills, District Sargodha, Punjab, Pakistan. Inf. Rel. Geol. Surv. Pakistan. **201**, 38p.

——— **& AHMAD, R.** (1990a) Aggregates resources of Kirana Hills, Sargodha District, Punjab, Pakistan. Inf. Rel. Geol. Surv. Pakistan **381.**

——— **JALEEL, A. & AHMAD, R.** (1990 b) Discovery of iron ore deposits in the Precambrain shield rocks of Punjab Plains, Chiniot area, Jhang District, Punjab, Pakistan. Inf. Rel. Geol. Surv. Pakistan **427**, 31 p.

DAVIES, R.G. & CRAWFORD A.R. (1971) Petrography and age of the rocks of Buland Hill, Kirana Hills, Distt. Sargodha, West Pakistan. Geol. Mag. **108** (3), pp. 235-246.

HERON, A.M. (1913) The Kirana and other hills in the Jech and Rechna Doabs. Recs. Geol. Surv. India **43**, (3) pp. 229-236.

SHAH, S.M.I. (1973) Occurrences of gold in Kirana group, Sargodha (Punjab), Pakistan. Inf. Rel. Geol. Surv. Pakistan **68**, 14 p.

Manuscript received on October 20, 1992; accepted for publication of December 31, 1992.

ACTA MINERALOGICA PAKISTANICA
VOLUME 6 (1992) PP. 101-114.

A COMPREHENSIVE GEOLOGICAL AND STRUCTURAL SKETCH OF PAKISTAN

ABDUL HAQUE
Centre of Excellence in Mineralogy, University of Balochistan,
P.O. Box 43, Quetta, Pakistan.

ABSTRACT: This paper is based partly on the compilation work already done by the national and international geologists upto 1980, and the rest based on the field observations carried out by the author himself during several geological excursions in different areas of Pakistan since 1972. The present studysuch as: the observations of different lithological and structural zones, the description of both sedimentary ranges and flysch deposits, and the age of emplacement of ophiolites, will give a broad picture to teh readers for understanding the whole geology of Pakistan. Since 1960's the progressive advancement of the concepts of plate-tectonics, a great change to the problems associated with the plate boundaries have been developed. Conseequently, the term "Axial Belt" part of geosynclinal theory is no more valid for the western boundary of Indian plate, which is to be overlapped by the "Suture Zone".

INTRODUCTION

In this paper attempt is made to trace the stratigraphic and structural boundary betwen the Indian shield and its Paleozoic sedimentary cover; to decipher the sedimentary ranges of Pakistan, to assign an age of emplacement of ophiolites, and to delimit the actual western limit of Indian plate.

Fig. 1, compiled by the author, enables us to differentiate the following successive stratigraphic and structural elements between the Indian-shield and the Noshi-Chaman fault: (1) Indian Sheild, (2) Pericontinental Ranges, (3) Ophiolitic zone, (4) Internal zone, (5) Volcanic zone, and (6) Suture zone.

INDIAN SHIELD

The most ancient outcrops in the Indian shield or foreland are the Bundelkhand gneiss of 2550 Ma age, which is covered by the Precambrian rocks of Aravalli Range. The bottom of this range is argillaceous associated with basic and ultrabasic rocks, apprised of the characteristics of geosynclinal environment (Gansser, 1964). The Aravalli Range is intensely folded and, metamorphosed and later on intruded by granites. These rocks are highly cratonized during Aravalli orogenesis, dating 1400 Ma ago (Stocklin, 1977). Overlying these rocks, reposing continental sediments are represented by the Vindhyan system of Lower Paleozoic age.

The sedimentary cover of the Indian plate commences by the outflow of Malani rhyolites about 745 Ma ago. These rhyolites are conformably underlain by the Jodhpur sandstones which gradually change into calcareous facies containing trilobites of Lower Cambrian and thick gypseous and salt belts, correlatable with the Cis-Indus Salt-Range in Pakistan.

The Indian Foreland alongwith the Indus basin is filled with molasse which represents the southern continuation of the Potwar basin, and is traceable along the whole eastern length of Kirthar-Sulaiman.

PERICONTINENTAL RANGES

The pericontinental or margin ranges are characterized by the rocks which were deposited in the semi-enclosed seas situated on the periphery of the continents. Such seas are floored by the submerged continental masses.

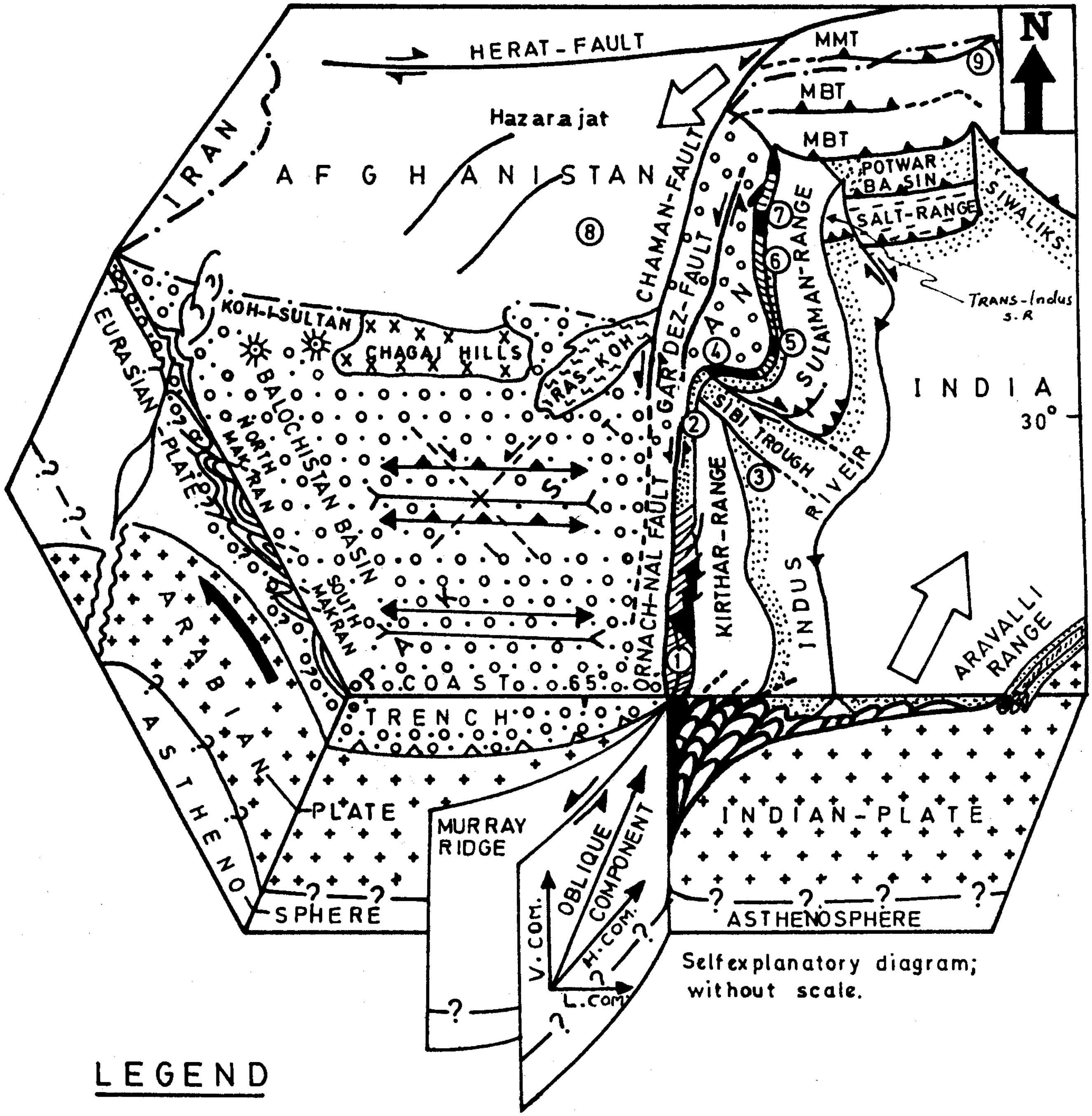

LEGEND

The numbers ① ② ③ ④ ⑤ ⑥ ⑦ ⑧ ⑨ respectively denote the names of different localities i.e; Las-Bela; Quetta; Sibi; Muslim-Bagh; Zhob; Waziristan; Dargai; Kandhar, and Hazara.

▨ Ophiolites associated with Cretaceous rocks.

▨ (a) (b) Internal Zone a) Katwaz Zone
b) Makran Zone

△ Indus-Delta

Fig. 1. Schematized three dimensional structural and geological diagram of Pakistan and the adjacent areas, compiled by the author through the references cited in the text.

SALTRANGE

Salt Range is situated in the south of Potwar plateau which is itself limited in north by the Himalaya and in the south by transgressive molasse (Fig. 1). Both these contacts are faulted; thus the later one is thrusted over the formar one. The presence of the Precambrian Saline Series at the base of the Salt Range played an important role of lubricant during these structural episodes.

Salt Range is divided laterally into two portions (Fig. 1) the western and eastern parts by a regional strike-slip fault. The western part is called "Trans-Indus Salt Range", and the eastern one is called "Cis-Indus Salt Range". Such regional fault is actually confounded with the passage of Indus river (Gansser, 1964, Fig. 3; Bernhard & Curt, 1970). The area of Trans-Indus Salt Range is 60 x 80 km^2 which constitutes the Surghar Range, Shinghar Range, Kirsor Range and Marwat Range. The eastern side is more complete stratigraphically than its western side.

The base of the Cis-Indus Salt Range starts with the Saline Series of Precambrian-Cambrian age. The Cambrian sequence shows repeated continental to marine-continental sedimentation.

Stratigraphically the Lower Paleozoic is absent. The series again begin by tillite of the Upper Carboniferous age (Bernhard & Curt, 1970) of Permian (Gansser, 1964).

Permian is represented by fossiliferous Amb Formation and Vargal Formation where the base is constituted of limestone and shale. Then, an emersion of the region is represented by lateritic bands.

Triassic is representd, amongst others, by the Mianwali Formation with *ammonites* which is typically Alpine facies. The succession continues to the west upto Cretaceous while Triassic to Paleocene is absent in its eastern side. Paleocene is absent in both sides of the Salt Range.

Middle Eocene is marked by evaporites named as Kohat Saline Series whereas Oligocene is represented by a stratigraphic discordance; than com classical marine formations of Murree and Siwaliks of Miocene age.

Structure

Salt Range is described like a thrusted block of slight inclination towards north. Such thrustings are due to the presence of Saline Series situated at its base. Such strengthless Series reposes verisimilitudely over Precambrian basement; thus producing an active tectonic "decollement" of the Series as well as dissociation of the Series itself (Armbruster et al., 1978). Gansser (1964) has indicated that the development of Salt Range is recent which affects only the deposits of Upper Siwaliks. Keller et al. (1977) consider that the recent work done over the eastern Salt Range shows that major upheaval movements had taken place during the past 1 Ma.

All such data conclude that the "decollement plane" is even now-a-days active, and is situated under the Potwar plateau and is probably attached in the north, with the Main Boundary Thrust.

SIWALIKS

Fluviatile continental molasse of Indus plane is contemporaneous to those of sub-Himalayan regions. Such molassic sediments have been named diversely by different geologists like "Sibi-Group", "Data Conglomerate", "Urak Group", "Siwaliks", etc., in which the stratigraphic code of Pakistan has accepted the name Siwaliks for these postorogenic sedimentary formations.

Siwaliks are classed as Upper, Middle, and Lower, which are well developed in the Sibi depression where in its central part, the upper Siwaliks are well exposed whereas Lower Siwaliks outcrop only in its periphery.

Moreover, the reduced thickness of Middle Siwaliks over the crests of anticlines in the central parts of Sibi depression shows that these anticlines had been in obducting state during its deposition, while the Upper Siwaliks in the interior of synclines give an average thickness of 800 m.

The contact between Lower Siwaliks (Miocene) and Middle Siwaliks (Pliocene) is transitional and is represented by the commencement of a thick series of sandstones and clays which shows Himalayan orogenic phase of Mio-Pliocene.

Potwar basin localized in the north of Salt Range (Fig. 1) and which is amassed by molassic sediments which have been classed as Rawalpindi and Siwalik Group of Mio-Quaternary age.

The first sedimentation in the Himalayan foredeep is represented by Rawalpindi Group (Murree and Kamlial Formation) of Oligocene to Lower Miocene age (Gary et al., 1979) where flora have been reported in its lower part.

Then, Middle Siwaliks (Miocene to Lower Pleistocene) which have had cyclic fluviatile (Pilbeam et al., 1977) and synorogenic sedimentations (Gary et al., 1979), begin by massive sandstones, becomes fine towards top and restarts by massive sandstones (Allen, 1965) where hominiens fossils are found which are considered as the first human ancestors (Pilbeam et al. 1977).

Siwaliks of the Indo-Gangetic plains are difficult to classify because of its lateral lithological variations. However, the classification is done on the one hand over the basis of flora which are found in the Rawalpindi Group and on the other hand over the existence of vertebrate fossils in the upper Siwaliks.

Laterally sandstones change to siltstones which change to shale and finally to mudstone. Moreover, in the interior of sandstones, bands of different characters are found which demonstrate a fluviatile history. The longest continental stratigraphic section in world belonging to Siwaliks is situated near Rhotas.

The huge thickness of molassic sediments in the Quetta-Sibi and in the Hazara-Kashmir depressions show a substantial and rapid subsidence of these basins (Gary et al., 1979).

The stratigraphic columns taken along the periphery of Sibi-depression reveal well lateritic band of Upper Oligocene and Lower Miocene age (Movstiovitch & Malik, 1965, fig. 4). Moreover, at the base of Lower Siwaliks, the conglomerate deposits lying directly over marine facies of Kirthar and Nari, reveal a complementary proof of this sedimentary hiatus (Gansser, 1964).

Structures

Since Siwaliks are postorogenic sediments, they make regional angular unconformities with the preexisting rocks, ranging in age from Maastrichtian to Eocene (Dunghan Limestone); Maastrichtian to Paleocene (Ghazij shale); Lower Eocene)Kirthar Limestone). These discordances are visible in the Kach and Ziarat as well as in other areas of Balochistan. In Ziarat such surface is represented by laterite of Oligocene age having variable thickness from 1 to 2 m.

In the north of Jhelum, the Jammu thrusting within the Siwaliks is examplified by Main Boundary Fault where Rawalpindi Group is thrusted over Siwaliks. This thrust plane is parallel to that of Pir Panjal Range situated more to the north.

KIRTHAR-SULAIMAN RANGES

General Characteristics

To the west of Salt-Range begin Kirthar-Sulaiman Ranges which turn towards south and take N-S orientation. The northern range (Sulaiman Range) from the southern range (Kirthar Range) is seperated near Quetta by Sibi depression which is oriented NW-SE (Fig. 1). These two ranges being 1000 km long seem to be the western continuation of Himalaya (Abdul Gawad, 1971). The Kirthar range turns towards west and rejoins Makran subduction zone which is oriented E-W and continues upto Iranian frontier. The width of the Kirthar-Sulaiman Ranges attaining 500 km near the Iranian border, reduces 200 km near Waziristan (Andrieux & Brunel, 1977).

Detrital formations (e.g., Shirinab Formation) from stratigraphically the lowermost part of these ranges, while neritic limestone (Chiltan Limestone) and pelagic calcareous limestone (Parh limestone) take the upper position. Besides, shales and carbonates are pelagic in its centre and very gypsiferous to detritic towards Indian plate. The Oman sea, the Arabian Sea and the Indus basin represent the external zones of Kirthar-Sulaiman-Makran-Zagros Ranges. The inner zones of these ranges are situated beyond the ophiolitic belt namely: Central mountains of Afghanistan and Helmond desert.

In the interior of these ranges the oldest formations like Shirinab Formation (Jurassic) and Alozai Group (Permo-Triassic) make the mountainous regions of Pakistan. The Jurassic limestones and dolomites are very thick (1500 to 2000m) constituting the core of enticlines.

Gretaceous is dominantly argillaceous (Sember & Goru Formations), calcareous (Parh Limestone) and arenaceous (Pab sandstone), having pelagic tendency (Parh Limestone) in the internal part of these ranges. Towards its external part, on the contrary, Cretaceous is specially represented by sandstone and marl. These two different facies are distributed in two different basins being seperated by Jacobabad-Sibi positive zones. Moreover, the volcanism in Late Cretaceous and in Paleocene, i.e., Ziarat basalt, doleritic veins, interstratified lava flow in Ranikot Formation had been worngly correlated (Auden, 1936) with that rrrepresented by Deccan Traps.

In most of the localities, Eocene is represented by a transgression. In Kirthar-Sulaiman ranges it is represented by lateritic discordance being out-cropped near Ziarat in Balochistan. One finds at the base of Eocene deltaic characters represented by coal deposits within Ghazij shale (Paleocene to Lower Eocene) in Balochistan (Sor Range & Degari mines) being exploited at present. Eocene is also described by Ras Koh intrusions.

Structure

Thes two ranges give a narrow belt of several curvatures which provide Jura-type foldings; strike-slip and reverse faults mostly diverted towards the exterior. Such curvatures have been differently named by diverse geologists, viz; oroclines; syntaxes; nodes; arcs, etc., (Kalat, Khuzdar, Quetta, Tank near Kalabagh Hazara) which have on the one hand a direct relationship with the form of the Indian basement and on the other hand related with most recent orogeneses dating Plio-Pleistocene.

Structural and orographical set up of these ranges show that the tectonic transport is always towards Indian Foreland. Moreover, seismic evidences suggest that these guirlands are because of decollement of supra-crustal rocks over Indian basement (Klootwijk & Canoghan, 1978). The presence of a low depth seismic event in the Sulaiman Range permits to consider that may be the Precambrian. Indian basement is slightly deformed due to subsequent accummulation of sediments (Powell, 1979).

Sulaiman Range seems to be displaced 250 km from that of Kirthar by a zone of right-lateral strike-slip faults (Klootwijk et al., 1981) being traced by Sibi depression which is subsequently filled by molasse of Miocene age. This depression will provide us synsedimentary faults, being oriented NW (Stocklin, 1977).

The extremities of Sulaiman Range show en echelon forms which allow to consider that its central part has moved towards foreland with respect to their two ends. Moreover, this range seems to be truncated in the north by E-W fault which is observed in the Safaid-Koh crystalline rocks.

The tectonics of Kirthar-Sulaiman Ranges is essentially Mio-Pliocene with the most recent fold affecting middle Pleistocene rocks. Anticlines and synclines of great width having parallel to subparallel horizontal and curved axes have been observed. Anticlines are named as: Central, Las-Bela, Sanjawi Raskoh, Hyderabad. Synclines are Karachi, Chinjan, Urak, etc., which are not visible since they have been subsequently filld by molassic sediments derived from neighbouring positive parts during Alpine Orogenesis.

Between such anticlines and synclines the undeformed sediments have been named as plateaus, viz: Kalat Plateau (Eocene sediments) is situated between Las Bela and Central anticiline; Mirjawa-Delbandin-Plateau, is covered by Cretaceous volcanic rocks.

Amongst other structures vertical to subvertical folds, tight overturned plunging and doubly plunging folds of different orientations are visible in Quetta, Kach, Chinjin, Killa Saifullah, Loralai and Zhob regions.

Folds often show length of 100 km and having feeble curvature produced a shortening of order of 30% (Andrieux & Brunel, 1977). Faults more or less vertical (7%) are of two natures: Inverse (thrusted towards exterior) and strike-slip faults. The altter are the most recent and intersect the former ones. Moreover, the trends of inverse faults are subparallel to the axes of regional folds. Strike-slip faults having both horizontal and vertical displacements are oblique to the directions of regioal structures. Sometimes extensional structural like grabens due to late phases of compressive tectonics are also seen over arial photographs.

Finally the tectonics phase of such structures in the interior of these folded ranges, is Plio-Pleistocene and towards Indian plate it is Pleistocene-Recent (Abdul Haque, 1985).

OPHIOLITIC ZONE

The ophiolitic zone of Pakistan commences in the south near Las-Bela, Balochistan (Fig. 1). This N-S oriented ophiolitic outcrops go upto Nal where it disappears. Reappears near Khanozai and passes by Muslim-Bagh, then more towards north near Waziristan, and lastly located near by Dargai and Dras (Fig. 1). This zone also passes in the north through Swat valley and by Nanga-Parbat and finaly terminates by oining the Indus suture line. Apart from the above description, Ras Koh ophiolites are situated in the extreme north west of Balochistan.

Las-Bela

Las-Bela ophiolites (Fig. 1) having more than 250 km length and 10 km width, at some places, are bordered in the west by Quaternary and in the north by Tertiary transgressive deposits (Kazmi, 1979). Porali massif part of Bela ophiolites constitutes small lenticular masses of serpentinized peridotites, gabbros and diorites which are obducted under Bela ophiolites of age varying from Upper Paleocene to Lower Eocene (Andrieux & Brunnel, 1977). The characteristic feature of these ophiolites is the presence of kilometric pieces of different rocks known as melanges. In the south of Bela ophiolites pillow-lavas and in its north either serpentinized ultramafic rocks or pillow lavas have been observed (Kazmi, 1979).

Further to the east of Porali mossif, are situated Mor-Range and Pub-Range both are constituted by continental sedimentary rocks. These two ranges have been subsequently intruded by sills and dykes. The tectonic style of Mor-Range (tight folds with axial plane schistosity specially in its shale) is quite different from that of Pub-Range wherein folds are virtually absent and the beds are monotonously dipping towards east. In the north of Mor-Range (south of Khuzdar) the ophilites have a direct tectonic contact with the Indian-Foreland; here the ophiolites are in course of erosion thus giving volcanic blocks and debris witin the "Khadro Formation" of Danian age. Moreover, Khadro Formation (Lowermost part of Ranikot Group) is well developed in both Kirthar and Sulaiman Provinces.

The presence of granite-blocks in the conglomerates of these formations are remarkable in the Wad region. Their existence indicates that during the emplacement of ophiolites towards Indian-Foreland, these blocks had been dragged, towards the surface and are subsequently eroded and deposited by sedimentary processes.

Bela ophiolites equally evokes an olistolith within volcanosedimentary formations called Rakhshani Formation (Paleocene age).

Volcanic rocks within Las-Bela ophiolites are of sub-marine origin and are older than that of Deccan Traps. Their age varies from Sentonian-Campanian to Paleocene of subserian origin (Stocklin, 1977). The age of transgressive sediments over Las-Bela ophiolites is upper Cusian to lower Lutenian, while north of Bela in the Sor-Dir region on the contrary its age is Oligocene (Franz, 1979).

Muslim-Bagh & Khanozai

Muslimbagh ophiolites are distributed in three outcrops: Jang-Tor ghar, Saplai-Tor ghar, and Nassai masif. These outcrops together with Khanozai ophiolites have been classed as:

Cumulates: commences by dunite, then pyroxenite (99% anstatite), next come gabbros and sometimes anorthosite. The cumulates series more or less 15 m thick repeats at least three times (Abbas & Ahmad, 1979).

Tectonites: constitute sills and dykes of harzburgite (70%) and of dunite (30%). Dolerite sills (1 to 15m thick) having high angle dips towards east and their geochemical models show that they have been derived from tholeiitic magma (Abass & Ahmad, 1979).

Ophiolites of the Muslim Bagh Khanozai represent an oceanic crust of dorsal origin, which are later on obducted over the western margin of the Indian Foreland. These ophiolites seem to resemble to Oman and Cyprus ophiolites.

The base of these ophiolites is a crushed zone where dynamic metamorphism had produced blueschist facies. Here the schistosity is feebly inclined affecting pelagic terrain of Upper Cretaceous. Moreover, the presence of one discontinuous slice of garnet-amphibole-gneiss, shows at least two phases of isoclinal foldings squeezed between ultrabasis rocks and epimetamorphosed sediments (Andrieux & Brunel, 1977). Jang-Tor-ghar peak is a tectonic klippe and the drag zone underneath constitues metamorphosed and serpentinized blocks defines melange of the area (Zaki & Abbass, 1979).

The age of emplacement of Muslim-bagh ophiolites is believed to be as Early Lutetian, while that of sedimentary blocks and lenses within serpentinites is Maastrichtian. Such data conclude that its age of emplacement is not before Paleocene (Franz, 1979). On the contrary, Zaki and Abbass (1979) give to these ophiolites Paleocene to Lower Eocene age, since they are bordered below by rocks of Maastrichtian age and above by that of Middle Eocene.

Zhob

In the north-east of Muslim-bagh (Fig. 1), Zhob ophiolites having a big outcrop is constituted by ultrabasic massif with alternative bands of harzburgite and serpentinized dunite rich in chromite, which is transected by doleritic veins of tholeiitic composition (Andrieux & Bruenel, 1977, Figs. 5 & 6). Bilgrami (1964) ascretained that its upper part consitutes gabbros. Basalt is represented by pillow-lavas, and the absence of thermal metamorphism instigated by sills intrusion.

Peridotites or this massif show neither any isolclinal folds nor foliations: but they are affected by conjugated east-west strike-slip faults in which chromitization and serpentinization are very intense.

Waziristan

Waziristan ophiolites (Fig. 1) are best studied in the region of Kosh in Afghanistan, where these ophiolites reveal periodotites pyroxenites, chromites associated with pillow-lavas, and the whole ophiolitic sequence is emplaced over pelagic sedimentary terrain of Cretaceous age (Asrarullah et al., 1979) and thus, representing a gigantic klippe (Andrieux & Brunel, 1977).

Dargai

An outcrop of 25 x 6 km Dargai ophiolites are found in the NNE of Peshawar, and it has been classified into:

Mafic Cumulates: containing gabbros plus serpentinite.

Ultramafic Cumulates: 80% harzburgite, nearly 20% dunite.

Ultramafic tectonites: More than 90% harzburgite and 10% dunite.

Dargai ophiolites show strong isoclinal folds with remarkable foliation and lineation. Such folds are mined for the mineral chrome. The upper and lower contacts of Dargai ophiolites are EW oriented faults dipping towards north (Asrarullah et al., 1979). Majority of the northern ophiolites of Pakistan are aligned with the Main Suture Line of Indian plate (Gansser, 1955; 1960; 1966; 1974a, b; 1979).

Ras-Koh

Ras-Koh ophiolites are found in the NW of Balochistan (Fig. 1). It contains peridotites, norites, gabbros, diorites, serpentinites in which chromite in lenticular form is present as a accessory mineral (Asrarullah et al., 1979). These ophiolites are tectonically intercalated with volcanic rocks and conglomerates (Bakr, 1964; Andrieus & Brunel, 1977) belonging to Rakhshani Formation of Paleocene age. Ras Koh ophiolites belong to a subduction zone probably of Eocene age (Asrarullah et al., 1979).

INTERNAL ZONE

This zone is divided by Quetta syntaxis, into Zhob-Katawaz and Makran zones (Fig. 1)

Zhob-Katawaz Zone

Located between Sulaiman Range and Nushki-Chaman fault (Fig. 1), and represent a depression filled by flysch sediments (Stocklin, 1975).

Argillaceous flysch and phyllite deposits (Eocene to Miocene) within this depression have 9000 metres thickness are subsequently transected by regional strike-slip faults of Tertiary age like that of Gardez fault (Fig. 1). The fissures and cleavages are Post-Mesozoic age, may be related to the movement of Tertiary faults (Stocklin, 1977).

The provenance of such flysch and phyllite is the Loger zone in Afghanistan, since this region lacks of Mesozoic and Lower Tertiary sediments. The fissures and cleavages within these flysch have been developed during Mesozoic orogeneses in which Pre-Senonian granites are intruded in the east of Baiman in Afghanistan. Hydrocarbon point of view Zhob-Katawaz zone seems to be very important, since this zone is escaped largely from post-Mesozoic tectonic.

Makran Zone

The southern extension of Zhob-Katawaz zone is named Makran zone also represented by flysch sediments of the same age (Fig. 1). Makran geology commences by Teritary sediments (Farhoudi & Karig, 1977) which were later on deformed due to the subduction of Arabic-Plate under the blocks of lout and of Dashst-i-Margo (Klootwijk et al., 1981).

Teritary formations of Makran zone start by Panjgur Formation of Upper Oligocene to Lower Miocene, though the base is not exposed. Its estimated thickness is 2000 m (Ahmed, 1969, fig. 2). This formation was before part of the Khojak Shale which was discovered firstly by Hunting group in 1960.

Than comes Makran group (Middle Miocene to Late Pliocene) constitutes the following beds (Ahmed 1969, Fig. 5), from bottom to top:

Parkini Mudstone: Age Miocene. The lower contact is conformable with Punjgur Formation but it is oftenly faulted. Thickness 1,600 m constitutes mainly calcareous mudstone with thin bands of siltstones. Ripple marks are abundant.

Telar Sandstone: Age Upper Miocene to Lower Pliocene. The lower contact with Parkini Mudstone is gradual, but one can put it at the end of resistant bands of sandstone. The Upper limit of Talar sandstone (1500 m) is transitional with Chatti Mudstone. But in the east of Makran this contact is faulted with Ormara Formation. One part of the sand-stone may be correlated with Diz Sandstone which is situated in the north of Makran. The lower part of Talar sandstone shows sandstone changing into mudstone with quartz pebbles, chert and jasper, while its middle portion contains thick bands of mudstone and sandstone which produce peaks in the south of Makran. Its upper portion is mainly marine shales and sandstones.

Chatti Mudstone: Age Middle Pliocene. *Chatti Mudstone* (1300 m) is conformably covered by Ormara Formation. Chatti Mudstone is mainly shale thin impure calcareous bands which differentiate it from Parkini Mudstone.

Ormara Formation: Pliocene to Pleistocene is the age. Thickness 70 m. It contains shales, sandstones, conglomerates and shells-fragments in its upper part.

Jiwani Formation: Its age is Pleistocene. Thicikness 30 m. It contains shales, limestone, conglomerates in which the pebbles and blocks derived from Talar Sandstone.

Structure

Makran zone is bounded in the east and west by two regional strike-slip faults: to the east sinistral Nushki-Chaman fault in Pakistan and to the west dextral Nayband fault (Franz, 1979) in Iran. The latter one has been considered as a trace of Oman-lineament which seperates Makran flysch (in the east) from calcareous series of Zagros (in the west) and in probably active presently (Falcon, 1967).

Landsat imagery of Makran zone shows an accretionary prism giving an emerged subduction zone (Girod & Conrad, 1975; Ahmed 1969, fig. 4).

The Oman Gulf has been considered as the rest of oceanic crust where the water depth is sufficiently great (Farhoudi & Karig, 1977).

Makran subduction zone nearly 1000 km, long and the subduction rate is more than 5 cm per year (Jacob & Quittmeyer, 1979). Near the trench the dip of the subducting plate is zero, the turning of benioff changes abruptly near Jaz Muran basin and at the level of volcanic arc the depth of benioff attains 100 km (Jacob & Quittmeyer, 1979, fig. 6). The development of foredeep basins, vis: Raddo-bassin; Hammun-i-Maskel bassin; Jaz-Muran bassin are due to the curvature of subducting benioff.

The argillaceous-sandy sediments of Pliocene age having maximum thickness of one km (Girod & Conrad, 1975), which show that sone Miocene, Makran region had been an active zone of subduction.

At the end of Cretaceous epoch, Makran region (Hinterland basin) had already been divided into south-Makran basin and north_makran basin by an EW positive topography which was named by H.S.C. (1960) as Central axis, influencing the development and the displacement of Tertiary rocks.

South-Makran basin is bounded in the east by Kirthar range and in the west by Straits of Hormuz; in the north by faults and mud volcanos. The structures within the southern basin are very simple; they are east-west faults, and volcanic muds.

The structures within north-Makran basin become complicated. East-West tight folds (assymetrical anticlines) diversed towards south and limited by high angle EW thrusting. The seismic date shows that the displacement over such thrusting is several hundred meters, but unfortunately they are masked by sedimentary cover of Pleistocene age. However, due to compressional forces directed from north the weak and resistant Cretaceous and Eocene rocks are compressed, upheaveled, and the limestones are lightly folded. The repetition of beds by inverse faults in the south give roughly 6000 m total displacement (Ahmed, 1969). Moreover, recent right and left lateral faults which cut the preexisting regional structures are also found in this basin.

These Tertiary basins repose over Cretaceous rocks (1200 m thick) which outcrop near Megas at the Irano-Pakistani frontier.

VOLCANIC ZONE

Quaternary or more ancient volcanos situated in the north of Makran are completely eroded or partially covered by recent sediments. They are namely as: Bazman volcano (3490 m altitude); Chagai Hills; Koh-i-Sultan (2510 m altitude), Koh-i-Taftan (4100 m altitude). The distance between these volcanos also called volcanic-arc) varies from 100 to 150 km. Between such volcanic arc and Makran subduction zone the distance varies from 400 km, in the west to 600 km in the east (Jocob & Quittmeyer,, 1979; Dykstra & Birnie, 1979, fig. 1)

In Iran, in the Lout region (north of Makran subduction zone) volumetrically important Paleogene acidic lava flow (hyolites and ignimbrites) have been derived through anatexis from crustal materials (Girod et al., 1977).

Structurally Dyksta & Birnie (1979) proposed" "Transverse breaks" model by which the Quaternary subduction plate is divide into four segments each one has its own dip. They are: outermost east and west segments; central east and west segments (fig. 2 of the same authors).

The orientations of these transverse breaks are more or less parallel to the direction of subduction. Over the surface they are distinguished in the form of volcanos which posses the given characteristics; high explosivity; continue activity; biomodal chemical composition, and rich sulphur emanation. Such characteristics are associated with Makran volcanos.

With the extreme west and east segments volcanos are absent, for which Barazangi and Isacks (1976) proposed that the dip of the sediments is less than 10 degrees. However, the least dips of these two segments might be related to the fact that they are adjacent to the zones of continental collision. For the central segments the dip of the benioff is estimated to be 25 to 30 degree, thus volcanism is present. Carr & al (1973) have shown that historically the active volcanos tend to group themselves near the transverse breaks.

Koh-i-Sultan in Pakistan is of Pleistocene age, while Bazman volcanos in Iran are of Pleistocene to Holocene spoch (Dykstra & Birnie, 1979).

SUTURE ZONE

Western limit of the Indian-Plate is represented by regional left lateral strike-slip fault, which has two segments; Ornach-Nal in the south and Nushki-Chaman in the north (Fig. 1).

Ornach-Nal Fault:

This fault situated in Balochistan, having 200 km length. Oriented north-south, passes by Ornach and terminates near Nal. Its southern extremity turns towards west and rejoin the Makran subduction zone (Kazmi, 1979, fig. 1). Ornach-Nal is actually represented by a north-south running fault zone passes within the ophiolites of Las-Bela in which the most recent and the most active faults are found in its east (Powell, 1979). This fault probably started in Eocene, cuts the most recent sediments (Auden, 1974). Such fault zone is defined by different faults of same nature and all are N-S oriented. These faults are Aghor fault, Ras-Malan fault, Hudishi fault, and Awaran fault.

Nushki-Chaman Fault

The northern continuation of Ornach-

Nal fault is called Nushki (in the south) Chaman (in the north) fault is also a regional left-lateral strike-slip fault.

The convexity of this fault is towards west having a radius of curvature of the order of 1000 km (Auden, 1974). This fault starts near Kharan depression (in the east of Nal), continues in the north-east, passing by Nushki, than by Chaman & next by Charikar in the north of Kabul (Auden. 1974), and finally it region a regional E-W right-lateral strike-slip fault, called "Herat Fault" (Fig. 1). The two faults (Chaman–Nushki and Herat) define the displacement of the Hazarajat region, in Afghanistan towards south-west (Desio, 1977).

Nushki-Chaman fault represents the persent western limit of the Indian-Plate (Klootwijk & al, 1981; Powell et al, 1980). The left-lateral sense of this fault is due to the northern movement of Indian-Plate (Templeton, 1973).

From the view point of structural geology, Nushki-Chaman fault is very important. It cuts recent deposits and the pledments which are visible both over areal photographs (Auden, 1974) and over the subrecent terrain of Gawal, Ghazaband pass of Balochistan. The large length (900 km.) of this fault, the abrupt terminations of geology on both side of this fault, and recently the discovery of gravimetric anomaly (McGinis, 1971), show the megatectonic importance of this fault. Thus, its place is in the category of Eyzincan fault in Turkey, Toktogul fault of Kirgizkaya in Russia (Auden, 1974).

This fault has been active since Eocene period, meterializing a displacement of the order of 300 km (Powell, 1979). Moreover, from 1892 earthquake the vertical left-lateral movement had the order of 0.75 m (Auden, 1974; Abdul Haque, 1985), which thus, considered it as capable to produce destructive earthquakes.

The Chaman segment is bordred to the east by flysch of Murgha Faquirzai and Shagula Formation of Oligocene and Lower Miocene age, while to the west it is limited by three distinct zones one from the others. (1) In Afghanistan, by Dasht-i-Margo block which contains igneous and metamorphic rocks: (2) In the exteme north of Pakistan by Chagai zone being represented by andesitic volcanic rocks of Cretaceous age, (3) Finally, by the Ras-Koh belt which contains volcano-clastic rocks of Cretaceous age, which are itself covered by marine limestone, sandstone and shale of Plio-Oligocene age. These marine sediments themselves covered by non marine deposits, i.e., variegated sandstone, mudstone, and conglomerate.

In the northern part of Makran, near the south of Ras-Koh, appears the flysch deposits which are similar to Margha Faquirzai and Shagula Formation. Such is the place where the difference in geology of the two sides of the fault disppears and consequently the fault vanishes here.

CONCLUSION

The Indian shield had been trangressed by Precambrian, highly folded and metamorphosd rocks of Aravalli Range.

The position of the Salt Range permits to consider that it had been thrusted towards south, otherwise it would have been located under th Potwar plateau.

The decollement plane within the Saline Series of Salt Range is acually active and probably connected with the Main Boundary Thrust which is observed in the north.

Marine stratigraphic succession from Permian to Triassic is, nevertheless, the only contactof such nature.

Siwaliks has been classed over the bases of flora and fauna and the presence of monotonous bands of sandstone and shale over the contacts of lower Siwaliks (Miocene) and Middle Siwaliks (Pliocene) reveal Himalayan orogenic phase of Mio-Pliocene age.

The reduced thickness of Middle Siwaliks over the anticlines situated in the central part of Sibi depression suggest that they had been upheavaled during Middle Siwaliks sedimentation.

Clays and carbonates with Kirthar-Sulaiman ranges are more pleagic in the interior and more gypsiferous and sandy towards Indian-Plate. These facial characteristics allowed to suppose that the changing of sedimentary regime is quitely related with the relative displacement of the Indian-Plate towards a subduction zone situated in the north and presently covered by flysch of Katawaz zone (Andrieux & Brunel, 1977).

In the interior of Kirthar-Sulaiman ranges the tectonic phase is Plio-Pleistocene and more far towards Indian-Foreland, it is Pleistocene-Recent.

Strike-frequency and density diagrams will elucidate on the one hand faults and fractures directions and on the other hand elaborate the orientations of principal deformations. Fracture orientations help to research for the mineralization of important minerals like the deposition of flourite in Dilband and Zhob areas; the barite deposits near Khuzdar, the chromite deposits near Muslim-Bagh the copper deposit of Saindak and Chagai etc. The orientations of the principal deformations define the X,Y,Z directions which are directly related to themovement of Indian-Plate.

Only Peive (1969) had shown that the ophiolites are tectonically emplaced and they are not like sills. These ophiolites are either thrusted over Indian-Foreland or well emplaced tectonically in the sedimentary rocks of trench origin.

Pleistocene and sub-recent foldings (which develop even now-a-days in the alluvium and sub-recent: Ghazaband, Nal, etc.,) show that the advancement of folded ophiolitic zone is continued, thus, give a continuous deformation (Auden, 1974).

The geology of the Makran region is composed of flysch type sediments varying in age from Miocene to Holocene. Such sediments interpreted as an accretionary Prism and are deposited over the roof of subducted plate (Dykstra & Birnie, 1979).

Deformations of the submarine sedimentary deposits of the Makran region reveal that this region has been a subduction one between well known two plates. Moreover the presence of insulary arc is a complementary proof.

East-west oriented regional folds and thrusts in the Makran range as well as strike-slip faults directed NW and NE which transect the convergence towards north inthe interior of accretionary prism of this region. This convergence is more intense from the indicated by the slip-vector oriented NNE for the relative movement of Arabic Plate with respect to that of Eurasian (Jacob & Quittmeyer, 1979).

The western limit of the Indian plate is traced by a zone of regional left-lateral strike-slip faults known as Chaman-Nushki fault. Such fault has both horizontal and vertical components. The horizontal one is defined by its relative longitudenal displacement while the vertical one is marked by eastward thrusting and imbrications which are due to the release of graviational forces.

ACKNOWLEDGEMENTS

The author of the paper expresses his gratitude to the anonymous reviewers for valuable comments and suggestions for the amendment and upgradation of its present preprint form, communicated to him twicely through Dr. Zulfiqar Ahmed, Director, Centre of Excellence in Mineralogy, University of Balochistan, Quetta. Special thanks are due to Mr. Sher Bahadur, Senior Geologist, ESSO Exploration and Production Pakistan Limited, Islamabad, for his valued reviews which substantially improvd the form and presentation of this paper.

REFERENCES

ABBAS, S.G. & AHMAD, Z. (1979) The Muslimbagh Ophiolites. *In*: Farah, A. & De Jong, K.A. (eds.) GEODYNAMICS OF PAKISTAN. Geol. Surv. Pakistan, Quetta, pp. 243-250.

ABDEL GAWAD, M. (1971) Wrench movements in the Balochistan arc & relation to Himalayan-Indian Ocean tectonics. Geol. Soc. America. Bull. **82**, pp. 1235-1250.

ABDUL-HAQUE, (1985) A proposal to study the Chaman-Nushki fault on the pattern of San Andreas Fault. Acta Mineralogica Pakistanica **1**, pp. 34-37.

AHMED, S.S. (1969) Tertiary geology of part of South Makran Balochistan, West Pakistan. Am. Asso. Petrol. Geol. Bull. **53**, pp. 1480-1490.

ALLEN, J.R.I. (1965) Fining upwards cyles in alluvial successions. Geol. Jour. **4**, pp. 229-246.

ANDRIEUX, J. & BRUNEL, M. (1977) L'evolution des chaines occidentals du Pakistan. Mem. h. serie Soc. Geol. Fr. **8**, pp. 189-207.

ARMBRUSTER. J., JACOB, K.H. & SEEBER, L. (1978) Tectonics of the Lesser Himalayas in north Pakistan based on microearth-quakes observations. Jour. Geophys. Recs. **83**, pp. 269-82.

ASRARULAH & AL. (1979) Ophiolites in Pakistan: An introduction. *In*: Farah. A. & De Jong K.A. (eds.) GEODYNAMICS OF PAKISTAN. Geol. Surv. Pakistan. Quetta, pp. 181-199.

AUDEN, J.B. (1936) The structure of the Himalaya in Gharwal. Rec. Geol. Surv. India **77**, pp. 407-433.

——— (1974) Afghanistan-West Pakistan. *In:* SPENCER, A.M. (ed.) MESOZOIC-CENOZOIC OROGENIC BELTS, DATA FOR OROGENIC STUDIES. Geol. Soc. London Spec. Publ. **4**, pp. 235-253.

BAKR, M.A. (1964) Geology of the western Raskoh Range, Chagai & Kharan districts, Quetta & Kalat Divisions, West Pakistan. Rec. Geol. Surv. Pak. **10**, pp. 1-28.

BARZANGI, M. & ISACKS, B.I. (1976) Spatial distribution of earth-quakes and subduction of the Naza plate beneath South America. Geology **4**, pp. 686-692.

BERNHART, K. & CURT. T. (1970) Stratigraphic Boundary Problems, Permian and Triassic of West Pakistan. pp. I-III.

BILGRAMI, S.A. (1964) Mineralogy and Petrology of the Central part of the Hindubagh Igneous complex, Hindubagh mining district. Zhob Valley, West Pakistan. Rec. Geol. Surv. Pak. **10** (2-C) 29p.

CARR, M.J., STOIBER, R.E. & DRAKE, C.I. (1973) Discontinuities in the deep seismic zones under the Japanese Arc. Geol. Soc. Amer. Bull. **84**, pp. 2917-2930.

DESIO, A. (1977) Correlation entre les structures des chaines due Nord-Est de l'Afghanistan et du Nord-Ouest du Pakistan. Mem. h. series Soc. Geol. Fr. No. **8**, pp. 178-188.

DYKSTRA, D.J. & BIRNIE, W.R. (1979) Segmenation of the Quarternary subduction zone under the Balochistan region of Pakistan and Iran. *In*: Farah. A. & De Jong K.A. (eds.) GEODYNAMICS OF PAKISTAN. Geol. Surv. Pakistan, Quetta, pp. 319-323.

FALCON, N.I. (1967) The geology at the North-East margin of the Arabian basement shield. Addv. Sci. Sept. pp. 31-42.

FARHOUDI, C. & KARIG, D.E. (1977) Makran of Iran and Pakistan as an active arc system. Geology **5** (Ii), pp. 664-668.

FRANZ, A. (1979) Time of Emplacement of the Zhob Valley ophiolites and Bela ophiolites, Balochistan (Preliminary Report). *In*: Farah. A. & De Jong K.A. (eds.) GEODYNAMICS OF PAKISTAN. Geol. Surv. Pakistan, Quetta, pp. 215-212.

GANSSER, A. (1955) New aspects of the geology in central Iran. 4th World Petrol. Cong. Proc. Rome, Sec. I/A/5. Paper 2, pp. 279-300.

——— (1960) Auseralpine ophiolith problem. Ecologae Geol. Helv. **52**, (2), pp. 659-680.

——— (1964) GEOLOGY OF THE HIMALAYA Wiley Interscience, London. 289 p.

——— (1966) The Indian Ocean and the Himalayas: A geological interpretation. Ecologae Geol. Helv. **59**, pp. 831-881.

——— (1974a) The ophiolitic melange, a world wide problem on Tethyan examples. Ecology Geol. Helv. **59**, pp. 497-507.

——— (1974b) Mesozoic-Cenozoic Orogenic belt, data for orogenic studies. Geol. Soc. London Spec. Publ. **4**, pp. 267-278.

——— (1979) Reconnaissance visit to the ophiolites in Balochistan and the Himalayas. *In*: Farah. A. & De Jong K.A. (eds.) GEODYNAMICS OF PAKISTAN. Geol. Surv. Pakistan, Quetta, pp. 193-214.

GARY, D. NOYEN, J. & AL. (1979) Magnetic reversal stratigraphy and sedimentary tectonic historyof the Upper Siwalik Group Eastern Salt Range and Southwestern Kashmir. *In*: Farah, A. & De Jong K.A. (eds.) GEODYNAMICS OF PAKISTAN. Geol. Surv. Pakistan, Quetta, pp. 149-165.

GIROD, M. A (1977) Les formations continentals tertiaires & quarternaire due bloc due Lout (Iran): Importance du plutonisme et du volcanisme. Mem. H. series. Soc. Geol. Fr., pp. 53-75.

——— **& CONRAD, G.** (1975) Les formations volcaniques recentes du sud de I'Iran (Kouh-e-shahsavaran) donnees petrologiques preliminaries, implications structurals. Bull. Volcanol. **39**, pp. 495-511.

HUNTING SURVEY CORPORATION LTD. (1960) RECONNAISSANCE GEOLOGY OF PART OF WEST PAKISTAN A Colombo Plan Co-operative Project. Government of Canada. Toronto, 550 p.

JACOB, K.H. & QUITTMEYER, R.C. (1979) The Makran region of Pakistan and Iran: Trench-arch system with active plate subduction. *In*: Farah. A. & De Jong K.A. (eds.) GEODYNAMICS OF PAKISTAN. Geol. Surv. Pakistan, Quetta, pp. 305-317.

KAZMI, A.H. (1979) Active fault system in Pakistan. *In*: Farah. A. & De Jong K.A. (eds.) GEODYNAMICS OF PAKISTAN. Geol. Surv. Pakistan, Quetta, pp. 285-294.

KELLER, H.M., TAHIRKHELI, R.A.K. & AL. (1977) Magnetic polarity stratigraphy of the upper Siwaliks deposits Pabbi Hills, Pakistan. Earth Planet. Sci. Lett. **46**, pp. 187-201.

KLOOTWIJK, C.T. & CANOGHAN, P.T. (1978) The extent of Greater India: Preliminary paleomagnetic data from the Hindukush, Chitral (Pakistan). Earth Planet. Sci. Lett. **42**, pp. 167-182.

——— **& AL.** (1981) A Paleomagnetic reconnaissance of northeastern Balochistan, Pakistan. Jour. Geophys. Res. **86** (B1), pp. 289-306.

Mc-GINIS, L.E. (1979) Gravity fields and tectonics in the Hindukush. Jour. Geophys. Res. **76**, pp. 1894-1904.

MOVSTIOVITCH, E.B. & MALI, M.A. (1965) Thickness and facies variations of molasse sediments of the Sibi re-entrant, West Pakistan. Geol. Bull. Punjab Univ. **5** pp. 31-43.

PEIVE, A.V. (1969) Ocean crust of the geological past. Geotectonics **4**, pp. 210-224.

PILBEAM, D.R. et al. (1977) Geology and palenotology of Neogene strata of Pakistan. Nature **270**, pp. 468-489.

POWELL, C.Mc. A. (1979) A speculative tectonic history of Pakistan and surrounding; some constrainte from the Indian Ocean. *In*: Farah A. & De Jong, K.A. (eds.) GEODYNAMICS OF PAKISTAN. Geol. Surv. Pakistan, Quetta, pp. 5-25.

——— **& CANOGHAN, P.J.** (1975) Tectonic models of the Tibetan Plateau. Geology **4**, pp. 727-731.

——— et al. (1980) A revised fit of East and West Gondwanaland. Tectonophys. **63**, pp. 13-29.

STOCKLIN, J. (1975) Possible ancient continental Margin in Iran: *In*: Buke & Drake (eds.) GEOLOGY OF CONTINENTAL MARGINS. Springer –Verlag, pp. 873-888.

——— (1977) Structural correlation of the Alpine range between Iran and Central Asia. Mem. Ser. Geol. Soc. Fr. **8**, pp. 333-353.

TEMPLETON, R.S.M. (1973) Ideas on the tectonics of the Afghan-Pakistan Geosyncline. Geonews **3**, pp. 7-10.

ACTA MINERALOGICA PAKISTANICA
VOLUME 6 (1992) pp. 115-117.

COMPUTER MODEL FOR CRACKS ANALYSIS

MUBARIK ALI,
SHAHID NADEEM QURESHI
&
SYED AZHER HUSSAIN
Department of Earth Sciences, Quaid-i-Azam University, Islamabad.

ABSTRACT: Based on mathematical formulation of Cheng and Toksoz (1979), a computer program is developed in Fortran 77 NEC compatible to resolve porosity of rock into a spectrum of concentration of pore / cracks of varied aspect ratio using seismic velocities (Vp, Vs) as a function of depth or pressure. The program is tested successfully on Westerly granite, and can effectively be used in other situations to achieve the distribution of cracks of different shapes.

INTRODUCTION

Seismic interpretations are improved with the precise knowledge of seismic velocities. Since these are influenced by several factors like crack shape, crack size, orientation, degree of saturation, inter communication and physical properties of the inclusion, the insight into porosity can give better understanding of velocity behaviour. Porosity by definition is a ratio between the volume of interstices and the total volume of rock, and comprises pores and cracks of various shapes. Porosity on the whole causes reduction in seismic velocity and that reduction phenomenon is significantly diminished with water saturation of pores / cracks. Wyllie et al. (1958) have given a relationship between the rock velocity, fluid velocity, grain velocity, and the porosity. Toksoz et al. (1976) have looked in detail into the effect of the porosity and saturation on seismic velocity and have come up with the conclusion that thinner cracks influence velocities more than those of spherical or near spherical pores.

If the rounded pores are gas saturated, the seismic velocities become higher than those of water / brine or oil saturation, whereas the flatter pores in case of gas saturation show lower velocities. The presence of a small amount of gas (5%) in brine as an immiscible mixture would reduce Vp even more than that of 100% gas saturation.

The observed seismic velocities (Vp, Vs) which increase with pressure or depth (3 km depth ~ I kbar pressure) due to deformation and closure of cracks in a porous medium, include the effects of porosity and saturation, and may be inverted to give information about the distribution of cracks. All approaches by Wyllie et al. (1958), Biot (1956), O'Connell & Budiansky (1974, 1977), and various others give a generalised guess, whereas the modelling of Toksoz et al. (1976) and Cheng and Toksoz (1979) provides details of volume concentration of the cracks of different aspect ratio effective on seismic velocities.

CHENG AND TOKSOZ MODEL

Since the actual crack geometries are unknown, modelling is attempted under a general assumption that cracks vary in shape from circular (a_m =1) to rather flat ($a_m = 010^{-2}$ to 10^{-4}). The formulation is based on looking into the Earth from surface the concentration of cracks of aspect ration a_m at pressure Pn, and their relation with effective moduli. The inversion is carried to determine crack spectrum from the given moduli or velocities.

Practically, the crack spectrum in two phase medium is modelled through specification of a set of aspect ratios (a_m, m=1, ..., M), and at each pressure Pn (n=1; ..., N), the relationship between volume concentration of cracks and effective moduli are taken from the observed velocities (Vp, Vs), density, and pressure or depth.

The estimation of volume concentration of microcracks related to a spectrum of aspect ratios is done through Cheng and Toksoz (1979), model the theoretical basis of which are discussed in their papers (Toksoz et al. 1976; Cheng Toksoz, 1979), however, the derived model is produced here for explaining the programming.

If (k, u, p) are bulk modulus, shear modulus, and density of the rock matrix, (k*, u*, p*) are the effective properties of the rock, and (k', u', p') are the properties of the fluid in pores, then the model has been defined as follows:-

$$\frac{k_n - k}{k' - k} \bullet \frac{3k + 4u}{3k_n^* + 4u} = \frac{1}{3} \sum_{m=1}^{M} a_m . [1 + dc/c (a^m , P_n)] \; T_1 (a_{nm}) . c (a_m)/a_m \quad ..(1)$$

$$\frac{U_n^* - u}{u' - u} \bullet \frac{25u (3k + 4u)}{6u_n^* (k+2u) + u (9k+8u) \; m = 1} =$$

$$M a_m . [1 + dc/c (a_m , P_n)] .$$

$$[T_2 (a_{nm}) - 1/3 \, T_1 (a_{nm})] . c (a_m) / a_m \; ...... (2)$$

Equations (1) and (2) generate a set of linear equations related to different saturation conditions and pressures. This set of linear equations is of the form Y=Ax, where Y is the data vector. A is a rectangular matrix of coefficients, and x is a parameter vector.

This model, as Cheng and Toksoz (1979) mention, can be approached through linear inversion method or linearized iterative inversion method. However, we have opted former approach due to simplification of the method to develop a computer program. Since we have NEC Mainframe facility, the program is written in Fortran 77, NEC compatible and is based on six subroutines and a function written to perform the desired calculations.

PROGRAM DESCRIPTION

The program converts initially the Vp and Vs information into effective bulk and shear moduli of the rock matrix at given pressures, and then generates data vector Y for the given pressures and saturation conditions; it calculates all the saturation changes at one pressure and then sequentially for all the pressures. After this, coefficient matrix A and its transpose are produced.

Table 1. Comparison of our results with those of Cheng (1979).

PORE ASPECT RATIO (a_m)	CONCENTRATION OF (c_m) GIVEN BY CHENG (1979)	CONCENTRATION OF (c_m) FOR DRY ROCK	CONCENTRATION OF (c_m) FOR SATURATED ROCK
1	(0.6929 ± 0.699) x 10^{-2}	0.7821958 x 10^{-2}	0.8014333 x 10^{-2}
0.01	(0.16 ± 0.04) x 10^{-2}	0.4810313 x 10^{-3}	0.4746446 x 10^{-3}
0.17 x 10^{-2}	(0.84 ± 0.93) x 10^{-4}	0.2721136 x 10^{-3}	0.2134515 x 10^{-3}
0.12 x 10^{-2}	(0.67 ± 0.68) x 10^{-4}	0.1078882 x 10^{-3}	0.1015858 x 10^{-3}
0.85 x 10^{-3}	(0.15 ± 0.05) x 10^{-3}	0.7795857 x 10^{-4}	0.9473844 x 10^{-4}
0.55 x 10^{-3}	(0.11 ± 0.03) x 10^{-3}	0.1341266 x 10^{-3}	0.6137978 x 10^{-4}
0.25 x 10^{-3}	(0.66 ± 0.13) x 10^{-4}	0.6895583 x 10^{-4}	0.2385681 x 10^{-4}
0.1 x 10^{-3}	(0.40 ± 0.06) x 10^{-4}	0.3596827 x 10^{-4}	0.1601068 x 10^{-4}

Then the damped least square inverse A_s^{-1} of the coefficient matrix is obtained and the smallest eigenvalue of the matrix A^TA, is determinated to add its squared value to the principle diagonal of the matrix $(A^TA + \varepsilon^2 I)^{-1}$ by A^T.

Finally, to calculate the volume concentrations, A_s^{-1} is multiplied with data vector and the resultant matrix gives the value of $c(a_m) / a_m$. From this the concentration $c(a_m)$ is obtained by multiplying a_m to the corresponding elements of the resultant matrix.

The program does all these calculations systematically to give resulting pore aspect ratios and their concentration at each pressure.

TEST

This program is tested specially on Westerly granite because that is well studied in terms of cracks spectrum. For the input to the program the velocity (Vp, Vs) data as a function of pressure (or depth) is taken from Nur and Simmons (1969); density, bulk and shear moduli and porosity of the rock at zero pressure, and saturation conditions are taken from Cheng and Toksoz (1979); the bulk and shear moduli of saturants are taken from Toksoz et al. (1976). The test study was made on Westerly granite with dry, and saturated pores / cracks. Our results alongwith previously known results of Cheng and Toksoz (1979) are given in Table 1.

It is to be observed that the total porosity (0.9%) of Westerly granite given by Cheng and Toksoz (1979) is divisible into voids / pores ($a_m = 1$) and elongated cracks ($a_m = 0.1$) as 0.7% and 0.2%, respectively. The results of our program are 0.8% and 0.1%. The comparison suggests that the calculated result concerned with the circular pores is appreciably closer to the known concentration, the noticeable difference as observed lies in the distribution of elongated cracks of varied aspect ratio. The possible reasons which could be responsible for this difference may be as follows:-

1. The technique used in this program is based on "Linear Inversion Method" while the results presented in Cheng and Toksoz (1979) are based on "Linearized Iterative Inversion".

2. The velocity versus pressure data used in our case is taken from Nur and Simmons (1969), which could be different from that used by Cheng and Toksoz (1979).

3. For simplification we have taken the smallest eigenvalue equal to 1.0 in the calculation of damped least square inverse, and it may also be different from that of Cheng and Toksoz (1979).

CONCLUSION

In general the program works very well and provides reasonably good results. This can effectively be used to look into the Earth from surface the spectrum of concentration of circular to elongated cracks of varied aspect ratios.

REFERENCES

BIOT, M.A. (1965) Theory of propagation of elastic waves in a fluid saturated porous solids-II, Higher frequency range. J. Acoust. Soc. Am. **28**, pp. 179-191.

CHENG, C.H., & TOKSOZ, M.N. (1979) Inversion of seismic velocities for the pore aspect ratio spectrum of a crack. J. Geophys. Res. **84.** pp. 5733-5743.

NUR, A. & SIMMONS, G. (1969) The effect of saturation on velocity in low porosity rocks. Earth Planet. Sci. Lett. **7**, pp. 183-193.

O'CONNELL, J.R. & BADIANSKY, B. (1974) Seismic velocities in dry and saturated cracked solids. J. Geophys. Res. **82**, pp. 5412-5426.

——— & BUDIANSKY, B. (1977) Viscoelastic properties of fluid saturated cracked solids. J. Geophys. Res. **82**, pp. 5719-5735.

TOKSOZ, M.N., CHENG, C.M. & TIMUR, A. (1976) Velocities of seismic waves in porous rocks. Geophys. **41**, pp. 621-645.

WYLLIE, M.R., GREGORY, A.R., & GARDNER, G.H.F. (1958) An experimental investigation of factors affecting elastic wave velocities in porous media. Geophys. **23**, pp. 459-493.

Manuscript received on July 7, 1992;
accepted for publication on September 20, 1992.

ACTA MINERALOGICA PAKISTANICA
VOLUME 6 (1992) pp. 118-125.

PETROGENETIC COMPARISON BETWEEN THE MAFIC DYKES OF CHILAS COMPLEX AND KOHISTAN BATHOLITH, NORTHERN PAKISTAN.

TAHSEENULLAH KHAN
Geoscience Laboratory, Geological Survey of Pakistan, Islamabad.
M. ASIF KHAN
NCE in Geology, University of Peshawar, Peshawar.
&
ABDUL AZIZ
Geoscience Laboratory, Geological Survey of Pakistan, Islamabad.

ABSTRACT: Kohistan island arc is formed due to the northward subduction of oceanic plate in Cretaceous. The arc sequence contains two major magmatic complexes: the layered mafic and ultramafic Chilas Complex at the base, and the Kohistan batholith in the middle part. Mafic dykes intrude the gabbronorite and pyroxene diorites of the Chilas Complex, north of Chilas, and the diorites of the Kohistan batholith west and south of Gilgit. Petrography and geochemistry divide the mafic dykes into three distinct groups. The mafic dykes of the Chilas Complex are rich in plagioclase, hornblende, and ilmenite and/or magnetite. The Kohistan arc batholith dykes contain hornblende and biotite in abundance. These are metamorphosed to amphibolites except the dykes intruding the batholith at shallower part. The Chilas Complex dykes are picrobasalt and basalt whilst in the batholith they are basaltic andesite and trachyandesite. Trace element geochemical patterns are similar for all the three type of dykes but the Chilas Complex dykes are more depleted in LIL elements with marked negative Nb and positive Sr anomalies. The Kohistan batholith dykes are comparatively enriched in the LIL elements and the trachyandesites are more enriched. The former are considered "D-type" and the later "E-type" dykes. They all show island arc affinities but the trachyandesite shows continental margin signatures. The three groups also reflect three different magmatic episodes, derived from the partial melting of less and more heterogeneous mantle sources, respectively.

INTRODUCTION

The Kohistan island arc in northern Pakistan is unique for its exposure of an almost complete island arc sequence, formed due to northward subduction of the oceanic lithospheric plate. It is obducted onto the Indian plate along the Indus suture (Tahirkheli et al., 1979, 1983; Khan & Thirlwall, 1988). It has been separated from the Eurasian-Karakoram plate to the north by the northern suture (MKT) and from the Indian plate by the Indus suture (MMT).

The Kohistan sequence comprises four major geological units (Fig. 1). The units trend east-west and are of Cretaceous to Oligocene age (Petterson & Windley, 1992). These units are from north to south: (1) Yasin sedimentary group (Albian-Aptian) and Chalt volcanic group (Cretaceous); (2) the Kohistan batholith (Cretaceous to Oligocene); (3) the Chilas and Jijal Complex (Cretaceous); and, (4) the Kamila amphibolite belt (Cretaceous). Volcanic rocks of Paleocene-Eocene age crop out between Kalam and Dir (for details, see Majid & Paracha, 1980; Coward et al., 1982, 1986). The Kohistan island arc underwent two major collisions (Petterson & Windley, 1992): (1) with Eurasia between 102 and 75 Ma (Petterson & Windley, 1985; Treloar et al., 1989) which transformed the island arc into Andean type continental margin; (2) and with Indian plate which began ca. 50-45 Ma, and is continuing to present (Rex et al., 1988) transforming Kohistan from Andean margin to a component of a major continent-continent col-

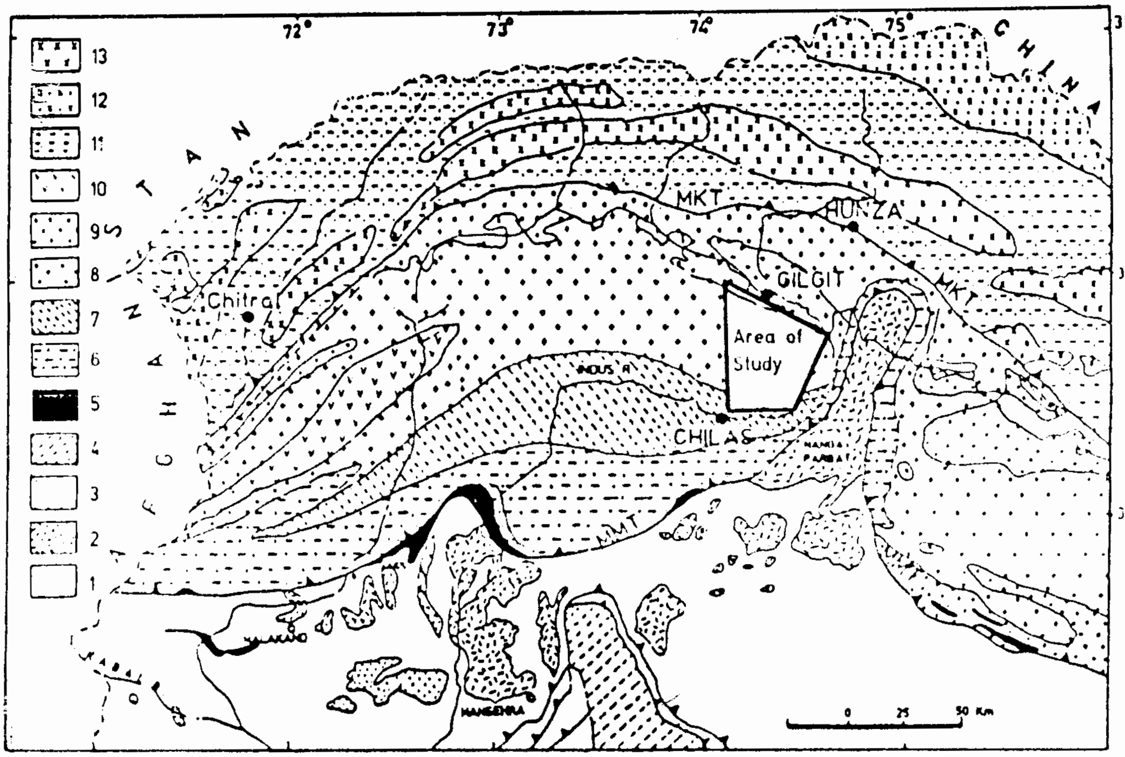

Fig. 1. Simplified geological map of northern Pakistan. (1) Precambrian to Mesozoic sedimentary rocks of the Indo-Pakistan plate; (2) Cambrian granitic rocks; (3) Permo-Triassic alkaline to sub-alkaline igneous rocks; (4) Middle Tertiary clastic sediments; (5) Ultramafic ophiolites; (6) Kamila amphibolites; (7) Chilas and Jijal mafic-ultramafic complex; (8) Kohistan-Ladakh granitic belt (in Kohistan, Kohistan arc batholith); (9) Cretaceous sediments and volcanics of the Yasin Group and Chalt volcanic group; (10) Creto-Eocene sediments and volcanics of Kalam-Dir area; (11) Sediments and metasediments of Karakoram plate; (12) Khunjrab-Wakhan-Tirichmir granites; and (13) Karakoram granitic belt. MMT: Main Mantle Thrust; MKT: Main Karakoram Thrust (modified after Jan et al., 1984).

lision zone (Rex et al., 1988; Petterson & Windley, 1992).

The mafic dykes of the Kohistan island arc, between Gilgit and Chilas belong to the Chilas Complex and Kohistan batholith (Petterson & Windley, 1992). A brief discussion on petrogenesis of the two dyke suites including comparison based on field features, petrography and geochemistry, is presented here.

FIELD FEATURES AND PETROGRAPHY

The mafic dykes were studied in Kiner Gah and Ames Ges Gah and also along KKH near Thurly Gah where they intrude the gabbronorite and pyroxene diorite and cut the NW foliation of the host Chilas Complex. These dykes range from 10 cm to 4 m in thickness and up to 10 m in length. They are greenish balck and fine grained. Igneous textures such as porphyritic, ophitic and poikilitic may be present. The rocks are equi- to sub-equigranular and in some cases foliated. The dykes are frequently present in the mafic and ultramafic association of the Chilas Complex at Thak valley confluence with KKH and in Thurli Gah. They are mainly N-S oriented but at places make networks. One of the porphyritic dykes exposed on the KKH near Thurli Gah separates the dunite from other rocks of the UMA and strikes N10°W with vertical dip. It is 1 m wide and 200 m long. The margins are fine grained and the core is porphyritic showing flowage differentiation. It has offshoots traversing the host rocks. Recrystallised mafic dyke swarms are intruded in the quartz orthopyroxene diorites, now amphibolites, in the southernmost part of Darel near Shatial. This part of the Chilas Complex represents ductile shear zone.

The minerals constituting the mafic dykes in Chilas Complex include plagioclase, hornblende with or without orthopyroxene as essential minerals, with quartz, epidote ± biotite ± muscovite ± sericite, magnetite, ilmenite ± rutile ± zircon and ± apatite as subordinates. They are hornblende rich with fair amounts of magnetite and limenite. In sample (KGT-26) orthopyroxene occurs in the rock in minor amounts and may be considered as secondary mineral (?). These are fresh and have very sharp boundaries with the adjacent minerals. Mafic dyke (KT-33), contains zircon and apatite as abundant trace minerals included in plagioclase and hornblende. The plagioclase shows albite twinning and is fresh, with the composition An_{40} - An_{60}. The amphibole is bluish green and pleochroic. It is altered at places into biotite and epidote. These dykes are basaltic in composition and metamorphosed to amphibolites but at places even higher grade metamorphism may be suspected because of their granoblastic texture (KT-26).

Mafic dykes occur in the Kohistan arc batholith which are exposed in the Kar Gah, Sai Nala and Huddar Gah. The total volume of the dykes, as elsewhere in the batholith (Petterson & Windley, 1992), is much less. The dykes are intrusive in the stage II and III plutons of the batholith (Petterson & Windley, 1992) and also the rocks of the Thelichi formation, Chalt volcanic group and the Gilgit paragneisses. They are absent in the younger plutons (< 30 Ma) which post-date the dykes. The dykes are generally thin (< 2 m) and strike NW. In Huddar Gah, within the quartz diorite, mafic dykes show isoclinal folding, trending N70°W and dip 60°SW. The dykes are deformed and recrystallised into amphibolites. In the middle part of the batholith at Jut (Kar Gah), a 2 m thick dyke cuts the foliation of its host quartz diorite. The contact is sharp and no visible chilling effects are observed. The dyke is fine grained and weakly porphyritic containing hornblende and plagioclase as megascopically recognisable minerals. The mafic dykes in the Kohistan batholith near the junction of Shinghai Gah with Kar Gah and at Hurkus, Sai Nala intrude the diorites (stage II plutons) which are metamorphosed into amphibolites. They are foliated, fine grained and non porphyritic. The apparent thickness of these dykes may reach upto 1 m. On the basis of petrography, the mafic dykes may be grouped into two types. The first one is the recrystallised (amphibolite) type with fine-grained and foliated textures (KGT-1A). Plagioclase (An_{45}) and hornblende are the essential minerals. Plagioclase is albite-twinned and subhedral. At places myrmekitic texture is noticed in the plagioclase showing slight deformation in the dyke . Hornblende is olive green to green and lepidoblastic. Biotite replaces hornblende and plagioclase. Epidote symplectites are also developed. Quartz, zircon, apatite and opaque oxides are present in traces. The dykes of second type (KGT-59) contain plagioclase and hornblende phenocrysts in the trachytic and intersertal groundmass. Plagioclase is albite twinned and its anorthite content is upto An_{45}. Hornblende is brown and twinned, marginally altered to secondary hornblende and/or chlorite. Biotite is developed at the expense of hornblende. Anhedral quartz grains are present but in traces and may be secondary. Muscovite is in traces and the opaque oxide is in the form of magnetite. The dyke KGT-59 does not show recystallisation to amphibolite and the primary mineral assemblages and trachytic and intersertal textures persist.

GEOCHEMISTRY

Geochemical data on the mafic dykes are presented in Table 1. The dykes of the Chilas Complex are low in SiO_2 (< 50%), Na_2O, K_2O, P_2O_5, high in TiO_2, Al_2O_3 , Fe_2O_3 (t), MgO and CaO and resemble compositionally the high alumina basalts because of their high Al_2O_3 content, except sample KT-33 with 15.16% Al_2O_3. The mafic dykes of Kohistan batholith are high in SiO_2 (>53%), Na_2O, K_2O and P_2O_5; and are low in Al_2O_3 (<19%), TiO_2, Fe_2O_3, MgO and CaO. Dykes KGT-1A and ST-45 have similar chemical composition whereas KGT-59 and ST-30 have also close chemical similarity, thus making two distinct groups. The dykes plot as picrobasalt, basaltic andesite and trachyandesite on the TAS diagram (Fig. 2). The analyses were also plotted according to the scheme of Miyashiro (1978). In the SiO_2 versus $Na_2O + K_2O$ plot (Fig. 3), the dykes occupy sub-alkalic field. The mafic dykes of the Chilas Complex are more primitive and lower in total alkali content as compared to the dykes of the Kohistan batholith. The AFM diagram (Barker & Arth, 1976) distinguishes the Chilas Complex dykes as tholeiitic and Kohistan batholith, tholeiitic to calc-alkaline (Fig. 4).

Spider diagrams have been used to illustrate the relative multi-variation in REE data and more recently for trace elements data (Thompson et al., 1984; Holm, 1985; Myers & Breitkopf, 1989) in which the elemental ratios have been normalized against average. The trace element contents from the volcanic and plutonic rocks are plotted

Table 1. Major and trace elements data (wt.% and ppm) of the mafic dykes of Chilas Complex and Kohistan arc batholith between Gilgit and Chilas.

Samples:	KT26	KT33	KT35	AGT6	KGT1	ST45	KGT59	ST30
SiO_2	44.66	47.64	42.18	42.11	53.25	53.55	57.70	57.47
TiO_2	1.31	1.16	1.09	1.36	0.87	0.79	1.14	1.21
Al_2O_3	20.46	15.16	19.54	20.97	18.31	19.06	16.94	17.39
Fe_2O_3	14.06	11.34	12.98	13.75	9.24	9.92	6.59	6.59
MnO	0.17	0.18	0.15	0.13	0.16	0.18	0.09	0.09
MgO	5.65	8.14	8.24	7.57	3.74	3.31	3.34	3.25
CaO	10.99	13.79	12.45	12.66	7.86	8.83	5.75	5.45
Na_2O	2.15	2.14	2.12	1.15	1.58	2.75	3.89	3.70
K_2O	0.34	0.41	0.15	0.24	1.58	0.72	2.59	2.61
P_2O_5	0.15	0.12	0.02	0.02	0.21	0.26	8.52	0.61
Total	99.94	100.08	99.92	99.96	98.81	99.37	98.37	98.37
FeO(t)	12.66	11.23	11.68	12.37	8.32	8.93	5.93	5.93
Trace elements in p.p.m. :								
V	310	241	346	436	165	145	131	139
Cr	20	343	24	19	19	52	81	94
Co	53	46	57	59	58	12	36	20
Ni	19	147	59	31	12	21	47	36
Zn	95	86	85	88	95	77	78	104
Y	21	29	20	29	24	24	16	15
Zr	15	99	23	19	88	69	184	167
Nb	3	2	1	1	4	3	20	20
Rb	7	12	12	5	42	17	65	91
Sr	497	190	346	355	433	471	802	1024
Ba	18	130	-	63	364	450	588	731
Ratios :								
Zr/Nb	5	49.50	23	19	22	23	9.20	8.35
Zr/Y	0.70	3.41	1.12	0.94	3.67	2.87	11.50	11.13
Nb/Y	0.14	0.07	0.05	0.05	0.17	0.125	1.25	1.33

Key: KT - Kiner Gah; AGT - Ames Ges Gah; KGT Kar Gah.
Analyses carried out in Geosciences Laboratory, Islamabad using XRF.

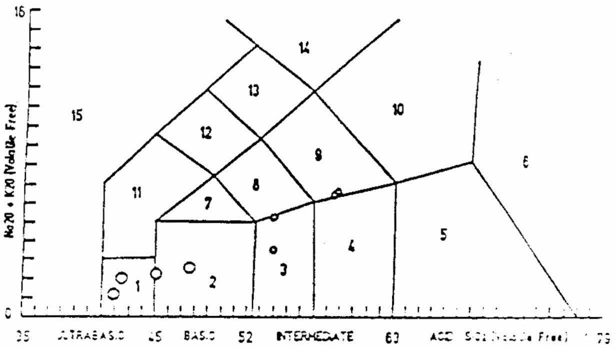

Fig. 2. The total alkali silica (TAS) diagram (after Le Bas et al., 1986).
Key: Large circles - mafic dykes of Chilas Complex. Small circles - mafic dykes of Kohistan arc batholith. (1) Picrobasalt; (2) Basalt; (3) Andesite; (4) Dacite; (5) Rhyolite; (6) Trachybasalt (7) Basaltic trachyandesite; (9) Trachyandesite; (10) Trachyte (Q < 20 in QAPF, Trachydacite (Q > 20 in QAPF)); (11) Basanite (ol > 10%, Tephrite (ol < 10%); (12) Phonotephrite; (13) Tephriphonolite; (14) Phonolite; (15) Foidite.

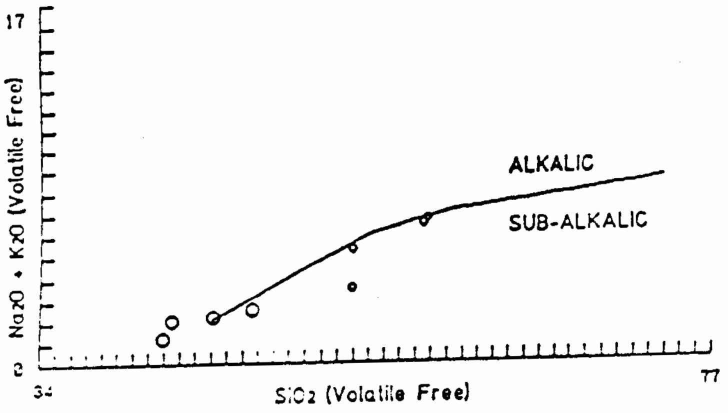

Fig. 3. SiO_2 versus Na_2O+. K_2O plot for the mafic dykes of the Chilas Complex and Kohistan batholith (after Miyashiro. 1978).

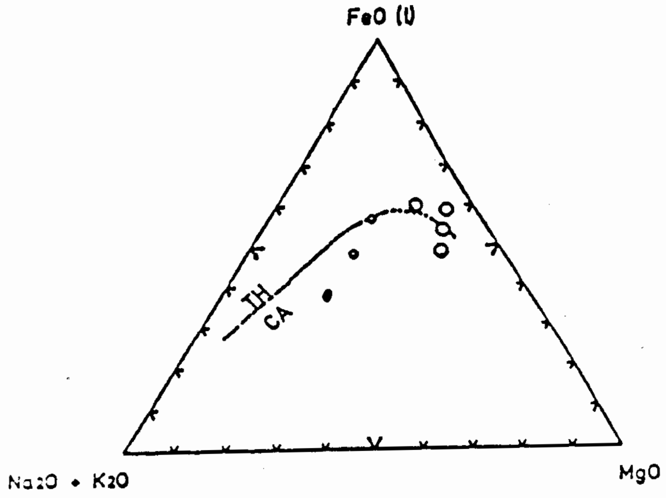

Fig. 4. AMF diagram used to accommodate the mafic dykes of Chilas Complex and Kohistan batholith into tholeiitic (TH) and calc-alkaline (CA) fields. The solid line separates tholeiitic from calc-alkaline (after Barker & Arth, 1976). Symbols as in Fig 2.

on a logarithmic scale. The elements are arranged in order of increasing KD values for partial melting under conditions of low PH_2O and fO_2 (Wood et al., 1979).

Fig. 5 shows spider diagrams for the mafic dykes of the Chilas Complex and Kohistan arc batholith. Sample C.C-1; KAB-2 and KAB-1 represent average data of the dykes of Chilas Complex and Kohistan arc batholith. They all show similar trace element patterns. A general feature is the negative Nb and positive Sr anomalies, which is typical feature of an island arc. The Chilas Complex dykes are more depleted in both the LIL and HFS elements as compared to the dykes of the Kohistan batholith which are enriched in the LIL elements, particularly the KAB-1 giving continental margin type affinity.

PETROGENESIS

It is generally understood that the partial melting of mantle lherzolite and peridotite results in the formation of basaltic magma which is injected through tensional fissures into narrow zones as pillow basalts on the surface, and dykes and layered intrusions at greater depths (Wilson, 1989). The partial melts from the deformed peridotites may be evacuated through dykes at maximum depth of 50 km (Nicholas, 1986). The mafic dykes of Chilas Complex as well as the Kohistan batholith are derived from the partial melting of the metasomatised mantle source as described by Petterson & Windley (1992) elsewhere in Kohistan. The trace elemental geochemical patterns define the mafic dykes of the investigated area as D-type (incompatible elements depleted) and E-type (enriched), (Petterson & Windley, 1992). Their Zr/Nb, Zr/Y and Nb/Y ratios also distinguish them into D-type and E-type dykes. The depleted dykes are tholeiitic and picrobasalt and basalt in composition and may be formed due to tholeiitic magmatism during the intra-arc rifting stage of the Kohistan island arc and intruded the Chilas Complex. This magmatism occurred before the closure of the Northern suture. The geochemical patterns of the mafic dykes of the Chilas Complex are very similar to the cumulate host rocks. These dykes are less contaminated, may be of greater depth of the magma chamber and the refractory nature of the host rocks through which the dykes intruded. The dyke width also does not exceed

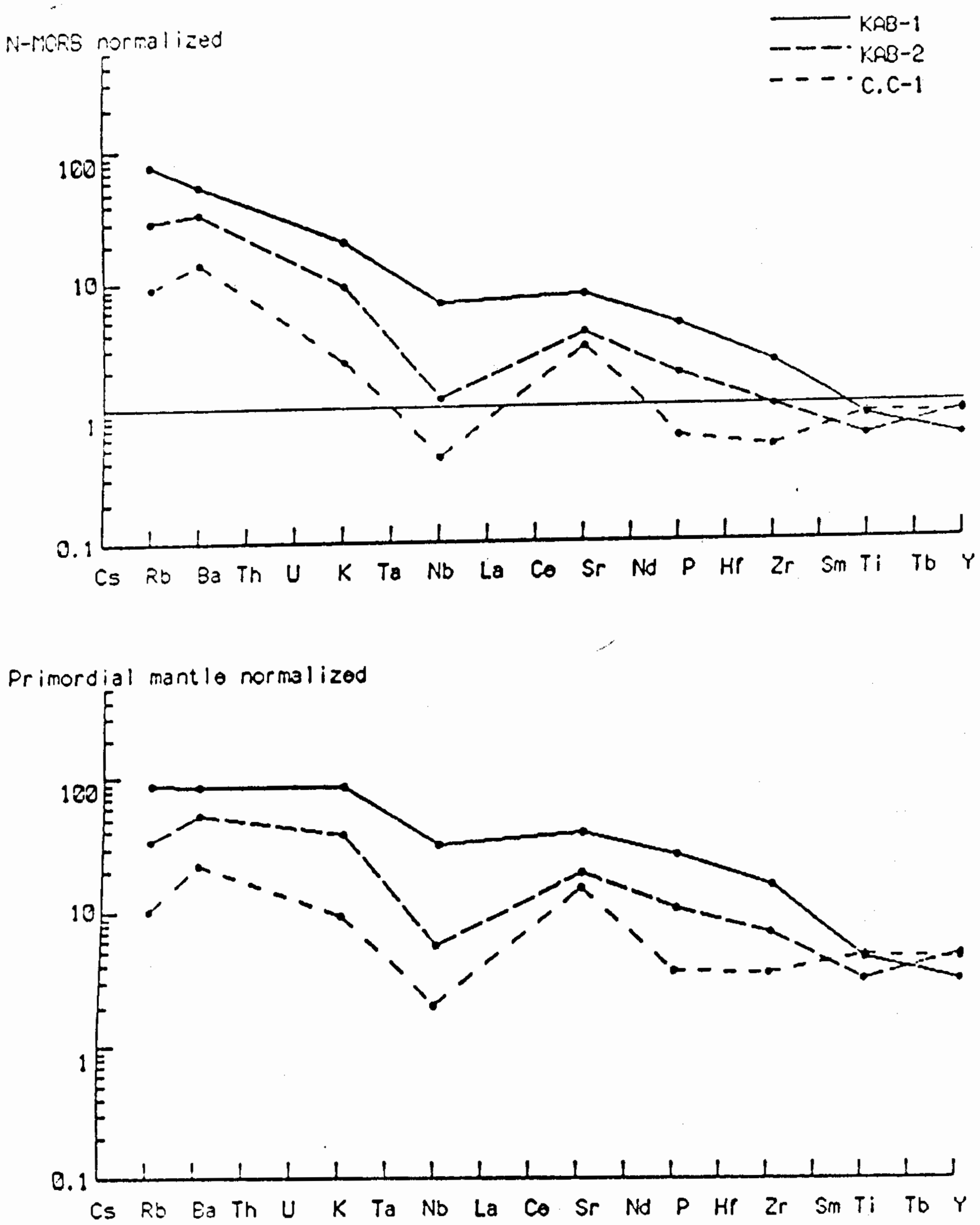

Fig. 5. N-MORB and Primordial mantle normalized trace element patterns for the average data of mafic dykes of Chilas Complex (C.C-1) and Kohistan arc batholith (KAB-2, KAB-1), after Wood et al. (1979).

3 m. According to Huppert & Sparks (1980) and Cambell (1985) the high temprature primitive magma become fully turbulent, if the dyke width exceeds 3 m and this will lead to ion exchange processes between the dyke and the wall rocks (Navon and Stolper, 1987). The D-type dykes of the Chilas Complex are less fractionated, and enriched in plagioclase, hornblende, and Al_2O_3, CaO and FeO (t). This enrichment may be considered as "cumulus enrichment" (Cox et al., 1979). Recrystallisation of these dykes to amphibolites may also enrich the aluminous phases (?). The tholeiitic reversal within the calc-alkaline layered magmatic rocks may be due to partial melting of the less metasomatised mantle to produce basaltic liquid which evacuated from the source, and solidified as mafic dykes during the subducting related processes within magma chamber at greater depth. This magma chamber underwent through continuous open system and new bath of magma periodically added resulting in producing the multiphases UMA rocks and the mafic dykes (?).

The dykes in the Kohistan batholith are of E-type, generally thin (<2 m), tholeiitic to calc-alkaline nature and may have been derived from the partial melting of the heterogeneous mantle source. Their production may be at shallow levels within the arc crust. The group I dykes as already discussed, intrude gabbroic-diorite. They are amphibolitised basaltic andesite and show similar geochemical patterns but grade towards calc-alkaline affinity. High contents of biotite and amphibole and low concentraction of the opaque oxides signify them to be derived under high volatile pressure. They have coherent geochemical patterns with the host rocks. These dykes are enriched in the incompatible elements and may be the result of the partial melting of the more metasomatised mantle source at shallow depth, but they are thin, and therefore, least contaminated by the host rock. The group II dykes of the Kohistan batholith are unmetamorphosd. They show trachytic texture and contain primary brown hornblende (KGT-59). These dykes show calc-alkaline trend and are more enriched in the incompatible elements as compared to the rest of the dykes. They show continental margin affinity, and are also developed by the partial melting of the more hetergeneous mantle source. The dykes of the Kohistan batholith were produced after the closure of the Northern suture (Petterson & Windley, 1985; Treloar et al., 1989). These are the components of singl igneous event dated at 75 Ma (Treloar et al., 1989) but the group II dyks may show 60-40 Ma magmatic episodes.

ACKNOWLEDGMENTS

This study is a part of Ph. D. research of Tahseenullah Khan, who is thankful to Hassan Gauhar, Project Director, Geoscience Laboratory for encouragment to conduct research work and M. Q. Jan, thesis supervisor who conducted field work with Tahseenullah Khan in the thesis area. Geoscience Laboratory, GSP, Islamabad is thankd for providing laboratory facilitie and NCE in Geology, Peshawar is also thanked for providing logistic support in field.

REFERENCES

BARKER, E. & ARTH, J.G. (1976) Generation of trondhjemitic tonalitic liquids and Archean bimodal trondhjemite-basalt suites. Geology **4**, pp. 596-600.

CAMBELL, I.H. (1985) The difference between oceanic and continental tholeiites: a fluid dynamic explanation. Contrib. Mineral. Petrol. **91**, pp. 37-43.

COX, K.G., BELL, J.D. & PANKHURST; R.J. (1979). THE INTERETATION OF IGNEOUS ROCKS. Allen and Unwin, London. 450 p.

COWARD, M.P., JAN, M.Q., REX. D.C., TARNEY, J., THIRLWALL, M. & WINDLEY, B.F. (1982) Geotectonic frame-work of the Himalaya of N. Pakistan. Jour. Geol. Soc. London, **139**, pp. 299-308.

——, WINDLEY, B.F., BROUGHTON, R.D, LUFF, I.W., PETTERSON, M.G., PUDSEY, C.G., REX, D.C. & KHAN, M.A. (1986) Collision tectonics in the NW Himalayas. *In*: Coward, M.P. & Ries, A.C. (eds.) COLLISION TECTONICS. Geol. Soc. London Spec. Publ. **19**, pp. 203-219.

HOLM, P.E. (1985). The geochemical finger prints of different tectonomagmatic environments using hygromagmatophile elements abundances of tholeiitic basalts and basaltic andesites. Chem. Geol. **51**, pp. 303-323.

HUPPART, H.E. & SPARKS, R.S.J. (1980). The fluid dynamic of a basaltic magma chamber replenished by influx of hot, dense ultrabasic magma. Contrib. Mineral. Petrol. **75**, pp. 279-289.

JAN, M.Q., PARVEZ, M.K., KHATTAK, M.U.K. & WINDLEY, B.F. (1984) The Chilas stratiform complex: field and mineralogical aspects. Geol. Bull. Univ. Peshawar **17**, pp. 153-169.

KHAN, M.A. & THIRWALL, M.F. (1988). Babusar amphibolites: Arc tholeiites from the southern Kohistan arc, N. Pakistan. Geol. Bull. Univ. Peshawar **21**, pp. 147-158.

LE BAS, M.J., LE MAITRE, R.W., STRECKEISEN, A. & ZANETTIN, B. (1986). A chemical classification of volcanic rocks based on the total alkali-silica diagram. J.

Petrol. **27**, pp. 745-750.

MAJID, M. & PARACHA, F.A. (1980). Calc-alkaline magmatism at destructive plate margin in Kohistan, Northern Pakistan. Proc. Inst. Com. Geodyn., Grp. Mtgs. Peshawar **13**, pp. 109-120.

MIYASHIRO, A. (1978) Nature of alkalic volcanic rock series. Contrib. Mineral. Petrol. **66**, pp. 91-104.

MYERS, R.E. & BREITKOPF (1989) Basalt geochemistry and tectonic setting: A new approach to relate tectonic and magmatic processes. Lithos **23**, pp. 53-62.

NAVON, D. & STOLPER, E. (1987) Geochemical consequences of melt percolation: the upper mantle as chromatographic column. J. Geol. **95**, pp. 285-307.

NICHOLAS, A. (1986) A melt extraction model based on structural studies in mantle peridotites. J. Petrol. **27**, pp. 999-1022.

PETTERSON, M.G. & WINDLEY, B.F. (1985) Rb-Sr dating of the Kohistan arc batholith in the Trans-Himalayan of the North Pakistan and tectonic implications. Earth Planet. Sci. Lett. **74**, pp. 45-57.

——— & ——— (1992) The field relations, geochemistry and petrogenesis of the Cretaceous basaltic Jutal dyke-suite, Kohistan, Northern Pakistan. J. Geol. Soc. London **149**, pp. 107-114.

REX, A.J., SEARLE, M.P., TIRRUL, R., CRAWFORD, M.B., PRIOR, D.J., REX, D.C. & BARNICOAT, A. (1988). The geochemical and tectonic evolution of the central Karakoram, N. Pakistan. *In*: Shackleton, R.M., Dewey, J.F. & Windley, B.F. (eds.) Tectonic evolution of the Himalayas and Tibet. Phil. Trans. R. Soc. London **A-326**, pp. 229-255.

TAHIRKHELI, R.A.K. (1983) Geological evolution of Kohistan island arc on the southern flank of the Karakoram-Hindukush in Pakistan. Bollitino Geofisica Teorica Applicata **25**, pp. 351-364.

———, MATTAUER, M., PROUST, F. & TAPPONNIER, P. (1979) The India-Eurasia suture zone in northern Pakistan. Synthesis and interpretation of data on plate scale. *In*: Farah, A. & Dejong, K.A. (eds.) GEODYNAMICS OF PAKISTAN. Geol. Surv. Pakistan, Quetta, pp. 125-130.

THOMPSON, R.N., MORRISON, M.A., HENDRY, G.L. & PARRY, S.J. (1984) An assessment of the relative roles of a crust and mantle in magma genesis: an elemental aproach. Phil. Trans. R. Soc. London. **A-310**, pp. 549-90.

TRELOAR, P.J., REX, F.C., GUISE, P.G., COWARD, M.P., SEARLE, M.P., WINDLEY, B.F., PETTERSON, M.G., JAN, M.Q. & LUFF, I.W. (1989) K-Ar and Ar-Ar geochronology of the Himalayan collision in NW Pakistan. Constraints on the timing of suturing, deformation, metamorphism and uplift. Tectonics **8**, pp. 881-909.

WILSON, M. (1989) IGNEOUS PETROGENESIS, A GLOBAL TECTONIC APPROACH. Unwin Hyman, London.

WOOD, D.A., JORON, J.L. & Teruil, M. (1979) A re-appraisal of the use of the trace elements to classify and discriminate between magma series erupted in different tectonic setings. Earth Planet. Sci, Lett. **45**, pp. 326-336.

ACTA MINERALOGICA PAKISTANICA
VOLUME 6 (1992) pp. 126-147.

SOME FUNDAMENTAL FIELD AND PETROGRAPHIC ASPECTS OF THE CHILAS MAFIC-ULTRAMAFIC COMPLEX, KOHISTAN ARC, NORTHERN PAKISTAN

M. ASIF KHAN
&
M. QASIM JAN
National Centre of Excellence in Geology, University of Peshawar, Peshawar, Pakistan.

ABSTRACT: Detailed field and petrographic studies of the Chilas complex, especially around Chilas, suggest that it is principally made up of gabbronorites with local pyroxenites, anorthosites, quartz diorites and tonalites. These contain, locally, up to 10 km^2 lensoid bodies of ultramafic rocks with associated anorthosites, troctolites, olivine gabbros, gabbros and gabbronorites. These latter are commonly layered and contain excellent sedimentary structures. However, the main gabbronorites are mostly uniform with only sporadic presence of igneous layering. The complex is remarkably coherent with rare evidence of multiple intrusions, suggesting that most of the crystallization took place in one or a few large, continuous magma chamber(s). The contact relations show that the Chilas complex intruded into a basement comprising metavolcanic amphibolites and paragneisses. The close association of the Chilas complex with arc-related rocks both in space and time, details of mineral and whole-rock geochemistry (presented elsewhere) and the absence of cyclically layered successions negate the possibility for the complex to have developed in mid-oceanic ridge conditions. The Chilas complex may represent rocks of the magma chamber to the Kohistan island arc, more likely, it developed from a mantle diapir in an intra-arc rift, similar to that documented in a number of recent island arcs, e.g., Mariana, Fiji.

INTRODUCTION

The Chilas complex (Fig. 1) forms the central spine of the Kohistan island arc of Tahirkheli et al. (1979). Attaining a maximum width of 40 km, it stretches for about 300 km between Nanga Parbat and western Dir. The complex generally trends ENE-WSW to E-W, but on its eastern side is tectonically rotated to N-S on the western margin of the Nanga Parbat massif near Raikot and pinches out near Thalichi. It covers about 8000 km^2 area, which is about 20% of the terrain occupied by the Kohistan arc. In terms of covered area, it is comparable to the Bushveld complex of S. Africa (Hunter, 1978), the Borde Range ultramafic-mafic complex of south-central Alaska (Burns, 1985), and the Dufekinter complex of Antarctica. The complex is principally made up of gabbronorites, which make it the largest body of its type in the world.

Localized accounts of the Chilas complex were presented by Wadia (1932), Misch (1949), Jan (1970), Desio (1974), Shams (1975), Bard (1983a,b), Khan et al. (1985), Khan (1988), and Ghazanfar et al. (1991) from the Indus valley, Martin et al. (1962), Jan & Mian (1971), Jan & Kempe (1973), Jan (1979), and Jan & Howie (1980) from Swat, Jan et al. (1969), Chaudhry & Chaudhry (1974) and Chaudhry et al., (1974) from Dir. Following general accounts of the petrography (Jan, 1979; Jan et al., 1984) and geochemistry (Hamidullah & Jan, 1985), Khan et al. (1989) presented data on mineral and whole-rock chemistry of the complex and discussed the petrology and tectonic setting of magma generation and emplacement.

On the basis of field, petrographic, mineralogical and geochemical data (Jan et al., 1984; Khan et al., 1985; 1989; Khan, 1988), the Chilas complex is broadly divisible into two associations of rocks: a rather uniform main gabbronorite association (MGA) making > 85% of the complex and a more diverse layered ultramafic- mafic-anorthosite association (UMAA). The UMAA is found mainly in the eastern parts of the complex

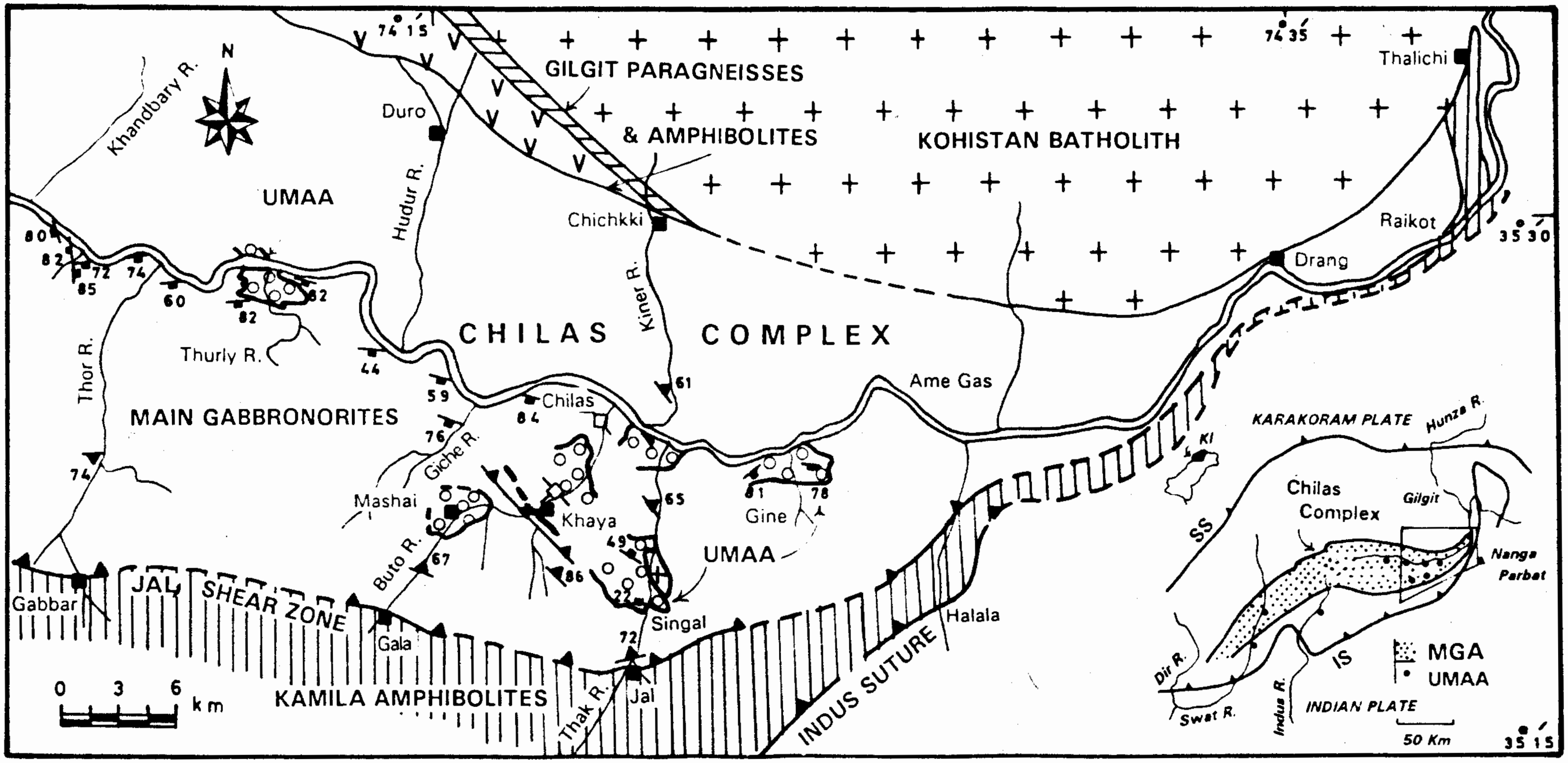

Fig. 1. Geological map of the south-eastern Kohistan arc. The Chilas complex (comprised principally of the main gabbronorites (MGA) with local bodies of the ultramafic-mafic-anorthosite association (UMAA) has a tectonic contact with the Kamila amphibolites in the south and intrudes paragneisses and amphibolites in the north. The Kohistan batholith intrudes all of these lithologies. See inset for the regional geology. Ki = Kohistan island arc; IS = Indus suture (= Main Mantle Thrust); SS = Shyok suture (= Main Karakoram Thrust)

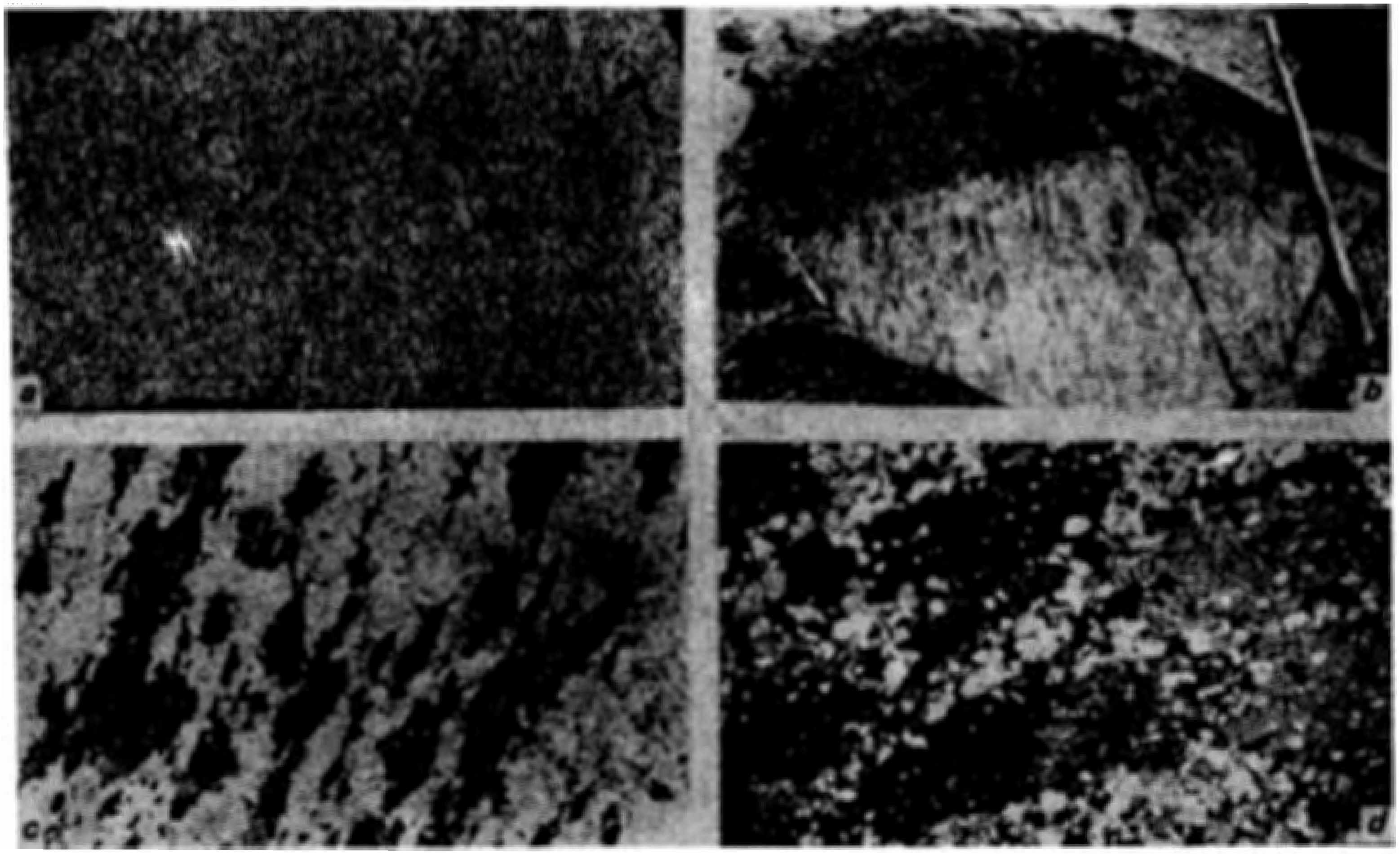

Fig. 2. Representative field and textural characteristics of the main gabbronorite association.(a) gabbronorite with magmatic lamination defined by mafic minerals (mainly pyroxenes). (b) fine-grained noritic xenoliths (earliest phase) in the leucogabbronorite. (c) photomicrograph of a laminated gabbronorite. The lamination is defined by lenticular aggregates of ortho- and clinopyroxene (length of the photograph 1.1 cm. (d) photomicrograph of the noritic xenolith (earlist phase) showing granular plagioclase and pyroxene and poikilitic clinopyroxene. Pg = Plagioclase; Pxns = Pyroxenes; Cpx = Clinopyroxene.

in the vicinity of Chilas (Fig. 1), but small bodies of such rock are sparsely scattered up to Swat valley and possibly beyond. It occurs as < 10 km^2 bodies emplaced in the MGA. The Chilas complex also contains dykes of (1) amphibole-plagioclase pegmatoids, and (2) fine-grained basic (amphibolitic) rocks, which are the youngest in the entire complex. The MGA contains a variety of xenoliths described in a later section.

This paper is aimed at highlighting some fundamental field and petrographic aspects of the Chilas complex as studied in east central Kohistan (i.e., Indus valley). Many of the features of the MGA are continuous along the belt and are therefore only briefly referred to from the Swat and Dir valleys. Various aspects are used to infer the nature of the Chilas complex and its mode of emplacement in the Kohistan sequence.

THE MAIN GABBRONORITE ASSOCIATION (MGA)

This association is characterized by an abundance of gabbronorites. These are commonly smoky to purplish, medium- grained, granular, massive to foliated (Fig. 2a) and essentially comprising plagioclase, orthopyroxene and clinopyroxene. Opaque oxides and apatite are ubiquitous accessories, together with quartz, calcic amphiboles and biotite in many and scapolite in a few. Large amounts quartz and K-feldspar may occur in intermediate members and Ca-amphibole in retrograde rocks. Local variations in the modes of the essential minerals result in melagabbronorites, plagioclase websterites, and anorthosites. These extreme compositions owe their origin to segregation of cumulus minerals and are commonly associated closely with layering. Locally one of the pyroxenes is absent or subordinate; thus gabbros or norites are developed instead of gabbronorites. At places the rocks grade into pyroxene-bearing diorites/tonalites, which appear to be their differentiates (e.g. NW of Matta, Swat). Locally, however, they occur as discrete intrusions, generally 1 km^2 in area, e.g., near Singal and Thurly, respectively, to the south and west of Chilas. Jan et al. (1984) and Khan et al. (1985) noted that a feature common to all thee rock types (i.e., gabbronorites, websterites, anorthosite and pyroxene diorites/tonalites) is the occurrence of plagioclase only moderately enriched in Ca (An_{45-65}).

There is evidence that the MGA comprises minor phases of magmatic activity both older and younger than the main-phase gabbronorites. In the vicinity of the Thalpan bridge, 2 km east of Chilas, and on the western slopes of the Thak valley, the gabbronorite and leuco-gabbronorite of the main phase contain numerous centimeter- to decimeter-scale enclaves of finer grain size and darker colour (Fig. 2b). As this area is relatively more sheared, the xenoliths are commonly tectonically stretched along the plane of foliation as flat lenticular masses. Similar xenoliths occur in the undeformed gabbronorites. In the roadside outcrops, just to the west of the KKH bridge on Buto Gah, undeformed leuco-gabbronorites have chilled contacts with a several meters large xenolithic block of fine-grained melanocratic composition. The important aspect of this xenolith is the presence of structures that depict one or more phases of deformation prior to incorporation in the main-phase gabbronorites (Fig. 3). Such xenoliths may represent an earlier phase of gabbronorite intrusion unless they belong to the basement of the Kohistan arc.

Evidence about the presence of a younger phase of gabbronorite/norite intrusions into the main-phase gabbronorites is met within the Thor area. About 500m to the east of the Thor bridge on KKH, a fine-grained dyke of amphibole-rich gabbronorite cuts through and carries xenoliths of the relatively coarser gabbronorites (Khan et al. 1985). Similar dykes are locally seen at several locations in the Thor and Thurly valleys. Fine-grained noritic dykes intrusive into relatively coarser gabbronorites also occur in the western part of the Chilas complex in the Swat valley (Jan, 1979).

Modal Composition

According to the IUGS nomenclature (Streckeisen, 1975), a large proportion of rocks in the MGA can be classified as gabbronorites comprising 45-65% plagioclase, 6 to 28% clinopyroxene and 10 to 27% orthopyroxene. A small proportion of the studied samples contains > 70% plagioclase and are termed anorthositic gabbronorites (nomenclature after McCallum et al., 1980). The layered zones in the MGA may contain rocks ranging from pure anorthosite to websterite, but locally there also are cm-scale veins of anorthosite in massive gabbronorites. Amphibole occurs in minor amounts in most rocks, but it is an important modal constituent (up to 30%) in some phase-3 dykes. The main-phase gabbronorites may also contain significant proportions of amphibole in low-grade shear zones or in zones of static retrogression, especially at the margins of the complex. Iron and iron-titanium oxides are ubiquitous in the rocks of the MGA, forming 1 to 8 model%. Magnetite and titaniferrous-magnetite are the main oxide phases but accessory amounts of ilmenite are also present in most samples. More than half of the studied samples from MGA lack modal quartz. The others contain up to 6% of quartz, generally interstitial.

Many rocks, especially those with > 2% quartz, also contain biotite, generally associated with oxide minerals or intergrown with amphibole. Minor amounts of apatite, both as interstitial anhedral grains as well as tiny prismatic grains inclusive in plagioclase, are ubiquitous, whereas traces of zircon occur in rocks with > 5% quartz. In Seo area, Jan (1970) has reported minor garnet and scapolite in some rocks. The modes of the leuco-gabbronorites, quartz-diorites and tonalites are also dominated by plagioclase but the latter two may have a high amount of quartz (up to 30 modal%). Ferromagnesian minerals include amphibole, bitite and pyroxenes. The latter make only a minor modal constituent and are, in many places, in the process of replacement by amphibole and quartz. A minor amount of alkali feldspar, locally in radial undergrowth with biotite and vermicular quartz, may be present in some of these rocks. Interestingly, both the feldspars may display exsolution, whereas the plagioclase is mostly characterized by simple twinning (Jan, 1979).

The gabbronorite xenoliths are similar in mineral composition to their host main-phase gabbronorites, but have distinct macroscopic appearance and textural characteristics. The principal constituent is plagioclase (up to 41%). The layered variety of xenolithic blocks contains ortho-and/or clinopyroxene-rich layers alternating with those of gabbronorite. Amphibole varies between 2 and 25 modal%, and quartz, biotite, magnetite and ilmenite occur in subordinate to minor proportions.

Textural Characteristics

The rocks of the MGA are predominantly medium-grained and granular but quartz-bearing leuco-gabbronorites and tonalites are relatively coarser grained (up to 6 x 5 mm plagioclase and pyroxene grains) when compared to gabbronorites. The gabbronorite dykes of the second phase and the rare norites grading into gabbronorites of the first phase are generally fine grained. The grain shapes of the minerals are largely determined by mutual interference. But proxenes tends to form aggregates which serve as the principal element defining layering, lamination and deformation (Fig. 2c). In the pyroxene-rich layers, the pyroxene aggregates form an inter-connected framework enclosing lenticular aggregates of plagioclase.

Although the texture in the rocks of the MGA can broadly be described as hypidiomorphic granular, in several cases it is transitional between hypidiomorphic and granoblastic granular. This is shown by polygonal plagioclase grains with straight to curved, sharp mutual grain-boundaries and 120° triple junctions. In several cases, both subhedral-tabular and polygonal plagioclase occurs in the same rock suggesting an incomplete requilibration of the originally plutonic igneous textures to deep-seated granulite facies conditions of crystallization. Around Madyan, Swat, deformed gabbronorites have lensoid pyroxenes imparting the rocks a look of augen gneisses (Jan, 1979).

The phase-1 gabbronorites, occurring as xenoliths in the main-phase gabbronorites, have distinct textural characteristics than their hosts. In handspecimen, they are finer-grained and have a darker colour than their medium to coarse-grained host. When occurring as small centimetric xenoliths, they are homogeneous, but the large block, described above, consists of thin pyroxene- and plagioclase-rich layers. Under the microscope, they are characteristically granular. Plagioclase is polygonal with 120° triple junctions, and sharp and straight mutual interfaces, furnishing a granoblastic rather than hypidiomorphic granular texture. Pyroxenes are either equidimensional or short prismatic (less than 1 x 1 mm in size), but they are associated with a generation of clinopyroxene grains which are large (~5 x 4 mm), prismatic and characteristically poikilitic, containing abundant granular inclusions of plagioclase and subordinate amphibole and orthopyroxene (Fig. 2d). These poikilitic clinopyroxene grains are randomly oriented in homogeneous rocks but are parallel to the layering in layered rocks. Amphiboles are also observed in dual textural forms, fine-grained polygonal in some layers, and prismatic poikilitic in others. The amphiboles contain quartz inclusions in addition to inclusions of plagioclase and orthopyroxene. It is likely that the prismatic poikilitic amphiboles, also found in some xenoliths, are a replacement product of clinopyroxene. This replacement of clinopyroxene by amphibole + quartz was probably due to a reaction between clinopyroxenes and a melt, which was either residual or was supplied externally by the host magma of the main-phase gabbronorites. However, some of the poikilitic amphibole may have grown during lower grade metamorphism (see below).

Retrogressed Gabbronorites: The 'Diorite" Problem

Fresh outcrops of all the above-mentioned lithologies are commonly seen in the Chilas complex. However, a major part of the complex, particularly on the margins, is retrogressed and contains variable amounts of secondary amphibole. Such rocks have loosely been termed diorites by some workers (e.g. Jan, 12970), thereby creating considerable confusion. Shams (1975) mapped the southern part of the Chilas complex in the Thak valleey (between Single in the north and Jal in the south) as metadiorites. Recently, Ghazanfar et al. (1991) have extended this so-called "diorite" domain westward through Buto and Thor valleys, and eastward into Niat and Bunar valleys, and ahve excluded it from the Chilas complex. Detailed petrography of these valleys reveals that amphibole is almost exclusively secondary, often bearing relics of ortho- and clinopyroxene (Khan, 1988). This clearly shows, as pointed out by us previously (Jan, 1979), that these amphibole-rich rocks are derived from gabbronorites and related rocks in the MGA. It is to be noted that an ultramafic body of dunite-peridotite composition associated with troctolites, olivine gabbros, and extensively layered pyroxenites-melgabbronorites-anorthosites occurs near village Mashai (or Dossar) in the Buto Gah. This occurrence is several kilometers south of the village Khae, within the "Thor diorites" of Ghazanfar et al. (1991). Ironically, they include this body of ultramafic and associated rocks in the Chilas complex but exclude the host rocks (cf. Ghazanfar et al. 1991; page 73 & Fig. 2). In valleys to the south of Chilas the gabbronorites of the Chilas complex have a direct tectonic contact with the amphibolites of the Kamila belt, marked by a 50-100 m thick mylonite zone (the Jal shear zone of Khan and Coward, 1990). No repetition of the complex is seen south of the contact here, a case opposite to that in the Indus and Swat valley sections.

Other parts of the Chilas complex which have been erroneously labelled as "diorite" domains, and excluded from the Chilas complex, include (1) its northern marginal part, and (2) the area around Sazin (see Desio, 1974). The area around Sazin is variably retrogressed to amphibolites and greenschists. Treloar et al. (1990) have recognized two hydration zones in this area and attributed them to two different mechanisms. Near Sazin, there is a high concentration of amphibole-plagioclase pegmatoids and amphibole-rich basic dykes, and the hydration is related to this intrusion event. SW of this the hydration is clearly controlled by a higher degree of deformation. The shear zones enhanced permeation of water into the rocks. This is reflected in the presence of amphibolite bands, some up to 200 m wide, which are formed within the unaltered gabbronorites.

The northern contact of the Chilas complex is well exposed in the upper reaches of valleys to the north of Indus. In Kiner and Hudur valleys the gabbronorites of the Chilas complex intrude Gilgit paragneisses and intercalated banded amphibolites (Tehseenullah Khan, unpublished data). Xenoliths of these lithologies (some several tens of meters large) occur within the gabbronorites of the Chilas complex, particularly in the middle Kiner Gah. (Khan, 1988). Fromhere eastward (i.e., between Ke Gas and Thalichi), the Chilas complex is in direct contact with the Kohistan batholith. The contact is typically intrusive; apophyses of quartz diorite, some several tens of meters thick, are seen emerging from the main body of the Kohistan batholith and intrude the Chilas gabbronorites near Drang confluence with Indus. In its northern marginal parts, the Chilas complex is only locally dioritic in composition (still retaining the essential assemblage of ortho-

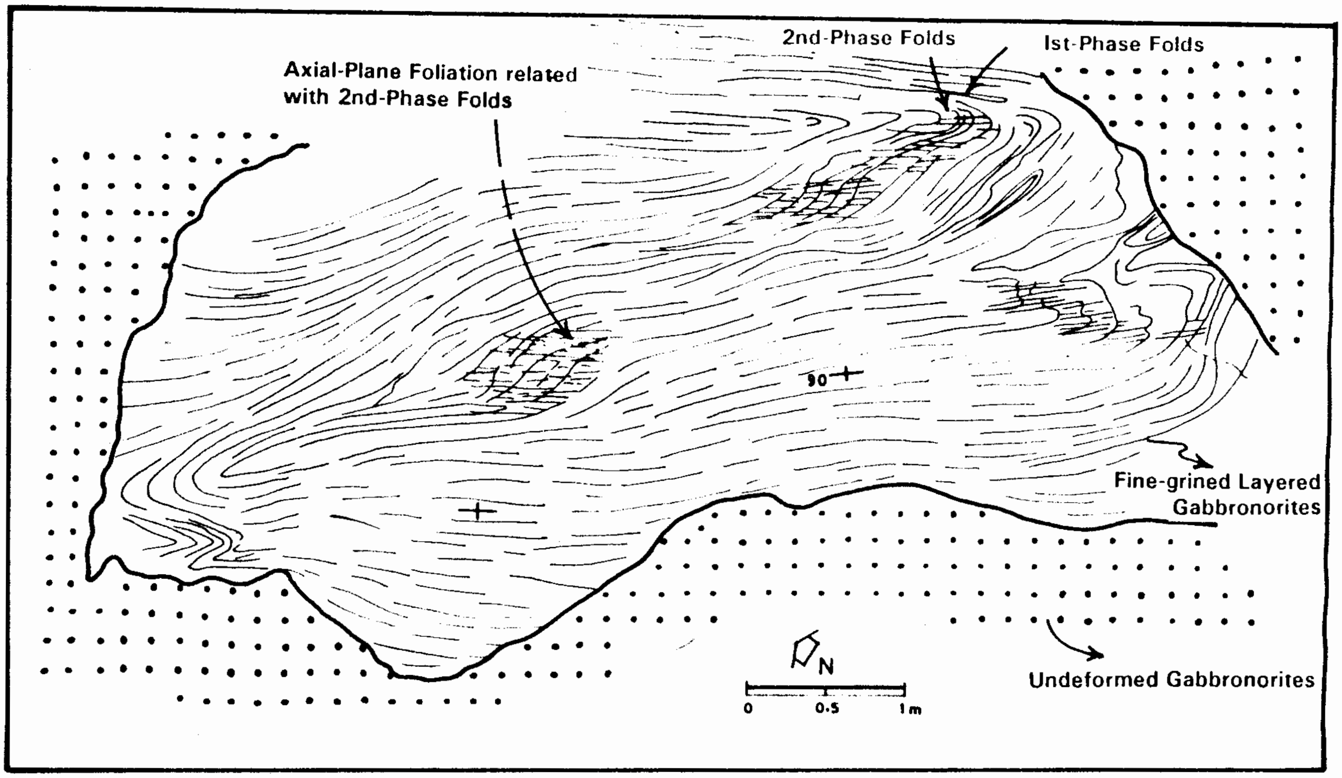

Fig. 3. Sketch map of a deformed xenolithic block of the earliest-phase norite containd in an undeformed leuco-gabbronorite of the main phase. Note the presence of two-phases of folding and tectonic fabric in the xenolith.

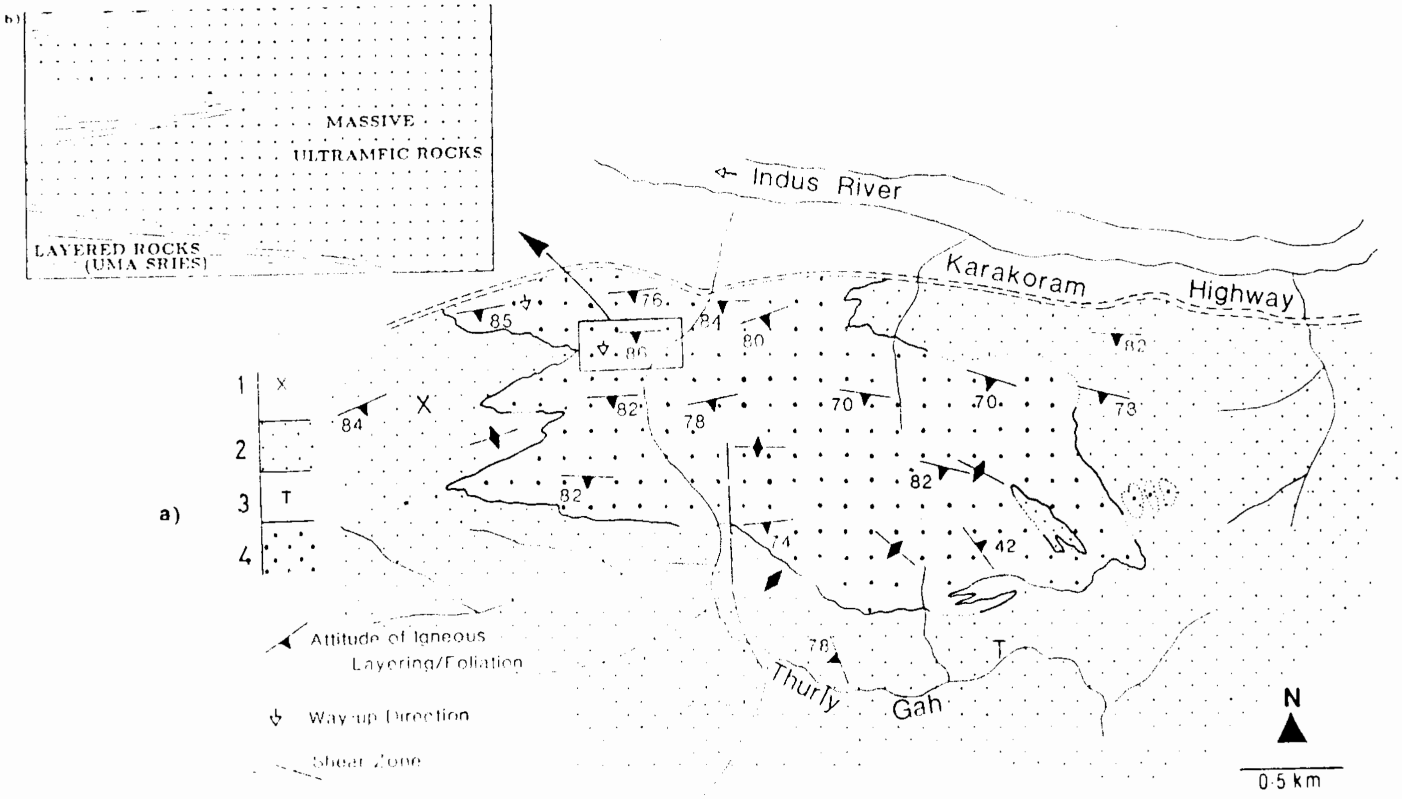

Fig. 4 A sketch geological map of the ultramafic-mafic-anorthosite (UMAA) body at the Thurly confluence, about 20 km west of Chilas. 1 = occurence of a calcsilicate xenolith; 2 = main gabbronorites; 3 = tonalite intrusion; 4 = ultramafic- mafic-anorthosite (UMA) body.

and clino-pyroxene) and is predominantly gabbronoritic. The relationship is particularly clear in the Kiner Gah, where medium-grained gabbronorites locally grade into leucogabbronorites and pyroxene tonalites but persist up to Gabbar village, where they intrude the Gilgit paragneisses and mark the northern limit of the Chilas complex. Thus, the Darel diorite unit of Ghazanfar et al. (1991) is non-existing, and is a misnomer for the retrogressed gabbronorites of the Chilas complex.

THE ULTRAMAFIC-MAFIC ANORTHOSITE ASSOCIATION (UMAA)

A subordinate but important component of the Chilas complex comprises ultramafic rocks: dunites, peridotites, orthopyroxenites clinopyroxenites, websterites and chromitites. They are intimately associated with anorthosites and mafic rocks ranging from troctolites, through olivine gabbros, to gabbronorites and gabbros all of which contain highly calcic plagioclase (An > 80). Almost all the occurrences of the UMAA have associated pegmatoids of both ultramafic and mafic composition. The ultramafic pegmatoids comprise pyroxenes (mainly orthopyroxene), olivine and large crystals of amphibole. The gabbroic pegmatoids contain essential plagioclase, commonly in aggregates. These pegmatoids are distinct from those referred to later in this paper (i.e., amphibole- plagioclase pegmatoids) which are not a part of the UMAA and make a separate phase of magmatic activity.

In terms of overall volume, the UMAA makes only a minor proportion of the Chilas complex. In the eastern parts of the complex, however, a number of ultramafic-mafic bodies are exposed in a 20 km radius around Chilas. The largest body of UMAA occurs 6 km south of Chilas near Single (Fig. 1). It reaches 3 km in width and extends ESE-WNW for >5 km, across the drainage divide between the Thak and Buto valleys. The rest of the UMAA bodies are generally less than 5 km^2 in area, the principal ones being those near Gine, Indus-Thak confluence, Mashai (upper Buto Gah), and Thurly-Indus confluence. Minor occurrences of the UMAA have been recorded at several places in the Chilas complex: the eastern face of the Buto Gah (now occupied by the parts of the old Chilas village), 2 km to the south of the Chilas rest house, between the Basha dam-site and Dudishal bridge on the Indus, along KKH to the west of Harban police station and, very locally, in Swat valley.

All the bodies of UMAA, irrespective of their location in the complex, comprise a complete spectrum of the rock types characteristic of this association, though their mutual proportions may vary from one body to the other. Most are predominantly ultramafic but the Gine body contains relatively higher proportions of the mafic rocks and pegmatites.

The rock of the UMAA occur in two principal modes; either in the form of layered successions or as thick homogeneous masses. Thick masses of dunite and peridotite, without much internal layering, make large proportions of all the UMAA bodies, particularly those of the Thak and Thurly confluences. Layered successions are common either in the plagioclase-rich rocks or where plagioclase-bearing rocks occur together with the ultramafic rocks. The Gine, Thak and Thurly confluence bodies show best developed layered successions.

The relationship between the massive ultramafic rocks and layered successions are variable, but the former occur mostly in the form of thick lenses conformable with the layered successions. This relationship is best exhibited in the Thurly confluence body, the core of which consists of massive ultramafic rocks comprising dunites and peridotites with minor showings of chromitites. When followed east or westward along the strike, the ultramafic mass splits up peripherally into fingers extending parallel to the intervening mafic-ultramafic layered successions. This relationship is portrayed schematically in Fig. 4. Exactly similar relations, though on a relatively smaller scale, are observed in the SW peripheries of the UMAA body at the Thak confluence (Fig. 5).

Unlike the conformable relations described from the Thurly and the Thak confluence bodies, the massive ultramafic rocks in the UMA body near the Gine confluence cut across the layered succession (Fig.6), and are intruded by an irregular mass of ultramafic to mafic pegmatoids. The intrusive emplacement of the massive ultramafic rocks here is apparently assisted by a locak fault. This is indicated by an offset of more than 45

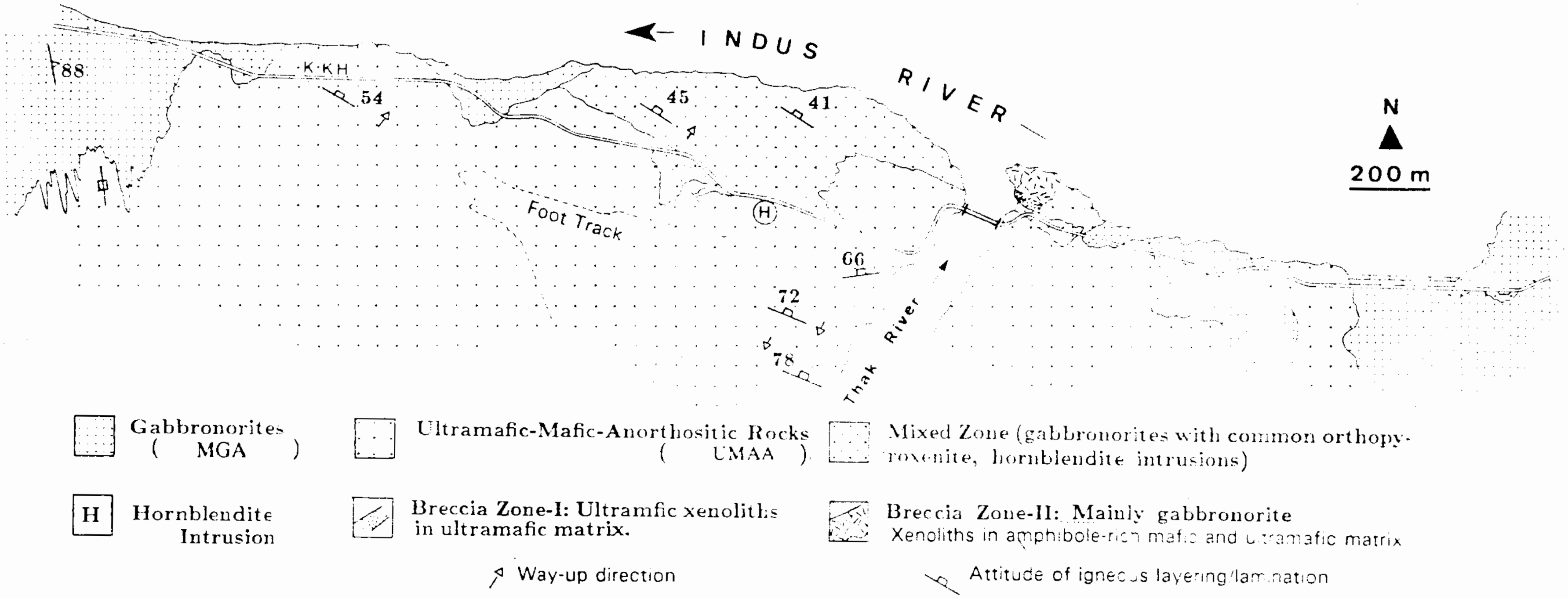

Fig. 5. A sketch geological map of the ultramafic-mafic-anorthosite (UMAA) body at the Thak confluence.

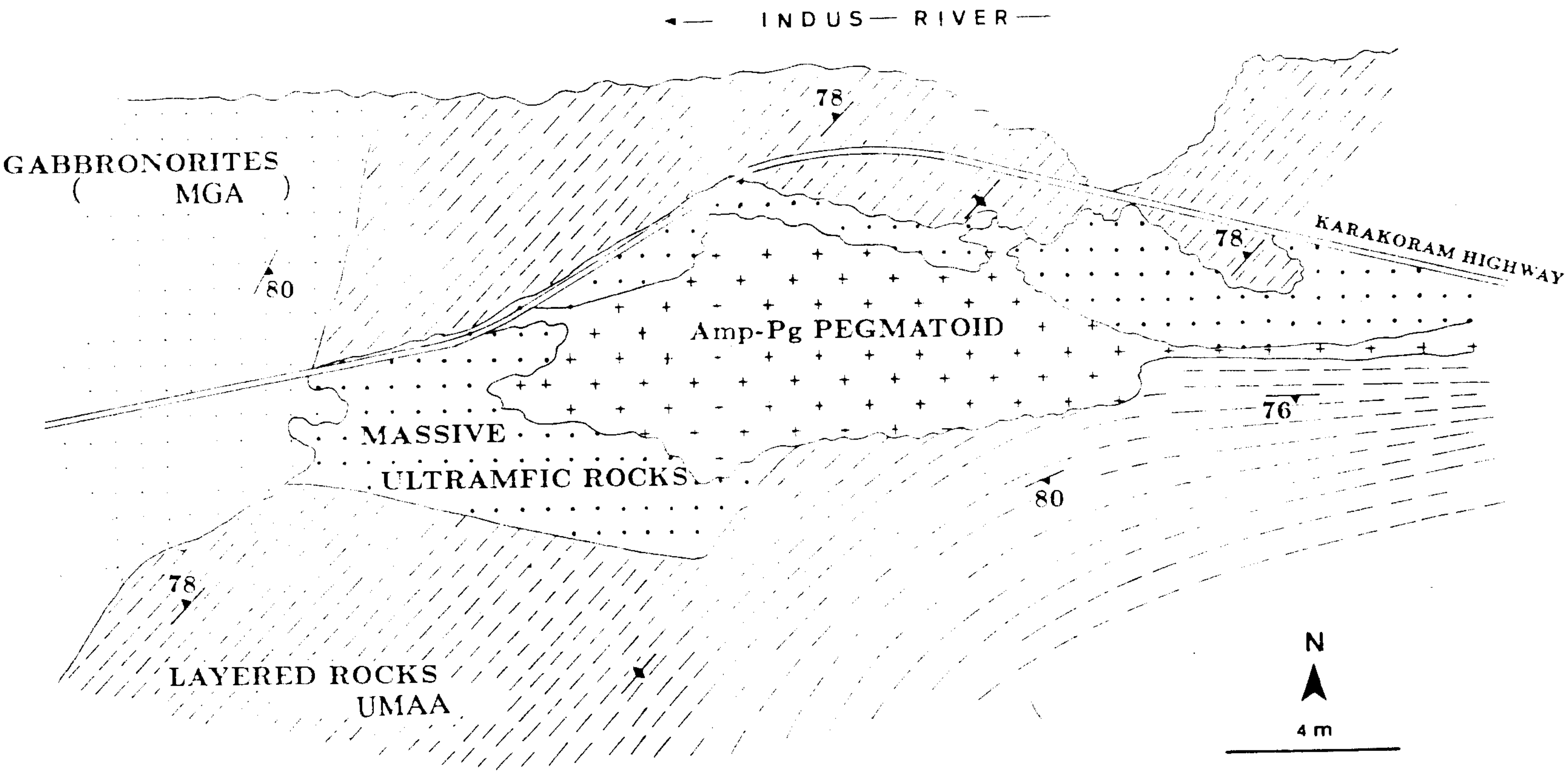

Fig. 6. A sketch geological map of the ultramafic-mafic-anothosite (UMAA) body at Gine, some 20 km east of Chilas. Tectonically remobilized massive ultramafics cut across the layered rocks of the same association.

degrees in the attitude of layering in the layered succession on the two sides (N & S) of the intrusive ultramafic mass. An interesting aspect of this UMA body is that ultramafic rocks, similar to those cross-cutting the layered succession, occur also as conformable layers in the layered succession.

The cross-cutting relations between various members of the UMAA are not uncommon elsewhere in the complex. In a number of places dykes of olivine-rich ultramafic rocks, anorthosites and gabbronorites, have been observed, but without any chilled margins. In some places, gabbronorite or anorthosite make the matrix of breccia containing blocks of ultramafic rocks and vice versa. Fig. 7a shows an outcrop in the Thurly confluence body, where a succession of layered mafic rocks and anorthosites is cut across and brecciated by veins of a granular dunite. Abut 100 m south of this location, a gabbronorite (UMAA) dyke runs between two mafic layers obliquely, cutting across an intervening meter-thick layer of dunite. The cross-cutting relations between rocks, which predominantly show interstratifed relationship, suggest emplacement of crystal mushes or remobilisation of rocks which crystallized originally as layered successions, rather than from multiple intrusion. Such a mechanism has also been suggested for similar relations in the Emigrant Gap area, California (James, 1971).

Late Intrusives

These rocks in the UMAA occur exclusively in cross-cutting bodies and are not related to layering. These include amphibole-rich orthopyroxenites, hornblendites, and amphibole-rich olivine-gabbro pegmatoids. These occur in the form of thin veins, small dykes and irregular bodies up to 10 m across. The principal concentration of the intrusive orthopyroxenites is seen in the UMA body at the Thak confluence (north side of KKH on the river-side), where several small subcircular bodies intrude both the dunites of the UMAA and the gabbronorites of the MGA. Elsewhere, e.g., Thak and Thurly confluence bodies, the orthopyroxenites occur as veins and dykes. In the Thak example, the orthopyroxenite dyke contains a few fractures which are apparently filled by the host gabbronorite. This suggests that the emplacement of the dyke took place while the host rock was still hot (and capable of plastic flow), a possibility also supported by the lack of chilled margins in the dyke.

The type occurrence of hornblendites in the Chilas complex, is about 30 m west of the Thak bridge on the KKH (Fig. 7b). In an outcrop covering an area of 8 m^2 granular hornblendites (±diopside) intrude and brecciate massive dunites as veined network. Abut 50 m northwards, on the other side of the road, small bodies of hornblendites intrude the layered gabbronorites and anorthosite. The contact is well-defined but not sharp, marked by thin apophyses of hornblendite running outward into layered mafic and anorthositic rocks along the plane of lamination and layering. East of the Thak bridge, the contact between the ultramafic body and the gabbronorites of the MGA is occupied by a ~ 20 m thick breccia zone, which is divisible into two sub-zones (Fig. 1) The internal breccia sub-zone, next to the ultramafic rocks, is exclusively ultramafic both in terms of included blocks (dunites and peridotites) and matrix (orthopyroxene-rich peridotites). The outer sub-zone consists predominantly of gabbronorite (MGA) but also contains dunite xenoliths (Fig. 7c). The interstices between the angular blocks are occupied by a matrix varying in composition between hornblendites and amphibolites. The amphibole-rich ultramafic and mafic rocks are thus a late phase intrusive activity in the UMAA, characterized by a high volatile content and explosive emplacement.

The pegmatoids of amphibole-rich olivine-gabbro to gabbronorite composition are common and are characteristically associated with the rocks of the UMAA. They are commonly in the form of veins and dykes (generally less than 10 cm thick), but also occur in irregular to subscircular, small bodies cross-cutting both homogenous dunites as well as layered successiosn. Locally they form networks of dykes enclosing large blocks of dunites. In places fragments derived from the pegmatoids occur between graded layers, the younger layers bulging around the fragments (Fig. 7d). This suggests that the pegmatoid formation inthe UMAA is spread over a considerable span of time both before and after complete crystallization of the layered rocks of the series. The close association of this group of rocks with UMAA, their similarity in mineral content (except for an abundance of hornblende)

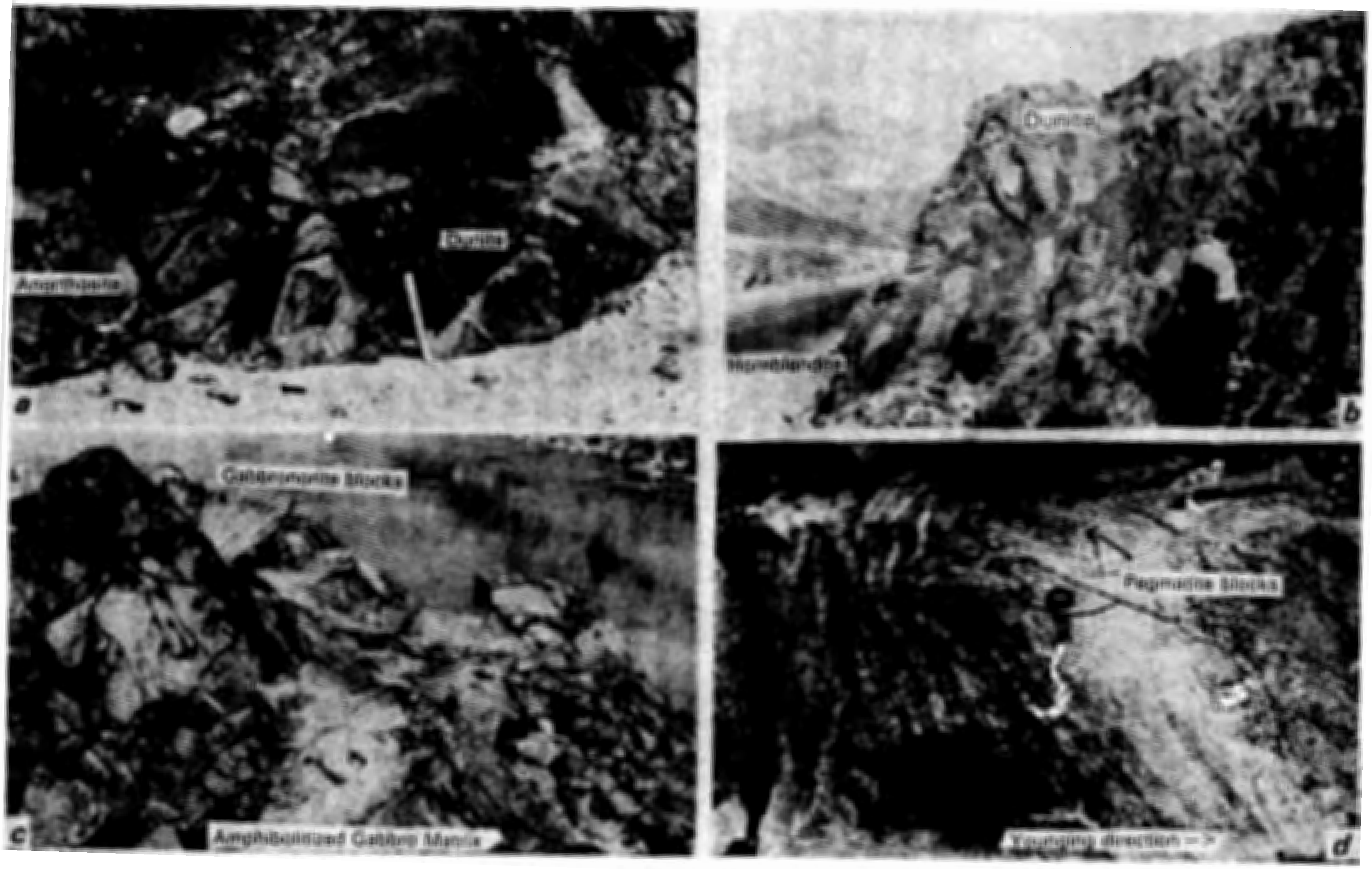

Fig. 7. (a) A brecciated mass of leuco-gabbronorites-anorthosites of the UMAA invaded by granular dunite (black). (b) A net-work of hornblendite (balck) intruding the granular dunite. (c) A brecciated mass of gabbronorites, set in a matrix of hornblendites (or hornblende gabbronorites). (d) A xenolithic block of gabbroic pegmatoid (just below and to the left of the lense cover). Note that underlying layers (those on the left) are depressed while the overlying bludge over the xenolith.

with the rocks of UMAA, and nearly similar time of emplacement are compelling arguments to suggest that they are genetically related to the UMAA. The following possibilities can be proposed for their origin. The pyroxenite dykes, which generally lack chilled margins, may represent remobilized layers, crystal mushes or partly crystallized magma. The hydrous pegmatoids and hornblendites may represent pockets of H_2O-rich differentiates of UMAA, or chimneys for the escape of volatiles, thereby altering the neighbouring rocks.

Modal composition

The UMA association of the Chilas complex, though subordinate in volume proportions, comprises a more diverse group of rock types than the MGA. About 50% (by volume) of it consists of ultramafic rocks ranging from dunites (olivine cumulates) to clino- or ortho-pyroxenites, with many having a peridotitic composition (including wehrlites and harzburgites). Aggregates or pockets of cumulus plagioclase, or its reaction products with olivine (discussed below), occur in most ultramafic rocks. There also are thin seams and pockets of chromitite inter-layered with dunites and pyroxenites. Modaly, the chromitiferous rocks range from olivine- or pyroxene - chromitites to dunites and pyroxenites containing accessory chrome spinel. Amphibole occurs in most ultramafic rocks, both as a post-cumulus and secondary mineral. Some meso-cumulate ultramafic rocks may contain up to 30% by volume of interstitial and poikilitic amphibole, but commonly it is from 1 to 5 modal%.

The mafic rocks of the UMAA are broadly divisible into olivine- bearing (troctolite, olivine gabbro, olivine gabbronorite) and olivine-free (gabbro, gabbronorite) varieties. A characteristic feature of the olivine-bearing rocks is the development of orthopyroxene (± clinopyroxene), hornblende and Al-spinel coronas resulting from subsolidus reaction between olivine and plagioclase (Jan et al., 1984b). In some gabbronorites all the olivine also has been consumed in the process. But for the abundance of plagioclase, the anorthosites are comparable with the mafic rocks in terms of mineral assemblage. Post cumulus amphibole is a common but minor phase in the mafic rocks and anorthosites (up to 5 modal%). Chrome spinel is an accessory phase in the olivine-bearing mafic and anorthosite rocks. In the olivine-free gabbronorites the oxide phases are characteristically magnetite and titaniferous- magnetite. Modal proportions of oxide minerals in the mafic and anorthositic rocks of the UMAA are generally lower than their counterparts of the MGA. The olivine-free mafic rocks of the UMAA are modally more or less identical to those of the MGA, and the distinction is possible only on the basis of mineral composition such as higher An-content of plagioclase and high Mg# of ortho- and clinopyroxene in the UMAA compared with the MGA.

Textural Characteristics

A great majority of the ultramafic rocks of the UMAA is characteristically granular. This is particularly so in the rocks rich in olivine (dunite and peridotite) where 3 x 3 mm size grains form equigranular mosaic with generally little or no post-cumulus material. A more or less similar granular texture is shown by the websterites, orthopyroxenites, clinopyroxenites, and interlayered granular chromitite (Fig. 8a, b). The pyroxenes in these rocks are equigranular with mostly equidimensional (1.5 x 1.5 mm) grains which hardly contain any post-cumulus material. All the ultramafic rocks of the association, however, are not adcumulate. Some of the olivine cumulates contain up to 30% by volume of the post-cumulus minerals such as clinopyroxene, orthopyroxene, plagioclase and amphibole (e.g., Fig. 8c-f). These post-cumulus minerals occur either as anhedral interstitial grains or, more commonly, as optically continuous, large (up to 8 x 8 mm) poikilitic grains enclosing cumulus olivine.

In addition to the straightforward cumulus textures described above, the ultramafic rocks also show some unusual textures: (1) granoblastic granular and (2) porphyritic. The granoblastic-granualr, ultramafic rocks (both dunites and pyroxenites) differ from the granular adcumulates in having polygonal grains with straight to curved mutual interfaces, common 120° triple junctions, and a finer grain size (Fig. 8a, b). These rocks are probably derived from the adcumulus dunites and pyroxenites as a product of sub-solidus annealing in response to the residual heat of magma (cf. Moore, 1978). The porphyritic-type

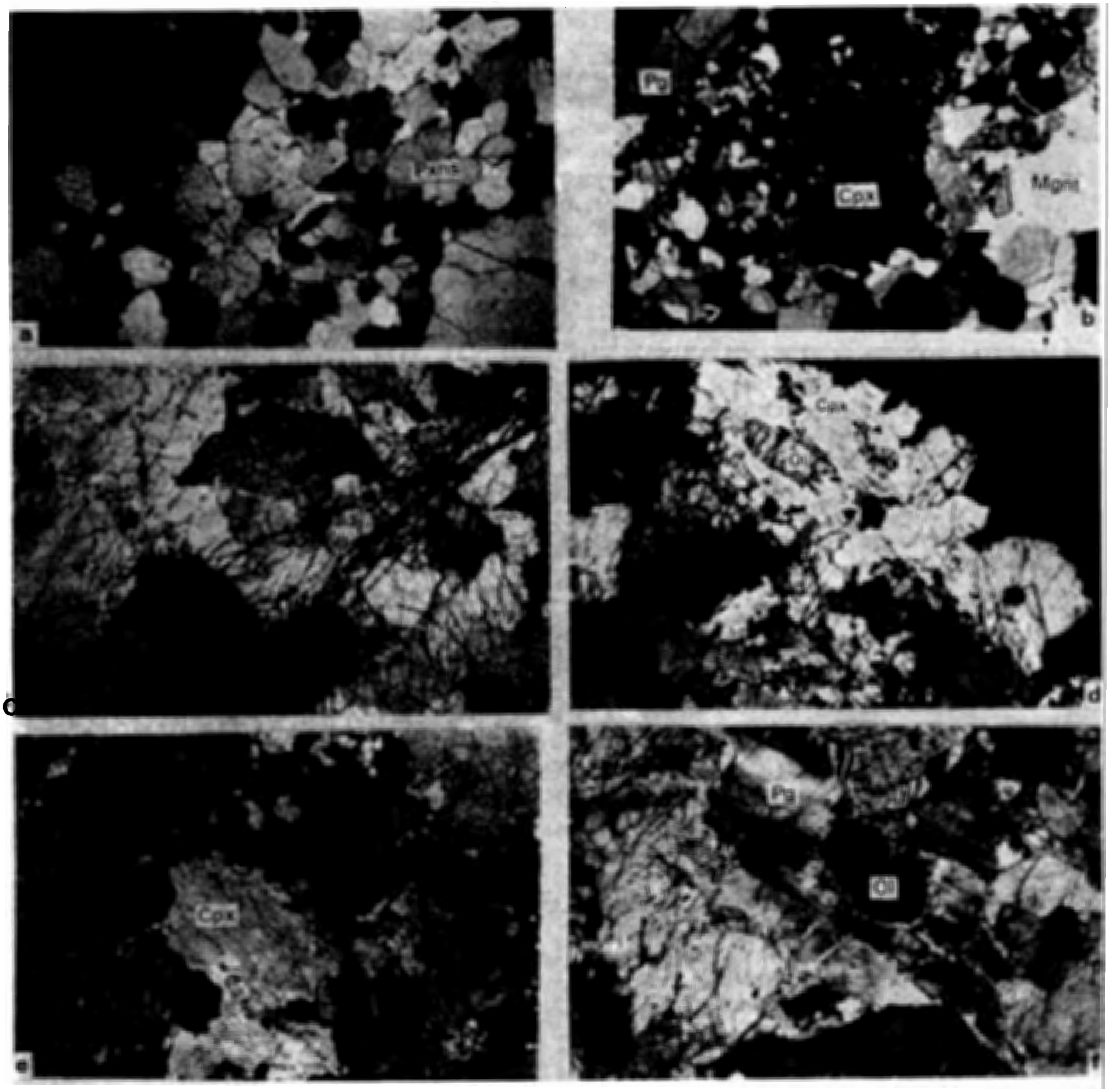

Fig. 8. Photomicrographs showing representative textures in the UMAA. (a) granular peridotite. (b) granular peridotite with an exsolved megacryst of clinopyroxene showing recrystallisation in its marginal parts. (c) a large clinopyroxene crystal (left one-third of the photo) poikilitically enclosing olivine megacryts. (d) Olivine megacrysts poikilitcally enclosed in clinopyroxene (upper right corner). (e) several megacrysts. of clinopyroxene enclosed in a granular groundmass of clinopyroxene, orthopyroxene and olivine. (f) olivine megacrysts enclosed in a poikilitic plagioclase. In all cases, photomicrographs length = 1.5 cm. Oi = Olivine; Amp = Amphibole; rest of the mineral abbreviations are same as in Fig. 2.

texture is characterized by the occurrence of large (3 x 3 to 8 x 8 mm size), isolated, equi-spaced grains of clinopyroxene and, rarely, of orthopyroxene and olivine in a fine-grained matrix (< 1 mm grain size) of the three minerals and amphibole (Fig. 8e). These megacrysts are generally tabular to equidimensional and only rarely contain inclusions. This latter feature indicates cumulus nature of the megacrysts (primocrysts of Wager & Brown, 1968), though the rocks do not qualify to be termed as cumulates due the lack of physical contact between the megacrysts to form a cumulus framework (cf. Irvine, 1980).

The mafic rocks of the UMAA have both hypidiomorphic and granoblastic granular textures. The clinopyroxene and orthopyroxene form lenticular aggregates (2-6 x < 10 mm) alternating with those of plagioclase of similar lenticular shape and dimensions, defining mm scale layering. Predominantly the texture is adcumulus, though post-cumulus amphibole occupying interstices between plagioclase and pyroxene-plagioclase interfaces occurs in majority of the rocks. Rarely, the clinopyroxene and orthopyroxene form large poikilitic crystals enclosing subhedral plagioclase inclusions, indicating post-cumulus crystallization.

Pegmatoids associated with the UMA bodies are highly variable in modal composition. Most ae rich in pyroxenes with appreciable amounts of amphibole, but some contain up to 80% olivine. Pyroxenes in these rocks occur as 10 x 10 mm size crystals enveloped in granular to tabular amphiboles. Plagioclase is a common consittuent of most pegmatoids, occurring both as large (8 x 8 mm) tabular, and small (2 x 2 mm) polygonal grains. Some pegmatoids consist exclusively of amphibole, with only minor amounts of diopside and are termed hornblendites.

AMPHIBOLE PLAGIOCLASE PEGMATOIDS

The pegmatoids, made up exclusively of plagioclase and hornblende, occur sporadically throughout the complex (Jan, 1979), but are more common in the central part. Unlike the gabbroic pegmatoids of the UMAA described above, these pegmatoids occur both in the gabbronorites of the MGA and in the UMAA. Furthermore, they lack pyroxenes and olivine, and contain plagioclase of only a moderate An content; these features distinguish them from the pegmatoids of the UMAA. They occur in the form of veins, dykes and irregular intrusive bodies. There is a wide range of grain size from one to another pegmatoid and, to a lesser extent, within the same pegmatoid body. The prismatic hornblende crystals range from a cm to half a meter in length (Jan & Kempe, 1973), and so does the accompanying plagioclase (Fig. 9a, b). The hornblende crystals are mostly randomly oriented, but in some cases they are grown perpendicular to the walls of the dykes or veins, suggesting a very slow crystallization and/or an abundance of fluids. Hydration (e.g., amphibolitizatin) of the host rock around these pegmatoids is observed in several places (Jan, 1979), especially between Sazin and Lotar on the KKH where the pegmatoids have a greater concentation (Treloar et al., 1990).

BASIC DYKES

Basic dykes are widespread in the east-central part of the complex. Although they have not been recorded in Swat and Dir valleys, Jan et al. (1983) reported sporadic, thin dykes in gabbronorites in the western end of the complex in Dir. Comminly only a few cm thick, they are locally thicker than a meter. The dykes are essentially fine-grained, massive and homogeneous, and have a dark appearance in hand specimens. Locally they occur in sub parallel sets, but no consistent trend could be detected on a regional scale. A majority of the dykes in the complex are internally undeformed, but their country rocks may or may not be foliatd. The dykes comprise comparable amounts of plagioclase and amphibole, both occurring in a granoblastic granualr texture, but in rare cases the hornblende may be over 2 cm long. Ilmenite and magnetite are common minor constituents of these dykes. Locally, they contain orthopyroxene which occurs in two modes: (a) forming large (5 x 5 mm) equidimensional discrete grains (Fig. 9c), and (b) as fine-grained polygonal/tabular grains in 6 x 6 mm size globular masses (Fig. 9d). Both are regularly disseminated in an amphibolite matrix, giving a similar general appearance in hand specimen. Whereas the discrete orthopyroxenes might have crystallized primarily as phenocrysts, the globular masses

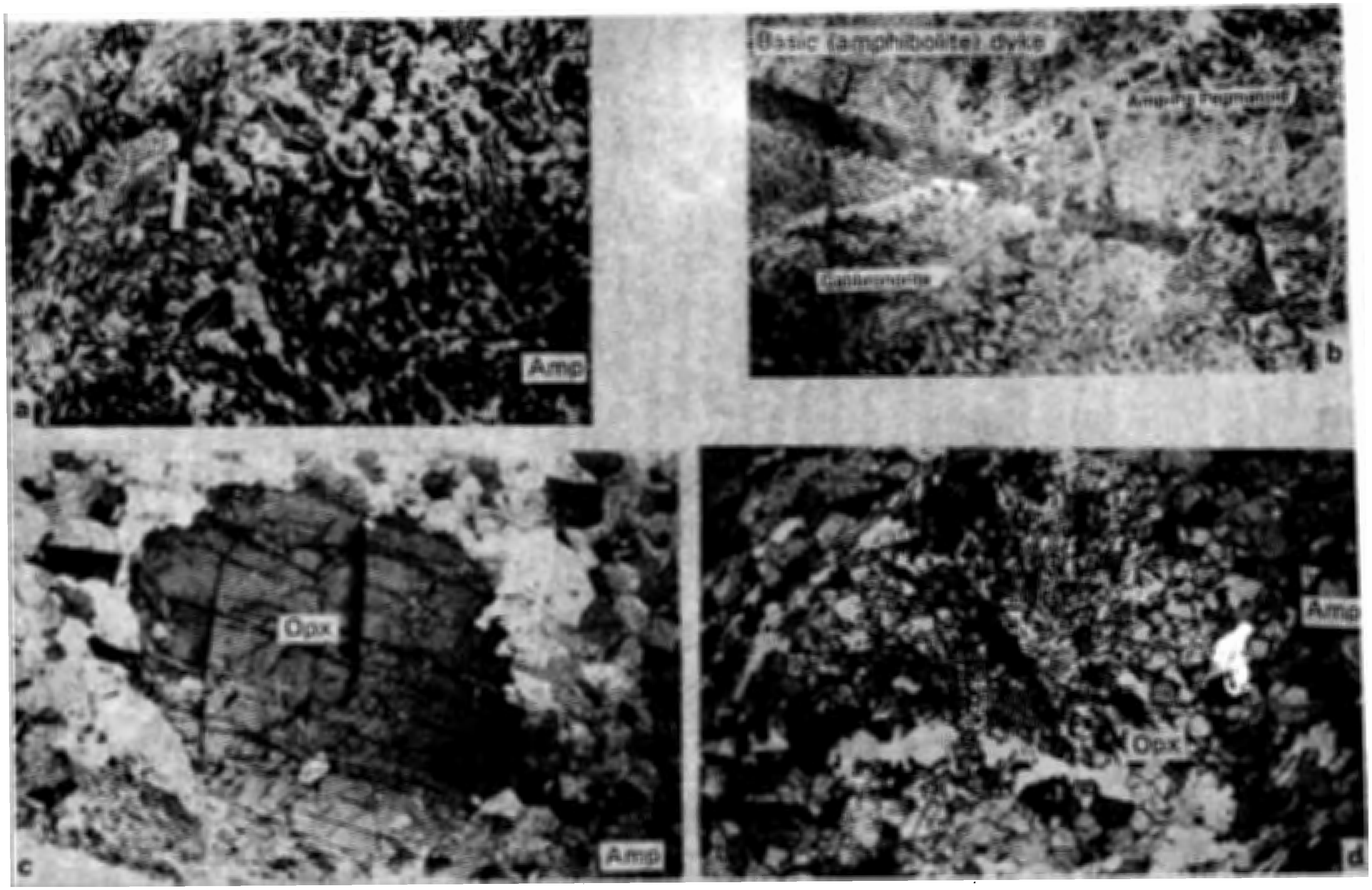

Fig. 9. (a) a close-up of the amphibole-plagioclase pegmatoid from an irregular massive body at Gine. (b) gabbronorite containing a plagioclase-amphibole pegmatoid cut by a basic (amphibolite) dyke. The two cut across all the other lithologies in the Chilas complex. (c) a photomicrograph of a basic dyke comprising a discrete phenocryst of orthopyroxene in a groundmass comprising granular amphibole and plagioclase (x10). (d) photomicrograph of the basic dyke containing a granular mass of orthopyroxene with abundant magnetite vermicules. The surrounding groundmass is that of plagioclase and amphibole (x10). The symplectite may be derived from olivine. Mgnt = Magnetite vermicules; for the rest of mineral abbreviations see Figs. 8 & 2.

of orthopyroxenes appear to be a replacement product of olivine. This is based on the observation that these orthoproxenes contain abundant magnetite granules and vermicules, particularly high in the core of globular masses (Fig. 9d), which is a characteristic feature of the corona orthopyroxenes and amphiboles in the Chilas complex.

COUNTRY-ROCK XENOLITHS IN THE CHILAS COMPLEX

These can broadly be divided in three major groups.

Calc-silicate Rocks

These occur in several places in the complex. The largest of them (70 x 40 cm^2) was recorded just to the east of Thor bridge on KKH. Such xenoliths are also found on the western ridge of the Thurly valley, and 20 km west of Sazin. It is notable that horizons of bedded calc-silicates occur near the base of or at the southern contact of the Chilas complx in Bunar Gah, at Seo (about 6 km N of Kamila, Shin (Swat), and there are interlayered marbles and calc-silicates in the Kamila amphibolites at Jal (Thak valley). All the xenoliths of this group contain combinations of quartz, plagioclase, alkali feldspar, wollastonite, grossular, clinopyroxene, epidote, scapolite, ilmenite and/or sphene. Most xenoliths are thinly banded; bands rich in garnet may alternate with bands rich in wollastonite.

Paragneisses

A second group of xenoliths is found in the Kiner valley, north of Chilas. They range from cm-scale xenoliths to meter-scale blocks. These are essentially banded rocks, with individual bands being comparable in mineral assemblages but highly variable in modal composition and texture. Common mineral assemblage comprises quartz, plagioclase and alkali feldspars, orthopyroxenes, garnet, biotite, and magnetite -titanomagnetite. The orthopyroxene and garnet are generally in sparate bands, and only rarely coexist. Garnet-bearing bands are also rich in quartz and biotite compared with orthopyroxene-rich bands which contain higher proportions of plagioclase. The thinly banded nature, and extremely variable modal composition from one band to the other suggest a derivation from a volcano-sedimentary sequence, probably tuffs. Similar xenoliths are reported by Bard (1983b) from Swat valley.

Basic metavolcanics and porphyritic diorites

These are restricted to the southern marginal part of the Chilas complex as observed in the Thor valley (to the north of village Gabar). The host rocks in this area are pyroxene tonalites which have a gradational contact with the main-phase gabbronorites northwards in the interior of the complex. Whereas the porphyritic diorite/ tonalite enclaves may be autoliths, related to the hosts, the fine-grained basic xenoliths may be derived from the Kamila amphibolites which occur nearby to the south of the contact.

SEDIMENTARY STRUCTURES

Like other large mafic-ultramafic complexes (e.g. Skaergaard, Bushveld, Stillwater, Duke island, Rhum), cumulate rocks in the UMA association of the Chilas complex also display a number of structures similar to those found in sedimentary rocks, especially turbidites (irvine, 1965) and marine evaporites (Wadsworth, 1973). While the main gabbronorite association displays local layers of pyroxenite and anorthosite (Jan, 1979), rocks of the UMAA, especially gabbronorites, are characterized by well-developed layers, generally 1-10 cm in thickness. The layering is commonly rhythmic, but rarely a set of layers is repeated cyclically. The layered sequences, at places several tens of meters thick, may consist solely of graded layers or, less commonly, of alternating isomodal layers of different composition (terminology of Irvine, 1982). The grading is commonly modal with base containing more of the mafic phases and top containing more plagioclase, however, in a few places size grading is also observed. The layers may end laterally within a few meters or extend for several hundred meters. Various sedimentary structures, to be described in detail in a separate paper, are shown in figures (10 & 11), and can be classified as follows.

(1) Crystal sorting under the influence of gravity and/or convection currents, or local growth due to diffusion leading to the development of layering and graded bedding.

(2) Structures related to the action of magmatic flow and currents during deposition, e.g., igneous lamiantion, current bedding, wedging of layers

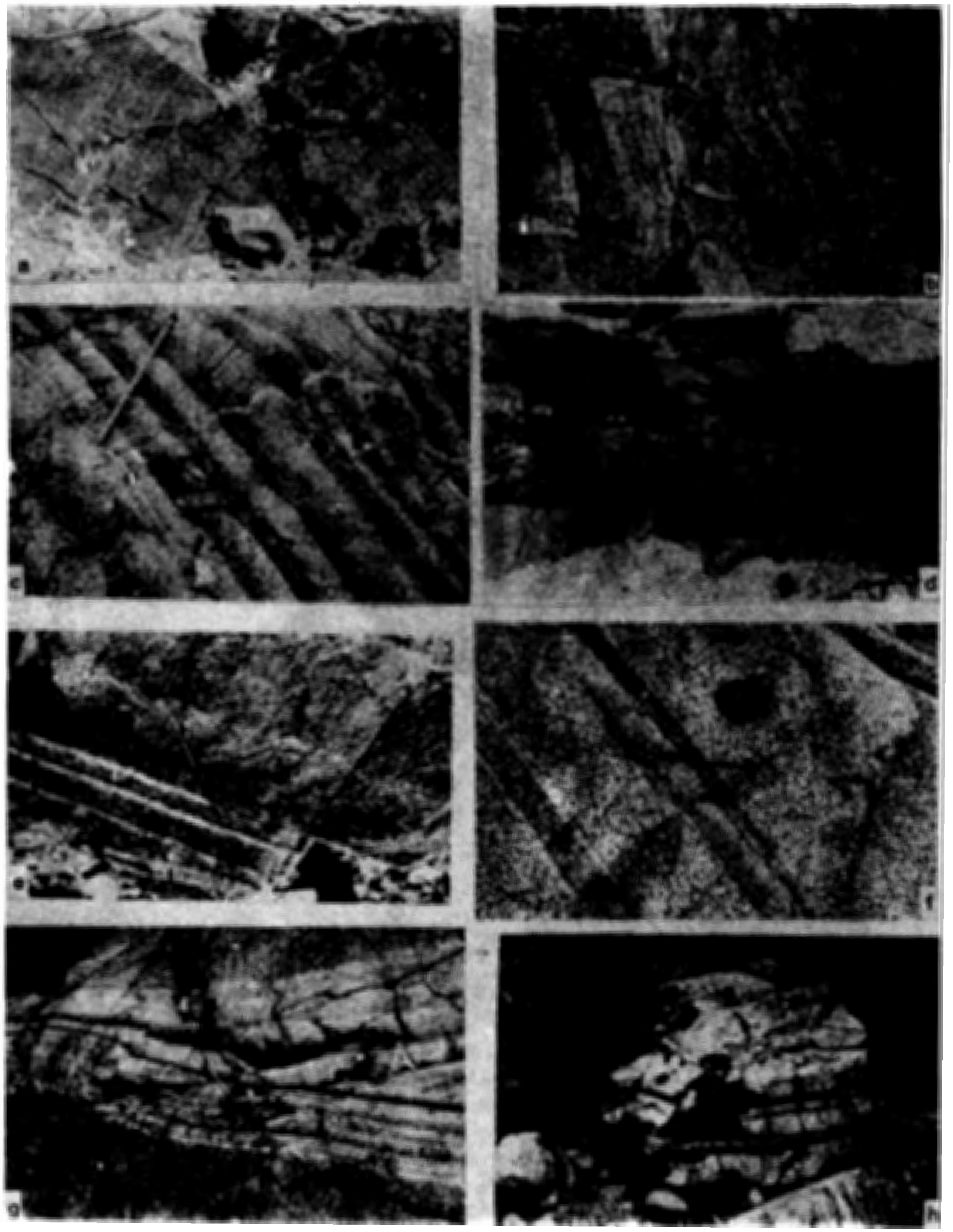

Fig. 10. Various types of igneous layering encountered in the Chilas complex. (a) Rare cm-scale layering in the gabbronorites of the MGA. (b) Isomodal anorthosite-gabbronorite layers in MGA. (c, d, e, f, g, h) Graded layering. Note the presence of synsedimentary faults in (g). In (h) the succession comprises isomodal dunite and anorthosite layers, but the former is locally remobilised to form apophyses cutting across the succession.

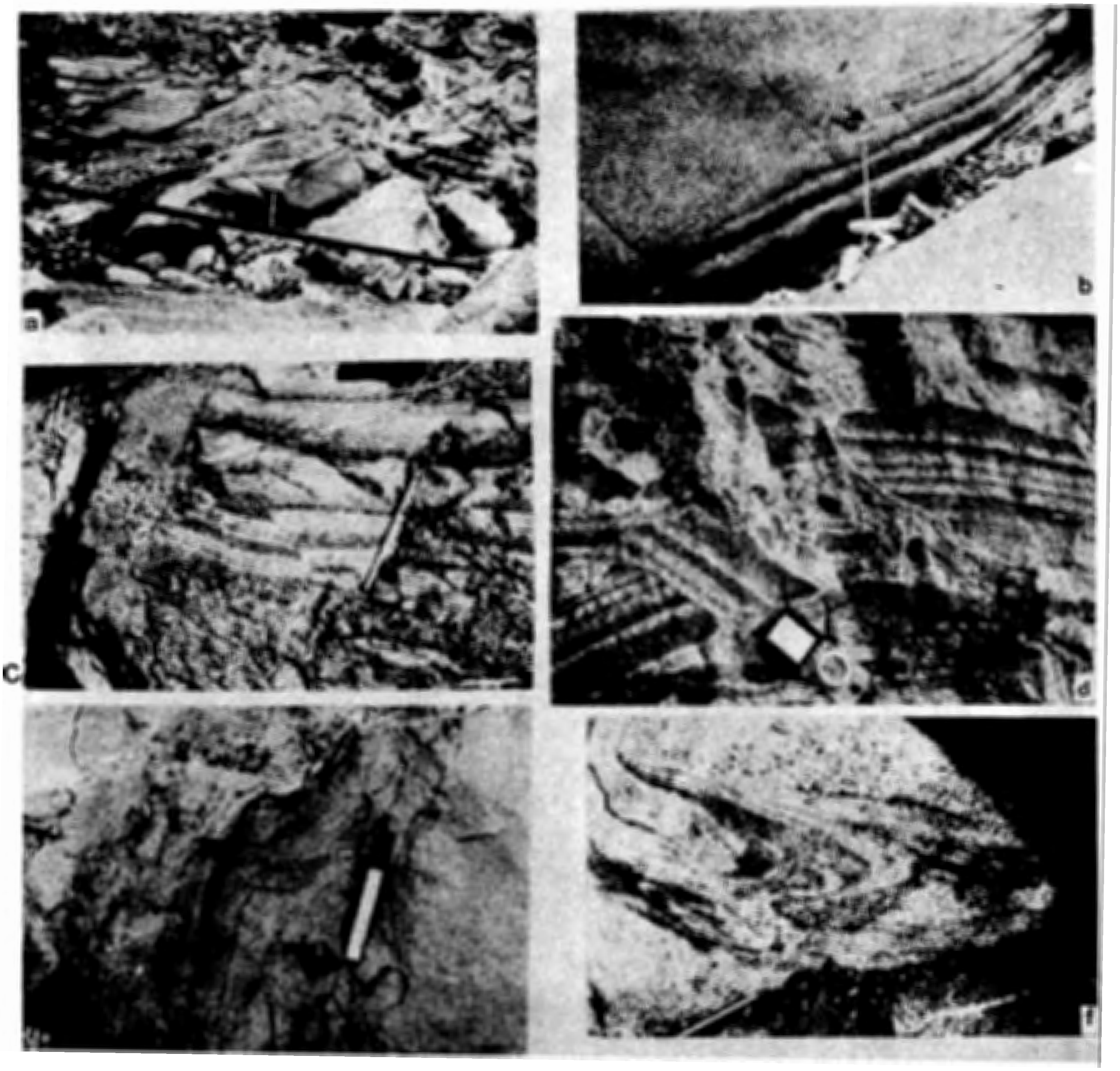

Fig. 11. Representative sedimentary structures in the UMAA. (a) A trough structure marked by layered rocks. This resembles greatly with chennel deposites in turbidites and may have similar origin. (b) An angular unconformity defined by erosive action of a pulse of gabbronorites truncating previously deposited layered gabbronorites-websterites (c) Syn-sedimentary faults in a graded sequence of layers. Note that the top-most two layers are undisturbed, deposited on lower layers in the sequence which are faulted and brecciated. (d) An example of breccia produced and deposited in response to turbidity currents in the slowly crystallizing magma chamber. (e, f) Slump folding. In (e) chromitite and dunite layeres are involved while in (f) anortosite and pyroxenite layers are involved.

where an earlier set of layers is truncated by a younger set to produce "angular unconformities", scour and fill structures and breccias.

(3) Syn-sedimentation faulting, resulting in offset of earlier (lower) layers under a cover of undisturbed younger layers. The occurrence of such faults and large joints may have led to secondary features such as diapirism of crystal mushes and fracture filling by feshly accumulated crystals.

(4) Structures related to gravitational instability, e.g., sagging, slump folding, and brecciation.

DISCUSSION

The petrographic and other aspects described in this paper have fundamental implications for the nature and origin of the Chilas complex. Field evidences, discussed earlier, suggest that the complex is autochthonous and intrudes the neighbouring amphibolites and paragneisses, although during subsequent crustal shortening it was thrust against the Kamila amphibolites to its south.

The compositional spectrum ranges from ultramafic rocks to diorites and tonalites. The mutual field relations suggest that though the two asociations (UMAA and MGA) might have crystallized from magmas with different initial compositions (Khan et al., 1985, 1989), the rocks within each association must be inter-related through the processes of crystal separation and magmatic differentiation. Such processes can operate only in conditions of slow cooling in magma chambers.

The ultramafic rocks in the UMAA are characterized by the crystallization of Cr-spinel, olivine, plagioclase, clinopyroxene and orthopyroxene as cumulus minerals, while the latter three minerals along with amphibole also occur as post-cumulus minerals. The mafic members of this association are characterized by a first crystallization of olivine, followed by a simultaneous crystallization of plagioclase, clinopyroxene and orthopyroxene. Amphibole is again either post-cumulus or secondary mineral. The gabbronorites of the MGA are characterized by the simultaneous crystallization of plagioclase, clinopyroxene and orthopyroxene more or less in cotectic proportions. These characteristics are intermediate between those of ophiolites and arc-related plutons. Whereas the early crystallization of plagioclase is a trait of the ophiolites (Basaltic Volcanism Study Project, 1981), the crystallization of pyroxenes as early as plagioclase, and in particular early crystallization of abundant orthopyroxene, is a characteristic feature of the arc-related plutons (Burns, 1985) crystallizing under moderate pressures of 5-10 kbar (Stolper, 1982).

Despite the presence of sedimentary-type structures, the Chilas complex differs from the type stratiform complexes in the preponderance of isotropic gabbronorites. Such rocks, however, may form in magma chambers undergoing continuous but slow convection (cf., Irvine, 1980), in magmas that are highly viscous or where there is turbulance in the magma chamber.

The mafic-ultramafic complexes with partly or wholly stratiform nature occur in diverse tectonic settings including intra-continental (e.g., Bushveld, Stillwater, Skaergaard), continental margin (Fongen-Hyllingen complex, Norway: Thy Esbensen, 1982), oceanic ophiolites (e.g., Bay of Islands: Komer et al., 1984), and island arcs (e.g., Grenada: Arculus & Wills, 1980). Most geoscientists working in Kohistan agree on the intra-oceanic nature of the Kohistan island arc and a majority of them considers the Chilas compex to be emplaced as a subduction-related magmatic body in the oceanic basement or in the lower parts of a volcanic arc crust (Tahirkheli et al., 1979; Bard et al., 1980; Bard, 1983a, b; Coward et al., 1982, 1986, 1987). Khan et al. (1989) drew attention towards the thermal problems in the generation and emplacement of such a large volume of magma as the Chilas complex, and suggested that the rise of a diapir in an intra-arc rift or back arc basin environment may be the most appropriate explanation. A different view is held by Chaudhry et al. (1984) and Ghazanfar et al. (1991). They consider the Chilas complex as an ophiolite body, tectonically emplaced between two other ophiolites, one to the north comprising the Chalt metavolcanics and the other to the south comprising the Kamila amphibolites, greenstones and the Jijal complex. These authors, for unknown reasons, consider only the diorites, granodiorites and granites as arc-related.

Mafic-ultamafic complexes similar to Chilas can occur within the lower parts of the oceanic crust, directly beneath the mid-oceanic ridges, but an essential feature of such magma chambers is the open-system fractionation. These magma chambers are continuously tapped by basalt extrusion along the mid-oceanic ridge, and simultaneous replenishment by fresh batches of magma from the underlying mantle. This results in cyclic repetition of fractionated sequences within the magma chambers (cf. Thy, 1987). Fractional crystallization under cumulate processes gives rise to a layered sequence comprising ultramafic rocks at the bottom followed by fractionated rocks like gabbro at the top. However, before all the magma is consumed in crystallization, a new pulse of basaltic magma replenishes the fractionated magma with a primitive composition wich starts crystallizing ultramafic cumulates on top of the fractionated gabbros.The frequency of this cyclic repetition depends upon the spreading rate; the fast-spreading ridges are underlain by larger bodies with greater number of cyclically repeated successions and vice versa (Sleep, 1975). The Chilas complexes has local cyclically repeated graded layers; however, cyclic repetition of layered successions is absent. Even if the UMAA bodies represent later pulses of magma emplaced on the floor of the then crystallizaing main Chilas magma chamber (Khan et al., 1985), they are too infrequent to be related to a spreading centre at the site of a mild-ocean ridge.

Subduction-related intrusives in island arcs or continental margins have a characteristic composite nature. The Kohistan batholith (Petterson & Windley, 1985) is a nice example. Hundreds of plutonic bodies, varying in composition from gabbro to granite, intrude the Kohistan crust, often cross cutting each other. Unlike the composite Kohistan batholith, the main trait of the Chilas complex is its coherent nature depicting crystallization in a single or a few contiguous magma chambers.

Jan & Kempe (1973), Jan (1977, 1980), Bard et al. (1980) and Bard (198a, b) postulated a subduction-related origin for the Chilas complex. Keeping in mind the heat problem in producing such a large amount of mafic magma, Khan et al. (1989) proposed that it may be related to a mantle diapir. Tatsumi et al. (1983) have experimentally determined the temperature of segregation of island-arc basalts in mantle, which is > 1300°C. This temperature is too high for a stable mantle geotherm, and can be satisfied only by invoking a mantle diapir. Mantle diapirs, however, would superimpose extensional environments over subduction-related environments. Hamilton (1989) has repeatedly pointed out the prevalence of extensional tectonics in island arcs. Initial stages of intra or back-arc spreading is the most suitable environment where extensive magmatism may generate with subduction-related signature. It is suggested that the Chilas complex crystallized from a magma generated in the late stages of island arc growth in Kohistan (prior to collision with Karakoram and the intrusion of the Kohistan batholith some 100 Ma ago), probably in the initial stages of an intra- or back-arc rifting event. Khan et al. (1989) have already demonstrated the calc-alkaline nature of the Chilas complex on the basis of trace- and rare-earth element data, suggesting an affinity with mature stages in arc growth.

ACKNOWLEDGEMENTS

Several people have contributed to this paper either through field assistance or discussions. M. P. Coward, R.J. Knipe, R. Butler, P. J. Treloar, B.F. Windley, P. Le Fort, F. Debon, and I.A. Abassi visited the authors in the field and provided useful guidance. B.F. Windley provided some of the field photographs presented here. Discussions with B.F. Windley, J. Tarney, K. Brodie, and M. Petterson were extemely informative. Recent field work in parts of the Chilas complex has been done in the company of Mr. Tehseenullah Khan, Ahmed Khan and Sufian Qazi. NCE in Geology, University of Peshawar, and NSRDB Research Project No. Esc. 24 paid the expenses for field work.

REFERENCES

BARD, J.P. (1983a) Metamorphism of an obducted island arc: example of the Kohistan sequence (Pakistan) in the Himalayan collided range. Earth Planet. Sci. Lett. **65**, pp. 133-144.

———, (1983b) Metamorphic evolution of an obducted island arc: Example of the Kohistan sequence (Pakistan) in the Himalayan collided range. Geol. Bull. Univ. Peshawar **16**, pp. 105-184.

BARD. P., MALUSKI, H., MATTE, P. & PROUST, F. (1980) The Kohistan sequence: crust and mantle of an obducted island arc. Geol. Bull. Univ. Peshawar., (Special Issue) **13**, pp. 87-93.

BASALT VOLCANISM STUDY PROJECT (1981) BASALTIC VOLCANISM ON THE TERRESTRIAL PLANETS. Pergamon Press Inc., New York. 1286 p.

BURNS, L.E. (1985) The Border Ranges ultramafic and mafic complex, south-central Alaska: Cumulate fractionates of island arc volcanics. Can. J. Earth Sci. **22**, pp.1020-1038.

CHAUDHARY, M.N., GHZANFAR, M. & ASHRAF, M. (1984) A plate tectonic model for NW Himalaya. Kashmir Journal of Geology **1**, pp. 109-112.

——— **& CHAUDHRY, A.G.** (1974) Geology of the Khagram area, Dir district. Geol. Bull. Punjab Univ. **11**, pp. 21-43.

———, **KAUSER, A.B., & LODHI, S.A.K.** (1974) Geology of Timurgara-Lal Qila area, Dir district N.W.F.P. Geol. Bull. Punjab Univ. **11**, pp.21-43.

COWARD, M.P., JAN, M.Q., REX, D., TARNEY, J., THIRLWALL, M. & WINDLEY, B.F. (1982) Geotectonic framework of the Himalaya of N. Pakistan. Journ. Geol. Soc. London **139**, pp. 299-308.

———, **WINDLEY, B.F., BROUGHTON, R.D., LUFF, I.W., PETTERSON, M.G., PUDSEY, C.J., REX, D.C. & KHAN, M.A.** (1986) Collision tectonics in the NW Himalaya. *In:* Coward, M.P. & Ries, A. (eds.) Geol. Soc. London Special Publ. **19**, pp. 203-219.

——— **BUTLER, R.W.H., KHAN, M.A., & KNIPE, R.J.** (1987) The tectonic history of Kohistan and its implications for Himalayan structure. Jour. Geol. Soc. London **144**, pp. 377-391.

DESIO, A. (1974) Geological reconnaissance in the middle Indus valley between Chilas and Besham Qila (Pakistan). Boll. Soc. Geol. Italy **93**, pp. 345-368.

GHAZANFAR, M., CHAUDHRY, M.N. & HUSSAIN, M.S. (1991) Geology and petrotectonics of Southwest Kohistan, Northwest Himalaya, Pakistan, Kashmir Journal of Geology **8 & 9**, pp. 67-98.

HAMIDULLAH, S. & JAN, M.Q. (1986) Petrochemical study of the Chilas Complex, Kohistan island arc, northern Pakistan. Geol. Bull. Univ. Peshawar **19**, pp. 157-182.

HAMILTON. W. (1989) Convergent plate tectonics viewed from the Indonesian region. *In:* Sengör, A.M.C. (ed.). TECTONIC EVOLUTION OF THE TETHYAN REGION. Kluwer Publishers, Dordrecht, Netherlands. pp. 655-698.

HUNTER, D. (1978) The Bushveld complex and its remarkable rocks. Amer. Scient. **66**, pp.551-559.

IRVINE, T.N. (1965) Sedimentary structures in the igneous intrusions with particular reference to the Duke Island ultramafic complex. *In:* Middletion, G.V. (ed.) PRIMARY SEDIMENTARY STRUCTURES AND THEIR HYDRODYNAMIC INTERPRETATION. Society of Economic Paleontologists & Mineralogists Spec. Publ. **12**, pp. 220-232.

——— (1980) Magmatic density currents and cumulus processes. Am. Jour. Sci. **280-A**, pp. 1-58.

———, (1982) Terminology for layered intrusions. J. Petrol. **23**, pp.127-162.

JAN, M.Q. (1979) Petrography of pyroxene granulites from northern Swat and Kohistan. Geol. Bull. Univ. Peshawar **11**, pp. 65-87.

——— (1977) The mineralogy, geochemistry, and petrology of Swat, Kohistan, NW Pakistan. Ph. D. thesis, Univeristy of London (Unpublished).

——— (1969) Petrography of the upper part of Kohistan and southwestern Gilgit Agency along the Indus and Kandia rivers. Geol. Bull. Univ. Peshawar **5**, pp. 27-48.

——— (1980) Petrology of the obducted mafic and ultramafic metamorphites from the southern part of the Kohistan island arc sequence. Geol. Bull. Univ. Peshawar **13**, pp. 95-108.

———, **KEMPE, D.R.C. & TAHIRKHELI, R.A.K.** (1969) The geology of the corundum-bearing and related rocks around Timurgara, Dir. Geol. Bull. Univ. Peshawar. **4**, pp. 83-89.

——— **& MIAN, I.**, (1971) Preliminary geology and petrography of Swat Kohistan. Geol. Bul. Univ. Peshawar **6**, pp. 1-32.

——— **& KEMPE, D.R.C.** (1973) The Petrology of the basic and intermediate rocks of Upper Swat, NW Pakistan. Geol. Mag. **110**, pp. 285-300.

——— **& HOWIE, R.A.** (1980) Ortho- and clinopyroxene from pyroxene granulites of Swat Kohistan, northern Pakistan. Mineral. Mag. **43**, pp. **715-728.**

———, **BANARAS, M., GHANI, A. & ASIF, M.** (1983) The Tora-Tigga ultramafic complex, southern Dir district. Geol. Bull. Univ. Peshawar **16**, pp. 11-29.

———, **KHATTAK, M.U.K., PARVEZ, M.K., & WINDLEY, B.F.** (1984b) The Chilas stratiform complex: field and mineralogical aspects. Geol. Bull. Univ. Peshawar. **17**, pp. 153-169.

———, **PARVEZ, M.K., & KHATTAK, M.U.K.** (1984a) Coronites from the Chilas and Jijal-Pattan complexes of Kohistan. Geol. Bull. Univ. Peshawar **17**, pp. 75-85.

JAMES, O.B. (1971) Origin and emplacement of the ultramafic rocks of the Emigrant Gap area, California. J. Petrol. **12**, pp. 523-560.

KHAN, M.A. (1988) Petrology and structure of the Chilas mafic-ultramafic complex, Kohistan, NW Himalayas, Pakistan. Ph.D. thesis, Imperial College of Science, Technology, and Medicine, University of London. (Unpublished).

———**, HABIB , M. & JAN, M.Q.** (1985). Ultramafic and mafic rocks of Thurly Gah and their relationship to the Chilas Complex, N. Pakistan. Geol. Bull. Univ. Peshawar **18**, pp. 83-102.

———**, JAN, M.Q., WINDLEY, B.F., TARNEY, J. & THIRLWALL, M.** (1989) The Chilas mafic-ultramafic igneous complex; the root of the Kohistan island arc in the Himalaya of northern Pakistan. Geol. Soc. America. Special Paper **232**, pp. 75-94.

——— **& COWARD, M.P.** (1990) Entrapment of an island arc in collision tectonics: A review of the structural history of the Kohistan arc complex, N.W. Himalayas. Phys. Chem. Earth. **17**, pp. 1-18.

KOMOR, S.C., ELTHON, D. & CASEY, J.F. (1985) Mineralogical variations in a layered ultramfic cumulate sequence at the North Arm Mountain massif of the Bay of Islands ophiolite, Newfoundland. J. Geophys. Res. **90**, pp. 7705-7736.

MARTIN, N.R., SIDDIQUI, S.F. & KING, B.H. (1962) A geological reconnaissance of the region between the lower Swat and Indus rivers of Pakistan. Geol. Bull. Punjab Univ. **2**, pp. 1-13.

McCALLUM, I.S., RAEDEKE, L.D. & MATHEZ, E.A. (1980) Investigation of the Stillwater complex: Part 1. Stratigraphy and structure of the banded zone. Am. J. Sci. **280-A**, pp. 487-554.

MISCH, P. (1949) Metasomatic granitization of batholithic dimensions. Am. J. Sci. **249**, pp. 209-245.

MOORE, A.C. (1978) Studies of igneous and tectonic textures and layering in the rocks of the Gosse Pile Intrusion, Cental Australia. J. Petrol. **14**, pp. **49-79.**

PETTERSON, M.G. & WINDLEY, B.F. (1985) Rb-Sr dating of the Kohistan arc-batholith in the Trans-Himalaya of north Pakistan, and tectonic implications. Earth Planet. Sci. Lett.**74**, pp. 45-57.

SHAMS, F.A. (1975) The petrology of the Thak Valley igneous complex, Gilgit Agency, Northern Pakistan. Acad. Nazionale Dei Lincei,Series V111. V.LIX. pp. 453-464.

SLEEP, N.H. (1975) Formation of oceanic crust, some thermal constraints. J. Geophys. Res. **80**, pp. 4037-4042.

STOLPER, E. (1980) A phase diagram for mid-oceanic ridge basalts: preliminary results and implications for petrogenesis. Contrib. Mineral. Petrol. **74**, p. 13-27.

STRECKEISEN, A. (1976) To each plutonic rock its proper name. Earth Planet. Sci. Review **12**, pp. 1-33.

TAHIRKHELI, R.A.K., MATTAURE, M., PROUST, F. & TAPPONNIER, P. (1979) The India-Eurasia suture zone in northern Pakistan: Synthesis and interpretation of data at plate scale. *In:* Farah, A. & De Jong, K.A. (eds.) GEODYNAMICS OF PAKISTAN. Geological Survey of Pakistan, Quetta, pp. 125-130.

TATSUMI, Y., SAKUYAMA, M., FUKUYAMA, .H. & KUSHIRO, I. (1983) Generation of arc basalt magmas and thermal structure of the mantle wedge in subduction zones. J. Geophys. Res. **88**, pp. 5815-5825.

THY, P. (1987) Magmas and magma chamber evolution, Troodos Ophiolite, Cyprus. Geology **15**, pp. 316-319.

——— **& ESBENSEN, K.H.** (1982) Origin of certain types of small-scale igneous layering from the Fongen-Hyllingen basic complex, Norway. Geologiska Foreningens i Stockholm Forhandlinger **104**, pp.33-42.

TRELOAR, P.J., BRODIE, K.H., COWARD, M.P., JAN, M.Q., KHAN, M.A., KNIPE, R.J., REX , D.C. & WILLIAMS, M.P. (1990) The evolution of the Kamila shear zone, Kohistan, Pakistan. *In*: Salisbury, M.H. & Fountain, D.M. (eds.) EXPOSED CROSS-SECTIONS OF THE CONTINENTAL CRUST. pp. 175-214.

WADIA, D.N. (1932) Notes on the geology of Nanga Parbat (Mt. Diamir) and adjoining portions of Chilas, Gilgit District, Kashmir. Rec. Geol. Surv. India. **66**, pp. 212-234.

WADSWORTH. W.J. (1973) Magmatic sediments. Minerals Science Engineering. **5**, pp. 26-35.

WAGER, L.R. & BROWN, G.M. (1968) LAYERED IGNEOUS ROCKS. Oliver & Boyd, Edinburgh.

Manuscript received on November 11, 1992; accepted for publication on December 12, 1992.

ACTA MINERALOGICA PAKISTANICA
VOLUME 6 (1992) PP. 149-158.

"UPWARD–CONTINUATION" FILTERING OF THE UTHAL GRAVITY DATA

NAYYER ALAM ZAIGHAM
Geological Survey of Pakistan, R–42, Block 6, PECHS, Karachi.
&
KHALIL A. MALLICK

Geological Survey of Pakistan, R–42, Block 6, PECHS, Karachi.

ABSTRACT: The southern mountainous part of the "Axial Belt" of Pakistan is enigmatic. In the triangular Bela Plain, the southward extension of the Bela ophiolite complex and other trends of the geologic features are obscure and create an apparent discontinuation of the geologic relationships between the land and the sea. The gravity investigation has been carried out to interpret the subsurface geological conditions in the area. The application of the "Upward-Continuation" filtering of the gravity data provides the valuable subsurface information in relation to the lateral and the vertical continuations of the ophiolite zone and the associated geologic structures. The upward-continuation maps show that the exposed part of the Bela ophiolites is about 1 km thick which has been shearedoff from the southern buried part as broken sheet and thrusted up in NW direction. The southern buried part of this zone is massive which extends laterally southward into the Arabian Sea and vertically upto a considerable depth.

INTRODUCTION

The largest exposures of the ophiolites occur in between the Khuzdar and Uthal towns of Balochistan Province, known as "Bela Ophiolites" in the southernmost part of the "Axial Belt" of Pakistan. Towards south, they disappear under the Quaternary Neogene sediments in the Bela Plain creating an enigmatic condition of geologic features between the land and the sea.

To study the subsurface geological environments, about 700 gravity observations have been made in the Uthal area covering 4000 sq. km from latitude 25° 15' to 26° 15' N and longitude 66° 30' to 67°E (Fig. 1). The gravity observations are made by using Worden gravity meters along paths and stream beds accessible by the four-wheel drive vehicles at an interval of about 1.6 km. In the areas of difficult accessibility, the observation stations are reached on foot.

In order to study the vertical continuation of the ophiolite zone with respect to the successive increase in depth, the "Upward-Continuation" filtering is applied to the gravity map data of the Uthal-Sonmiani area. The filtering process is completed at the Computer Centre of the Geophysics Department, Colorado School of Mines, Golden USA. This paper describes the results of the filtering and the interpreted resultant pictures of the subsurface structural trends of the southern part of the "Axial-Belt".

GEOLOGICAL SETTING

Tectonically, the area is delineated by the Ornach-Nal-Chaman fault system(s) in the west and the north, and by the Kirthar fold-thrust mountainous belt and the Indus Basin in the east. In the SE, it is bounded by the Karachi-Hyderabad Arch of gently folded Tertiary rocks, and in the south by the Arabian Sea which consists of exotic submarine features, like the Murray Ridge and the Owen Fracture Zone.

The major stratigraphic units exposed

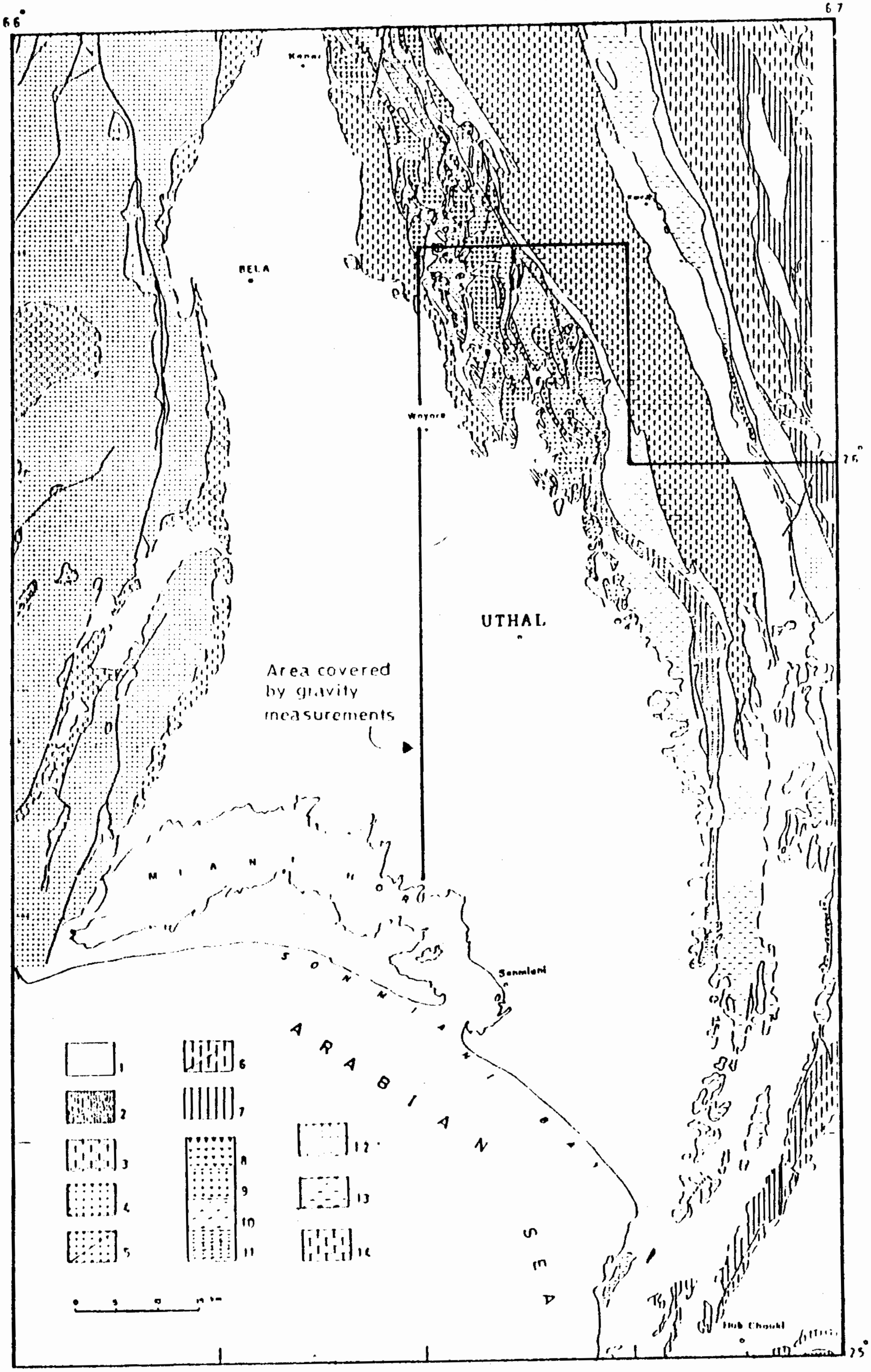

Fig. 1. Geological map of Bela region. Inside frame shows the area covered by gravity measurements. 1: Alluvium, 2: Extrusive mud (Holocene), 3: Haro Conglomerate (Pleistocene), 4: Hinglaj Group (Pliocene), 5: Parkini/Gaj Formation (Miocene), 6: Nari Formation (Oligocene), 7: Jakker Group (Eocene), 8: Volcanics, 9: Gabbros, 10: Ultramafics, 11: Mélange, 12: Pab Sandstone (Cretaceous), 13: Sembar Formation (Cretaceous), 14: Shirinab Formation (Jurassic). [Compiled from Hunting Survey Corporation Ltd., 1960; Bakr & Jackson, 1964; Shah, 1977; Sarwar & De Jong, 1984; Fariduddin & Pasha, 1988].

in the area are of Jurassic to Quaternary age (Fig. 1). The Bela Ophiolite complexes emplaced during Paleocene-Eocene (Allemann, 1979; Sarwar & De Jong, 1984), are exposed only in the northern part of the study area and have contact with the Neogene flysch sediments in the west. The remaining western side of the ophiolite zone extending towards south is covered under the Quaternary sediments. The eastern margin of the ophiolite zone has tectonic contacts with the Mesozoic rocks (De Jong & Subhani, 1979).

THE GRAVITY MAP

Fig. 2 shows the Bouguer gravity map of the Uthal area of Balochistan, and Fig.3 shows the residual gravity map after having filtered out the polynomial surface of second order, superimposed on the geological map of the area.

The predominent trend on the Bouguer gravity map is the elongated N-S trending gravity high anomaly bounded by the steep gradients on the east and the west sides extending southward into the Arabian Sea and plunging out northward. This map also shows the superimposition of the anomalies of noticeably different orders and sizes. The composite map (Fig. 3) shows that the relatively smaller anomalies in the NW corner are associated with the ophiolite units; otherwise, most of the anomalies are found in the area covered by the alluvium from the coast of the Arabian Sea to the north of Uthal town indicating the possible subsurface continuation of the Bela ophiolite complexes (Zaigham, 1991).

"UPWARD-CONTINUATION" FILTERING

The "Upward-continuation" of the potential field data has been used to investigate the perspective concerning the large regional sources beneath the study area. In "upward continuation" the gravity data measured on one surface, is transformed to some higher surface using a simple filter operation. The Fourier transform of a function on level z is obtained by multiplying the transform of a function on level z=0 by e^{2zw} . In general, the transform on level z_1 is converted to the transform on level z_2 by multiplying by $e^{2w\,(z2-z1)}$. The "Upward-Continuation" filter tends to smooth the original data by attenuation of short-wavelength anomalies relative to their longer-wavelength counterparts.

The upward continuation filtering technique is applied on the gravity data of Uthal area for different higher surfaces to study the behaviour of the deep-seated regional structures. Fig.4 shows the results of applying an "upward-continuation" filter for the levels of 1, 2.5, 5, and 10 km. Likewise Fig. 5 shows results for further higher levels of 20, 25, 35 and 40 km.

The comparative study of different "upward-continued" levels indicates that relatively short-wavelength anomalies do exist approximately upto a depth of 1 km. These short-wavelength anomalies superimpose upon an elongated, almost N-S striking high density regional structural feature, most probably due to the presence of the buried obducted sequence of the ophiolites. The N-S striking high density regional structural feature has been filtered out on 2.5 and 4 km "upward-continued" levels. At 10 km continued-level, this gravity structural high plunges out just north of Uthal, but it continues from Uthal town in the south extending into the Arabian Sea as indicated by the presence of partial gravity anomaly which appears to continue further south of the study area. The continued-transformed levels upto 20 and 25 km indicate that the high density structural features do exist approximately upto 25 km. The "upward-continued" levels at 35 and 40 km seem to represent the possible continuation of gravity gradient due to the density contrast at that depth.

Fig. 6 shows comparative study based on the longitudinal profiles taken from different levels of "Upward-Continuations." In general, it is significant that the higher density crust, which appears to be oceanic, dominates in the south but vanishes in the north with respect to the depth.

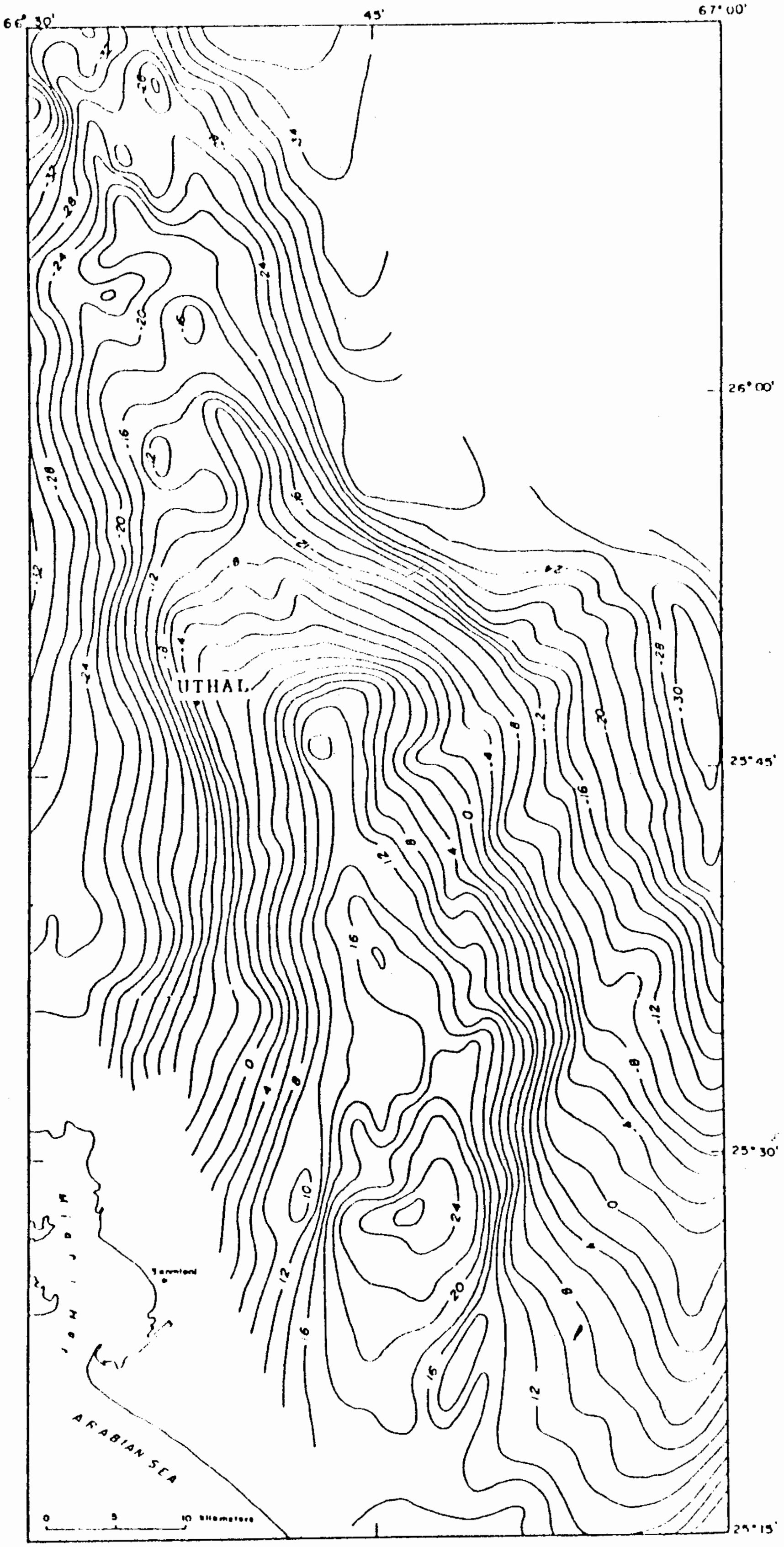

Fig.2. Bouguer gravity anomaly map of southern Bela ophiolite zone. Contour interval is 2 mGal.

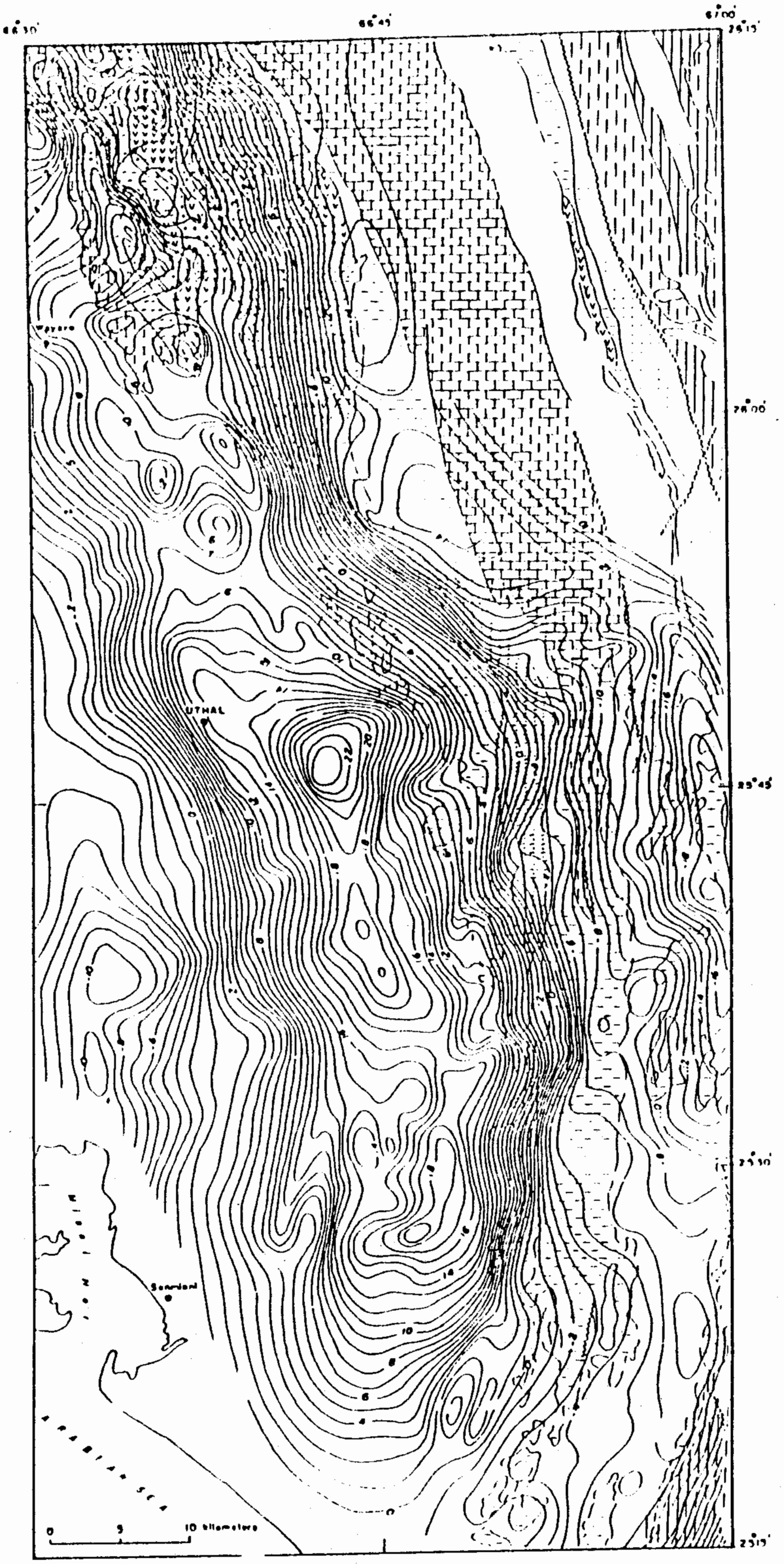

Fig. 3. Overlay of residual gravity anomalies over the geological map of souther Bela Ophiolite Zone which shows the subsurface continuation of the ophiolites. A, B & C: anomalies of probable subsurface ophilite zone.

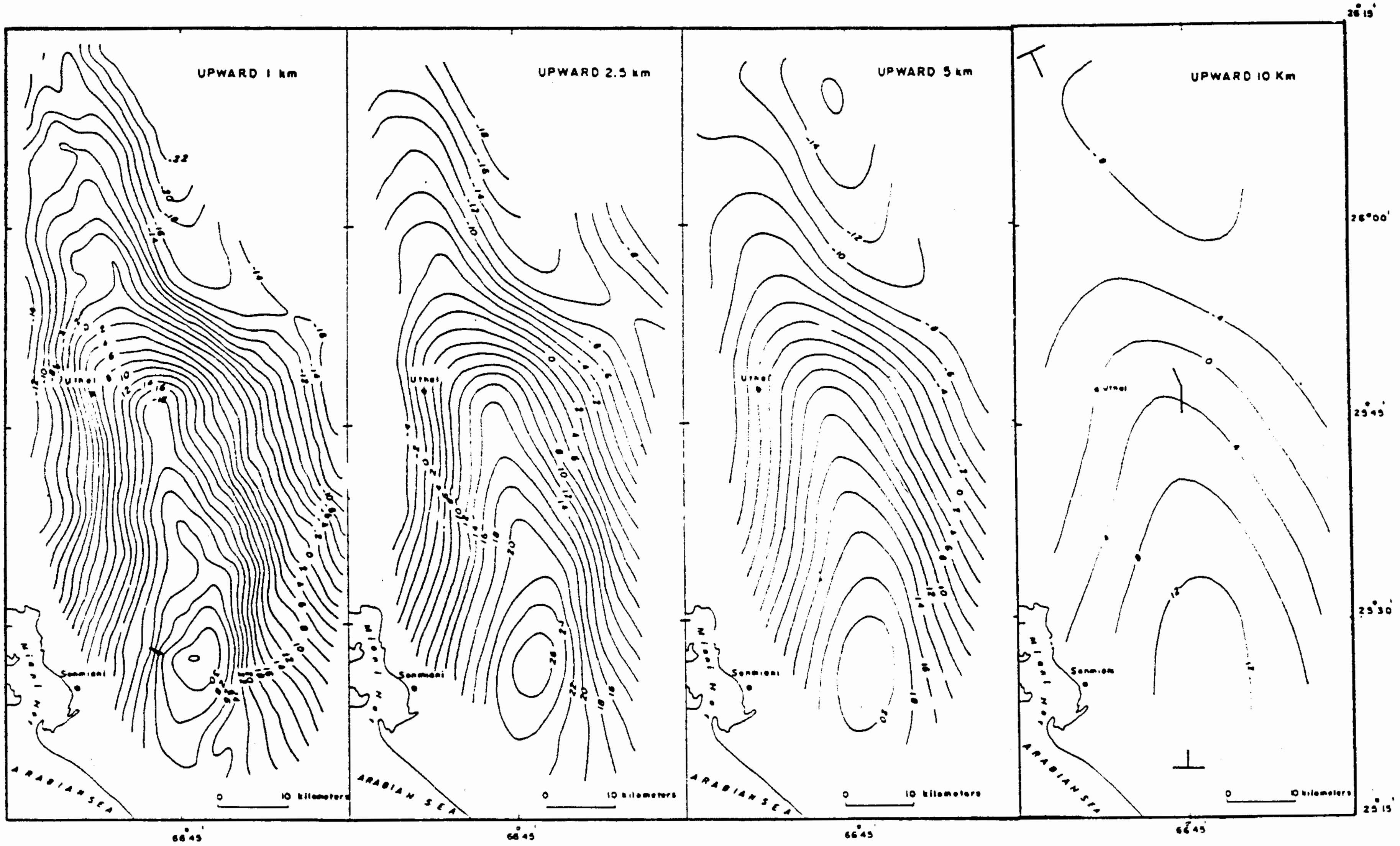

Fig. 4. Maps showing results of applyign "upward-continuation" filter to the Bela Bouguer gravity map data for the levels at 1, 2.5, 5 and 10 km.

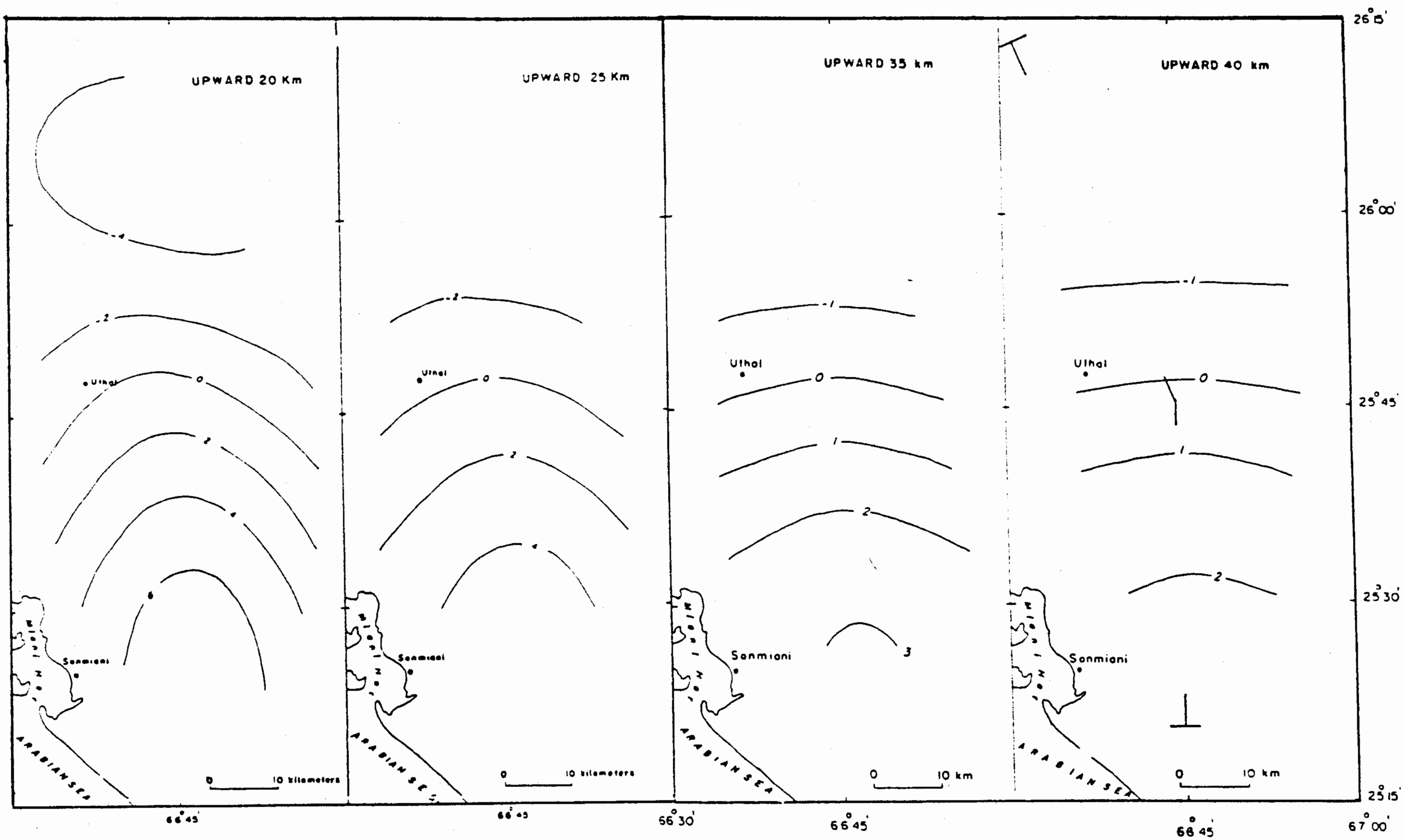

Fig. 5. Maps showing results of applying upward-continuation filter to the Bela Bouguer gravity map data for the levels at 20, 25, 35 and 40 km.

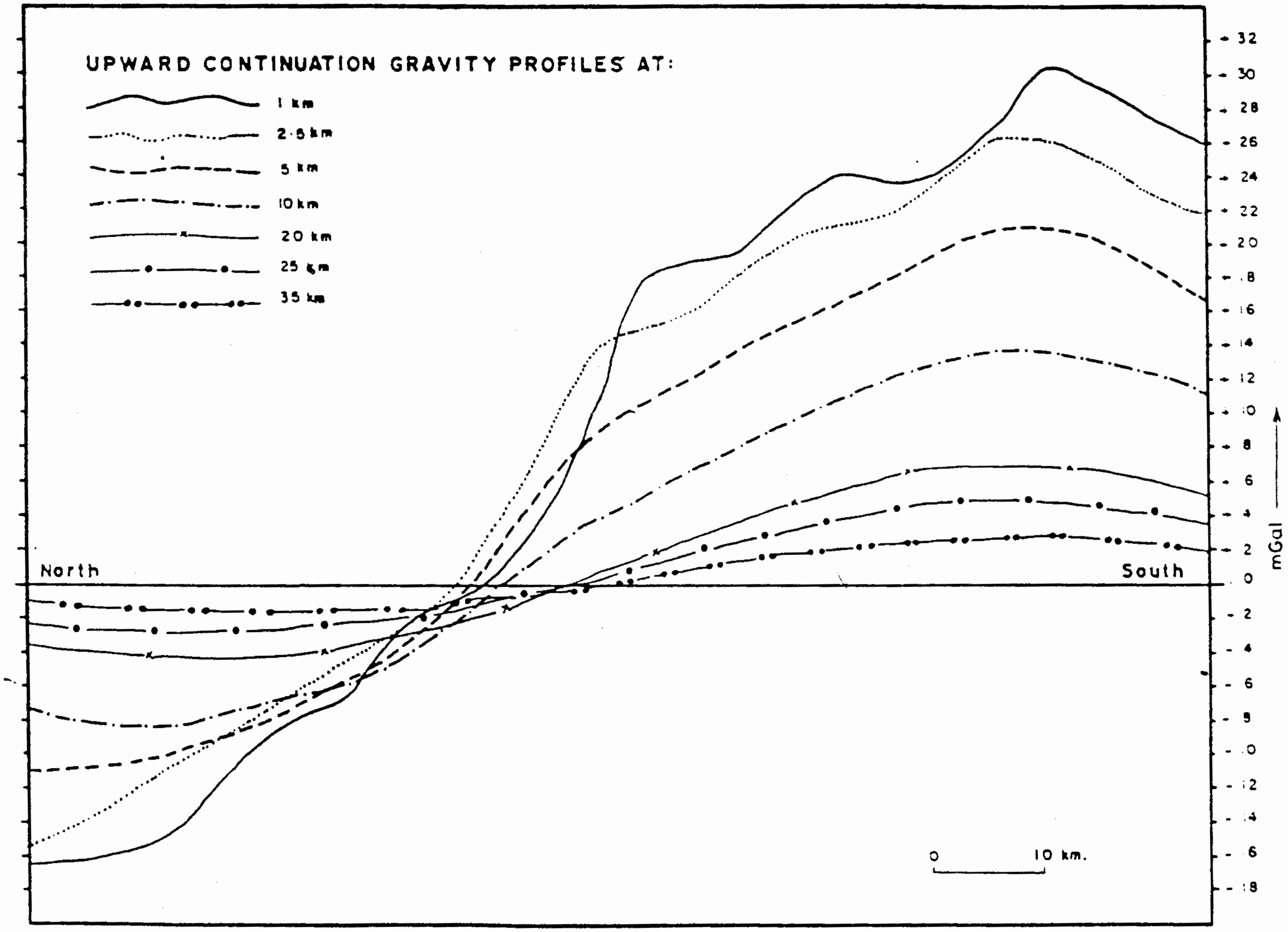

Fig. 6. Comparative study of "upward-continuation" gravity profiles at different levels derived from Figs. 4 & 5.

A prominent zone of gravity gradient is observable on profile at 1 km and onward upto profile at 10 km "Upward-Continued level". This gravity gradient appears to be associated with the zone of decollement along which the exposed part of the Bela ophiolites have been thrusted up with the older Mesozoic sediments along a ramp-like thrust plane (Berger & Johnson, 1980; Zaigham, 1991) in the NW part of the study area. From the qualitative analysis of the "Upward-continuation" gravity profiles, it is inferred that the obducted Bela ophiolites in the northern part of the study area are only restricted to shallow depths, ranging from surface to a depth of approximately 1km, whereas the relatively shorter-wavelength anomalies associated with the buried ophiolite bodies, can be seen in the southern half of the profile at 2.5 km level superimposed on the deep-seated longer-wevelength anomalies.

CONCLUSION

The "Upward-Continuation" filtering indicates that the exposed zone of the Bela ophiolites has a finite thickness. It is about 1 km thick. This zone has been sheared off from its originally emplaced main zone under the intense deformational process and thrusted up north-westward alongwith mélange(s) and metamorphic suit along NW-SE striking ramp-type structure just north of Uthal town.

In the south of Uthal town, massive and thick part of the ophiolite zone continues subsurface upto the coast and appears to extend further into the Arabian Sea.

Based on the conspicuous trend of the elongated gravity high anomaly upto the "Upward-Continued-Level" at 25 km, it appears that this zone of high density materials exists vertically upto considerable depth and belongs to the upper crustal features.

ACKNOWLEDGEMENTS

The permission granted by the Director General, Geological Survey of Pakistan, to avail the departmental facilities and to publish the work is gratefully acknowledged. The authors wish to express many thanks to Mr. Anwaruddin Ahmad, Chief Geophysicist, GSP, for the review of the manuscript. The help, guidance and cooperation of Dr. Richard O. Hansen, Research Professor of Geophysics, Colorado School of Mines, during the filtering & analysis of the gravity data at the Computer Center of the School, is acknowledged.

REFERENCES

ALLEMANN, F. (1979) Time of emplacement of the Zhob valley ophiolites and Bela ophiolites. *In*: Farah, A. & De Jong, K.A. (eds.) GEODYNAMICS OF PAKISTAN, Geol. Surv. Pakistan, Quetta, pp. 213-242.

BAKR, A. & JACKSON, R.O. (1964) Geological map of Pakistan, Scale 1:2,000,000. Geological Survey of Pakistan, Quetta.

BERGER, P. & JOHNSON, A.M. (1980) First-order analysis of deformation of a thrust sheet moving over a ramp: Tectonophys. **70**, pp. T 9-T24.

DE JONG, K.A. & SUBHANI, A.M. (1979) Note on the Bela ophiolites with special reference to the Kanar area. *In*: Farah,A. & DeJong, K.A. (eds.) GEODYNAMICS OF PAKISTAN, PP. 263-269. Geological Survey of Pakistan, Quetta.

FARIDUDDIN, G. & PASHA, M.A. (1988) Geology of Kanraj area, Lasbela district, Balochistan: Inf. Rel. Geol. Surv. Pakistan, 299 p.

HUNTING SURVEY CORPORATION LTD. (1960) RECONNAISSANCE GEOLOGY OF PART OF WEST PAKISTAN. Colombo Plan Cooperative Project, Government of Canada, Toronto, 550p.

SARWAR, G. & De JONG, K.A. (1984) Composition and origin of the Kanar mélange of southern Pakistan. Geol. Soc. Amer. Spec. Pap. **198**, pp. 127-137.

SHAH, S.H.A. (1977) STRATIGRAPHY OF PAKISTAN Geol. Surv. Pak. Mem. **12**, pp. 37-50.

ZAIGHAM, N.A. (1991) Bela Ophiolites and associated mineralization in southern part of axial-belt of Pakistan. Ph.D. dissertation Geology Department, University of Karachi, 370p (Unpublished)..

ACTA MINERALOGICA PAKISTANICA
VOLUME 6 (1992) pp. 158-160.

SHORT COMMUNICATIONS

A BURIAL HISTORY OF THE STRATA AT COVE EAST BERWICKSHIRE, SCOTLAND

GHULAM NABI
Geology Department. University of Balochistan, Quetta.

The study area is covered by a part of sheet 33 of the 1 : 50,000 geological map of Scotland and occurs at the NE end of the Southern Uplands Massif in East Berwickshire about 36km north of Berwick Upon Tweed (TN 7853 7171) (Fig. 1).

The sediments accumulated in the so-called Oldham Stocks Basin (Lagios, 1983) and the Cove sequence represents the western margin deposit of the structure. This succession is the eastern equivalent of the Cementstone and Lower Oil Shale group of the Scottish Midland Valley (Greig, 1988). The rocks are well-exposed on the shore and are classified as the Calciferous Sandstone Measures (Greig, 1971). Fig. 1 shows the principal outcrop features of the sequence. The beds dip towards the N and NW at 10° - 45° except near the Cove Fault where the dip steepens to about 70°.

To determine the burial history and constrain the effect of burial diagenesis on the studied strata a compacted burial depth versus time curve (Fig. 2) has been constructed, using the base of Heathery Heugh Sandstone as a datum. It can be observed from the curve that the maximum burial depth was probably 2000 m and that this was achieved by the end of Carboniferous time. The curve has been compiled by using various information on the thickness of the strata and estimated rates of deposition and erosion. It must be stressed that the curve can only be an order of magnitude approximation.

Thickness of the present strata is calculated during the fieldwork, while the thickness of the strata which has been

Table 1. Carboniferous strata thicknesses in East Berwickshire overlying the Kip-Carle Sandstone.

STRATA	THICKNESS	SOURCE
Heathery Heugh Sandstone.	56m	Measured during fieldwork
Series of strata from Heathery-Heugh to Cove Harbour-Sandstone.	50m	Measured during fieldwork
Cove Harbour Sandstone.	50m	Measured during fieldwork
Strata between Cove Harbour Sandstone and Bilsdean Sandstone.	50m	Measured during fieldwork
Bilsdean Sandstone.	50m	(Davies et al., 1986)
Lower Limestone Group.	26m	(Davies et al., 1986)
Limestone Coal Group.	255m	(Cameron & Stephenson, 1985)
Upper Limestone Group.	320m	(Browne et al., 1985)
Passage Group.	200m	(Cameron & Stephenson, 1985)
Lower and Middle Coal Measures	220m	(Greig, 1971).
Upper Coal Measures	800m	(Greig, 1971).

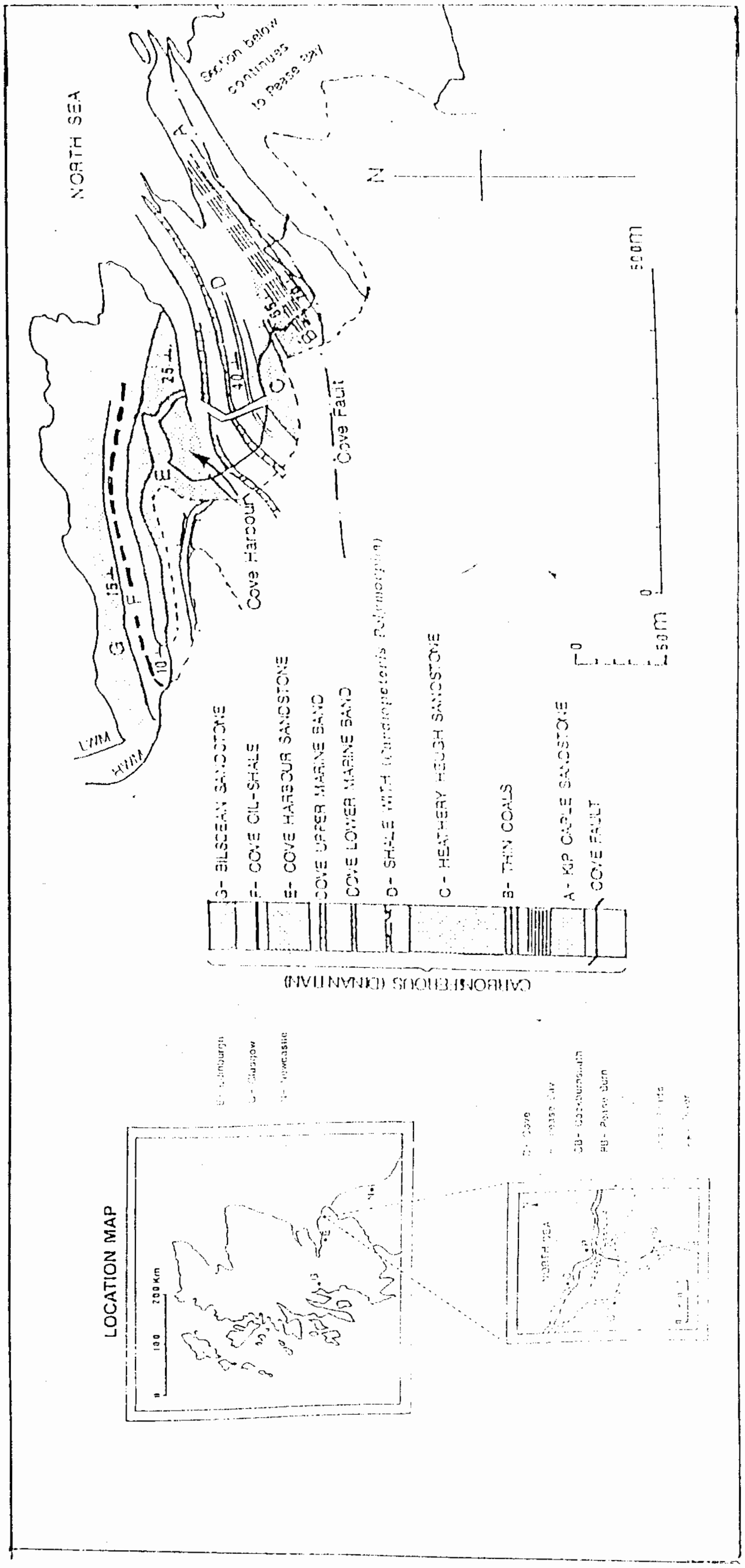

Fig. 1. Map (modified from Greig, 1971) showing outcrop features of the sequence of calciferous Sandstone Measures between Kip-carle Sandstone and Bilsdean Sandstone. Insert gives location.

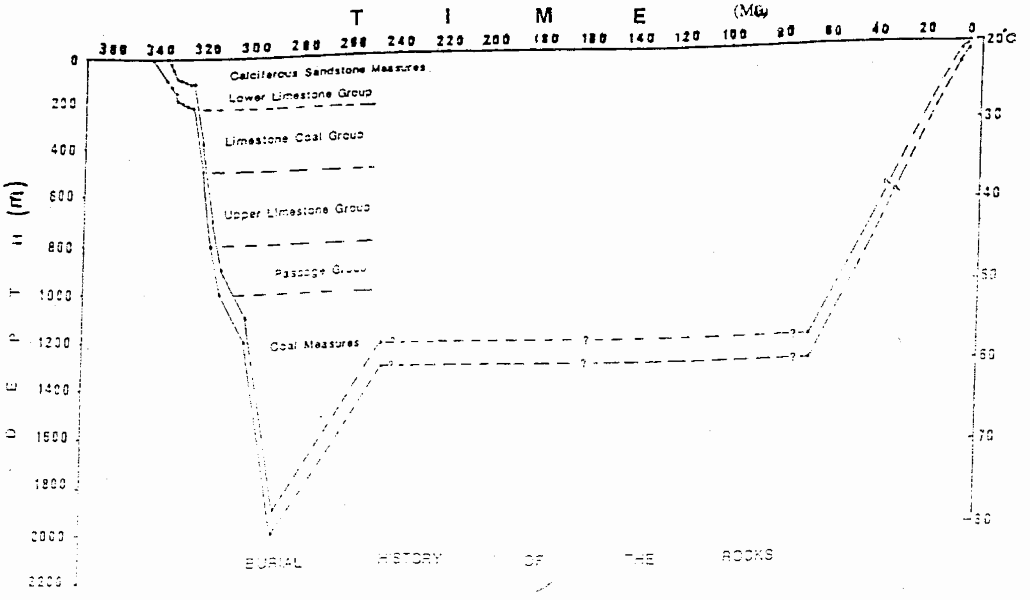

Fig. 2. Time versus depth curve showing burial history of the rocks.

removed can only be approximated using literature sources. Therefore, the thickness of the strata (Table 1) from upper Limestone Group to Coal Measures has been determined using various references.

During the Permian to Triassic the area was mostly a low-lying landmass, and it is inferred that much weathering occurred during this time. It is impossible to accurately determine the rate of erosion at this time. Paleogeographic maps (Owen, 1976) suggest that the area remained a low lying landmass through the Jurassic. Erosion rates may not have been great during this period of non-deposition (Greig, 1971). Since the Tertiary to the present was a period of further erosion and during the Pleistocene the rate of erosion probably increased due to glaciation (Anderton et al., 1979).

REFERENCES

ANDERTON, R., BRIDGES, P.H., LEEDER, M.R. AND SELLWOOD, B.W. (1979). A DYNAMIC STRATIGRAPHY OF THE BRITISH ISLES. Allen and Unwin London, **301** p.

BROENE, M.A.E., HARGREAVES, R.L. & SMITH, I.F. (1985) The Upper Palaeozoic basins of the Midland Valley of Scotland. British Geological Survey Geothermal Resource Programme, **48** p.

CAMERON, I.B. & STEPHENSON, D. (1985). BRITISH REGIONAL GEOLOGY, THE MIDLAND VALLEY OF SCOTLAND, H.M.S.O., London, **172** p.

DAVIES, A., MACADAM, A.D. & CAMERON, I.B. (1986). Geology of the Dunbar district. Mem. British Geol. Surv. (Scotland Sheets **33E** & **41**), 69 p.

GREIG, D.C. (1971), British regional geology, the south of Scotland. Institute of Geological Science Special Report, 125 p.

——— **(1988)** Geology of the Eyemouth district. Mem. British Geol. Surv. (Scotland Sheet No. **34**), 78 p.

LAGIOS, E. (1983). A gravity study of the Eastern Berwickshire basins, S.E. Scotland Scot. Jour. Geol. **19**, pp. 189-203.

OWN, T.R. (1976) THE GEOLOGICAL EVOLUTION OF THE BRITISH ISLES. Pergamon Press, Oxford, 161 p.

Manuscript received on October 12, 1992; accepted for fublication on October 14, 1992.

ACTA MINERALOGICA PAKISTANICA
VOLUME 6 (1992) pp. 161-163.

A NOTE ON THE USE OF NEPHELINE SYENITE FROM N.W.F.P., PAKISTAN

ABDUR RAUF NIZAMI, FAYAZ UR REHMAN
& IZHAR UL HAQ KHAN
Pakistan Council of Scientific & Industrial Research,
Laboratories Complex, Ferozepur Road, Lahore, Pakistan.

Nepheline syenite of the Swat area has been reviewed for the purpose of its use in industries. Some practical suggestions are forwarded regarding nepheline syenite-based industries.

Nepheline syenite is mined for its industrial use (Ashraf et al., 1987; Khan et al., 1987; Naqvi et al., 1987). It contains nepheline as its major component alongwith other feldspathoids such as cancrinite and sodalite. The use of this rock as a raw material in glass, ceramics and continuous steel casting has been studied by PCSIR Laboratories Complex, Lahore, (PCSIR Lahore, 1988).

The occurrence of nepheline syenite has been reported from Swat, NWFP, Pakistan; and studied in detail by many workers (Siddiqui, 1965; Siddiqui et al., 1968; Kempe & Jan, 1970; Kempe, 1973; E.C.L., 1979; Kempe, 1983; Chaudhry et al., 1984; Ashraf et al., 1987; Khan et al., 1987a, b; Naqvi et al., PCSIR Lahore, 1988).

Nepheline syenite was first reported from Swat District by Siddiqui (1965). The occurrence was previously correlated with the Shewa Formation, comprising albite-porphyries of Martin et al. (1962). Nepheline syenite and associated alkaline rocks are also known from certain other areas, i.e., Loe Shilman, Warsak, Malakand, Shewa, Koga and Tarbela (Kempe, 1973). A preliminary study of nepheline syenite of southern Swat regarding its industrial use in glass and ceramics was conducted by E.C.L . (1979) Petrography of nepheline syenite and associated rocks of Koga area was given by Chaudhry et al. (1984). The mineralogy and geochemistry of these rocks alongwith the other alkaline rocks of the area was investigated by Ashraf et al. (1987a, b) and Khan et al. (1987). The bene-ficiation and pilot plant studies of the same rocks were carried out by Khan et. al., (1987). The utilization of nepheline syenite of the Koga area in glass and ceramics were examined by Naqvi et al. (1987). A report on the neheline syenite of Koga Swat (NWFP) was published by PCSIR, Lahore (1988) pertaining to its evaluation and beneficiation for local industrial use. Potential reserves of nepheline syenite from the Koga area are 6000 million tons (Ashraf et. al., 1987).

Koga is situated in the Swat District. It is a small village of Chamla valley, Bunair area (latitude 34° 23' N and longitude 70° 32' E). The area can be approached through either of the two regular bus routes : one from Mardan via Rustam (total distance about 56 km); and the other from Mangora via Karar Kandao and Daggar (total distance about 90 km). Another way to reach the area is from Swabi via Chingalai by a jeepable road.

The Koga syenite occupies a roughly oval to elliptical form with irregular outline. Its outcrop forms a horse shoe shape open to the NE. The headward erosion of the tributaries of the Chamla river has eroded the NE part of the Koga nepheline syenite except for a small hill called Bibi Dherai. The Koga nepheline syenite lies in the central part of the alkaline complex, and is spread over Koga. Naranji Kandao, Miane Kandao and Sura areas. However, in places this rock has intruded the host Babaji syenite as dykes. The colour of the fresh surface of these rocks is whitish grey to light grey with black specks of mafics while the weathered surfaces of these rocks are generally grey, rusty grey or dark grey. The rock is affected by typical granitoidal weathering and extensive jointing. The rocks has also been intruded by many nepheline-bearing or nepheline-free microcline peg-matites. The rocks, rich in nepheline are exposed at Landi Pataô Sar, south of the villages of Agarai and Miane Kandao. At Kharkhal and Bagoch Sar the rock is low in nepheline. At a number of localities the nepheline syenite has been altered hydrothermally. It forms a discontinuous belt stretching from north of Landi Patao Sar to south of Landi Patao.

The nepheline syenite is medium- to coarse-grained. Chilling and flow structure can frequently be observed. Fine- to medium-grained dykes are exposed to the W, SW and S of Koga village, and at Bibi Dherai and south of Agarai and Sura. The central and eastern parts of the nepheline syenite form small to large dykes intruded into the Babaji syenite. These dykes show chilled margins.

The nepheline syenite contains nepheline, microcline, albite, sodalite, pyroxene, biotite, sphene, zircon, apatite, fluorite, magnetite and pyrite (Chaudhry et al., 1984; Ashraf et al., 1987). Calcite is abundant in the nepheline syenite exposed along Naranji Kandao. The age of the Koga nepheline syenite known from K/Ar determination on biotite is reported as 50 m.y. (Kempe, 1973).

The nepheline syenite of the Koga area is a part of the alkaline province extending from Loa Shilman to Chamla. The Koga nepheline syenite intruded during the later stages of the Himalayan orogeny (Ashraf et al., 1987). In addition to nepheline the nepheline syenite rocks also contains other feldspathoidal minerals such as sodalite, cancrinite, albite and microcline. Petrographic and chemical investigations indicate the following sequence of formation of the Koga nepheline syenite : peralkaline syenites (with or without quartz) — nepheline syenite — nepheline sodalite syenite — carbonatite.

The reported chemical and mineralogical analyses of different bodies of Koga nepheline syenite s given by Ashraf et al. (1987) who divided the rocks of the Koga area that into six major classes, i.e., nepheline syenite (sensu stricto), foyaites, nepheline syenite dykes, sodalite-nepheline syenite, litchfieldites and pegmatite.

The use of nepheline syenite as a substitute for feldspar in glass and ceramic industries is a common practice in many parts of the world because of it low melting point. However, the high iron content sometimes makes its use doubtful. A study carried out by PCSIR shows that the iron contents of the Koga nepheline syenite can be reduced to the minimum (0.1%) by magnetic separation (PCSIR Lahore. 1988). This concentration is acceptable to the galss industies (Khan et al., 1987b). The acceptable iron as Fe_2O_3 for the manufacturing of glass ranges from 0.05 to 0.07% (Naqvi et al., 1987). Another likely use of nepheline syenite from the Koga area is in slag-forming powder in steel industries for the continuous flow of steel during casting (PCSIR Lahore, 1988). Nepheline syenite can be used in whiteware and sanitary-ware, glazes and porcelain enamels, abrasive grinding wheels, portland and refractory cements, heavy clay products and as an extender in pigments and fillers in paints, plastics and rubbers (Naqvi et al., 1987; Ashraf et al.,1987). It is also used as a popular building stone due to its toughness (Siddiqui et al., 1968).

It is proposed that the industies based on Koga nepheline syenite be erected near the mining sites in the Koga area. This will lower the manufacturing cost of the products and help cope with the prevailing un-employment in this mountainous area.

REFERENCES

ASHRAF, M., CHAUDHRY, M.N. & HUSSAIN, S.S. (1987) Mineralization associated with the alkaline rocks and carbo-natites in NWFP, Pakistan. Kashmir Jour. Geol. 5. pp. 51-64.

CHAUDHRY, M.N., ASHRAF, M. & HUSSAIN, S.H. (1984) Petrology of Koga nep-heline syenite and pegmatite of swat district. Geol.

Bull. Punjab Univ. **16**. pp. 83-97.

KEMPE, D.R.C. (1973) The petrology of the Warsak alkaline granites, Pakistan, and their relationship to other alkaline rocks of the region. Geol. Mag. **110 (5)**, pp. 385-495.

——— **(1983)** Alkaline granites, syenites and associated rocks of the Peshawar plain alkaline igneous province, NW pakistan. *In:* Shams, F.A. (ed.) GRANITES OF HIMALAYAS, KARAKORUM & HINDU KUSH. Institute of Geology, Punjab University, Lahore, Pakistan, pp. 341-354.

——— **& JAN, M.Q. (1970).** An alkaline igneous province in the North-West Frontier Parovince, West Pakistan. Geol. Mag. **107**, pp. 395-398.

KHAN, I.H., QAZI, M.A. MAHMOOD, F. & KHAN, B. (1987a) Evaluation, beneficiation and utilization of Koga nepheline syenite as glass and ceramics raw material. Part I, Geochemical evaluation and concentra-tion studies. Pakistan J. Sci. Ind. Res. **30(1)**, pp. 54-59.

——— ——— ——— & ——— **(1987b)** Evaluation, beneficiation and utilization of Koga nepheline syenite as glass and ceramics raw material. Part II, Beneficiation and pilot plant studies. Pakistan. J. Sci. Ind. Res. **30(6)**, pp.466-471.

MARTIN, N.R., SIDDIQUI, S.F.A. & KING, B.H. (1962) A geological reconnaissance of the region between the lower Swat and Indus rivers of Pakistan. Geol. Bull. Punjab Univ. **2**, pp. 1-14.

NAQVI, A.A., FAROOQ, M.K., SOHAIL, M. & CHAUDHRY, M.S. (1987) Utilization of nepheline syenite in glass founding. Pak. J. Sci. Ind. Res. **30(8)**, pp. 590-594.

E.C.L. (1979). Report submitted to Directorate of Mineral Development, NWFP., Engineering Combine Limited, **111** p. (Un-published).

PCSIR LAHORE (1988) Report on nepheline syenite of Koga, Swat (NWFP); **135** p.

SIDDIQUI, F.A. (1965) Alkaline rocks of Swat and Chamla. Geol. Bull. Punjab Univ. **5** p. 52.

———**, CHAUDHRY, M.N. & SHAKUR, A. (1968)** Geology and pertrology the feldspathoidal syenites and the associated rocks of the Koga area, Chamla valley, Swat, West Pakistan. Geol. Bull. Punjab Univ. **7**, pp. 1-30.

Manuscript received on October 16, 1992; accepted for publication on December 31, 1992.

ACTA MINERALOGICA PAKISTANICA
VOLUME 6 (1992) pp. 164-166.

LEAD-ZINC-COPPER MINERALIZATION IN TRERI-MANJHOTAR AREA, DISTRICT MUZAFFARABAD (AZAD KASHMIR), PAKISTAN

SHAFEEQ AHMAD,
RIAZ A. SHEIKH
Institute of Geology, Punjab University, Lahore.
IZHARUL HAQUE
&
MUSTANSAR NAEEM
PCSIR Laboratories Complex, Lahore.

Ore microscopic study of the samples from Treri Manjhotar area show the deposit to have formed at below 200°C. The ore is comprised of lead-zinc-copper mineralization in which galena replaces the earlier minerals.

Lead-zinc mineralization has been reported from Treri-Manjhotar area, District Muzaffarbad, Azad Kashmir. Qureshi & Malik (1988) described in detail the geology of the area. The oldest rocks are the Precambrian Salkhala Formation which mainly comprises shists, phyllites, marbles and gneisses. These rocks are followed by Punjal Group of Triassic age which consists of volcanic rocks and dolomitic limestones which contain lead-zinc-copper mineralization. The ore is concentrated in four major bands.

The ore microscopic study of the polished samples and various tests applied to the minerals show the presence of pyrite, galena, sphalerite and chalcopyrite (Fig. 1). Pyrite is of bright yellow colour with Vicker's Hardness Number (VHN) of 1150. It occurs as anhedral to subhedral grains. Sphalerite occurs as irregular anhedral light grey grains with VHN 215. Chalcopyrite occurs as yellow to brassy yellow medium- to coarse- grained anhedral aggregates with VHN 208. Galena appears white with high lustre. It is coarse-grained, interstitial to pyrite and sphalerite with VHN 80. The occurrence of galena as coarse grains indicates its crystallization without disturbance and it replaces the earlier crystallised minerals.

DISCUSSION

The most significant feature about the mineral association pyrite-sphalerite-chalcopyrite-galena is the co-occurrence of sphalerite and chalcopyrite. Ramdohr (1969) described two types of sphalerite. One type shows exsolution of sphalerite and chalcopyrite indicative of solid solution and the other is devoid of this phenomenon. The second type does not show exsolution although chalcopyrite exists as discrete grains. According to him highest temperature sphalerite associated with chalcopyrite contains blebs of chalcopyrite. Oelsner (1966) described the hypothermal sphalerite to have a high iron content and epithermal sphalerite a low iron content. According to him high temperature sphalerite can include foreign substances in its lattice which are rejected again with the fall of temperature. The inclusion of chalcopyrite is temperature dependent: a hypothermal sphalerite can take up more chalcopyrite than an epithermal sphalerite. An epithermal vein or an altered sphalerite shows absence of segregated chalcopyrite.

However, the ore sample under study is devoid of exsolution of sphalerite and chalcopyrite although significant amount of chalcopyrite is present in the ore sample in association with sphalerite and galena. Such type of mineral association has been reported by many workers in sedimentary dolomites, limestones and magnesian limestones. These also occur in associated sandstones, shales or conglomerates. Workers like Brown (1967, 1970), Beales & Jackson (1966), Heyl (1969) and Assereto et al. (1977) reported similar mineral assemblages. The vein-type ores at temperatures below 200°C.

Assereto et al. (1977) described the Pb-Zn mineralization in dolomites to be due to the precipitation as sulphides of the metals carried out by the brines as chloride complexes, by the presene of reduced sulphur.

Zheng & Wang (1991) described the Pb-Zn mineralization to be divisible into three periods. Sedimentary periods mainly include dolomite, lesser pyrite (chiefly as framboids), and rare sphalerite.

The hydrothermal period may be divided into three stages: pyrite-arsenopyrite, sphalerite-galena and sphalerite-quartz. During the stage of sphalerite-galena, sphalerite has a black colour and occurs in high energy forms such as grape and band forms caused by rapid crystallization. Chalcopyrite grains also occur within sphalerite.

The minerals of a higher idiomorphic degree are formed in the sphalerite-quartz stage and include sphalerite, calcite, quartz and galena. There are no chalcopyrite grains within sphalerite. The weathered minerals include smithsonite and cerussite.

Zheng & Wang (1991) suggested that such deposits are formed by the ore-forming fluid of meteoric source belonging to a Ca-Mg-Cl-HCO_3 type of weak acidic to near-

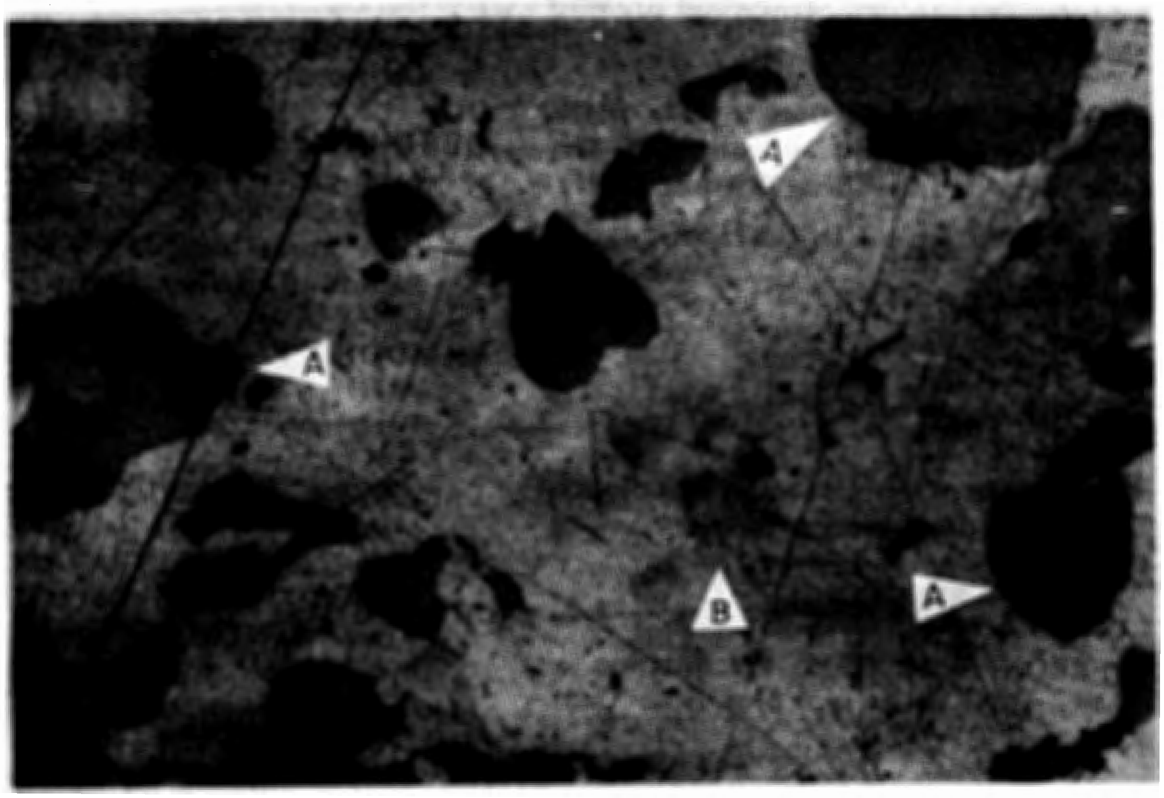

Fig. 1. Galena replacing sphalerite (A) and chalcopyrite segregations (B).

neutral pH solution with salinity of about 4 wt.% NaCl. The metals are transported as chloride complexes such as $PbCl^{-3}$, and $ZnCl_2$ and react with reduced sulphur and precipitate as sulphide minerals. The textures of minerals are controlled by the rate of supply of reduced sulphur.

The deposition of Treri Manjhotar sulphide ores may have resulted from the extraction of ore materials (Pb, Zn) by the heated meteoric waters resulting in ore-forming solution with low salinity; and the metals migrated as chloride complexes in weakly acidic to alkalic ore solutions reacted with the reduced sulphur giving rise to the formation of sulphide minerals at temperature of 150° to 200°C. The availability of reduced sulphur may have resulted by the reduction of sulphate water by methane, formed by the decomposition of organic matter.

The most likely reaction to take place under such environment appears to be the same as suggested by Zheng & Wang (1991).

$$CaSO_{4\,(s)} + PbCl^{-}_{3(aq)} + CH_{4\,(g)} + H_2SiO^{-2}_{4\,(aq)} =$$

$$PbS_{(s)} + CaCO_{3\,(s)} + SiO_{2\,(s)} + 3H_2O_{(1)} + 3Cl^{-}_{(aq)}$$

$$FeS_{2\,(s)} + 2PbC1^{-}_{(3(aq)} + 4e =$$

$$2PbS_{(s)} + Fe^{+2}_{(aq)} + 6Cl^{-}_{(aq)}.$$

The increase of ferrous ions in the solution resulted in redeposition of pyrite.

REFERENCES

ANDERSON, G.M. (1975) Precipitation of Mississippi Valley type ores. Econ. Geol. **70**, pp. 937-942.

ASSERETO, R., BRUSCA, C., GAETANI, M. & JADOUL, F. (1977). The Pb-Zn mineralization in the Triassic of the dolomites geological history and genetic interpretations. Industrial Mineraria Publicazioni degli Instituti di Geologia e di Paleonologia dell 'Universita degli studi di Milano, **231**, pp. 1-33.

BEALES, F.W. & JACKSON, S.A. (1966) Precipitation of lead zinc ores in carbonate reservoirs as illustrated by Poine Point orefield. Trans. Instn. Min. Metall. **B75**, pp. 278-285.

BROWN, J.S. (editor) (1967) Genesis of stratiform lead-zinc-barite fluorite deposit. Econ. Geol. Monog. **3**, pp.

BROWN, J.S. (1970) Mississippi Valley-type lead-zinc ore. Mineral. Deposita **5**, pp. 103-119.

HEYL, A.V. (1969) Some aspects of genesis of zinc-lead-barite-fluorite deposit in the Mississippi Valley, U.S.A. Trans. Instn. Min. Metall. Eng. **78**, pp. B148-B160.

OELSNER, O. (1966) ATLAS OF THE MOST IMPORTANT ORE MINERAL PARAGENESES UNDER THE MICROSCOPE. Pergamon Press, Oxford, pp. 3-71.

QURESHI, M.S. & MALIK, R.H. (1988) First geologic report on lead-zinc-silver mineralization at Treri Manjhotar, District Muzaffarabad, A.K. AKSMIDC Report. (Unpublished).

RAMDOHR, P. (1969) THE ORE MINERALS AND THEIR INTERGROWTHS. Pergamon Press, Oxford, pp. 502-516.

SANGSTER, D.F. (1976) Carbonate hosted lead zinc deposits. *In:* Wolf, K.H. (ed.) HANDBOOK OF STRATABOUND AND STRATIFORM ORE DEPOSITS. Elsevier, Amsterdom-Oxford-New York, Vol. **6**, pp. 447-456.

ZHENG, M. & WANG, X (1991) Genesis of the Daliangzi Pb-Zn deposit in Sichuan, China. Econ. Geol. **86**; pp. 831-846.

ACTA MINERALOGICA PAKISTANICA
VOLUME 6 (1992) pp. 167-170.

ANNUAL REPORT OF THE CENTRE OF EXCELLENCE IN MINERALOGY, QUETTA (1992)

ACADEMIC STAFF

	Date of Joining C.E.M.
Professor & Director	
1. ZULFIQAR AHMED Ph. D. (London), PG.DIP. (Mining Univ. Austria) M.Sc. & B. Sc. Honours (Punjab)	August 25, 1984
Associate Professors	
2. ABDUL HAQUE Dr. Troisieme Cycle (Caen, France), M.Sc. (Balochistan)	November 21, 1989
3. AKHTAR M.KASSI Ph. D. (St. Andrews, UK).	August 11, 1991 to August 18, 1992
Assistant Professor	
4. JAWED AHMED M.Sc. (Karachi), M. Phil. (Balochistan).	April 1, 1980
Lecturer-Cum-Research Associates	
5. KHALID MAHMOOD M. Phil., M.Sc. (Balochistan) (On doctorate-study leave to University of Montpellier II, France).	November 5, 1989
6. MOHAMMAD AHMED FAROOQUI M.Sc. (Balochistan) (on doctorate study leave to Montana University, USA)	Novermber 5, 1989
7. MEHRAB KHAN M.Phil., M.Sc. (Balochistan)	November 5, 1989
8. AMJAD RASHID M.Sc. (Balochistan)	November 5, 1991 to August 18, 1992

GENERAL STAFF

Administrative Officer	
1. S. SHAHABUDDIN M.Sc. (Balochistan)	May 21, 1977
Accounts Officer	
2. MIRZA MANZOOR AHMED B.Com. (Karachi)	May 7, 1980
Senior Technician	
3. KHUSHNOOD AHMED SIDDIQUI Dip. Assoc. Engr. (Hyderabad)	March 1, 1976
Assistant Librarian	
4. ABDUL GHFOOR M.L.S. (Balochistan)	May 2, 1985
Superintendent (Office)	
5. LAL MOHAMMAD DURRANI	May 12, 1973
Photographer	
6. HUSSAINUDDIN	June 16, 1981
Stenotypists	
7. M. GHALIB SHAHEEN KHAN	July 17, 1985
8. SAID RASOOL MAHJOOR	June 6, 1990
Draftsman	
9. AHMED KHAN MANGI	July 1, 1981
Assistant	
10. MOHAMMAD ANWAR	September 18, 1977
Laboratory Assistant	
11. SHER HASSAN	August 22, 1977
Store Keeper	
12. MUSA KHAN	August 20, 1977
Senior Clerk	
13. JUMA KHAN	June 12, 1985
Junior Clerk	
14. ABDUL MALIK	April 28, .1987
Drivers	
15. ALI MOHAMMAD	July 17, 1984
16. SALEH MOHAMMAD	August 18, 1990
Junior Mechanic	
17. ABDUL QADIR	August 21, 1977
Laboratory Attendents	
18. GHULAM RASOOL	August 20, 1977
19. MEHRAB KHAN	August 21, 1977
Naib Qasid	
20. SIKANDAR KHAN	April 30, 1976
21. MOHAMMAD RAFIQUE	October 12, 1978
22. ATTA MOHAMMAD	March 25, 1986
Loader	
23. RAWAT KHAN	July 2, 1977
Sweeper	
24. NAZIR MASIH	April 1, 1977
Chowkidar	
25. ABDUL WADOOD	January 26, 1992

M.PHIL. STUDENTS

1. **Din Mohammad**
   Supervisor : Akhtar M. Kassi
   Dissertation Title : Structural and sedimentological studies of the coal-bearing Ghazij Formation of Sor Range area, Quetta District.

2. **Mian Hassan Ahmad**
   Supervisor : Jawed Ahmad
   Dissertation Title : Petrography and stratigraphy of Chiltan Formation, south of Quetta, Balochistan.

3. **Masood Iqbal**
   Supervisor : Abdul Haque
   Dissertation : The ophiolitic rocks of Sra Salwat, south of Muslim Bagh, Balochistan.

4. **Mohammad Ibrahim Baloch**
   Supervisor : Mehrab Khan
   Dissertation Title : Structural, stratigraphic and petrographic studies of ophiolitic rocks of a part of Lukh Abdul Rehman, Khuzdar District, Balochistan.

5. **Qaiser Mahmood**
   Supervisor : Zulfiqar Ahmed
   Dissertation Title : Geology of Wadh-Goth Haji Shakar area, Khuzdar District, Balochistan.

The University of Balochistan kept pending the registration of the following fourteen M. Phil. students which were accepted for admission by C.E.M. during 1991.

1. Mohammad Sadiq.
2. Amjad Rashid.
3. Mohammad Ayub Baloch.
4. Mohammad Abdullah.
5. Khalid Rehman.
6. Masud Tariq.
7. Mohammad Omar.
8. Mohammad Rahim Jan.
9. Zulfiqar Ali.
10. Khan Bakhsh Bugti.
11. Mohammad Saeed.
12. Abdul Razak Khilji.
13. Munir Ahmad Baloch S/O Dr.Habibullah.
14. Munir Ahmad Baloch S/O Mohammad Gul.

In 1992, following students applied for M.Phil. admission.

1. Mr. Abdul Shakur.
2. Mr. Muhammad Din.

The Centre has recommended their admission; but they cannot begin the academic activity until the meeting of University's Committee for Advanced Studies & Research approves their registration.

C.E.M. RESEARCH PUBLICATIONS (1992) IN JOURNALS OTHER THAN ACTA MINERALOGICA PAKISTANICA

Ahmed, Zulfiqar

Leucocratic rocks from the Bela ophiolite, Khuzdar District, Pakistan. In: Searle, M.P. & Treloar, P.J. (Editors) HIMALAYAN TECTONICS Geological Society of London Special Publication. (Submitted).

Ahmed, Zulfiqar

Bulk-rock and mineral chemistry of anatectic and magma-fractionated rock suites from the Bela ophiolite. Kashmir Journal of Geology (submitted).

Kassi, A.M. & Kakar, D.M.

Preliminary assessment of the active landslides and gapping fissures in Sor Range-Zharai China area, Quetta District. Pakistan. Journal of Earth Sciences, Vol. 1 (Submitted).

Kassi, A.M. & Weir, J.A.

The stratigraphy, sediments and structure of the Lower Palaeozoic succession of the Gala Valley. Transactions of the Royal Society of Edinburgh, Scotland: Earth Sciences Section (Accepted for publication).

ABSTRACTS (1992)

Abstract are condensed but informative summaries of presentations made at meetings of scientific and professional organizations.

Ahmed, Zulfiqar

Ophiolitic leucocratic rocks from Khuzdar District, Pakistan. 7th Himalaya-Karakoram-Tibet Workshop. April 6-8, 1992, Oxford University, England. p.2.

Ahmed, Zulfiqar

Western margin of the Indian plate in terms of the geochemistry of Bela ophiolite, Pakistan. UNESCO Postgraduate Advanced Course in Plate Tectonics, Punjab University, Lahore; December 20, 1992 - January 2, 1993.

OTHER ACADEMIC ACTIVITIES

Prof. Francoise Boudier, of the Tectonophysics Laboratory, University of Montpellier II, France, conducted joint collaborative field work with the C.E.M. staff from April 11, to May 5, 1992.

Mr. Khalid Mahmood of C.E.M. continued the field studies in Muslim Bagh area from April 14, till June 20, 1992.

Mehrab Khan accompanied Professor F.Boudier from April 14, 1992 to May 10, 1992. Mr. Mehrab Khan proceeded to France for six months period in September, 1992, to conduct laboratory work on the samples collected from field work in Balochistan.

Activities on the linkage programme sponsored by the British Council, linking CEM with Department of Geology, Royal Holloway & Bedford New College, University of London, England, have been persued actively.

Zulfiqar Ahmad visited the U.K. institution from February 9 to April 15, 1992 (10 weeks). During this visit he completed the rare-earth element analyses on 50 whole-rock samples of the igneous rocks of Balochistan. He did this work using the Inductively coupled plasma atomic emission spectrometry (ICP-AES) technique at the laboratory of Dr. J.N. Walsh. The results have been presented for publications in journals.

Zulfiqar Ahmed also conducted other researches on the lead-zinc and fluorite mineralizations of 3 areas of Balochistan jointly in collaboration with R. J.L. Colvine and David H. Alderton of the U.K. institution.

Zulfiqar Ahmed also held meeting with other staff at the U.K. institution and discussed other research projects that can be undertaken under the link programme. In this connection, he met Prof. A.J. Smith (Chairman of the Department), Dr. J.N. Walsh, Dr. A.Hall, Prof. R.A. Howie (Emeritus Professor), Dr. M.F. Thirlwall, Dr. Martin A.

Menzies & Dr. Lewis A. Owen.

Zulfiqar Ahmed, visited Reading University and conducted research work on the rare-earth element analyses of the kimberlitic lamprophyre, associated basalts and diabase rocks of the Pishin District, Balochistan, in collaboration with Mr. Salim A. Malik, University of Reading, U.K.

Zulfiqar Ahmed participated in the 7th Himalaya-Karakoram-Tibet workshop held from April 6 to 8, 1992, at the Department of Earth Sciences,University of Oxford. He presented a research paper entitled "Ophiolitic leucocratic rocks from Khuzdar District, Pakistan". The paper was appreciated because of its first-time recognition of the supra-subduction zone geochemical signatures in the Bela ophiolite of Balochistan.

Mehrab Khan visited Department of Geology, Royal Holloway & Bedford New College, University of London, U.K., from January 13, 1992, till March 3, 1992. He studied 24 igneous rock samples from Nal area, Khuzdar District. He received training in rock crushing, powdering, preparation of rock samples into glass discs and powder pellets for the XRF analyses, X-ray diffraction and computer microscope. The prepared samples for XRF were analysed by Dr. David H. Alderton.

Drs. D. H. Alderton and R.J.L. Colvine from the RHB New College, U.K., and Hazel Prichard from the Open University, U.K. have planned to visit C.E.M. in the spring of 1993 to conduct a workshop at Quetta. This will be followed by the exchange short visit of two C.E.M. scholars to the RHB New College, England. A proposal has been sent to the British Council for sponsorship. Jawed Ahmad plans to work on the clay mineralogy and neotectonics of the Bostan Formation rock outcrops in Balochistan.

Mr. Boem van Ravenswaiij, Director, SOCRATES Insernational Consultancies, The Hague, Netherlands, visited C.E.M.on October 4, 1992, and discussed plans for the development of the library of CEM. He promised to advocate for material assistance for CEM in the form of books and journals published in Holland, computer hardware, laser printer, and other requirements of the CEM library.

In September, 1992, Zulfiqar Ahmed joined the Pakistan-Italy-France Joint Research Programme, 1992, on the geology of the Karakorum Range (Project on the Karakoram axial batholith). However, due to unusual landslides and floods in the project areas (Karambar-Imit and Yasin Valley in Gilgit Agency), the programme was disrupted. The programme is to be conducted now in the year 1993.

Zulfiqar Ahmed attended the one-day seminar on environmental profile of Balochistan held at Quetta on November 30, 1992, under the auspices of International Union for Conservation of Nature and Natural Resources (IUCN) and sponsored by the Royal Netherlands Embaassy at Islamabad.

Zulfiqar Ahmed participated in the Punjab University-UNESCO Regional Postgraduate Training Course in Plate Tectonics held at Lahore from December 20, 1992, to January 2, 1993. He presented his paper entitled "Western margin of the Indian plate in terms of the geochemistry of Bela ophiolite" on December 24, 1992.

1992 PAPERS OF REGIONAL INTEREST FROM OTHER JOURNALS

BUTLER, R.W.H., GEORGE, M., HARRIS, N.B.W., JONES, C., PIRIOR, D.J., TRELOAR, P.J. & WHEELER, J. Geology of the northern part of the Nanga-Parbat massif, Northern Pakistan, and its implications for Himalayan tectonics. Journal of the Geological Society, London, Vol. **149**, part 4, pp. 557-568.

JADOON I.A.K., LAWRENCE, R.D. & LILLIE. R.J. Balanced and netrodeformed geological cross section from the frontal Sulaiman lobe, Pakistan : Duplex development in thick strata along the western margin of the Indian plate. *In* : McClay, K.R. (Ed.) THRUST TECTONICS, pp. 343 - 356. Chapman & Hall.

JAN., M.Q., KHAN, M.A. & WINDLEY, B.F. Exsolution in Al-Cr-Fe $^{3+}$ -rich spinels from the Chilas mafic-ultramafic complex, Pakistan. American Mineralogist Vol. **77**, pp. 1074-1079.

Petterson, M.G. & Windley, B.F. Field relations, geochemistry and petrogenesis of the Cretaceous basaltic Jutal dykes, Kohistan, northern Pakistan. Journal of the Geological Society, London Vol. 149, pp. 107-114.

POGUE, K.R., WARDLAW, B.R., HARRIS, A.G. & HUSSAIN, A. Paleozoic and Mesozoic stratigraphy of the Peshawar basin, Pakistan: Correlations and implications. Geological Society of Ameria Bulletin, Vol. **104** (8), pp. 915 - 927.

SARWAR, G. (1991) Tectonic setting of the Bela ophiolites, southern Pakistan. Tectonophysics, Vol. **207**, pp. 359 - 381.

ABSTRACTS

7TH HIMALAYA-KARAKORAM-TIBET WORKSHOP, APRIL 6-8, 1992, DEPARTMENT OF EARTH SCIENCES. OXFORD UNIVERSITY, ENGLAND :

Ahmed, Z. Ophiolitic leucocratic rocks from Khuzdar District, Pakistan.

Allen, M.B., Windley, B.F. & Chi, Z. Cenozoic tectonics in the Urumqi-Korla region of the Chinese Tien Shan.

Arif, M. & Jan. M.Q. Mineralogy of the Indus suture ophiolite and an investigation of the associated mineralizations in Swat, NW Pakistan.

Bossart. P., Chaudhry. M.N., Dietrich, D., Ghazanfar, M.D., Greco, A., Meier, A., Ottiger, R., Papriz, K., Ramsay, J.G., Rey, R., Spencer, D., & Wahrenberger, C.A. A review of the geology of the northern Indian Plate, Kaghan Valley, NE Pakistan.

Brookfield, M.E. Was the Pamir arc pre-indented ? Stratigraphic and sedimentologic evidence for Mesozoic-early Tertiary back arc basins in the North Pamir and adjacent areas.

Brunel, M., Tapponier., P., Arnaud, N., Pan, Y. & Wang, Y. Tectonics of the Eastern Pamir.

Caporali, A. Recent gravity measurements in the Karakoram.

Chambers, A.F. & Izatt, C.N. The evolution of the external Himalayas. North Pakistan: the Galiat and eastern Potwar, Punjab.

Crawford, M.B. & Searle, M.P. Crustal structure and collision-related granitoid magmatism of the Hunza Karakoram, north Pakistan.

Coward, M.P., Izatt. C.N., Ries. A.C. & Williams. M.P. Passive margin subsidence and inversion along the western margin of the Indian Plate.

Cronin,V.S, Schurter, G.J., & Sverdrup, K.A. Landsat image analysis of drainage lineaments to locate possible faults and structural discontinuities along the Nanga Parbat - Haramosh massif, northwest Himalaya.

Dipietro, J.A., Pogue, K.R., Lawrence, R.D., Baig, M.S. , Hussain, A. & Ahmad, I. Stratigraphy and dome structure, Lower Sawat, Pakistan.

Fuchs, G. & Sinha, A.K. A terrain map of the Himalaya.

Gaetani, M., Erba, E., Jadoul, F. & Angiolini, L. Age constraints on Karakorum early deformations derived from sedimentary rocks.

Gaetani, M., Pasini, M. & Angiolini, L. The Permian of the Shaksgam Valley (Aghil and Karakorum Ranges).

George, M.T., Harris, N.B.W. & Butler, R.W.H. Granite magmatism and thermochronology across the Main Mantle Thrust, NW Pakistan.

Izatt, C.N. & Chamber, A.F. Stratigraphy and mountain front geometry of the Kalachitta and Hazara Hill Ranges, Pakistan.

Jadoon, I.A.K. Fault tip-lines and evolution of foreland structures : an example from the Sulaiman foredeep of Pakistan.

Jan, M.Q. & Khan, M.A. The Spatgali mafic-ultramafic complex, Kohistan arc, N. Pakistan.

Khan, M.A. & Jan, M.Q. Magmatic evolution of the lower island arc crust, Kohistan, N. Pakistan.

Le Fort, P., Pognante, U. & Benna, P. The Himalaya-Karakorum contact : eastern termination of the Nanga Parbat spur (Pakistan).

Matte, P., Tapponier, P., Bourjot, L., Pan, Y. & Wang, Y. Tectonics of western Tibet from the Kunlun to the Karakoram.

McDougall, J.W. The Main Boundary Thrust and propagation of deformation into the foreland fold-thrust belt in northern Pakistan.

Meier, A. & Wahrenberger, C. Metamorphism and tectonics of the Higher Himalayan crystalline of the Upper Kaghan Valley, NE Pakistan.

Nicora. A., Angiolini, L., & Gaetani, M. The Permian/Triassic boundary in the Hunza Valley (North Karakorum).

Pettersen, M.G., Crawford, M.B. & Humayun, M. Sr, Nd and O isotope data from the Kohistan batholith, N. Pakistan : constraints on the evolution of the Kohistan mantle and crust from 102 Ma to 30 Ma.

Pivnik, D.A. & Sercombe. Out-of-sequence, evaporite controlled faulting and folding in the Kohat Plateau, NW Pakistan.

Potts, G.J., Treloar, P.J. & Wheeler, J. Faulting history of the Nanga Parbat syntaxis, northern Pakistan : constraints from modern earthquake data.

Reddy, S.M., Kelley, S.P. & Magennis, L. A microstructural and ^{40}Ar/^{39}Ar laserprobe study of a greenschist facies shear zone from the Liachar Thrust. North-west Pakistan.

Scott, C. Glacial sediment production by the steep valley glaciers of the Nanga Parbat massif, Pakistan Himalaya.

Searle, M.P., Dransfield, M.W., Waters, D.J., Rex, D.C. & Wilson, R. Macro and Micro- structural evolution of the High Himalayan metamorphic rocks from Zanskar and Kashmir.

Smith, H.A. & Chamberlain, C.P. Evidence for late Eocene anatexis within the Indian plate as a result of Eocene Himalayan orogeny.

Spencer, D.A. & Spencer-Cervato, C. Exhumation and cooling history of eclogite and amphibolite facies rocks in the Upper Kaghan nappe, NW Himalaya, Pakistan.

Sullivan, M.A. A palaeogeographic reconstruction of the Dir Group : evidence for magmatic arc migration in the NW Himalaya.

Spring, L., Bussy, F., Vannay, J.-C. & Huon, S. Permocarboniferous " alkaline" granitic magmatism in the Indian High Himalaya (Upper Lahul-SE Zanskar) : geochemical characterisation and geotectonic implications.

Tapponier, P., Avouac, J.P. & Liu, Q. Active faulting and crustal folding in west Tibet and the Pamirs.

Treloar, P.J., Rex, D.C. & Hurford, A.J. Geochronology of the Indus gorge section through the Nanga Parbat syntaxis : constraints on uplift history.

Vannay, J. & Spring, L. Geochemistry of continental basalts within the Tethyan Himalaya of Lahul-Spiti and SE Zanskar (NW India).

Villa, I.M., Tonarini, S., Oberli, F., Meier, M., Spencer, D.A., Pognante, U. & Ramsay, J.G. Eocene age of eclogite metamorphism in Pakistan Himalaya.

Warwick, P.D. & Wardlaw, B.R. Paleocene-Eocene stratigraphy in northern Pakistan: depositional and structural implications.

Windley, B.F. & Allen, M.B. The Mongolian plateau : evidence for a mantle plume under Asia.

Zanchi, A. Structural evolution of the Karakoram sedimentary cover : preliminary data.

Zeitler, P.K., Chamberlain, C.P. & Smith, H.A. Quaternary anatexis and Neogene metamorphism at Nanga Parbat, Pakistan.

INFORMATION FOR AUTHORS

ACTA MINERALOGICA PAKISTANICA publishes in English annually the results of original scientific research in the multifaceted field of mineral sciences, covering mineralogy, petrology, crystallography, geochemistry, economic geology, isotope geoscience, petrography, petrogenesis, mineral chemistry and related disciplines. Review articles and short notes are also considered for publication. Priority is given to geoscientific papers with impact on Pakistani region.

In general, the manuscripts be organized in the following order: title; name(s) and institutional address(es) of the author(s); abstract; introduction; methods, techniques, material studied and area descriptions; results; conclusions; acknowledgements; references; tables; figure captions. The abstract should not exceed 300 words. All tables and figures should be referred in the text and numbered according to their sequence in the text. All references to publications are given in the text by author's name and year of publication; and are listed at the end of text alphabetically by author's names and chronologically per author.

Authors of the articles submitted for publication in ACTA MINERALOGICA PAKISTANICA should send two complete copies of the manuscript, typed double-spaced on one side of the paper only. Copies of tables should be in final format. As far as possible, tables and figures should be prepared for reduction to the single column size or to the page size (204mm x 278mm). Use of mineral symbols by Kretz (The American Mineralogist, 1983, Volume 68, pp. 277-279) is recommended for superscripts, subscripts, equations, figures and tables. The Concise Oxford Dictionary is adopted for spelling. Underlining of text by a single line will mean printing in italics; that by a double line will mean printing in bold letters. The use of metric system and S.I. units is recommended. Bar scales should be used in all figures rather than numerical scales.

Only articles not previously published and not about to be published, wholly or in part, in either Pakistani or foreign journals, are considered for publication. Submission of an article is understood to imply that the article is original and unpublished and is not being considered for publication elsewhere. Publication is subject to the discretion of the Editor. All manuscripts are refereed before being accepted. Accepted papers become copyright of the Centre of Excellence in Mineralogy, Quetta. Authors alone are responsible for the accuracy of the contents and views expressed in their respective papers. Fifty off-prints of each published paper will be sent to authors free of charge. Additional copies may be ordered just after receiving the acceptance letter from the Editor. Manuscripts should be sent to: Acta Mineralogica Pakistanica C/O Centre of Excellence in Mineralogy, University of Balochistan, G.P.O. Box 43, Quetta, Pakistan. Phone Nos. are (081) 41974 & 40500.

ACTA MINERALOGICA PAKISTANICA VOLUME 6, 1992

CONTENTS